Development of 2nd Row Molybdenum (0) Dearomatization Agents

Philip Joseph Shivokevich
West Chazy, New York

B.S., Chemistry, SUNY Plattsburgh, 2010
B.A., History, SUNY Plattsburgh, 2010

A Dissertation Presented to the Graduate Faculty
of the University of Virginia in Candidacy for the Degree of
Doctor of Philosophy

Department of Chemistry

University of Virginia
May 2017

I am fortunate to have so many people to thank. I truly would not be here, having written all of the pages before you if it weren't for the huge amounts of love and support that I have received from so many along the way. Most of the people listed in this section know that I have a difficult time expressing my feelings. I will attempt to overcome that difficulty here and hopefully give a small amount of something back to all those who have contributed so much to me. I know that I will not do justice to the feelings that I have, but will try my best to express them here. With that in mind, know that as you read on that this was the most difficult, and time consuming part of my thesis to write. It is because I have been fortunate enough to come into contact with a great many wonderful people that any of the subsequent chapters exist; so to say that these acknowledgements are the foundation of my thesis would be an understatement.

So here we go. I will start with those who have supported me from the start, my parents. My parents have always encouraged, nurtured, loved and supported me in any venture that I have undertaken. As teachers, they have shown me the importance of education in so many ways. As their way of life, in their professional lives, and also at home. They always stressed the importance of reading, but also looked to establish education in other less traditional ways. These have included travel, and along the way sparked my love of both history and the outdoors, which have continued to be passions of mine to this day. Through my parents I also learned a great deal about the world around me that was not covered in the classroom curriculum. Learning how to build and fix things from my Dad has been a skill that has helped me countless times throughout life, although it also came with the unfortunate side effect of having to constantly fix the rotovap. My Dad also instilled in me the time and money sinks of boating and woodworking, both of which have given me countless hours of joy, and a means of finding peace at stressful times in my life as an adult. In the classroom my parents taught me to

appreciate all subjects, which I did (except for English class, I hate grammar as anyone at Dean's writing workshop could tell you). This eventually led me to chemistry, which astonished my parents. I went off to college and pursued chemistry, becoming more interested as classes progressed, although I still could not shake my humanities leaning, and ended up with degrees in both chemistry and history.

My parents continued to give me support when I set off for Charlottesville. They helped in my apartment search and moving the large amount of stuff that I had accumulated. They then made several house hunting trips, and we drove circles around Charlottesville and the surrounding counties. When I finally bought my first home in the spring of my first year, they both used nearly all of their vacation time to come down and help me with the seemingly endless remodels. I never could have finished it without them. All throughout graduate school they have been tirelessly supporting me, with frequent trips, and also from a distance. They have always been there if I needed anything from someone to talk to in difficult times, to life advice, to plane tickets for holidays when money was tight. I would not have made it to graduate school without the wonderful influence of my parents, and surely would not have made it through all of the trials without their love and support. To you both I owe nearly all that I am. I love you, and thank you.

Next up would be my little sister Priscilla. Over the past 26 years we have assumed many roles as siblings, from partners in crime, to archrivals, to protectors, and even co-workers (now getting the mail for Day Brothers, Chip-it-103!). All along the way I have antagonized my little sister, to the point when I look back on it I am a little surprised that she still talks to me. Now we joke about it, and I claim that all of the, let's call them 'tests,' that I put her through made her stronger. I have been and continue to be astonished by her resilience, a quality that I wish I had on the same level as her. Throughout the years she has challenged me and pushed

me to be better and stronger, and when I needed it she has given me protection. Throughout graduate school she has always been there to talk about difficult things. My sister has also given me one of the happiest days of my life when she married my brother in law, Hrishi. Hrishi, also known as Mr. Chop-Chop, has been a wonderful husband to my sister, and over the last few years has become the brother that I never had. I am so happy that Priscilla made the cross-country trek for my defense, it certainly wouldn't have been the same without her. Thank you Priscilla for all that you have done for me and mean to me, I love you.

This brings me to the band of misfits in Virginia more commonly known as the Harman Lab. From this elite group of mad scientists I have received more support, knowledge, friendship, kindness, and love than is quantifiable. Lab members past and present have profoundly impacted both my heart and my mind, and I will do my best to show the depths of my gratitude.

I have to start with our fearless leader, Dean. Dean was the reason that I wanted to come to UVA. In my limited interactions with him on visitation weekend he catapulted UVA from a maybe school to my top contender. In those few days I experienced what I'm sure many before me have and what many more after me will, a strange inexplicable draw to Dean Harman. Once at UVA I met with Dean when it was time to decide your preference of research groups. I remember that day well (or at least think I do). I had been up for nearly 30 hours before our meeting working on another retake of an Organic III test (gross), followed by finishing the take home portion of an Analytical test, then taking the corresponding in class portion. After all of that non-stop chemistry I was pretty sure that I was delusional, and thought to myself that I just needed to stay awake a little longer. Perhaps I hallucinated, but I remember feeling a bit down after the meeting. It seemed as though Dean only planned on taking one student, and some lame kid from South Carolina had already claimed that spot by doing summer

research. Lucky for me Dean always takes more students than he says/thinks (a trend which continues today), and decided to take a chance on me.

Once in the Harman Lab (to my initial surprise and delight), I began my journey into organometallic chemistry. I was lucky to have Dean as a devoted mentor/tutor, along with a few others (which we'll get to shortly) who really helped me establish a strong foundation to build on. Dean has been available for weekly meetings from the beginning, always fostering and gently pushing my intellectual development, and was always there if I needed more time. These early discussions helped deepen my understanding as a scientist, and have helped me as a teacher in formal and informal settings. I have continually benefited over the years from Dean's uncanny ability to explain extremely complicated topics. Over the years this experience and encouragement has helped me develop my own interest in teaching, which put me in contact with a great many wonderful influences later on in my career at UVA. Dean, you have been the best advisor that I can imagine, thank you for taking a chance on me.

Another giant in my development within the Harman Lab was Bill Myers. Bill hailed from the University of Richmond, where he was an established inorganic professor. I remember when my first semester in the Harman Lab was nearly completed the lab was buzzing with anticipation for the arrival of 'Bill.' This all seemed very odd to me, but from my first interaction with Bill I understood the hype. Bill was the epitome of the gentle giant. His imposing physical presence was accented by his kind and giving nature. Throughout the summer of 2013 Bill gave me huge amounts of time and patience as he explained the intricate details of nearly any topic that one could encounter in the Harman Lab. Throughout future summers Bill continued to give his time and knowledge selflessly.

More than a mentor however, Bill Myers was a dear friend. He was always ready with a story, either to help illustrate a point in teaching, or for comic relief. But as quick as Bill was

with a story for any occasion, he was just as quick to lend an ear. Bill cared deeply about all those that he came into contact with. He was always ready to listen to any problem that we had, big or small, in lab or in our personal lives. His persona resonated as endearing and trustful. You could tell Bill anything and count on him not to pass judgement on you, but rather to listen with genuine concern and provide pillars of support. I was able to talk to Bill about anything, and could talk to him about things that I have been unable to do with anyone else. Over the years Bill has been a great mentor, therapist, and friend. Sadly Bill passed away in the fall of 2017. In his passing students have lost an educator, science a champion, and the Harman Lab a mentor and dear friend. It is telling of his influence that Bill was instrumental in bringing a great deal of former students and Harman Lab alumni together twice in his last months with us; once to celebrate his retirement, and the other to celebrate his life. I miss you Bill, and wish that you could be with us today, thank you for all that you have done for me.

My next mentor was my trainer and recruiter Dr. Jared Pienkos. I first met Jared at visitation weekend in the spring of 2012. Jared was certainly the most memorable graduate student that I encountered. We hit it off well, and spent a great deal of time together over my first few days at UVA. He was a tireless recruiter for both UVA and Dean, and his persistence and outgoing personality really started to get me thinking about coming to UVA. After joining the lab, we would joke that he was a bit obsessed with me. In hindsight this might have been true, since one night he snuck me in for a peak at the new (current for the younger folks) lab space, which he wasn't supposed to do as it was under renovation (sshhh, don't tell). After joining the lab Jared became my graduate student mentor, and trained me in many of the ins-and-outs of lab. I was always in awe of Jared's ability both in the lab, and in explaining what seemed to be inexplicable concepts, while also making connections between the tungsten system that he knew, and the molybdenum system that he was training me on. I did not realize

how difficult this was, much less the patience that he showed me as I fumbled with lab techniques and concepts, until I began training people as a senior lab member. Jared taught me the essentials of lab, including how to detect and when to ignore Dean's truly crazy ideas. Jared, thank you for all of the time that you spent in training me and prepping me for candidacy, I wouldn't have made it without you.

Dr. Ben Liebov and Dr. Bri MacLoed were rising senior members when I joined the lab. Initially my interactions with both of them were limited, as they were both gearing up for their candidacy exams. I remember going to their practice talks and thinking that knowing the answer to even a quarter of the questions that other graduate students posed to them was impossible. I couldn't imagine what type of questions that professors would ask; and I tried to block out the thought completely, telling myself that was a long way in the future… how time does fly. Both Ben and Bri passed their exams, and along with Jared spent massive amounts of time helping me prepare for mine. I owe a great deal of my success to their time and efforts, the enormity of which I didn't realize until it was time to help younger members with their preparations. Like Jared before them Ben and Bri contributed a great deal to their fellow lab members, and helped to foster a sense of community that I shared with them for four years.

What can you say about Ben? Enthusiastic might be the best word. I don't think I can imagine a better personification. Ben was enthusiastic, about everything. His always positive attitude helped to keep morale through the constant failed experiments that are the nature of science. Although our projects didn't overlap much, Ben was always there for a question about a variety of random topics. Ben also brought a great deal of culture to the lab. With Ben I felt a kindred nature, as he was also a weird humanities guy trying to convince people that he was a scientist (although we departed on topics, since his other degree is in English, which we've already established as gross). Ben was always there to discuss the random books that we were

reading, and a few times we even convinced each other on some titles, no regrets there. Thank you Ben for your constant optimism, giving nature, and friendship, you made my years in lab truly enjoyable.

On to Queen Bri. Although perhaps the most outspoken person in lab, Bri's presence really helped maintain order. This was especially evident after Jeff and I passed candidacy (more on this soon), and realized that we would then be difficult to get rid of. This led to a general rambunctiousness; of which Bri, as the only woman in lab, was the constant target. Bri provided a great deal of leadership, and was always there if I had an organic question (which despite my best efforts to avoid, I produced many). She was also a thorough editor, and her relentless slashing really helped me to hone my science writing skills by becoming more concise. So if the remainder of this thesis is terrible, I blame Bri. Despite all of my madness Bri managed to tolerate me, which like my sister is rather surprising. I owe her a great deal as a senior lab member, friend, and endless source of in-lab entertainment.

Dr. Jeff Myers joined the lab in the same year as me, formally in fall 2012, although he had already established himself by doing summer research with Dean (that's right he was the lame one from South Carolina). Despite the fact that we shared the same class schedule, Jeff and I didn't become close until after I joined the lab. In fact, my first memory of Jeff is g-chatting in November 2012. We both had made it into the Harman Lab. I was happy to have someone to lean on, and I think he was too (although at times he might regret it). Over the last five years Jeff has been my partner in crime, competitor, box-mate, and friend. We have shared the same meetings, classes, and struggles throughout graduate school. These started with our meetings with Dean and Jared, and in the summer Bill. These meetings quickly became a competition, with us trading victories each week. These competitions have continued in our later years in the form of chess matches, although I'm sad to say that they have been much

more one-sided in favor of the South (I blame Jeff's lack of history knowledge there, although he still won't defer to my degree on the chess matter). Jeff has always been there to update me on the e-mails that I would never read (thanks Dr. Secretary); and help me in my various fights with technology, which happen continuously, and were highlighted with my inability to print copies of my thesis for my committee without his generous rescue. Together we have grown in science, although along slightly different paths. I am proud of the contributions that we have made to the Harman Lab together, and am proud of the amazing scientist that Jeff has become. I am happy to know that he will be staying in lab as a post-doc, and I know that his presence will help maintain the order and culture of the Harman Lab. Jeff, thanks for all of the random, nonsensical arguments, and all of the memories, graduate school would not have been the same without you.

To Steven Dakermanji, my one-time trainee, who has risen to a 3rd year graduate student (this makes me feel so old). I appreciate the amount of time that you have dedicated to helping the lab function smoothly. You constantly give your time to change or help change tanks, refill acetone bottles, and many other greatly underappreciated tasks. As a scientist you have made some important strides over the years, and I hope that your continued growth helps to solve the racemization of molly. You have a tough task ahead, batten down the hatches. I wish you well in your future endeavors. Oh, and I nearly forgot…Sing us a song Steven!

To Jacob Smith, the rising star of the Harman Lab. Jacob, you have provided interest and intrigue from the first time I met you on visitation weekend. Since joining the lab about two years ago Jacob has become an integral part of the Harman Lab, both in terms of science and community. Over the years we have shared beers, sunburns, and best of all memories. Thanks for all of the random stuff that you helped me with, from attempting to help grout my kitchen floor, to moving heavy stone slabs. I am continually amazed by Jacob's prowess in lab, which is

truly astonishing for his mere two years. I know that with the amazing science that Jacob has done so far that he will do some great things in his graduate career and beyond. Thanks for all of the help on Tz, and the random questions about a variety of topics. Jacob always asks good questions, and I greatly appreciate our conversations. Keep up the good work Mr. Smith!

To Ben Cavanaugh. Bento Box has floated around the lab a bit since he joined a year and a half ago. I was lucky enough to inherit Mr. Box as a 2nd undergraduate mentee in November following Dr. Leibov's graduation. In the few months since he has switched projects he has made great strides, and I am proud of the contributions that he has made to the Tz army. My only regret with Ben is my inability to give him more time, due to my having to write this thesis thing. Ben, you are a soft-spoken, kind soul. Thanks for the research work and friendship that you have given me.

To Dr. Kevin Welch. It was really strange and exciting to meet and talk with a person from the Harman Lab past, and seeing the person behind the articles that I've read. While I have only known Kevin a short time, I am glad that he has returned to UVA. Kevin has provided me with a person to discuss a wide range of topics with, and has even engaged in the odd argument. I have greatly enjoyed these interactions, and in the process have also learned a ton. Kevin has also made our trivia team immediately relevant, and has catapulted 'Kevin and the Spaceys' to continual contender status. Kevin, thanks for your knowledge on a wide range of useless information, your humor, and for editing that one chapter of my thesis.

I'd now like to switch gears and thank a few folks outside of the lab. I need to thank my friend and one-time supervisor Chuck Arrington. Over the past 5 years Chuck has helped me prep for organic labs, deal with difficult students, and provide some excellent lab stories. After my formal ties to the organic labs have ended Chuck has continued to be a great friend, sharing drinks, talking sports, and of course giving me an outlet for Civil War discussions and swapping

some historical reading. Chuck helped to keep my inner humanities nerd nourished in a sea of science. Thanks, for all of the memories, and helping to make my teaching experiences truly enjoyable.

To Lauren Russell in chemical engineering. We have shared many great memories and ridiculous times. It's always great to go out with Lauren and having the server think that I must be a child because I only order 1 or 2 meals/sides to her entire menu order. I have really appreciated you keeping me out on the trail over the last few years. It's always great to share a hike with her, and I'll always cherish the countless sunrises that we have taken in together. This has been especially helpful over the last few months, as those hikes have helped me to maintain my sanity during the writing process. Lauren, thank you for all of the memories and support, I don't know what I'd do without my hiking buddy.

To change gears a bit more I need to thank my many friends in the Music department at UVA. You guys have taken me in over the last two years and have made me an honorary department member. You have collectively given me an escape from science, and an audience to talk about 'normal' people things. Chief among these musicians I need to thank Amy Coddington and Kyle Chattleton. While these two will likely never read these words, I am indebted to them a great deal. They have given me support, shoulders to cry on, love, and friendship. I don't think that I would have made it through the last two years without them in my life. Their patience and understanding are beyond belief, I have never felt judged by them…except for that time that Amy found Bud Light in my fridge. Amy and Kyle, thank you for all that you have done for me and your continuing friendship, I love you both very much.

Since I began with the family that was instrumental on getting me here, and helped me through many struggles, I think that it's only fitting to end with my 2nd family. There are three members of the Harman Lab which have become that 2nd family, and have helped to shape me

more than any other people expect for my original family. From our random trips together to sharing meals at family dinner night, you guys have helped to keep me going, for that I owe you a great deal, and I love you all.

To Alex Heyer, my academic son. Alex it is odd how close that we have become over the years, especially since our age difference was highlighted in the pairing of the oldest and youngest members of lab for quite some time. This age discrepancy has contributed to an unfortunately large number of times when Alex's younger associates thought that I was his actual father…terrible times. Over the last two years Alex has made dramatic steps as a scientist. I am so proud of the work that he has done, and his stubbornness when it comes to science. I was continually surprised that when I offered to take to the optimization of Tz back over from Alex, that he always responded with 'No, I'm going to fix this thing.' He eventually did, and his outside the box thinking eventually led to the memorable kg reaction and the Tz video. These efforts showed me that Alex's immense intellect was tied to his even bigger refusal to give up, I knew that I hit the jackpot in the lottery of undergraduate researchers.

Excitingly, Alex's drive for knowledge extends well beyond the bounds of chemistry. This is clearly seen by his ridiculous level of involvement in student associations, as well as his legendary 'hypothetical of the day' questions. With Alex I have found a friend with which to argue chemistry, politics, religion, and the meaning of anything and everything. These colorful conversations have opened up new points of view, and have provided some truly comical anecdotes. I feel privileged to have played a role in the academic development of Alex, and even more so to have earned his friendship.

Moving on to his betrothed, Hannah Nedzbala. Hannah, like Alex has become a force within the lab, and within my world. This duo has taken graduate classes, performed excellent research, and pestered their mentors. Unfortunately for me Hannah has a stellar graduate

student mentor, so my interactions with her in terms of science have been rather limited. However, in those few interactions I have been impressed with her knowledge and understanding, and how she uses them to shape her questions.

Hannah has helped to keep both me and Alex in line over the last two years, while also providing a target for our provocations. I always admire how she is able to be very blunt with me, especially in the many times that I annoy her. Hannah is always quick with a smile, and her good nature really helps to keep the spirits up in lab. Hannah you have been a great friend to me, and I'll never forget the memories we have made together, from the Hannah heads to your exquisite garlic bread. You have been like a second sister to me, thanks for taking my abuse and giving some in return.

This leaves Katy Wilson, who has been my closest friend for the past three years. When Katy and I bonded over a discussion of the pros and cons of capitalism in the fall of 2014 while watching Riley in Jeff's backyard, we began to form a friendship that would change my life. Over the past few years we have spent incalculable amounts of time arguing and discussing many topics. The bulk of this time has been dedicated to science, since that is our common language. These arguments/discussions began under the guise of Katy 'learning' from me. It is amazing how quickly that changed from her trying to 'learn' from me to proving me wrong, and showing me that she is truly worlds beyond me in terms of science. One of my favorite memories of these arguments is the Saturday that we spent hours in the conference room arguing about entropy. I remember that day Ben came in, did some experiments, went home to eat dinner, then came back to get something and we were still there. When he asked what we were talking about, and we responded that we were still arguing about entropy, he rolled his eyes, said eww, and left us to continue our argument. Over the years I have learned a great deal from Katy in these arguments, which regrettably I lose in nearly all cases. Other than the influence of Dean,

which isn't really fair given that has had two extra years, Katy has been the greatest influence on my career as a scientist. Her never-ending drive for knowledge and incessant questions have helped me to stay motivated, looking for that one chance to finally win an argument.

Despite Katy's enviable ability as a scientist, she are an even better friend. Together we have shared more memories than I could possibly list. From late night shenanigans, to book club, to kicking my butt at a plethora of sports (except bowling, my redemption from Taco Bell). Katy has given me a friend to share endless hours of happiness. Thank you for your friendship, support, and knowledge. You have made me a better scientist and a better person, I am truly in your debt beyond what words could describe.

Abstract

Chapter 1 outlines the history of π-basic dearomatization chemistry, beginning with the introduction of the 1st generation $\{Os(NH_3)_5\}^{2+}$ fragment. The requisite properties for π-basic dearomatization are identified through the development of the replacement 2nd generation {TpRe(MeIm)(CO)} system. We then follow application of the Tp ligand set to current group 6 tungsten and molybdenum dearomatization agents, and detail their ability to activate aromatic molecules.

Chapter 2 outlines the synthetic procedures for access to molybdenum dearomatization. Within the discussion of these optimized conditions, we explore a range of ancillary ligand options, and discuss changes to the steric and electronic properties of the resulting molybdenum complexes. Finally, we outline the characteristics that make {TpMo(DMAP)(NO)} the preferred choice for molybdenum dearomatization chemistry.

Chapter 3 explores methods to resolve the racemic molybdenum center. Here we detail a variety of strategies for enantioenrichment of our chiral molybdenum dearomatization agent. Following the resolution of the molybdenum center, we probed the ability to transfer molybdenum chirality to synthetically interesting ligands, and establish a means to determine the success of the chirality transfer.

Chapter 4 illustrates an alternative synthesis to dihapto-coordination via ligand exchange. Here we report initial studies in the development of a molybdenum precursor, similar to 3rd row metal – dihapto-benzene complexes.

Chapter 5 explores a dual bidentate ligand set, as a means to overcome racemization of the molybdenum center. Here we synthesized a range of complexes in an effort to mimic the steric and electronic properties of the {TpMo(L)(NO)} fragment. While we were able to produce

similar electrochemical properties to molybdenum dearomatization agents, we were unable to overcome unfavorable steric interactions to produce a dihapto-coordinate complex.

Chapter 6 applies the tunable hydridotris(1,2,4-triazolyl)borate (Tz) scorpionate to group 6 dearomatization chemistry. We explore the synthesis of classical scorpionate complexes, and compare their reactivity to analogous Tp complexes. We demonstrate the ability of Tz complexes to undergo reversible modulation of electronic and physical properties, which provide stabilization in highly oxidative environments. Efforts to develop a Tz – based group 6 dearomatization agent are outlined, along with preliminary results for both tungsten and molybdenum complexes.

Table of Contents

Acknowledgements ii

Abstract xv

Table of Contents xvii

List of Abbreviations xxi

List of Figures xxiii

List of Schemes xxvi

List of Tables xxx

Chapter 1 : Introduction

1.1 Introduction: The Utility of Dearomatization Agents 2

1.2 The First Dearomatization Agent: $\{Os(NH_3)_5\}^{2+}$ 3

1.3 Design of a Dearomatization Agent 5

1.4 Exploration of a Rhenium Dearomatization Agent: The Importance of Electronics 6

1.5 Exploration of a Rhenium Dearomatization Agent: The Importance of Sterics 9

1.6 Tp Motif and a 2nd Generation Re-Dearomatization Agent: {TpRe(L)(CO)} 11

1.7 Design of a 3rd Generation Dearomatization Agent: {TpM(L)(NO)} (M = Mo or W) 17

1.8 Synthesis of a 3rd Generation Dearomatization Agent: {TpMo(MeIm)(NO)} 18

1.9 Synthesis of a 3rd Generation Dearomatization Agent: $\{TpW(PMe_3)(NO)\}$ 22

1.10 Conclusion 24

1.11 References 25

Chapter 2 Development of the Molybdenum Dearomatization Agent {TpMo(DMAP)(NO)}

2.1 Introduction 32

2.2 Optimization of Mo-Dearomatization Synthesis: {TpMo(MeIm)(NO)} 32

2.3 Increasing the Scope of Ancillary Ligands, Synthesis of TpMo(L)(NO)(X) 35

2.4 Synthesis and Optimization of TpMo(MeIm)(NO)(η^2-naphthalene) 38

2.5 The Synthetic Utility of Mo-Dearomatization: {TpMo(MeIm)(NO)} 39

2.6 Molybdenum Dearomatization Tunability: TpMo(L)(NO)(η^2-naphthalene) 42

2.7 Current Mo-Dearomatization: {TpMo(DMAP)(NO)} 47

2.8 Conclusion 50

2.9 Experimental 51

2.10 References 61

Chapter 3 Exploration of a General Method for the Resolution of {TpMo*(L)(NO)}

3.1 Introduction 65

3.2 Initial Attempts for Mo-Resolution: Chiral Ancillary Ligand {TpMo*(L*)(NO)} 65

3.3 The Re-Resolution Method: Coordination of α-Pinene 71

3.4 Application of α-Pinene Method to Mo-Resolution 74

3.5 Accessing Enriched TpMo(DMAP)(NO)(η^2-aromatic) 75

3.6 Mo-Racemization Studies: *S*-β-Pinene 76

3.7 Mo-Racemization Studies: Exploration of a Reporter Ligand 79

3.8 Mo-Racemization Studies: TpMo(DMAP)(NO)(η^2-α-Pinene) Exchange Conditions 82

3.9 Mo-Racemization Studies: TpMo(L)(NO)(η^2-α-Pinene) Exchnage Conditions 83

3.10 Mo-Racemization Studies: TpMo(DMAP)(NO)(η^2-α-Pinene) Redox Conditions 85

3.11 Mo-Racemization Studies: Redox Catalyzed Exchange of TpMo(DMAP)(NO)(η^2-α-Pinene) 87

3.12 Conclusion 90

3.13 Experimental 91

3.14 References 99

Chapter 4 Application of TpMo(DMAP)(NO)(η^2-α-pinene) as an Exchange Reagent

4.1 Introduction 103

4.2 Accessing η^2-Aromatic Complexes via α-Pinene Exchange 104

4.3 Accessing η^2-Carbonyl/Alkene Complexes via α-Pinene Exchange 106

4.4 Solvent Effects Influencing Coordination Diastereomer Ratio 109

4.5 Current Mo-Exchange: TpMo(DMAP)(NO)(η^2-α,α,α-trifluorotoluene) 112

4.6 Conclusion 113

4.7 Experimental 114

4.8 References 119

Chapter 5 Investigation of a Dual Bidentate Molybdenum Dearomatization Agent

5.1 Introduction 122

5.2 Bis(pyazolyl)borate (Bp) Complexes 122

5.3 2,2'-Bipyridal Complexes 125

5.4 Polypyridal Molybdenum Complexes 127

5.5 Conclusion 133

5.6 Experimental 134

5.7 References 137

Chapter 6 Development of Next Generation Group 6 Dearomatization with Incorporation of the Tunable Tz Scorpionate Ligand

6.1 Introduction 140

6.2 The Scorpionate Ligand Tris(1,2,4-triazolyl)borate (Tz) 141

6.3 Exploration of a Tz Dearomatization Agent: {TzM(L)(NO)} (M = Mo or W) 143

6.4 pH Modulation of Group 6 Tz Complexes 152

6.5 Exploration of Alternative Tz Dearomatization Agents: $\{TzM(L)(CO)\}^-$ (M = Mo or W) 156

6.6 Conclusion 160

6.7 Experimental 162

6.8 References 167

Concluding Remarks 169

Appendix 174

List of Abbreviations

OTf	trifluoromethylsulfonate (triflate) anion
CV	cyclic voltammetry
VT	variable temperature
NMR	nuclear magnetic resonance
Terpy	2,2',2''-terpyridal
t-Bupy	4-*tert*-butylpyridine
MeCN	acetonitrile
ETPB	4-ethyl-2,6,7-trioxa-1-phosphabicyclo[2.2.2]octane
t-BuCN	*tert*-butyl isocyanide
bpy	2,2'-bipyridal
IR	infrared
dien	diethylaminetiramine
Cp	cyclopentadienyl
L_π	π-acidic ligand
L	ancillary ligand
Tp	hydridotris(pyrazolyl)borate
py	pyridine
MeIm	*N*-methylimidazole
BuIm	*N*-butylimidazole
Im	imidazole
4-pic	4-picoline
3-pic	3-picoline
nic	*S*-nicotine
DMAP	4-dimethylaminopyridine
npam	*N*-propylamine
aam	allylamine
pyr	pyrrolidine
mor	*N*-methylmorpholine

Fpy	4-fluoropyridine
HOpy	2-hydroxypyridine
pz	Tp pyrazolyl ring
ampy	2-aminomethylpyridine
Bp	hydridobis(pyrazolyl)borate
Tpm	tris(pyrazolyl)methane
Tz	hydridotris(1,2,4-triazolyl)borate
DphAT	diphenyl ammonium triflate
DMA	*N,N*-dimethyl acetamide
DMF	*N,N*-dimethyl formamide
DMSO	dimethylsulfoxide
THF	tetrahydrafuran
DCM	methylene chloride
Et_2O	diethyl ether
EtOAc	ethyl acetate
DME	dimethoxy ethane
PAH	polycyclic aromatic hydrocarbon
ERG	electron releasing group
TEA	triethylamine

List of Figures

Figure 1.1 2

Metal donation from filled d orbital into a π* orbital of the aromatic ligand allows for dihapto-coordintation. The coordinated arene can be shown as an η^2-species, and reacts as an isolated diene.

Figure 1.2 7

Selected polypyridal rhenium frameworks yielding dihapto-complexes.

Figure 1.3 17

The electrochemical properties for {M(σ-donor)$_4$L} complexes for Os^{II}, Re^{I}, Mo^0, and W^0 dearomatization agents.

Figure 1.4 18

Design of group 6 Mo^0 and W^0 dearomatization complexes compared to 2nd generation Re^{I} (M= Mo or W).

Figure 2.1 34

Crystal structure of $[TpMo(MeIm)_2(NO)]^+$.

Figure 2.2 44

Coordination diastereomers formed by coordination of prochiral naphthalene to the chiral {TpMo*(L)(NO)}.

Figure 2.3 45

Quadrant analysis of ligand coordination and the impact of the steric profile of the ancillary ligand.

Figure 3.1 68

Molybdenum – *S*-nicotine diastereomers and coordination diastereomers of **29**.

Figure 3.2 69

Coordinated protons of **29**, VT ^{1}H NMR resolution of rotamers shows 'chiral splitting' (1 = room temperature, 2 = -14°C).

Figure 3.3 71

^{1}H NMR signals of coordinated protons (I-IV) for **26**, **29**, and **30** (A, B, and C, respectively).

Figure 3.4 72

Possible coordination modes of TpRe(MeIm)(NO)(η^2-*R*-α-pinene).

Figure 3.5 77

^{1}H NMR signals for DMAP methyl groups of **36** isomers.

Figure 3.6 79

Proposed coordination isomers of **36**.

Figure 3.7 79

Chiral reporter ligands.

Figure 3.8 80

^{1}H NMR signals for DMAP methyl groups of **38**, **39**, and **40** isomers (A, B, and C, respectively).

Figure 3.9 82

1 : 1 dr ^{1}H NMR signals for **41**.

Figure 3.10 88

10 : 1 dr ^{1}H NMR signals for **41** via Scheme 9.

Figure 4.1 107

Coordination diastereomers of **47**.

Figure 4.2 109

Dihapto-coordination of ethyl acetate (**48**).

Figure 4.3 110

Possible coordination diastereomers of **50** (A) and **51** (B).

Figure 4.4 111

DMAP signals for coordination isomers of **50** (A and B) and **51** (C and D) from exchanges in THF (A and C) and xylenes (B and D).

Figure 5.1 122

Comparison of proposed dual bidentate ligand set (A) with the established Tp – based ligand set (B).

Figure 5.2 128

Coordination isomers of **57**.

Figure 5.3 131

Coordination isomers of **60**.

Figure 6.1 140

Scorpionates applied to dearomatization chemistry.

Figure 6.2 142

Possible means to modulate electron density at the metal center by interactions with 4-N lone pairs.

Figure 6.3 146

Comparison of cyclic voltammograms of scorpionate complexes $[LMo(CO)_3]^-$ (A) and $LMo(NO)(CO)_2$ (B) with the presence of internal standards cobalicinium hexafluorophosphate (A) and ferrocene (B).

Figure 6.4 153

Cyclic voltammagrams desmonstrating the reversible modulation of the electrochemical behavior of **63** upon protonation/deprotonation with DPhAT/TEA. Red: initial solution of 3 (~0.02 M). Blue: addition of 10 eq of DPhAT; purple: addition of an excess of TEA.

Figure 6.5 154

Cyclic voltammagrams demonstrating the decomposition of **69** upon treatment with one molar equivalent of DPhAT in the presence of a cobaltocenium hexafluorophosphate internal standard. Red = initial scan; blue = addition of 1 eq DPhAT.

Figure 6.6 155

Cyclic voltammagrams of **63** in aqueous solution. Red: **63** (~0.02 M) in aqueous solution. Blue: addition of $HOTf_{(aq)}$ causes precipitation and loss of current; purple: addition of $NaOH_{(aq)}$ results in irreversible multi-electron oxidation.

List of Schemes

Scheme 1.1 2

General reaction pattern for tandem electrophilic – nucleophilic additions to η^2-aromatic complexes with stereo- and regiocontrol.

Scheme 1.2 4

Aromatic coordination scope for the initial $\{Os(NH_3)_5\}^{2+}$ dearomatization agent (R = H or Me, X = OMe, OH, or NR_2).

Scheme 1.3 9

The synthesis of a variety of dihapto-species with *fac*-$\{Re(dien)(PPh_3)(PF_3)\}$, providing more versatile π-donation than the previous polypyridal rhenium complexes.

Scheme 1.4 10

Synthesis of *fac*-$[Re(dien)(PPh_3)(CO)(\eta^2\text{-furan})]^+$, the first rhenium – based dearomatization agent developed in the Harman Laboratory.

Scheme 1.5 12

Synthesis of η^2-alkene and μ^2-η^2-aromatic complexes from $TpRe(CO)_2(THF)$.

Scheme 1.6 14

Synthetic pathways to $TpRe(L)(CO)(L_\pi)$ complexes.

Scheme 1.7 16

Substitution of TpRe(MeIm)(CO)(η^2-benzene) for various aromatic ligands.

Scheme 1.8 20

Synthetic pathways for group 6 $TpM(L)(NO)(L_\pi)$ dearomatization agents (M = Mo or W).

Scheme 1.9 23

Aromatic coordination scope of $\{TpW(PMe_3)(NO)\}$.

Scheme 2.1 33

Optimized pathways for the synthesis of a molybdenum dearomatization agent.

Scheme 2.2 40

Organic transformations to **24** and **25**, yielding novel organic products.

Scheme 2.3 41

Redox – based recycling of {TpMo(MeIm)(NO)}.

Scheme 2.4 42

One-pot synthesis of TpMo(L)(NO)(η^2-arene) complexes.

Scheme 2.5 48

Synthetic utility of accessing a stable allylic complex (**24-H**, **25-H**).

Scheme 2.6 49

{TpMo(DMAP)(NO)} Synthesis and stabilization of naphthalene allylic cation complexes (**26-H**).

Scheme 3.1 67

The racemic synthesis of a molybdenum dearomatization agent.

Scheme 3.2 73

Resolution of {TpRe*(MeIm)(CO)} by coordination of *R*-α-pinene.

Scheme 3.3 78

Synthetic pathways to **36** to test for transfer of molybdenum chirality.

Scheme 3.4 83

Proposed racemization of {TpMo(DMAP)(NO)}**.**

Scheme 3.5 86

Proposed redox scheme to overcome molybdenum racemization.

Scheme 3.6 87

Synthesis of **34** from TpMo(DMAP)(NO)(TFT) (**I**).

Scheme 3.7 89

Proposed redox catalyzed ligand exchange and molybdenum chirality transfer.

Scheme 4.1 103

Access to dihapto-aromatic complexes via benzene ligand exchange.

Scheme 4.2 104

Access to molybdenum – dihapto complexes via α-pinene ligand exchange.

Scheme 4.3 113

Exchanges from **I** illustrating expanded molybdenum coordination scope.

Scheme 5.1 124

Proposed synthesis of a molybdenum dearomatization agent featuring two bidentate ligands (**IV**).

Scheme 5.2 125

Alternate synthetic pathway to **IV**.

Scheme 5.3 127

Alternate synthetic pathway to **IV**, with incorporation of literature reports of **56** and **57**.

Scheme 5.4 129

Proposed synthesis of a polypyridal molybdenum dearomatization agent (**VI**).

Scheme 5.5 130

Proposed synthesis of a mixed polypyridal molybdenum dearomatization agent (**X**).

Scheme 5.6 133

Proposed polypyridal molybdenum dearomatization agent featuring a CO π-acid (**XII**).

Scheme 6.1 147

Proposed synthesis of dihapto-complexes (**III**) for group 6 tungsten and molybdenum Tz complexes.

Scheme 6.2 149

Proposed synthesis of **III** via redox reactions.

Scheme 6.3 150

Proposed disproportionation during the synthesis of **72**.

Scheme 6.4 157

Proposed synthesis of group 6 tungsten and molybdenum dearomatization agents $\{TzM(L)(CO)\}^-$ (**VIII**) by thermolysis of **63**-**64**.

Scheme 6.5 158

Proposed synthesis of **VIII** via tandem oxidation/thermolysis of **63**-**64**.

List of Tables

Table 1.1 8

d^5/d^6 reduction potentials for selected polypyridal rhenium and osmium – pentaamine dihapto-complexes (*a* = potential reported for $E_{p,a}$)

Table 1.2 15

Modulation of electron density within $TpRe(L)(CO)(L_\pi)$ complexes by changes to the ancillary ligand. Comparison of d^5/d^6 reduction potentials to $[Os(NH_3)_5(L_\pi)]^{2+}$. (a = potential reported for $E_{p,a}$).

Table 1.3 21

IR and electrochemical data for group 6 {TpM(L)(NO)} complexes (M = Mo or W).

Table 2.1 36

Electronic characteristics of a range of {TpMo(L)(NO)} complexes (a = complex observed *in situ*).

Table 2.2 43

Effects of the ancillary ligand on the electronic properties of $TpMo(L)(NO)(\eta^2$-arene) complexes (reported reduction potentials measured as $E_{p,a}$).

Table 2.3 46

Coordination diastereomer ratios of $TpM(L)(CO/NO)(\eta^2$-naphthalene) complexes (M = Re, W, or Mo).

Table 5.1 132

Reduction potentials for molybdenum bidentate complexes and their {TpMo(L)} analogs.

Table 6.1 145

Reduction potentials and IR stretches for selected group 6 Tp and Tz complexes.

Table 6.2 154

The effects of acid on $[LM(CO)_3]^-$ complexes (L = Tz or Tp, M = Mo or W).

Table 6.3 160

Comparison of reduction potentials for $\{TzM(L)(CO)\}^-$ and {TpM(L)(NO)} dearomatization agents (M = Mo or W).

Chapter 1

Introduction

1.1 Introduction: The Utility of Dearomatization Agents

Over the last 30 years π-basic transition metal dearomatization agents have shown great efficacy in accessing a variety of novel chemistry with aromatic substrates. These powerful transition metal fragments coordinate aromatic molecules in a dihapto-fashion, resulting in dearomatization of the coordinated ligand. This unique coordination mode occurs via backdonation of electron density from the π-basic metal center into an anti-bonding orbital on the aromatic ligand (Figure 1).[1-5] Dearomatization is illustrated with the coordination of a ligand such as benzene, as evidenced by changes to the bond lengths compared to those of the free

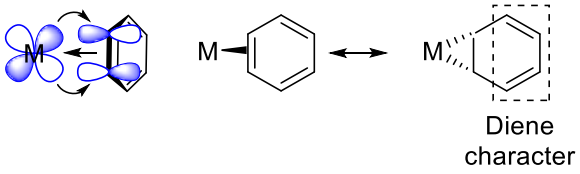

Figure 1: Metal donation from filled d orbital into a π* orbital of the aromatic ligand allows for dihapto-coordination. The coordinated arene can be shown as an η^2-species, and reacts as an isolated diene.

ligand ,and takes on the appearance and reactivity of a diene species (Figure 1).[1-2, 4-5] The η^2-aromatic species is now activated toward tandem electrophilic –nucleophilic *additions*,[1-5] rather than the substitutions which are readily accessed on the free aromatic via traditional synthetic methods.[6] Moreover, these transformations occur regio- and stereoselectively, as shown by the general reaction Scheme 1.[2, 4, 7]

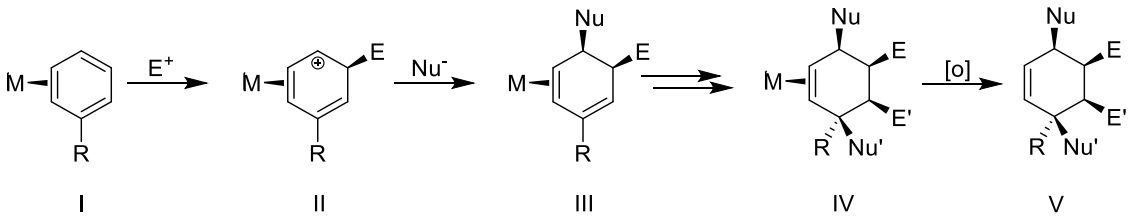

Scheme 1: General reaction pattern for tandem electrophilic – nucleophilic additions to η^2-aromatic complexes with stereo- and regiocontrol.

Stereocontrol is provided by the metal complex, which occupies one face of the ligand. Due to the steric bulk of the metal complex, additions to the coordinated ligand occur *anti* to the metal. As shown in Scheme 1, the initial addition of an electrophile occurs regioselectively, yielding an allylic carbocation species (**II**) which is subsequently stabilized by donation from the metal. The resulting species is activated toward nucleophilic addition, which also occurs stereoselectively producing a dearomatized tandem addition product (**III**, Scheme 1). The remaining uncoordinated double bond can undergo similar reactions (**IV**), and the novel organic molecule (**V**) can be liberated from the dearomatization agent by oxidation of the metal complex. Over the past 30 years these general methods have been used to access a range of small molecules occupying new chemical space.[1-2, 7-14]

1.2 The First Dearomatization Agent: $\{Os(NH_3)_5\}^{2+}$

The first dearomatization agent was reported by Harman and Taube in 1987. However, despite the synthetic power that this osmium system would eventually display, it arose from accidental beginnings.[5] The accidental dihapto-coordination of acetone from the reduction of $[Os(NH_3)_5(OTf)](OTf)_2$ is fitting given the accidental formation of its Os^{II} precursor, $[Os(NH_3)_5(N_2)](OTf)_2$, by Borod'ko et al. in the 1960s. Rather than yielding the desired osmium – nitrogenyl complex, Borod'ko synthesized one of the first known dinitrogen complexes.[15-17] After reporting of one of the first examples of dihapto-coordinated ketone complexes, Harman and Taube began to probe the reactivity of the electron rich $\{Os(NH_3)_5\}^{2+}$ fragment.[18] The electrochemical reduction of $[Os(NH_3)_5(OTf)](OTf)_2$ in the presence of benzene resulted in a dihapto-benzene complex, evidenced by CV, and later confirmed by VT NMR.[19] A variety of dihapto-aromatic complexes were synthesized according to Scheme 2, with the reduction of $[Os(NH_3)_5(OTf)](OTf)_2$ to generate the powerful π-base $\{Os(NH_3)_5\}^{2+}$.

The variety of dihapto-coordinated species that the $\{Os(NH_3)_5\}^{2+}$ fragment produced was somewhat unexpected given the metal's oxidation state, as well as the overall 2+ charge of the complex. However, despite these characteristics, which are typically associated with electron deficient species, the five ammonia ligands provide strong σ-donation to the osmium metal center while offering little in terms of backbonding ability.[15-16, 18, 20-21] Since its introduction by Harman and Taube, the $\{Os(NH_3)_5\}^{2+}$ fragment has produced a variety of interesting η^2-aromatic complexes (Scheme 2).[5, 22-23] These complexes differed from previous literature reports of dihapto-coordinated aromatics,[24-39] in that they are thermally stable and are able to undergo a variety of chemical reactions.[1, 5] With the demonstrated efficacy of the $\{Os(NH_3)_5\}^{2+}$ system to yield novel chemistry, the synthetic utility of π-basic dearomatization methodologies was established.

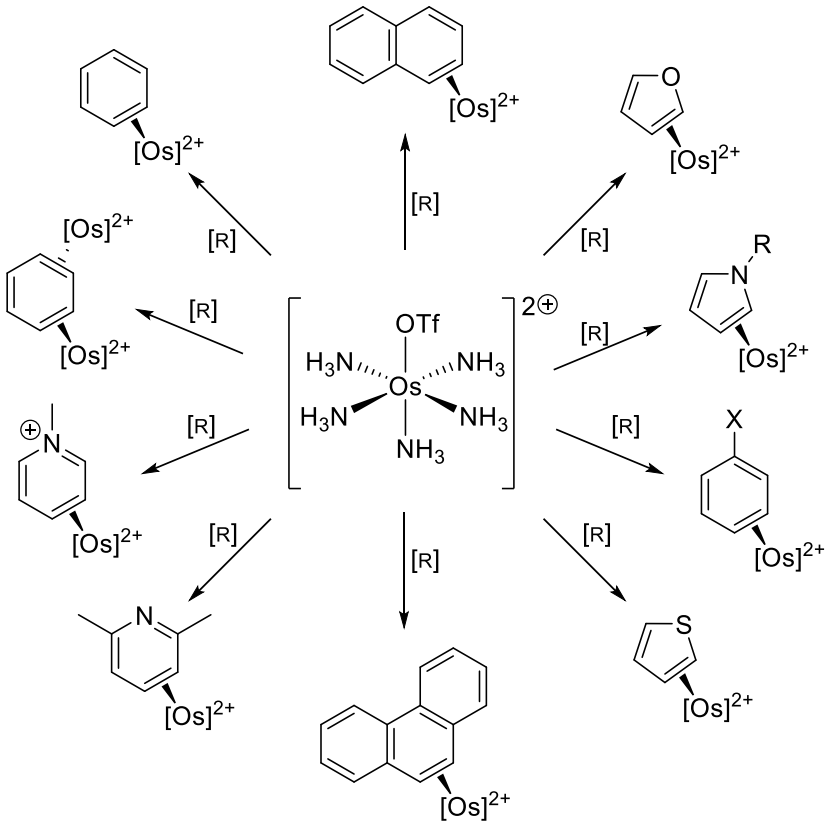

Scheme 2: Aromatic coordination scope for the initial $\{Os(NH_3)_5\}^{2+}$ dearomatization agent (R = H or Me, X = OMe, OH, or NR_2).

1.3 Design of a Dearomatization Agent

While the $\{Os(NH_3)_5\}^{2+}$ fragment demonstrated great synthetic utility over the course of 15 years, with a range of aromatic substrates, and producing a variety of novel products, it was not without its limitations.[1] Perhaps one of the biggest limitations of the osmium system is its lack of tunability. Changing a single ammonia ligand yields a complex which is no longer able to access novel η^2-aromatic coordination modes.[40] This problem directly impacted the small molecule products, which despite the *relative* regio- and stereocontrol offered by osmium coordination, lacked the desired *absolute* control due to the achiral nature of the osmium fragment.[1, 5, 41] Moreover, the osmium system was limited by cost, an especially important consideration given the stoichiometric use of the complex, as well as by synthetic difficulties due to the 2+ charge (low solubility in organic solvents, incompatibility with chromatography).[1] All of these drawbacks led to the design of a second generation dearomatization agent to build upon the foundational chemistry laid with $\{Os(NH_3)_5\}^{2+}$.

The initial design of a dearomatization agent began by dissecting the characteristics of the original $\{Os(NH_3)_5\}^{2+}$ system. This analysis yielded the importance of σ-donors arranged around a d^6 metal in an octahedral geometry. The importance of σ-donors was a direct reflection of the osmium system, whose entire ligand set is composed of σ-donating ammonia ligands which have negligible π-acid characteristics. This ligand set provides the electron density required for effective backdonation into aromatic ligands.[1, 5] The octahedral geometry is important for two reasons; both of which are essential to protect the electron-rich metal from undesired side reactions. First, the octahedral geometry helps prevent oxidative addition as a competing pathway to dihapto-coordination, which is commonly observed with highly reducing metal fragments. This protection comes with the coordinatively saturated environment upon η^2-coordination within d^6 metals, as well as the steric bulk to disfavor the resulting seven-coordinate

product of an oxidative addition.[1, 5] The sterics inherent within octahedral complexes also serve to protect the metal center from reagents used in subsequent reactions to the coordinated aromatic ligands.

1.4 Exploration of a Rhenium Dearomatization Agent: The Importance of Electronics

With the identification of the key characteristics required for a 2nd generation dearomatization agent, the investigation began into the development of a capable Re^{I} fragment. Rhenium provided a logical starting place for an Os^{II} replacement, as the majority of the previously reported η^2-aromatic species were rhenium complexes.[1, 24-28, 32, 34-35, 38-39] Another advantage was the reduced cost of the starting materials compared to the established osmium system (~1/12), immediately removing some of the cost limitation.[1]

Initial efforts to produce a d^6 Re^{I} dearomatization agent followed a similar synthetic approach to that of the osmium system, in which the proposed rhenium – η^2-aromatic species was achieved from subsequent oxidation and reduction of a rhenium dinitrogen complex. However, the syntheses of Re^{I} complexes with five σ-donors proved challenging, as the d^5 Re^{II} species were difficult to reduce due to the instability of the resulting highly reducing Re^{I} product.[1, 42]

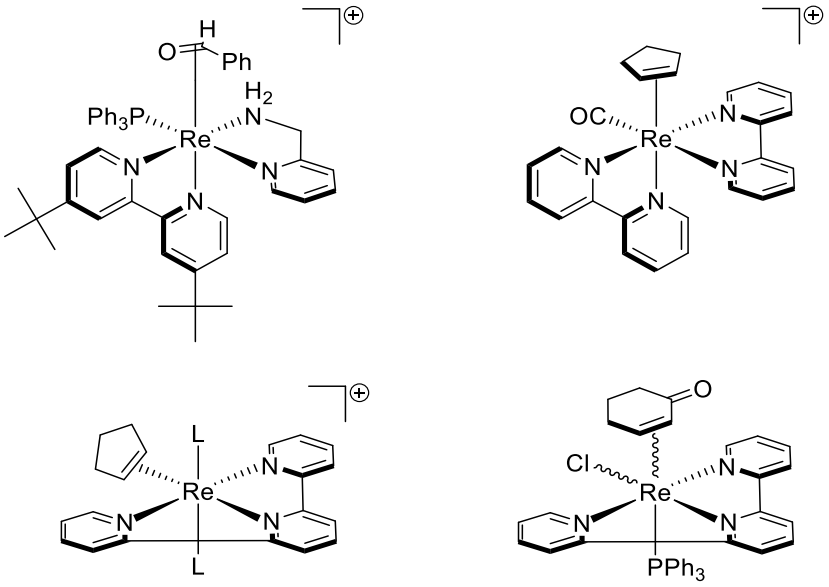

Figure 2: Selected polypyridal rhenium frameworks yielding dihapto-complexes.

The synthetic difficulties associated with an exclusively σ-donor ligand set led to incorporation of polypyridal ligands (*e.g.*, bpy, terpy). While these ligands act primarily as σ-donors in a variety of systems, their increased conjugation relative to that of a single pyridine results in increased π-acidity (bpy vs 2 pyridines, terpy vs 3 pyridines). Due to the increased π-acidity of the ligand set, coupled with σ-donation from the lone pairs of the pyridal nitrogens, the incorporation of polypyridal ligands results in complexes which can stabilize multiple metal oxidation states.[43] A variety of complexes were synthesized around bpy and terpy scaffolds (Figure 2), and demonstrated the ability to modulate the electronic properties of the complex by changes to ancillary ligands (1-14, Table 1). The polypyridal rhenium complexes yielded η^2 – alkene and carbonyl complexes, but were unable to coordinate aromatic ligands.[1, 43-47]

Entry	Re Polypyridal Complexes	d^5/d^6 Reduction Potential (V)
1	$[Re(terpy)(PPh_3)(Br)(\eta^2\text{-acetone})$	-0.04
2	$[Re(terpy)(PMe_3)_2(\eta^2\text{-cyclohexanone})]^+$	0.36
3	$[Re(terpy)(PMe_3)_2(\eta^2\text{-cyclopentene})]^+$	0.22
4	$[Re(terpy)(PMe_3)_2(\eta^2\text{-benzaldehyde})]^+$	0.28
5	$[Re(terpy)(PMe_3)_2(\eta^2\text{-acetone})]^{+,\,a}$	0.08
6	$[Re(terpy)(PMe_3)_2(\eta^2\text{-acetophenone})]^{+,\,a}$	0.22
7	$[Re(terpy)(t\text{-Bupy})(PPh_3)(\eta^2\text{-cyclohexanone})]^{+,\,a}$	0.50
8	$[Re(terpy)(NH{=}CMe_2)(PPh_3)(\eta^2\text{-cyclohexanone})]^+$	0.18
9	$[Re(terpy)(t\text{-BuNC})(PPh_3)(\eta^2\text{-cyclohexanone})]^+$	0.18
10	$[Re(terpy)(PPh_3)(MeCN)(\eta^2\text{-cyclohexanone})]^+$	0.42
11	$[Re(terpy)(t\text{-BuNC})_2(\eta^2\text{-cyclopentene})]^+$	0.52
12	$[Re(terpy)(t\text{-BuNC})_2(\eta^2\text{-acetone})]^{+,\,a}$	0.46
13	$[Re(terpy)(t\text{-BuNC})_2(\eta^2\text{-acetophenone})]^+$	0.34
14	$[Re(terpy)(ETPB)_2(\eta^2\text{-cyclohexanone})]^+$	0.66
	Os Complexes	
15	$[Os(NH_3)_5(\eta^2\text{-acetone})]^{2+,\,a}$	0.36
16	$[Os(NH_3)_5(\eta^2\text{-cyclopentanone})]^{2+,\,a}$	0.40
17	$[Os(NH_3)_5(\eta^2\text{-2-butanone})]^{2+,\,a}$	0.45
18	$[Os(NH_3)_5(\eta^2\text{-benzophenone})]^{2+,\,a}$	0.75

Table 1: d^5/d^6 reduction potentials for selected polypyridal rhenium and osmium – pentaamine dihapto-complexes (a = potential reported for $E_{p,a}$)

Despite the inability of polypyridal rhenium complexes to act as dearomatization agents, their alkene and carbonyl complexes provided a match to the electrochemical profiles of analogous osmium complexes (Table 1).[1, 43-47] These complexes also provide similar backdonation ability based on the IR stretches of their dinitrogen complexes.[20-21, 45] These results demonstrated that despite the ability to mimic the electronic requirements of the $\{Os(NH_3)_5\}^{2+}$ fragment, sterics also play an important role in the dihapto-coordination of aromatic molecules. With this in mind a closer look was given to the steric profile of the ligand set, especially the impact of ligands cis to the coordination site.

1.5 Exploration of a Rhenium Dearomatization Agent: The Importance of Sterics

With the importance of sterics accounted for in the design of our 2nd generation dearomatization agent, a new ligand set was explored. The new ligand set once again incorporated strong σ-donors, while the electronics of the complex were tempered with the inclusion of a sterically small π-acid, in order to mimic the redox chemistry of the $\{Os(NH_3)_5\}^{2+}$ fragment and the various polypyridal rhenium systems. These attempts produced a $\{Re(dien)(PPh_3)(PF_3)\}$ species, which provided a good electronic match for the $\{Os(NH_3)_5\}^{2+}$ forerunner.[48-50] Like the previously discussed polypyridal ligand set the new rhenium species also afforded a variety of dihapto-complexes (Scheme 3), with similar electronic properties. However, despite the success in once again reproducing the electronic requirements of the osmium system, η^2-aromatic complexes remained elusive. This was overcome by substitution of the PF_3 ligand for CO, which provided similar π-acidity with a slimmer steric profile.[48] The resulting *fac*-$\{Re(dien)(PPh_3)(CO)\}$ fragment established a chiral, second generation dearomatization agent, successfully coordinating furan (Scheme 4).[1, 48]

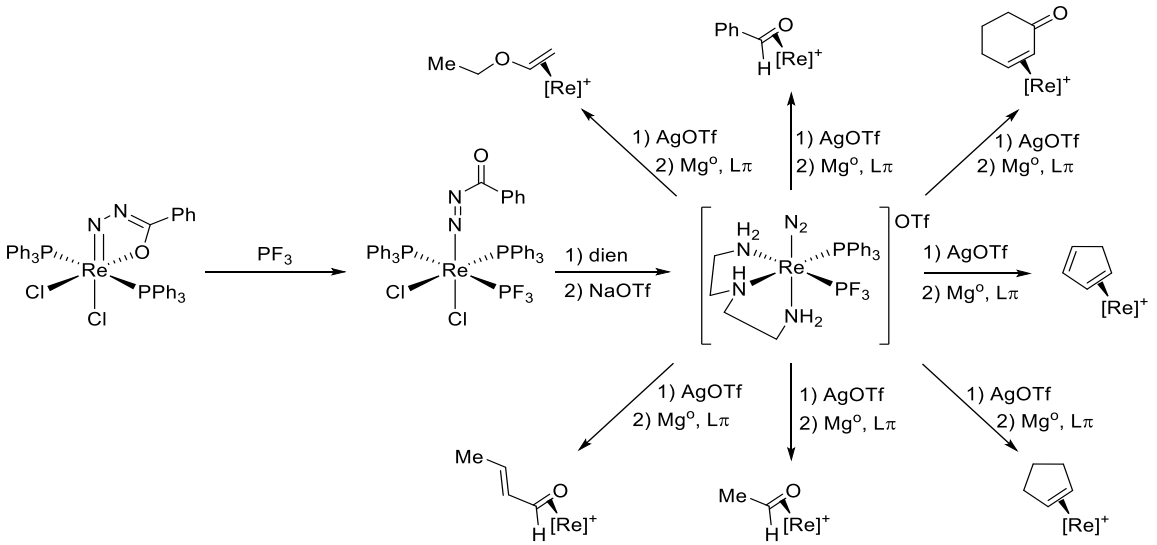

Scheme 3: The synthesis of a variety of dihapto-species with *fac*-$\{Re(dien)(PPh_3)(PF_3)\}$, providing more versatile π-donation than the previous polypyridal rhenium complexes.

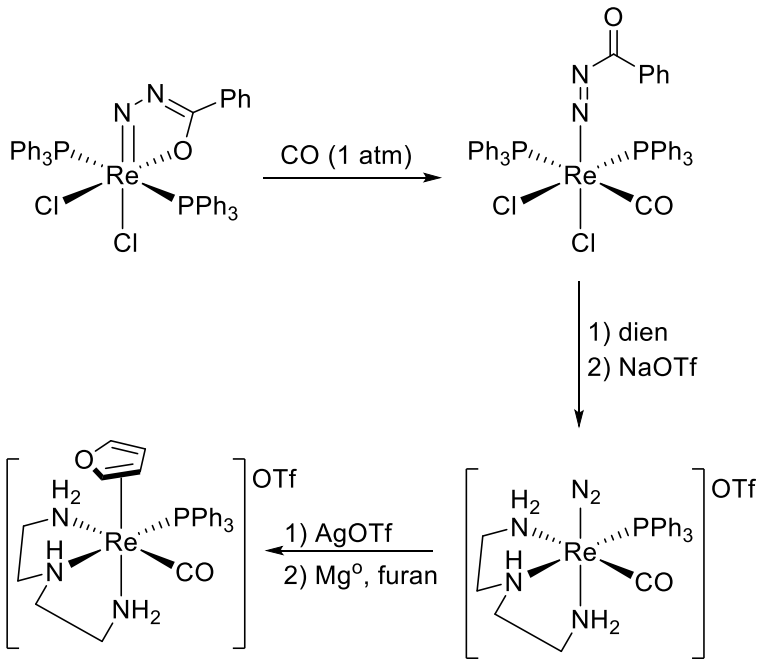

Scheme 4: Synthesis of *fac*-[Re(dien)(PPh_3)(CO)(η^2-furan)]$^+$, the first rhenium – based dearomatization agent developed in the Harman Laboratory.

Despite the success of the *fac*-{Re(dien)(PPh_3)(CO)} species to access the second example of thermally stable η^2-aromatic complexes, it had drawbacks which severely limited its synthetic utility. The main drawback was the propensity of the dien ligand to undergo isomerization from the desired *fac* coordination to a *mer* form, which proved too sterically bulky to effect dihapto-coordination. Although the prototype of the 2nd, rhenium based dearomatization agent was accompanied by difficulties due to undesired ligand isomerization, its development provided a great deal of insight into the steric and electronic requirements of π-basic dearomatization agents. The lessons learned through the early exploration of rhenium systems paved the way for the establishment of a ligand set which would not only provide a 2nd generation rhenium dearomatization agent, but would later be applied to group 6 molybdenum and tungsten systems as well.

1.6 Tp Motif and a 2nd Generation Re – Dearomatization Agent: {TpRe(L)(CO)}

With the realization that a dearomatization agent must operate within stringent steric and electronic constraints, literature precedent was explored for inspiration. This literature search provided several examples centered on a Cp (cyclopentadienyl) motif.[24-38] However, given the requirement for an octahedral geometry, initial investigations in our lab substituted the isoelectronic Tp (hydridotris(pyrazolyl)borate) for the Cp ring. Tp has long been compared to Cp,[51-53] however, within the strict constraints for dearomatization agents Tp offered a better fit. While both ligands are similar in their donor ability, Tp has been known to more rigidly enforce the desired octahedral geometry, unlike Cp, which has been documented to ring slip, providing access to coordinatively unsaturated complexes.[51-56] Moreover, Tp complexes are less prone to oxidative additions, an important consideration given the highly reducing nature of the metal centers in question.[53, 55-58]

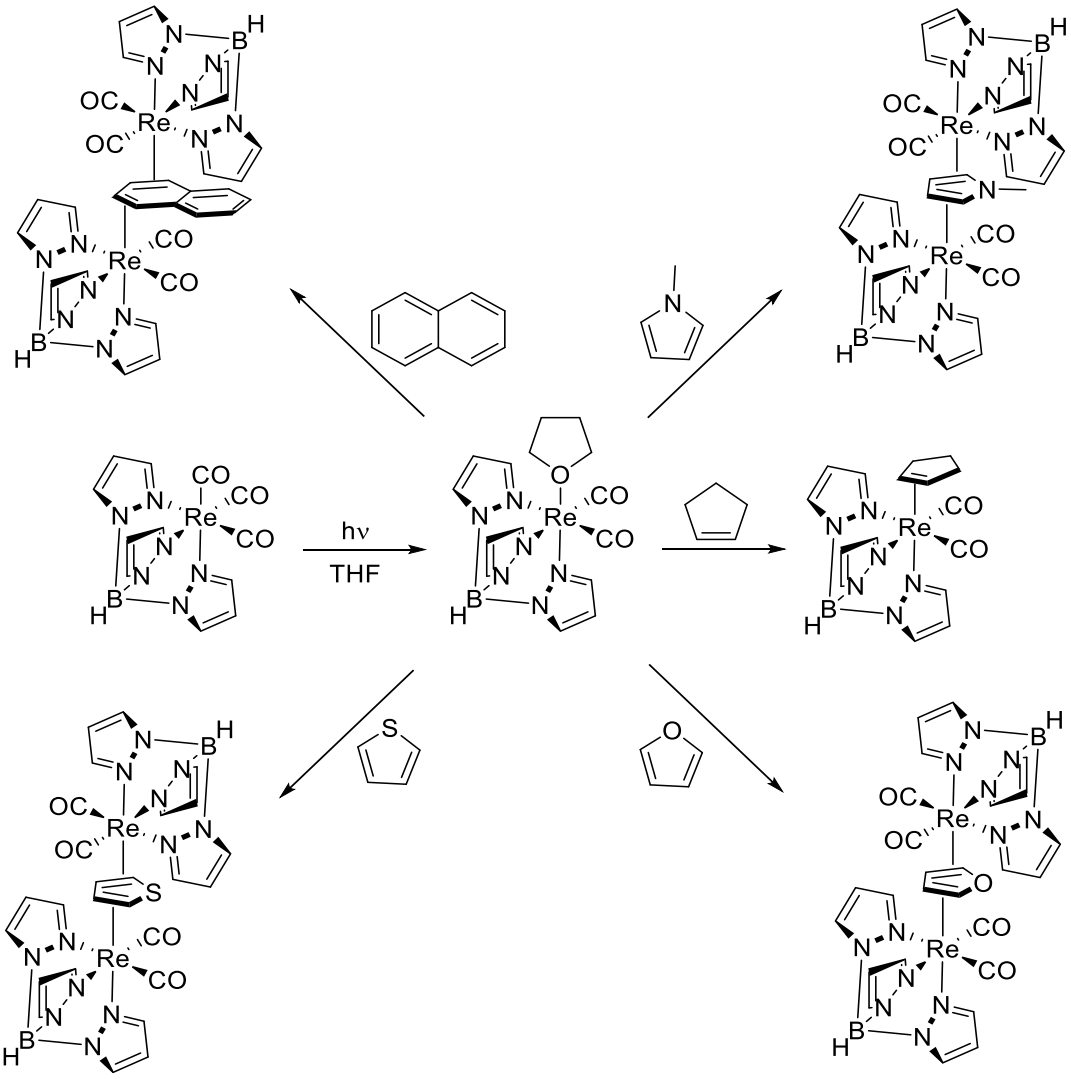

Scheme 5: Synthesis of η^2-alkene and μ^2-η^2-aromatic complexes from $TpRe(CO)_2(THF)$.

With a Tp foundation in place, the rest of the ligand set was considered. Initially the achiral $\{TpRe(CO)_2\}$ fragment was explored due to the relative synthetic ease to access the complex, and its similarity to previous CpRe – η^2-aromatic complexes.[59-60] This initial complex proved less electron-rich than the osmium system, yet was able to access dihapto-coordination with a range of ligands. Dihapto-aromatic complexes were also isolated, although only in a bridging fashion (Scheme 5). While these complexes are thermally stable, the bridging nature of aromatic coordination offers little ability to functionalize the ligand, due to the imposing sterics of the two metal complexes, each blocking off one face of the coordinated aromatic.[60]

Given the inability to form mononuclear η^2-aromatic species with the {TpRe(CO)$_2$} fragment, a variety of {TpRe(L)(CO)} fragments were proposed in which one CO was replaced with a more donating ligand.[61-62] The resulting complexes increased electron density to the range of {Os(NH$_3$)$_5$}$^{2+}$ and *fac*-{Re(dien)(PPh$_3$)(L)} fragments, and reestablished chirality at the rhenium center. Several synthetic routes were developed to access these rhenium dihapto-complexes. The synthetic flexibility illustrated in Scheme 6 allowed for the incorporation of a range of ancillary ligands to probe the impact of sterics and electronics within the {TpRe(L)(CO)} framework (Table 2). Initial attempts were made with nitrile, phosphine, and pyridine based ancillary ligands (L) (entries 1 – 10, Table 2), which provided good electronic agreement with the previous osmium system (18-22, Table 2).[63-64] However, despite the close electronic match to the {Os(NH$_3$)$_5$}$^{2+}$ fragment, these complexes provided a limited scope of aromatic coordination, likely due to increased sterics exhibited by the rhenium ligand set. [61, 63]

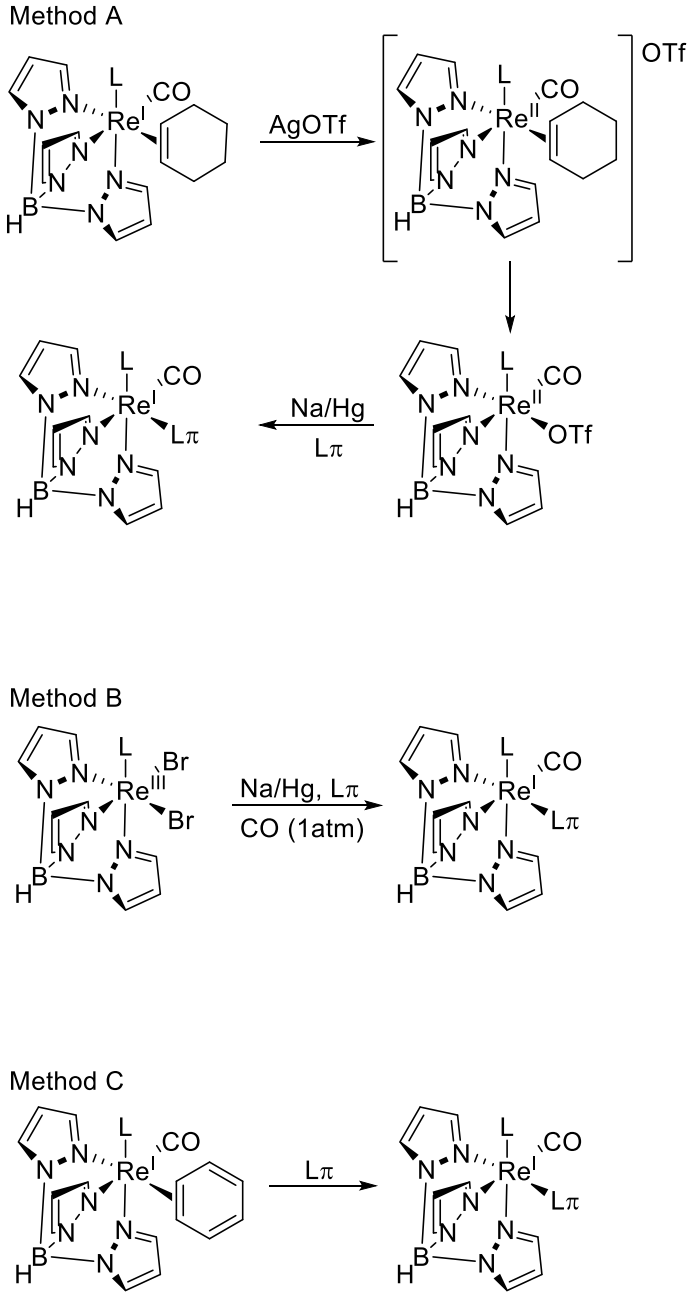

Scheme 6: Synthetic pathways to TpRe(L)(CO)(L_π) complexes.

Entry	Re Complexes	d^5/d^6 Reduction Potential (V)	ν_{CO} (cm^{-1})
1	TpRe(*t*-BuNC)(CO)(η^2-cyclohexene)	0.45	1826
2	TpRe(*t*-BuNC)(CO)(η^2-naphthalene)	0.47	1847
3	TpRe(*t*-BuNC)(CO)(η^2-furan)[a]	0.47	1846
4	TpRe(*t*-BuNC)(CO)(η^2-thiophene)	0.55	1831
5	TpRe(PMe_3)(CO)(η^2-cyclohexene)	0.23	1796
6	TpRe(PMe_3)(CO)(η^2-naphthalene)	0.19	1825
7	TpRe(PMe_3)(CO)(η^2-furan)[a]	0.30	1826
8	TpRe(py)(CO)(η^2-cyclohexene)	0.11	1783
9	TpRe(py)(CO)(η^2-naphthalene)	0.20	1812
10	TpRe(py)(CO)(η^2-furan)[a]	0.16	1810
11	TpRe(NH_3)(CO)(η^2-cyclopentene)	0.00	1776
12	TpRe(NH_3)(CO)(η^2-naphthalene)	0.02	1796
13	TpRe(MeIm)(CO)(η^2-cyclohexene)	-0.05	1775
14	TpRe(MeIm)(CO)(η^2-naphthalene)	0.02	1803
15	TpRe(MeIm)(CO)(η^2-furan)[a]	-0.02	1798
16	TpRe(MeIm)(CO)(η^2-thiophene)[a]	-0.03	1804
17	TpRe(MeIm)(CO)(η^2-benzene)[a]	-0.16	1794
	Os Complexes		
18	$[Os(NH_3)_5(\eta^2$-cyclopentanone$)]^{2+}$, [a]	0.40	--
19	$[Os(NH_3)_5(\eta^2$-naphthalene$)]^{2+}$, [a]	0.41	--
20	$[Os(NH_3)_5(\eta^2$-2-furan$)]^{2+}$, [a]	0.67	--
21	$[Os(NH_3)_5(\eta^2$-thiophene$)]^{2+}$, [a]	0.55	--
22	$[Os(NH_3)_5(\eta^2$-benzene$)]^{2+}$, [a]	0.15	--

Table 2: Modulation of electron density within TpRe(L)(CO)(L_π) complexes by changes to the ancillary ligand. Comparison of d^5/d^6 reduction potentials to $[Os(NH_3)_5(L_\pi)$. (a = potential reported for $E_{p,a}$).

In order to overcome the increased sterics of the Tp – based motif, more-donating ligands were explored. The syntheses of complexes incorporating thiazole, pyrazole, imidazole, and amine based ancillary ligands provided access to more electron-rich rhenium complexes (11-17, Table 2). The increased electron density with the incorporation of strong σ-donor ancillary ligands is also demonstrated by comparing ν_{CO} of entries 1-10 with 11-17 in Table 2. However, despite the increased electron density of the complexes, only the complex employing MeIm reproduced the

coordination scope of the 1st generation osmium system (Scheme 7); which was achieved by exchange of the weakly coordinating benzene ligand (Method C, Scheme 6).[63, 65]

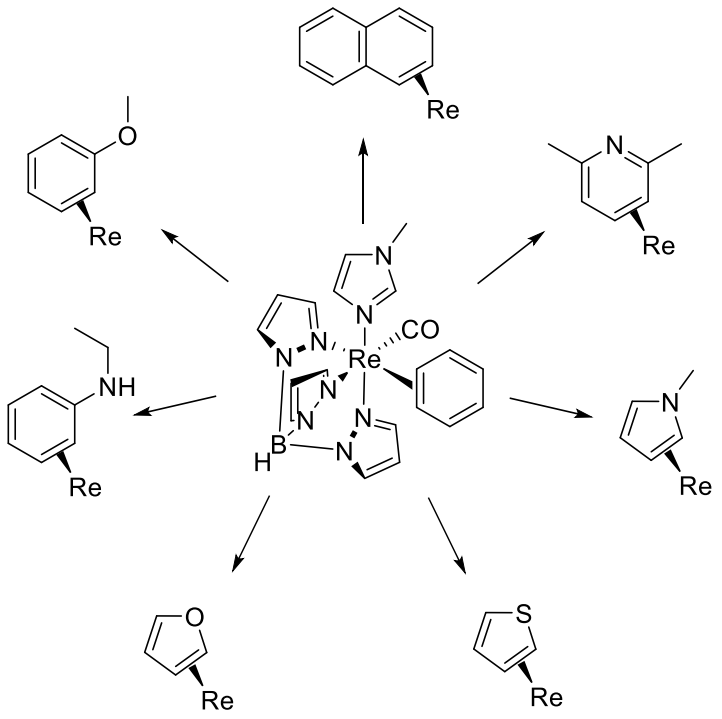

Scheme 7: Substitution of TpRe(MeIm)(CO)(η^2-benzene) for various aromatic ligands.

The scope of η^2-aromatic coordination established {TpRe(MeIm)(CO)} as a viable successor to $\{Os(NH_3)_5\}^{2+}$, providing a more cost effective and activating chiral dearomatization agent. Moreover, the ability to modulate the electronic and steric characteristics of the rhenium metal center by changes to the ancillary ligand and still afford η^2-aromatic complexes provides greater versatility than $\{Os(NH_3)_5\}^{2+}$.[1, 65] Despite the limited coordination scope of {TpRe(L)(CO)} fragments compared to $\{Os(NH_3)_5\}^{2+}$ and {TpRe(MeIm)(CO)}, the ability to modulate the chemical environment within a given aromatic ligand (*e.g.*, naphthalene, furan) with changes to L ({TpRe(L)(CO}) allows possible access to range of reactivity for each aromatic ligand.

1.7 Design of a 3rd Generation Dearomatization Agent: {TpM(L)(NO)} (M = Mo or W)

Despite the many improvements offered within the 2nd generation {TpRe(MeIm)(CO)} dearomatization agent, a variety of synthetic limitations remained. While the rhenium system was significantly less expensive (~1/12) than the 1st generation osmium complex that it replaced, given its stoichiometric use it was still cost prohibitive as a general synthetic method. Moreover, the {TpRe(MeIm)(CO)} fragment posed synthetic challenges, which made it difficult to synthesize on a large scale.[2, 7, 66-67] Given these disadvantages, earth abundant group 6 molybdenum and tungsten systems were proposed.

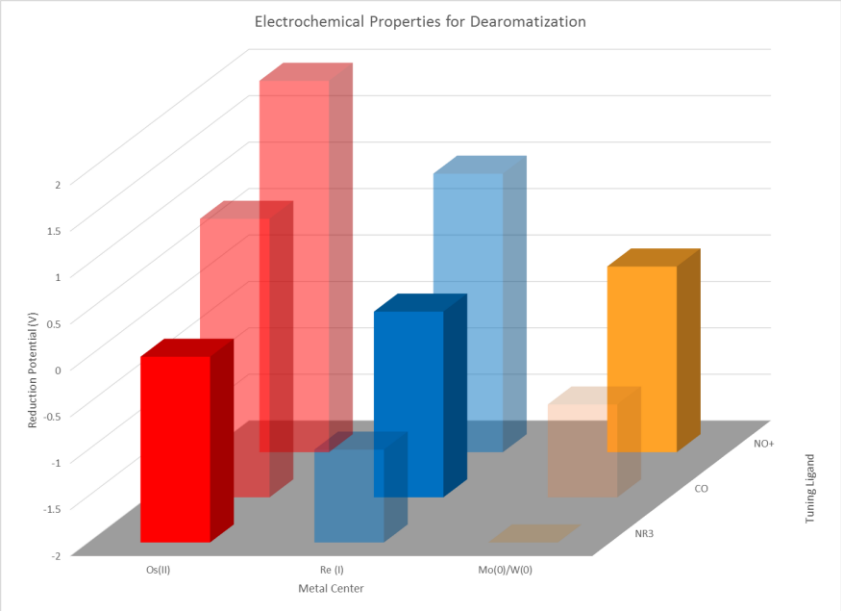

Figure 3: The electrochemical properties for {M(σ-donor)$_4$L} complexes for Os^{II}, Re^{I}, Mo^{0}, and W^{0} dearomatization agents.

Unlike the difficulties that were inherent in the development of the 2nd generation rhenium dearomatization agent, 3rd generation group 6 dearomatization agents could be built upon the foundation laid by the rhenium ligand set ({TpM(L)(CO)}). However, looking back on the knowledge gained during early rhenium development, group 6 metals with a (0) oxidation state would be inherently more electron-rich than Re^{I} complexes, and therefore require substitution of

CO for a stronger π-acid. The change in oxidation state of the dearomatization agents resulted in ~1 V shift in their reduction potentials, as shown in Figure 3.[2, 7, 66-69] With this in mind NO^+ was proposed as a replacement for CO, as its formal positive charge results in greater withdrawal of electron density. Changes to electron density are illustrated by comparing d^5/d^6 reduction potentials of the classical group 6 scorpionate complexes $[TpM(CO)_3]^-$ and $TpM(NO)(CO)_2$ (M = Mo or W), previously reported by Trofimenko and McCleverty, respectively, with that of the $TpRe(MeIm)(CO)(\eta^2\text{-arene})$ precursor $TpRe(MeIm)(CO)_2$ (Figure 4).[64, 70-71] These data showed that group 6 analogs of the initially investigated $\{TpRe(CO)_2\}$ fragment would likely prove to be too reducing. Incorporation of a NO^+ ligand would require a stronger σ-donor than CO, but would provide a better match for the electronic characteristics exhibited by the 2nd generation {TpRe(MeIm)(CO)} fragment.

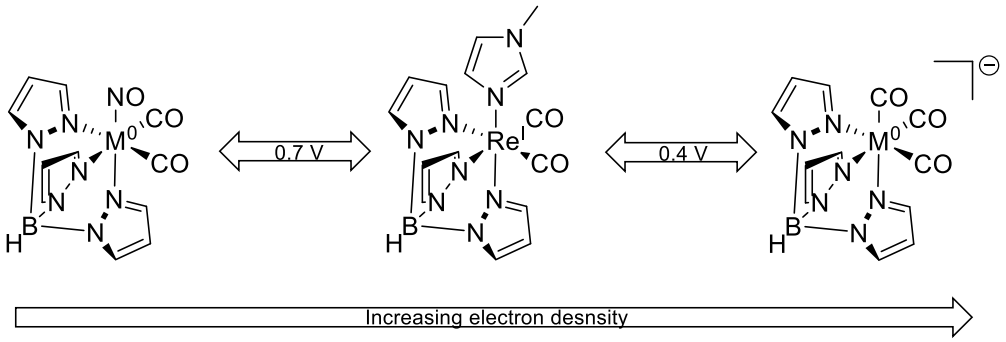

Figure 4: Design of group 6 Mo^0 and W^0 dearomatization complexes compared to 2nd generation Re^I (M= Mo or W).

1.8 Synthesis of a 3rd Generation Dearomatization Agent: {TpMo(MeIm)(NO)}

With a synthetic target in place, the inexpensive and commercially available $Mo^0(CO)_6$ was used as a starting material, from which $TpMo(NO)(CO)_2$ is easily accessed using established procedures in a large scale with high yields.[70] From here was the difficult task of replacing a CO from a relatively electron rich metal center with a (0) oxidation state. In order to overcome this strong metal-ligand bond, oxidation to Mo^{II} was explored by treatment of the $TpMo^0(NO)(CO)_2$

with a halogen (Br_2 or I_2) to afford $TpMo^{II}(NO)(X)_2$, as reported by McCleverty (Method A, Scheme 8).[70] The resulting Mo^{II} species could then be reduced in the presence of the desired ancillary ligand (L) to yield $TpMo^{I}(NO)(L)(X)$, the precursor to the proposed η^2-aromatic species.[7, 66, 68] An alternative to the introduction of the ancillary ligand by redox reaction is the thermolysis of $TpMo^{0}(NO)(CO)_2$ in the presence of the desired ligand to produce $TpMo^{0}(NO)(L)(CO)$ (Method B, Scheme 8). From here the desired $TpMo^{I}(NO)(L)(X)$ precursor could be generated by oxidation with a halogen (Br_2 or I_2).[7-8, 66] Within this framework a variety of ancillary ligands were investigated, and the electron density of the resulting complexes were analyzed by IR and CV (Table 3). These complexes gave a similar electronic profile to the {TpRe(MeIm)(CO)} fragment, and with a nearly identical steric profile offered the potential to provide a 2nd row dearomatization agent.[63, 66, 68, 72]

The coordination of the aromatic ligand is achieved in a manner similar to that of the 2nd generation rhenium system (Method A, Scheme 6), by reduction in the presence of the desired ligand (Scheme 8).[7, 66, 68] In some cases these η^2-aromatic complexes are also available via a one-pot reaction from $TpMo(NO)(X)_2$, when L is amendable to the highly reducing reaction conditions required (Method C, Scheme 8).[66] However, despite the range of $TpMo^{I}(NO)(L)(X)$ complexes synthesized, and their more reducing nature than the {TpRe(MeIm)(CO)} fragment (Table 3); the molybdenum based dearomatization agent was found to have a limited coordination scope (naphthalene, furan, and thiophene).[7, 66, 68, 72] This result is likely due to the less effective backbonding ability of the 2nd row molybdenum center compared to the 3rd row osmium and rhenium forerunners.

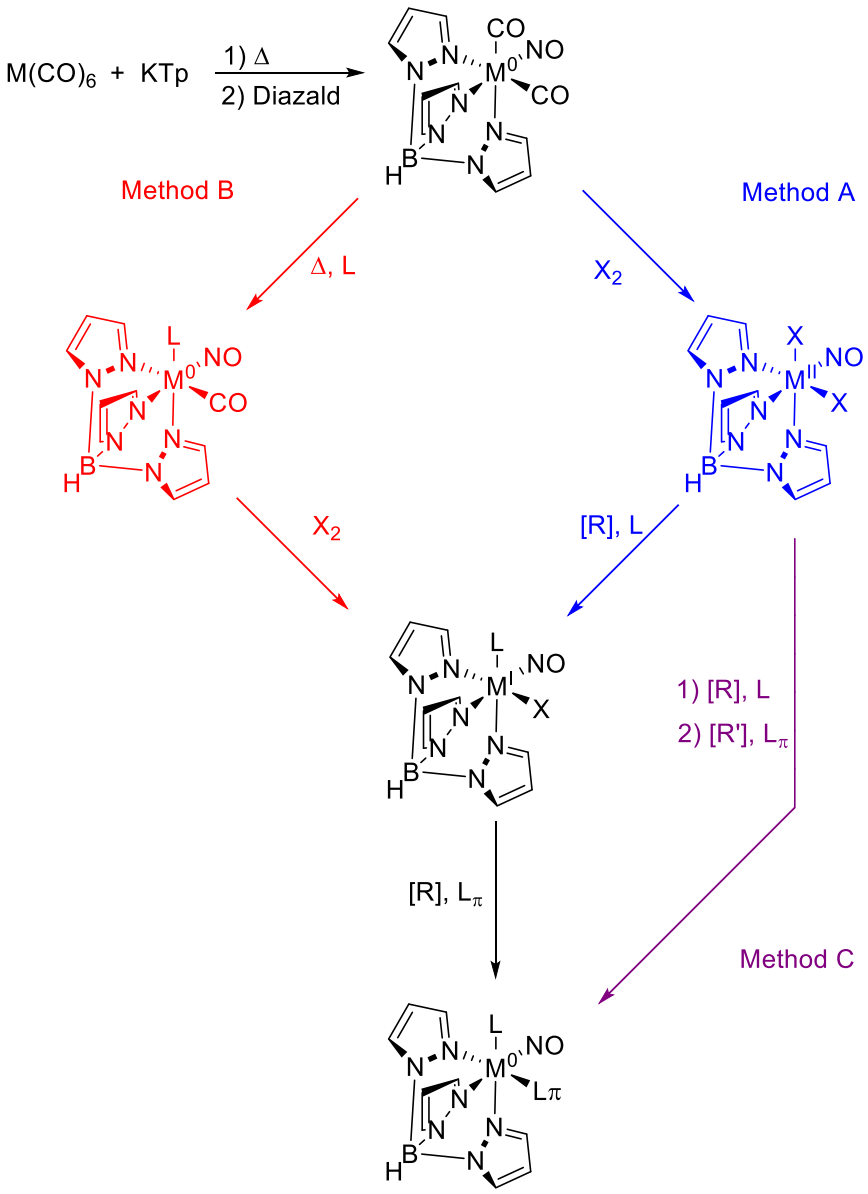

Scheme 8: Synthetic pathways for group 6 TpM(L)(NO)(L_π) dearomatization agents (M = Mo or W).

Entry	Mo Complexes	d^5/d^6 Reduction Potential (V)	ν_{NO} (cm^{-1})	% Yield
1	TpMo(MeIm)(NO)(CO)[a]	0.22	1583	60
2	TpMo(NH_3)(NO)(Br)[a]	-1.69	1593	72
3	TpMo(4-pic)(NO)(Br)	-1.42	1605	89
4	TpMo(*t*-BuNC)(NO)(Br)	-1.23	1618	45
5	TpMo(PMe_3)(NO)(Br)	-1.19	1617	76
6	TpMo(MeIm)(NO)(Br)	-1.33	1610	72
7	TpMo(DMAP)(NO)(Br)	-1.53	1613	61
	Mo - η^2-arene Complexes			
8	TpMo(NH_3)(NO)(η^2-naphthalene)[a]	-0.23	1556	15
9	TpMo(NH_3)(NO)(η^2-furan)[a]	-0.38	1560	10
10	TpMo(MeIm)(NO)(η^2-naphthalene)[a]	-0.18	1579	60
11	TpMo(MeIm)(NO)(η^2-anthracene)[a]	-0.11	1583	62
12	TpMo(MeIm)(NO)(η^2-furan)[a]	-0.36	1571	45
13	TpMo(MeIm)(NO)(η^2-thiophene)[a]	-0.33	1574	60
14	TpMo(DMAP)(NO)(η^2-naphthalene)[a]	-0.16	1580	45
	W Complexes			
15	TpW(py)(NO)(Br)	-1.31	1567	36
16	TpW(nic)(NO)(Br)	-1.35	1572	10
17	TpW(*t*-BuNC)(NO)(Br)	-0.71	1600	30
18	TpW($P(OMe)_3$)(NO)(Br)	-1.04	1597	78
19	TpW(PMe_3)(NO)(Br)	-1.38	1578	67
20	TpW(PEt_3)(NO)(Br)	-1.40	1578	58
21	TpW(MeIm)(NO)(Br)	-1.55	1563	--
22	TpW(DMAP)(NO)(Br)	-1.36	1567	1
	W - η^2-arene Complexes			
23	TpW($P(OMe)_3$)(NO)(η^2-naphthalene)[a]	0.23	1585	38
24	TpW($P(OMe)_3$)(NO)(η^2-furan)[a]	0.20	1569	47
25	TpW(PMe_3)(NO)(η^2-naphthalene)[a]	0.11	1569	26
26	TpW(PMe_3)(NO)(η^2-furan)[a]	0.03	1561	26
27	TpW(PMe_3)(NO)(η^2-thiophene)[a]	0.05	1564	31
28	TpW(PMe_3)(NO)(η^2-benzene)[a]	-0.13	1564	38

Table 3: IR and electrochemical data for group 6 {TpM(L)(NO)} complexes (M = Mo or W).

1.9 Synthesis of a 3rd Generation Dearomatization Agent: {TpW(PMe$_3$)(NO)}

With the ineffective backbonding of molybdenum based dearomatization agents, a 3rd row tungsten alternative was explored. Synthesis of the tungsten complexes followed Scheme 8, as described for molybdenum. However, due to the increased electron density and backbonding ability of the tungsten system, introduction of the ancillary ligand via thermolysis (Method B, Scheme 8) proved inaccessible.[66] Moreover, reduction of the previously reported TpW^{II}(NO)(X)$_2$ (X = Br or I) species gave disproportionation and low yields for a variety of the ligands successfully incorporated into rhenium and molybdenum complexes (Table 3).[2, 66] Within the scope of synthetically viable ancillary ligands, {TpW^{I}(L)(NO)} species were less electron-rich than their molybdenum and rhenium analogs (Table 3).

{TpW^0(PMe$_3$)(NO)} is able to coordinate the full complement of ligands accessed by the 1st and 2nd generation osmium and rhenium dearomatization agents. Continued investigation of the 3rd generation tungsten dearomatization agent showed it to be *more* activating than its chemical ancestors, despite its less reducing potential.[2, 73] This is likely due to the low (0) oxidation state in comparison to Os^{II} and Re^{I}, and also its more effective backdonation than the 2nd row Mo^0 fragment.

The synthetic power of {TpW(PMe$_3$)(NO)} was demonstrated by its increased coordination scope, as illustrated in Scheme 9.[2, 9-14, 66-67, 69, 72-83] Within the increased scope of coordination offered by the tungsten system is access to a variety of aromatic ligands with biologically interesting cores. Chief among these is pyridine, which offers access to the piperidine, indolizidine, and quinolizidine cores frequently found in natural products.[9-11, 14, 80] Moreover, the ability of the tungsten dearomatization agent to directly coordinate indolines and quinolines as their cationic salts allows for facile functionalization of these biologically important cores.[10-11, 80]

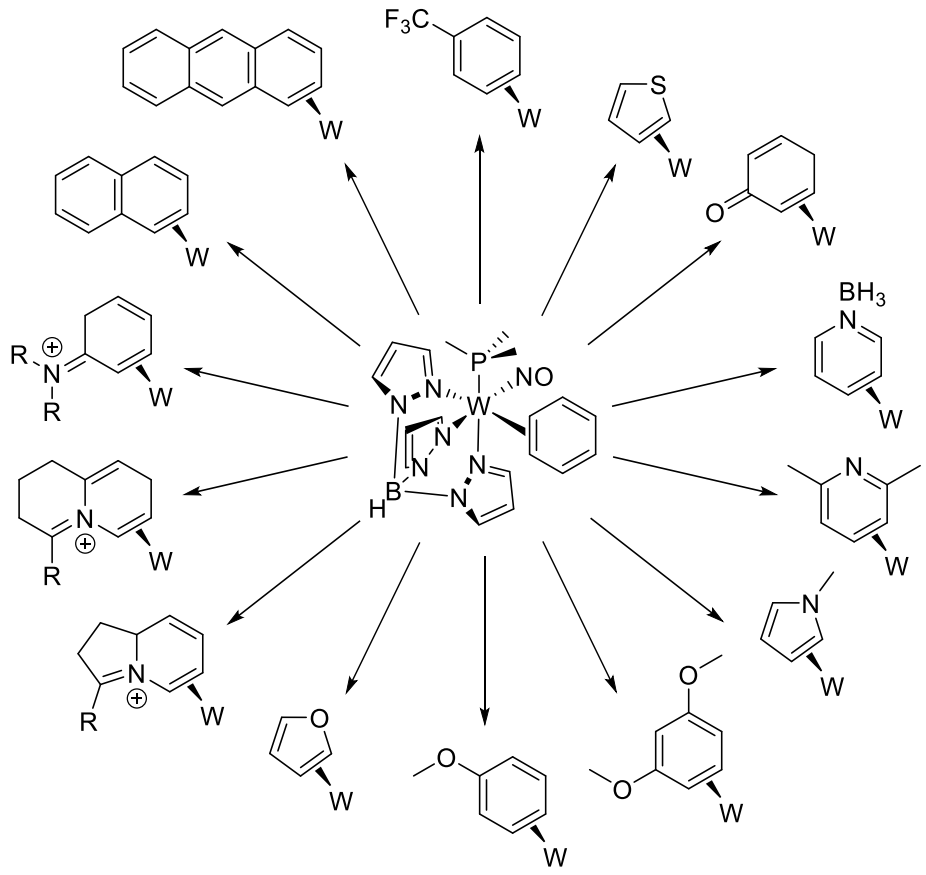

Scheme 9: Aromatic coordination scope of {TpW(PMe_3)(NO)}.

Despite the remarkable success of the tungsten dearomatization agent, the system has its own limitations. Chief among these are the harsh conditions required for liberation of the novel organic products. Due to the highly donating nature of the tungsten system, liberation of the organic product following synthetic transformations to the initial aromatic ligand requires a strong oxidant. These highly oxidizing conditions can result in decomposition of the liberated organic products, and often results in low yields for the isolation step.[10-11, 13, 80-81] Another limitation is the relatively low stability of the resulting W^{I} species, which is prone to undergoing a second oxidation.[2, 8, 66] This low oxidative stability results in an irrecoverable metal, whereas the previous Os^{III} and Re^{II} systems offered recyclable d^5 complexes (*vide supra*).

1.10 Conclusion

The $\{Os(NH_3)_5\}^{2+}$ system established the synthetic utility of π-basic dearomatization chemistry. The unique, thermally stable η^2-aromatic complexes allowed access to novel reactivity, with stereo- and regiochemistry dictated by the metal center, affording facile access to new chemical space from aromatic starting materials.

The development of a more widely applicable 2nd generation dearomatization agent was made by investigation of a replacement Re^{I} species. These endeavors demonstrated the strict steric and electronic requirements which must be met for π-basic dearomatization agents. This work culminated in development of the chiral {TpM(L)(π-acid)} ligand motif that has become the foundation of 2nd and 3rd generation dearomatization agents. The rhenium system {TpRe(MeIm)(CO)} exhibited increased reactivity compared to the initial, less reducing, $\{Os(NH_3)_5\}^{2+}$. However, the cost and synthetic difficulties associated with rhenium dearomatization resulted in the development of 3rd generation group 6 dearomatization agents.

The initial group 6 dearomatization agent {TpMo(MeIm)(NO)}, while more reducing than its osmium and rhenium predecessors, was also less activating, and provided a limited scope of η^2-aromatic coordination. The development of the 3rd row $\{TpW(PMe_3)(NO)\}$ system resulted in the greatest activation of all dearomatization agents to date. The powerful backdonation capabilities of the tungsten system has resulted in an increased coordination scope, and access to biologically interesting ligands through unprecedented reactivity. However, despite the dramatic success of the $\{TpW(PMe_3)(NO)\}$ fragment, the harsh oxidative conditions required to liberate η^2-ligands, and the inability to recycle the tungsten metal center has led to reopening the investigation into a 2nd row molybdenum based dearomatization agent.

1.11 References

1. Brooks, B. C.; Brent Gunnoe, T.; Dean Harman, W. *Coord. Chem. Rev.* **2000,** *206*, 3-61.

2. Keane, J. M.; Harman, W. D. *Organometallics* **2005,** *24*, 1786-1798.

3. Pape, A. R.; Kaliappan, K. P.; Kündig, E. P. *Chem. Rev.* **2000,** *100*, 2917-2940.

4. Ding, F.; Harman, W. D. *J. Am. Chem. Soc.* **2004,** *126*, 13752-13756.

5. Harman, W. D. *Chem. Rev.* **1997,** *97*, 1953-1978.

6. Solomons, T. W. G.; Fryhle, C.; Snyder, S., *Organic Chemistry, 11th Edition*. 2012.

7. Meiere, S. H.; Keane, J. M.; Gunnoe, T. B.; Sabat, M.; Harman, W. D. *J. Am. Chem. Soc.* **2003,** *125*, 2024-2025.

8. Myers, J. T.; Shivokevich, P. J.; Pienkos, J. A.; Sabat, M.; Myers, W. H.; Harman, W. D. *Organometallics* **2015,** *34*, 3648-3657.

9. Harrison, D. P.; Zottig, V. E.; Kosturko, G. W.; Welch, K. D.; Sabat, M.; Myers, W. H.; Harman, W. D. *Organometallics* **2009,** *28*, 5682-5690.

10. MacLeod, B. L.; Pienkos, J. A.; Wilson, K. B.; Sabat, M.; Myers, W. H.; Harman, W. D. *Organometallics* **2016,** *35*, 370-387.

11. Pienkos, J. A.; Knisely, A. T.; MacLeod, B. L.; Myers, J. T.; Shivokevich, P. J.; Teran, V.; Sabat, M.; Myers, W. H.; Harman, W. D. *Organometallics* **2014,** *33*, 5464-5469.

12. Pienkos, J. A.; Zottig, V. E.; Iovan, D. A.; Li, M.; Harrison, D. P.; Sabat, M.; Salomon, R. J.; Strausberg, L.; Teran, V. A.; Myers, W. H.; Harman, W. D. *Organometallics* **2013,** *32*, 691-703.

13. Strausberg, L.; Li, M.; Harrison, D. P.; Myers, W. H.; Sabat, M.; Harman, W. D. *Organometallics* **2013,** *32*, 915-925.

14. Welch, K. D.; Harrison, D. P.; Sabat, M.; Hejazi, E. Z.; Parr, B. T.; Fanelli, M. G.; Gianfrancesco, N. A.; Nagra, D. S.; Myers, W. H.; Harman, W. D. *Organometallics* **2009,** *28*, 5960-5967.

15. Allen, A. D.; Senoff, C. V. *Chem. Commun.* **1965,** 621-622.

16. Allen, A. D.; Stevens, J. R. *Chem. Commun.* **1967,** 1147-1147.

17. Yu, G. B. k.; Aleksandr, E. S. *Russ. Chem. Rev.* **1969,** *38*, 355.

18. Harman, W. D.; Fairlie, D. P.; Taube, H. *J. Am. Chem. Soc.* **1986,** *108*, 8223-8227.

19. Harman, W. D.; Taube, H. *J. Am. Chem. Soc.* **1987,** *109*, 1883-1885.

20. Lay, P. A.; Magnuson, R. H.; Taube, H.; Sen, J. *J. Am. Chem. Soc.* **1982,** *104*, 7658-7659.

21. Lay, P. A.; Taube, H. *Inorg. Chem.* **1989,** *28*, 3561-3564.

22. Harman, W. D.; Sekine, M.; Taube, H. *J. Am. Chem. Soc.* **1988,** *110*, 5725-5731.

23. Harman, W. D.; Taube, H. *J. Am. Chem. Soc.* **1988,** *110*, 5403-5407.

24. Agbossou, S. K.; Bodner, G. S.; Patton, A. T.; Gladysz, J. A. *Organometallics* **1990,** *9*, 1184-1191.

25. Choi, M. G.; Angelici, R. J. *J. Am. Chem. Soc.* **1989,** *111*, 8753-8754.

26. Choi, M. G.; Angelici, R. J. *J. Am. Chem. Soc.* **1990,** *112*, 7811-7812.

27. Choi, M. G.; Angelici, R. J. *J. Am. Chem. Soc.* **1991,** *113*, 5651-5657.

28. Choi, M. G.; Angelici, R. J. *Organometallics* **1992,** *11*.

29. Jones, W. D.; Dong, L. *J. Am. Chem. Soc.* **1989,** *111*.

30. Jones, W. D.; Feher, F. J. *J. Am. Chem. Soc* **1984,** *106*, 1650-1663.

31. Jones, W. D.; Feher, F. J. *Acc. Chem. Res* **1989,** *22* (3), 91-100.

32. Kowalczyk, J. J.; Agbossou, S. K.; Gladysz, J. *J Organomet. Chem.* **1990,** *397*, 333-346.

33. Jones, W. D.; Feher, F. J. *J. Am. Chem. Soc* **1982,** *104* (15), 4240-4242.

34. Sweet, J. R.; Graham, W. A. G. *J. Am. Chem. Soc.* **1983,** *105*, 305-306.

35. Sweet, J. R.; Graham, W. A. G. *Organometallics* **1983,** *2*, 135-140.

36. Sweigart, D.; Stone, N.; Rieger, P.; Mocellin, E.; Mann, T. *Organometallics* **1992,** *11,* 871-876.

37. Tagge, C. D.; Bergman, R. G. *J. Am. Chem. Soc.* **1996,** *118*, 6908-6915.

38. van der Heijden, H.; Orpen, A. G.; Pasman, P. *J. Chem. Soc. Chem. Comm.* **1985,** 1576-1578.

39. White, C. J.; Angelici, R. J.; Choi, M. *Organometallics* **1995,** *14*.

40. Barrera, J.; Orth, S. D.; Harman, W. D. *J. Am. Chem. Soc.* **1992,** *114*, 7316-7318.

41. Chordia, M. D.; Harman, W. D. *J. Am. Chem. Soc.* **1998,** *120*, 5637-5642.

42. Orth, S. D.; Barrera, J.; Sabat, M.; Harman, W. D. *Inorg. Chem.* **1993,** *32*, 594-601.

43. Gunnoe, T. B.; Meiere, S. H.; Sabat, M.; Harman, W. D. *Inorg. Chem.* **2000,** *39*, 6127-6130.

44. Helberg, L. E.; Barrera, J.; Sabat, M.; Harman, W. D. *Inorg. Chem.* **1995,** *34*, 2033-2041.

45. Helberg, L. E.; Gunnoe, T. B.; Brooks, B. C.; Sabat, M.; Harman, W. D. *Organometallics* **1999,** *18*, 573-581.

46. Helberg, L. E.; Orth, S. D.; Sabat, M.; Harman, W. D. *Inorg. Chem.* **1996,** *35*, 5584-5594.

47. Orth, S. D.; Barrera, J.; Sabat, M.; Harman, W. D. *Inorg. Chem.* **1994,** *33*, 3026-3027.

48. Brooks, B. C.; Chin, R. M.; Harman, W. D. *Organometallics* **1998,** *17*, 4716-4723.

49. Chin, R. M.; Barrera, J.; Dubois, R. H.; Helberg, L. E.; Sabat, M.; Bartucz, T. Y.; Lough, A. J.; Morris, R. H.; Harman, W. D. *Inorg. Chem.* **1997,** *36*, 3553-3558.

50. Spera, M. L.; Chin, R. M.; Winemiller, M. D.; Lopez, K. W.; Sabat, M.; Harman, W. D. *Organometallics* **1996,** *15*, 5447-5449.

51. Crabtree, R. H., *The organometallic chemistry of the transition metals*. John Wiley & Sons: 2009.

52. Tellers, D. M.; Skoog, S. J.; Bergman, R. G.; Gunnoe, T. B.; Harman, W. D. *Organometallics* **2000,** *19*, 2428-2432.

53. Bergman, R. G.; Cundari, T. R.; Gillespie, A. M.; Gunnoe, T. B.; Harman, W. D.; Klinckman, T. R.; Temple, M. D.; White, D. P. *Organometallics* **2003,** *22*, 2331-2337.

54. Curtis, M. D.; Shiu, K. B.; Butler, W. M. *J. Am. Chem. Soc.***1986,** *108* (7).

55. Gelabert, R.; Moreno, M.; Lluch, J. M.; Lledós, A. *Organometallics* **1997,** *16*, 3805-3814.

56. Trofimenko, S., *Scorpionates: the coordination chemistry of polypyrazolylborate ligands*. World Scientific: 1999.

57. Oldham, W. J.; Hinkle, A. S.; Heinekey, D. M. *J. Am. Chem. Soc.* **1997,** *119*, 11028-11036.

58. Wiley, J. S.; Oldham, W. J.; Heinekey, D. M. *Organometallics* **2000,** *19*, 1670-1676.

59. Angaroni, M.; Ardizzoia, G. A.; D'Alfonso, G.; La Monica, G.; Masciocchi, N.; Moret, M. *J. C. S. Dalton* **1990,** *6,* 1895-1900.

60. Gunnoe, T. B.; Sabat, M.; Harman, W. D. *J. Am. Chem. Soc.* **1998,** *120*, 8747-8754.

61. Gunnoe, T. B.; Sabat, M.; Harman, W. D. *J. Am. Chem. Soc.* **1999,** *121*, 6499-6500.

62. Gunnoe, T. B.; Sabat, M.; Harman, W. D. *Organometallics* **2000,** *19*, 728-740.

63. Meiere, S. H.; Brooks, B. C.; Gunnoe, T. B.; Carrig, E. H.; Sabat, M.; Harman, W. D. *Organometallics* **2001,** *20*, 3661-3671.

64. Meiere, S. H.; Dean Harman, W. *Encyclopedia of Reagents for Organic Synthesis*, John Wiley & Sons, Ltd: 2001.

65. Meiere, S. H.; Brooks, B. C.; Gunnoe, T. B.; Sabat, M.; Harman, W. D. *Organometallics* **2001,** *20*, 1038-1040.

66. Ha, Y.; Dilsky, S.; Graham, P. M.; Liu, W.; Reichart, T. M.; Sabat, M.; Keane, J. M.; Harman, W. D. *Organometallics* **2006,** *25*, 5184-5187.

67. Graham, P. M.; Meiere, S. H.; Sabat, M.; Harman, W. D. *Organometallics* **2003,** *22*, 4364-4366.

68. Mocella, C. J.; Delafuente, D. A.; Keane, J. M.; Warner, G. R.; Friedman, L. A.; Sabat, M.; Harman, W. D. *Organometallics* **2004,** *23*, 3772-3779.

69. Surendranath, Y.; Harman, W. D. *Dalton Trans.* **2006,** 33, 3957-3965.

70. McCleverty, J. A.; Seddon, D.; Bailey, N. A.; Joe' Walker, N. W. *J. C. S. Dalton* **1976,** 898-908.

71. Trofimenko, S. *J. Am. Chem. Soc.* **1969,** *91*, 588-595.

72. Harman, W. D.; Trindle, C. *Journal of Computational Chemistry* **2005,** *26* (2), 194-200.

73. Lis, E. C.; Delafuente, D. A.; Lin, Y.; Mocella, C. J.; Todd, M. A.; Liu, W.; Sabat, M.; Myers, W. H.; Harman, W. D. *Organometallics* **2006,** *25*, 5051-5058.

74. Delafuente, D. A.; Myers, W. H.; Sabat, M.; Harman, W. D. *Organometallics* **2005,** *24*, 1876-1885.

75. Graham, P. M.; Delafuente, D. A.; Liu, W.; Myers, W. H.; Sabat, M.; Harman, W. D. *J.Am. Chem. Soc.* **2005,** *127*, 10568-10572.

76. Graham, P. M.; Mocella, C. J.; Sabat, M.; Harman, W. D. *Organometallics* **2005,** *24*, 911-919.

77. Keane, J. M.; Chordia, M. D.; Mocella, C. J.; Sabat, M.; Trindle, C. O.; Harman, W. D. *J. Am. Chem. Soc.* **2004,** *126*, 6806-6815.

78. Lis, E. C.; Salomon, R. J.; Sabat, M.; Myers, W. H.; Harman, W. D. *J. Am. Chem. Soc.* **2008,** *130*, 12472-12476.

79. Liu, W.; Welch, K.; Trindle, C. O.; Sabat, M.; Myers, W. H.; Harman, W. D. *Organometallics* **2007,** *26*, 2589-2597.

80. MacLeod, B. L.; Pienkos, J. A.; Myers, J. T.; Sabat, M.; Myers, W. H.; Harman, W. D. *Organometallics* **2014,** *33*, 6286-6289.

81. Salomon, R. J.; Todd, M. A.; Sabat, M.; Myers, W. H.; Harman, W. D. *Organometallics* **2010,** *29*, 707-709.

82. Todd, M. A.; Sabat, M.; Myers, W. H.; Smith, T. M.; Harman, W. D. *J. Am. Chem. Soc.* **2008,** *130*, 6906-6907.

83. Welch, K. D.; Harrison, D. P.; Lis, E. C.; Liu, W.; Salomon, R. J.; Harman, W. D.; Myers, W. H. *Organometallics* **2007,** *26*, 2791-2794.

Chapter 2

Development of the Molybdenum Dearomatization Agent {TpMo(DMAP)(NO)}

2.1 Introduction

While a {TpMo(L)(NO)} fragment was initially explored as an alternative to the synthetic challenges which accompanied the 2nd generation {TpRe(MeIm)(CO)} dearomatization agent, it provided access to a limited coordination scope of aromatic ligands compared to previous 3rd row systems. Due to the synthetic power of the subsequently established {TpW(PMe_3)(NO)} dearomatization agent, which, like its osmium and rhenium based predecessors, could effect dihapto-coordination of benzene, work on molybdenum dearomatization was largely abandoned.[1-2] The 3rd generation tungsten system has provided access to a greater range of η^2-aromatic coordination, and resulting novel reactivity, than 1st and 2nd generation osmium and rhenium systems.[2-9] However, the backbonding proficiency of the tungsten complex results in synthetic challenges in the liberation of the organic ligand following functionalization of the previously aromatic core. Highly oxidative conditions are required to isolate the organic product, resulting in low yields and possible product decomposition.[6-8, 10-11] Moreover, these highly oxidative conditions result in over-oxidation of the tungsten fragment to an irrecoverable state.[11-12] In order to avoid the synthetic difficulties associated with the isolation of the organic products, as well as to explore the potential to access a new window of reactivity, investigation into a molybdenum based dearomatization agent was reopened.

2.2 Optimization of Mo – Dearomatization Synthesis: {TpMo(MeIm)(NO)}

The exploration of a molybdenum based dearomatization agent was initially focused on the most successful {TpMo(MeIm)(NO)} fragment, which displayed the greatest scope for η^2-aromatic coordination (naphthalene, furan, thiophene).[12-14] Synthesis of the dearomatization agent followed the synthetic scheme established during the initial investigation (Scheme 1).[12, 14] While initial reports employed displacement of a CO ligand of TpMo(NO)$(CO)_2$ by thermolysis in

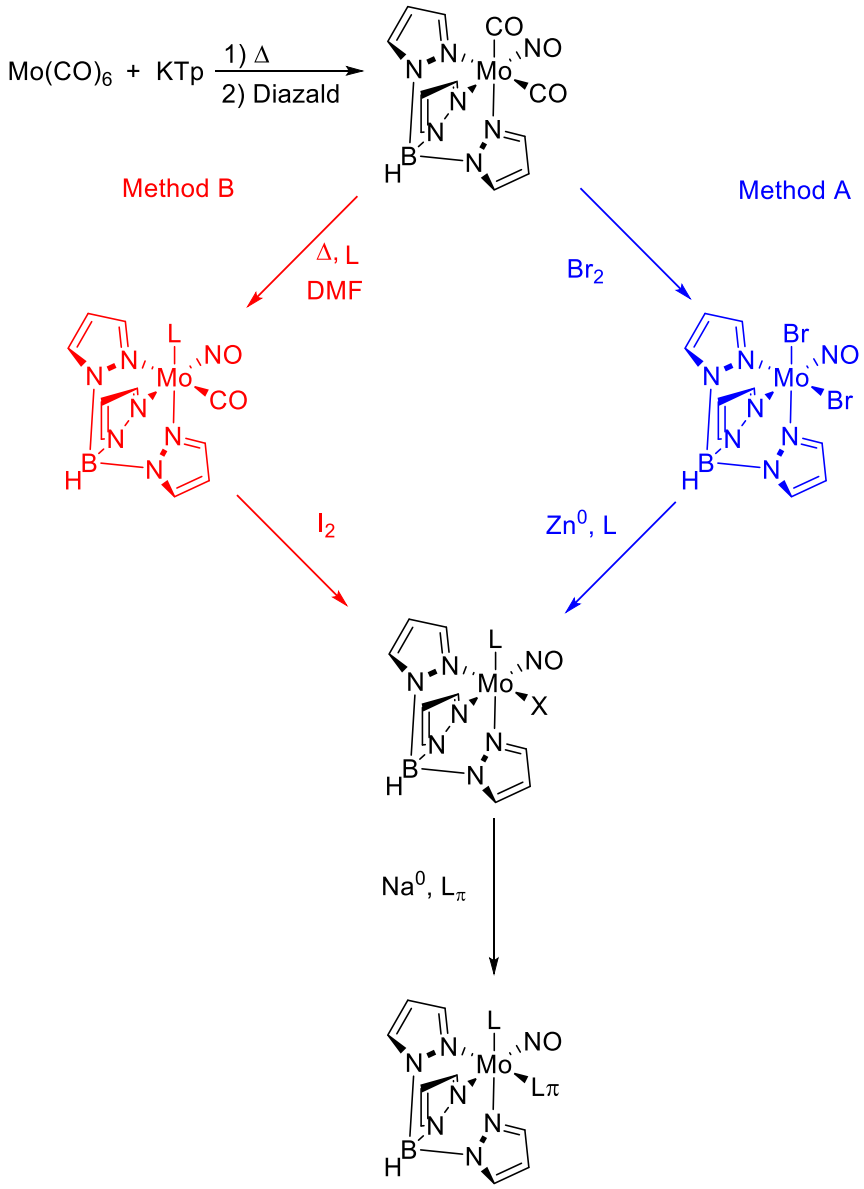

Scheme 1: Optimized pathways for the synthesis of a molybdenum dearomatization agent.

xylenes (Method B, Scheme 1), a variety of other solvents were explored by Jeff Myers as a means to reduce the 3 day time requirement, while also increasing yield and providing for a less laborious work-up. Within this work, the previous conditions which afforded the desired TpMo(MeIm)(NO)(CO) (**1**) in 3 days and 60 % yield, xylenes were replaced with DMF.[14] The solvent change increased the solubility of the starting material and provided higher reflux temperatures (138 vs 153 °C), reducing the reaction time to 5 h. Moreover, the change to DMF as the reaction

solvent allowed for water precipitation of **1**, eliminating the need for chromatography while simultaneously increasing the yield to 80%.[11] The product can then undergo oxidation by X_2 (Br_2 or I_2) to access the precursor to dihapto-coordination (TpMo(MeIm)(NO)(X) (X = Br^- (**2**) or I^- (**3**)), without the need for chromatography, and in near quantitative yield (Method B, Scheme 1).[11, 15]

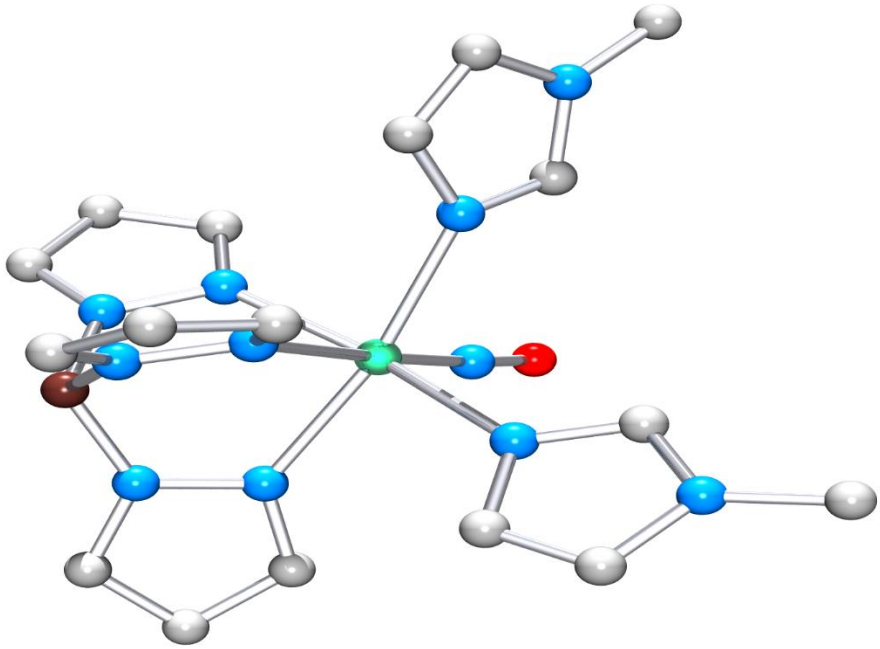

Figure 1: Crystal structure of $[TpMo(MeIm)_2(NO)]^+$.

The original synthetic pathway to the dearomatization precursor **2** was also explored. Within the context of the MeIm ligand, a variety of conditions were explored from the well-established $TpMo(NO)(Br)_2$ complex, reported by McCleverty in 1976 (Method A, Scheme 1).[16] The synthesis of **2** followed the procedure previously reported by Mocella et al.[14] However, when the solvent was changed from THF to DCM, as a means of increasing the solubility of the initial Mo^{II} complex, a new product was detected in the CV. The voltammagram showed the presence of two I/0 redox couples at -1.33 and -1.53 V, with the latter matching that of the reported product, as well as the products from the analogous reduction in THF and via Method B. We postulate that the more positive redox couple is due to the double displacement of Br^- for MeIm,

yielding $[TpMo(MeIm)_2(NO)]^+$, the presence of which was confirmed by a crystal structure isolated by Jeff Myers (Figure 1). Unfortunately, the high levels of disorder within the crystallographic data set prevented full analysis of the structure. Despite the presence of this side product, present in a 1 : 1 ratio with the desired product, the yield of subsequent reductions of **2** prepared from both DCM and THF is unchanged, suggesting that a MeIm ligand is easily displaced upon reduction to Mo^0.

2.3 Increasing the Scope of Ancillary Ligands, Synthesis of TpMo(L)(NO)(X)

Within the context of Method B, explored by Jeff Myers, the incorporation of two imidazole ligands is inaccessible due to the difficulty is displacing two CO ligands by thermolysis without reaching temperatures which favor decomposition of the metal center. *N*-Butylimidazole (BuIm) was pursued as a means to influence the solubility characteristics of the complex, providing increased solubility in nonpolar solvents. This proved to be a bit too successful, as the increased solubility demonstrated in TpMo(BuIm)(NO)(CO) (**4**) made isolation of subsequent complexes difficult, and as such BuIm complexes were not pursued past the synthesis of **4**. The incorporation of imidazole (Im) was also explored as a possible means to access NHC – type coordination. Table 1 compares the yield and electronic characteristics of the imidazole family of thermolysis products (**1**, **4**-**5**).

Jeff Myers also optimized the oxidation of the air stable thermolysis products **1** and **5**, affording the also air stable Mo^I – X products (**2**-**3**, **6**), allowing for preparation of dearomatization precursors outside of the glovebox.[15] While **1** was initially oxidized to **2** with Br_2, the I/0 reduction potential of **1** is sufficiently negative to undergo oxidation by the milder I_2 (0.54 vs 1.07 V). Due to this result I_2 was employed for the oxidation of molybdenum complexes accessed via Method B.[11, 15] A direct comparison of **2** and **3** illustrates the moderate increase in donor ability of Br^- compared to I^- (Table 1). However, this result has no impact on the ability of **2** and **3** to act as

dearomatization agents, as the halides are displaced upon reduction to the active {TpMo(MeIm)(NO)} fragment.

Complex	d^5/d^6 Reduction Potential (V)	ν_{NO} (cm^{-1})	% Yield
TpMo(MeIm)(NO)(CO) (**1**)	0.22	1583	60
TpMo(BuIm)(NO)(CO) (**4**)	0.18	1589	56
TpMo(Im)(NO)(CO) (**5**)	0.16	1585	54
TpMo(DMAP)(NO)(CO) (**22**)	0.27	1589	80
TpMo(nic)(NO)(CO) (**23**)	0.20	1593	78
TpMo(MeIm)(NO)(Br) (**2**)	-1.53	1610	80
TpMo(MeIm)(NO)(I) (**3**)	-1.47	1602	95
TpMo(Im)(NO)(Br) (**6**)	-1.66	--	99
TpMo(*t*-BuNC)(NO)(Br) (**7**)	-1.23	1618	45
TpMo(PMe_3)(NO)(Br) (**8**)	-1.19	1617	76
TpMo(NH_3)(NO)(Br) (**9**)	-1.69	1593	72
TpMo(npam)(NO)(Br) (**10**)	-1.62	1616	53
TpMo(aam)(NO)(Br) (**11**)	-1.60	1612	40
TpMo(pyr)(NO)(Br) (**12**)	-1.63	1585	56
TpMo(mor)(NO)(Br) (**13**)	-1.56	1601	61
TpMo(py)(NO)(Br) (**14**)	-1.23	a	a
TpMo(4-pic)(NO)(Br) (**15**)	-1.42	1605	89
TpMo(nic)(NO)(Br) (**16**)	-1.25	1631	38
TpMo(Fpy)(NO)(Br) (**17**)	-1.53	1616	24
TpMo(HOpy)(NO)(Br) (**18**)	-1.60	1601	92
TpMo(DMAP)(NO)(Br) (**19**)	-1.53	1613	81
TpMo(DMAP)(NO)(I) (**20**)	-1.43	1607	88
$[TpMo(CN)(NO)(Br)]^-$ (**21**)	-1.54	1608	89

Table 1: Electronic characteristics of a range of {TpMo(L)(NO)} complexes (a = complex observed *in situ*).

Expanding beyond imidazole based ancillary ligands, a variety of complexes were synthesized according to Method A (Scheme 1). Within the various resulting {TpMo(L)(NO)(Br)} systems (**7** – **21**), a 0.5 V range of I/0 reduction potentials were accessed (Table 1). Interestingly,

the production of the $[TpMo(L)_2(NO)]^+$ side product was only observed within the previously discussed MeIm system, and may be related of the propensity of $TpMo(NO)(Br)_2$ to disproportionate upon coordination of the relatively strong donation and small steric profile of the MeIm ligand.[14]

While several these complexes were unlikely to yield η^2-aromatic complexes, their Mo^I species provided important synthetic insight. Among these likely unsuccessful ancillary ligands was PMe_3 (**8**), whose relatively weak reducing nature is further hampered by its imposing steric profile. However, the inclusion of PMe_3 provided a means of comparing molybdenum donor capabilities (**8**, -1.19 V (Table 1)) to successful $TpRe(PMe_3)(CO)(OTf)$ (-0.65 V) and $TpW(PMe_3)(NO)(Br)$ (-1.33 V) dearomatization precursors. Within this context, we see that among the d^5 species incorporating PMe_3 as the ancillary ligand, the group 6 molybdenum and tungsten complexes are much more electron rich than the rhenium complex (> 0.5 V). These data are important in understanding the backbonding ability of the three metal systems. The most reducing $\{TpW(PMe_3)(NO)\}$ fragment is the most activating π-base yet explored, while the $\{TpRe(PMe_3)(CO)\}$ fragment is capable of only a limited coordination scope (*vide supra*). However, the $\{TpMo(PMe_3)(NO)\}$ fragment, which is nearly as reducing as the 3rd row tungsten fragment, is unable to coordinate the limited scope of the more electronegative $\{TpRe(PMe_3)(CO)\}$ center, or even to produce any dihapto-species to date. With these results in mind, a 2nd row dearomatization agent must work within tighter steric and electronic constraints than its heavy metal analogs to overcome its limited backdonation capabilities.

Similarly, the incorporation of a bulky 3° amine in the form of *N*-methylmorpholine (mor) seems an unlikely choice given the strict steric constraints required for dearomatization agents; although the synthesis of TpMo(mor)(NO)(Br) (**13**) allowed for characterization of NH_3, 1°, 2°, and 3° amines within the context of the Mo^I framework (**9** – **13**, Table 1). These data show that despite

the possible increase of donation from alkyl groups compared to that of H, the inverse effect is observed by CV with **9** being the most reducing and **13** being the least reducing. This may be explained by the increasing steric profile of the amine ligands, which cause lengthening of the Mo – N bond, and less donation to the metal center. However, the ν_{NO} shows no defining pattern, with the 2° amine complex **12** being the most donating, **9** and **13** equally donating, and the 1° amine complexes **10** and **11** the least donating.

The third major family of ancillary ligands explored were pyridines. Within this context TpMo(py)(NO)(Br) (**14**), TpMo(4-pic)(NO)(Br) (**15**), and TpMo(nic)(NO)(Br) (**16**) provided a similar electronic profile (Table 1). Among these complexes **16** was chosen for chiral resolution studies, discussed in greater detail in Chapter 3. The incorporation of an ERG at the 2- or 4-position of the pyridine ring produced complexes TpMo(Fpy)(NO)(Br) (**17**), TpMo(HOpy)(NO)(Br) (**18**), and TpMo(DMAP)(NO)(X) (X = Br^- (**19**) or I^- (**20**)) with a more reducing profile, comparable to that of the previously established imidazole family (**2**-**3**, **6** in Table 1). Among these ligands 4-fluoropyridine (Fpy) was of great interest, as it would provide a ^{19}F handle for resulting Mo^0 species. However, the synthesis of **17** was hampered by synthetic difficulties (24% yield).

Despite the range of TpMo(L)(NO)(Br) species produced, few proved effective as dearomatization agents. While **9**-**12** showed the ability to coordinate naphthalene, only **2**-**3**, **6**, **19**-**20**, and the less donating family of pyridines **14**-**16** were able to produce the desired dihapto-aromatic complexes in significant yield (> 25 %, Table 2). From this sub-set of ancillary ligands, the MeIm complex **3** was pursued due to the established success of the MeIm ligand within molybdenum and rhenium systems.[11-14, 17-18]

2.4 Synthesis and Optimization of TpMo(MeIm)(NO)(η^2-naphthalene)

Within the context of a MeIm ancillary ligand the reduction conditions of **2** and **3** to TpMo(MeIm)(NO)(η^2-naphthalene) (**24**) were explored in collaboration with Jeff Myers. These

initial studies began with the established reduction procedure for **24**, which employed Na/Hg amalgam as the reducing agent.[4-5, 12-14, 19] However, efforts to increase upon the reported 42% yield were unsuccessful. This result, in concert with the desire to avoid the environmental hazards of a reducing agent incorporating mercury, led to the investigation of Na^o as the reducing agent, similar to the established reduction procedures for tungsten dearomatization.[1-2, 9] These initial studies were hampered by the increased reducing power of Na^o compared to Na/Hg amalgam (-3.59 vs -2.91 V). The increased reactivity of the Na^o reducing agent quickly reduced naphthalene to sodium naphthalenide, which although a weaker reducing agent than Na^o (-2.81 vs -3.59 V), provides more facile electron transfer due to its homogeneous nature. As a result, **2** and **3** often underwent decomposition due to over-reduction within minutes. The over-reduction issue was eventually overcome by slowing the formation of sodium naphthalenide. This result was achieved through two strategies: reducing the molar equivalents of Na^o from 16.2 to 3.1, or by using Na-dispersion still immersed in its wax coating.[11] Both approaches limited the surface area of Na^o, producing a reduced concentration of the naphthalenide species.

2.5 The Synthetic Utility of Mo – Dearomatization: {TpMo(MeIm)(NO)}

The optimized reduction conditions for **24** were applied to TpMo(MeIm)(NO)(η^2-naphthalene) (**25**) by Jeff Myers, who transformed the aromatic cores into novel organic products. A variety of additions were performed on the polycyclic aromatic hydrocarbon (PAH) cores with the tandem addition of H^+, followed by a range of nucleophiles, to access a variety of novel hydro-naphthalene and anthracene products (Scheme 2).[11]

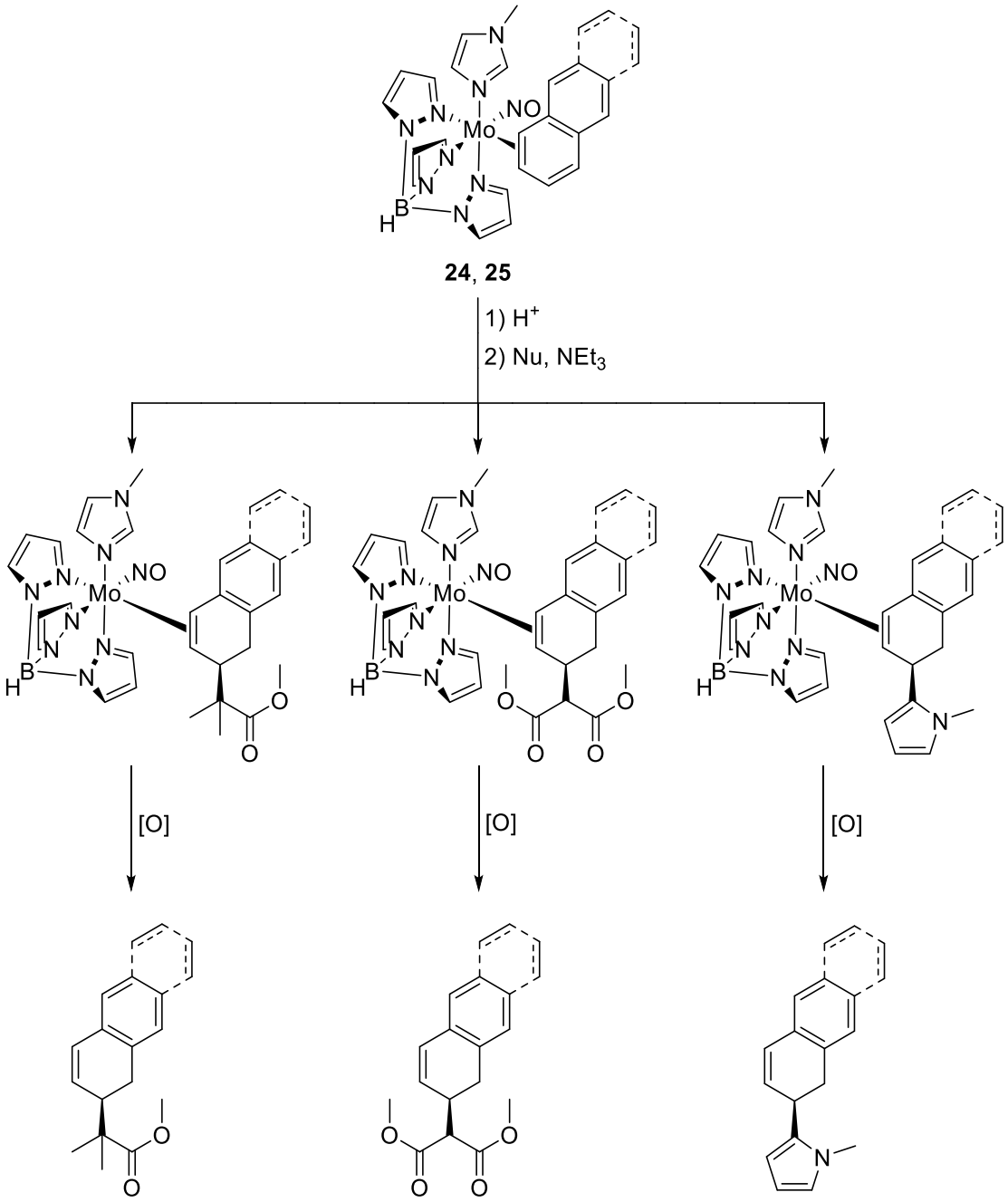

Scheme 2: Organic transformations to **24** and **25**, yielding novel organic products.

In addition to expanding the scope of synthetic transformations accessed via molybdenum dearomatization from the lone previous report, Jeff Myers also demonstrated the ability to recycle the {TpMo(MeIm)(NO)} dearomatization fragment.[11, 14] The ability to recycle the molybdenum fragment illustrates a synthetic advantage of the more reducing 2nd row metal in

comparison to the more activating 3rd row tungsten system. The lower reduction potentials of dihapto-molybdenum species than analogous dihapto-tungsten complexes allows for liberation of the dearomatized product from the metal center with a mild oxidant, such as I_2 (0.54 V).[11] Moreover, **3** provides a greater range of electrochemical stability than the analogous $TpW(PMe_3)(NO)(Br)$ complex. The electrochemical stability of **3** allows for the formation of the Mo^{I} species without over-oxidizing the resulting species to an irrecoverable state, as seen with the tungsten system (*vide supra*).[11] The combined effects of mild oxidizing conditions and the electrochemical stability of the molybdenum fragment allows for liberation of dearomatized products with I_2, regenerating **3**, the precursor to molybdenum – η^2-aromatic complexes (Scheme 3).

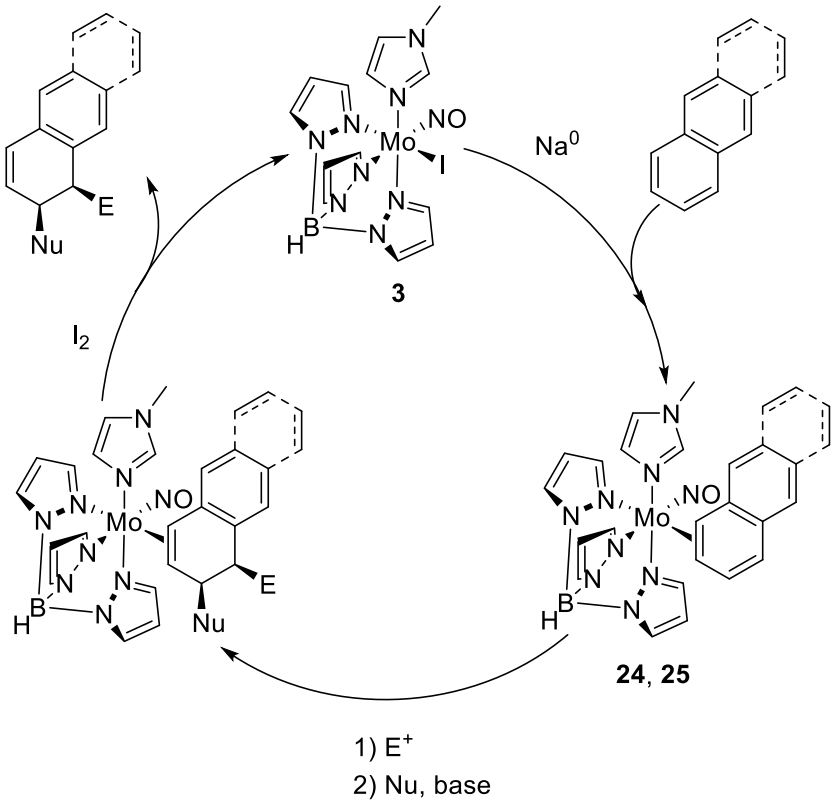

Scheme 3: Redox – based recycling of {TpMo(MeIm)(NO)}.

2.6 Molybdenum Dearomatization Tunability: TpMo(L)(NO)(η²-naphthalene)

The mild oxidizing conditions and development of molybdenum recyclability showed the first synthetic advantages of molybdenum dearomatization in comparison to the 3rd row tungsten system. We looked to further expand the utility of molybdenum dearomatization by demonstrating the adjustability of the ligand set, as seen with rhenium, to achieve differences in the reactivity of coordinated aromatic cores.[12, 17-18, 20-22] With this framework in mind DMAP was explored as an alternative to the previously reported MeIm system.

DMAP was chosen as an alternative ancillary ligand due to its similar electronics to the MeIm ligand set (**2**, **3** vs **19**, **20**, Table 1), while also providing a similar, although slightly larger, steric profile. Incorporation of the DMAP ancillary ligand also proved to be amenable to both synthetic pathways outlined in Scheme 1. **19** and **20** exhibited a similar difference in reduction potentials based on the donor ability of the X^- ligand, as seen with **2** and **3** (Table 1).

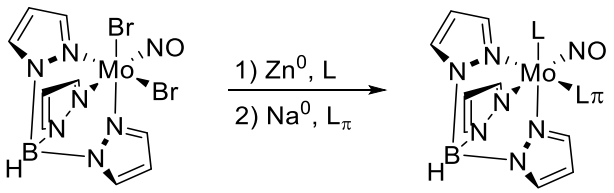

Scheme 4: One-pot synthesis of TpMo(L)(NO)(η²-arene) complexes.

TpMo(DMAP)(NO)(η²-naphthalene) (**26**) could also be accessed through a third synthetic pathway, a one pot double reduction in which **19** is created *in situ* (Scheme 4).[12] This synthetic pathway is applicable to a variety of pyridine derivatives for the isolation of dihapto-complexes (**26**, **28**-**30** in Table 2). The synthetic procedure outlined in Scheme 4 provided important advantages compared to the two-step pathways in Scheme 1, as there is no need to isolate the intermediate Mo^I species, allowing for quicker access to the desired molybdenum – η²-aromatic

complexes. Scheme 4 also allows for incorporation of ancillary ligands which are difficult to isolate through Scheme 1 (*e.g.*, nicotine complexes, which are discussed in greater detail in Chapter 3). Additionally, in the case of naphthalene and anthracene coordination, the one pot reduction of $TpMo(NO)(Br)_2$ produces conditions which inhibit decomposition by over-reduction of the metal complex.[12] This is likely due to the simultaneous presence of Na^o and Zn^o dust used for *in situ* formation of the active Mo^I species. The presence of the Zn^o dust inhibits the formation of the homogeneous sodium naphthalenide and anthracenide species by limiting the available surface area of the Na^o, similar to the steps required for reduction in Scheme 1.

Complex	d^5/d^6 Reduction Potential (V)	ν_{NO} (cm^{-1})	% Yield
TpMo(MeIm)(NO)(η^2-naphthalene) (**24**)	-0.25	1576	42
TpMo(MeIm)(NO)(η^2-anthracene) (**25**)	-0.11	1583	65
TpMo(DMAP)(NO)(η^2-naphthalene) (**26**)	-0.16	1580	50
TpMo(DMAP)(NO)(η^2-anthracene) (**27**)	-0.04	1585	47
TpMo(py)(NO)(η^2-naphthalene) (**28**)	-0.07	1585	24
TpMo(nic)(NO)(η^2-naphthalene) (**29**)	-0.09	1585	25
TpMo(3-pic)(NO)(η^2-naphthalene) (**30**)	-0.09	1577	26
TpMo(NH_3)(NO)(η^2-naphthalene) (**32**)	-0.23	1566	15
TpMo(pyr)(NO)(η^2-naphthalene) (**33**)	-0.25	1570	2

Table 2: Effects of the ancillary ligand on the electronic properties of TpMo(L)(NO)(η^2-arene) complexes (reported reduction potentials measured as $E_{p,a}$).

The dihapto-coordination of PAHs proved more difficult with the incorporation of amine ancillary ligands. While NH_3, 1^o, and 2^o amines meet the steric constraints for dihapto-coordination, the highly reducing nature of the {$TpMo^0$(amine)(NO)} fragments made isolation of the resulting naphthalene complexes difficult. While these ligands did provide access to molybdenum – η^2-naphthalene complexes via Method A (Scheme 1), only TpMo(NH_3)(NO)(η^2-naphthalene) (**32**) and TpMo(pyr)(NO)(η^2-naphthalene) (**33**) were isolated in low yields (Table 2). The synthetic difficulty of incorporating amine ancillary ligands was also seen in the context of

{TpRe(NH_3)(CO)}, which like the NH_3 and pyrrolidine molybdenum analogs are unstable due to the highly reducing nature of their d^6 complexes.[12, 14, 17, 23-25]

The molybdenum dearomatization agent has shown a similar ability to modulate the ancillary ligand as the rhenium system, resulting in the isolation of a variety of TpMo(L)(NO)(η^2-naphthalene) complexes with, a range of electronic characteristics (Table 2). The electronic characteristics of the η^2-naphthalene complexes mirrors the pattern seen at the Mo^{I} stage (Table 1). However, comparing the range of I/0 reduction potentials and ν_{NO} stretches for $TpMo^{I}$(L)(NO)(X) complexes (**2**-**3**, **6**, **9**, **12**, **14**, **16**, **19**-**20**, Table 1) with their reduced $TpMo^{0}$(L)(NO)(η^2-naphthalene) products (**24**, **26**, **28**-**33**, Table 2), we see the moderating effect of increased π-acidity (naphthalene vs X^-). The increased π-acidity helps to normalize the electronics across ancillary ligands, reducing the range of I/0 reduction potentials from 0.5 to 0.18 V and the range of ν_{NO} from 48 to 15 cm^{-1} (Tables 1 and 2). Despite the reduced differences in the electronics across $TpMo^{0}$(L)(NO)(η^2-naphthalene) complexes (**24**, **26**, **28**-**33**) compared to their Mo^{I} precursors, the different electronic characteristics within **24**, **26**, **28**-**33** may allow access to distinct reactivity patterns.

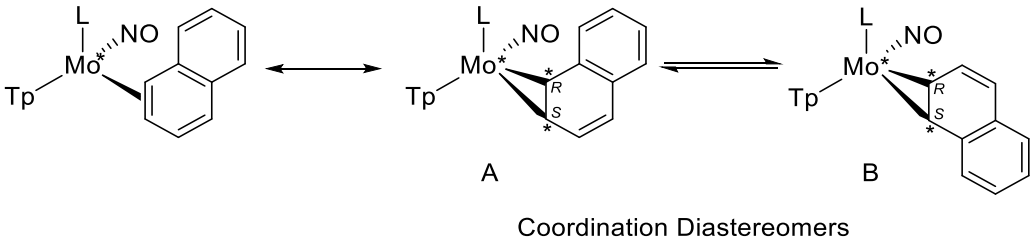

Figure 2: Coordination diastereomers formed by coordination of prochiral naphthalene to the chiral {TpMo*(L)(NO)}.

With an understanding of the range of electronics required for molybdenum dearomatization, we explored the effect of sterics among TpMo(L)(NO)(η^2-naphthalene) complexes (**24**, **26**, **28**-**33**), and the impact on the ratio of coordination diastereomers. Due to the chiral nature of the {TpMo(L)(NO)} fragment, the coordination of a prochiral ligand (*e.g.*,

naphthalene) results in the formation of new stereocenters (Figure 2). This is most clearly illustrated if we examine a resonance structure of our TpMo(L)(NO)(η^2-naphthalene) complex shown as A in Figure 2. Within this representation, the coordinated carbon atoms are sp^3-hybridized, and because they lack a mirror plane they become co-dependent stereogenic centers. The creation of these new stereocenters, in conjunction with the chiral nature of the molybdenum center, results in the formation of diastereomers (A and B, Figure 2), termed *coordination diastereomers*.[21-22, 26]

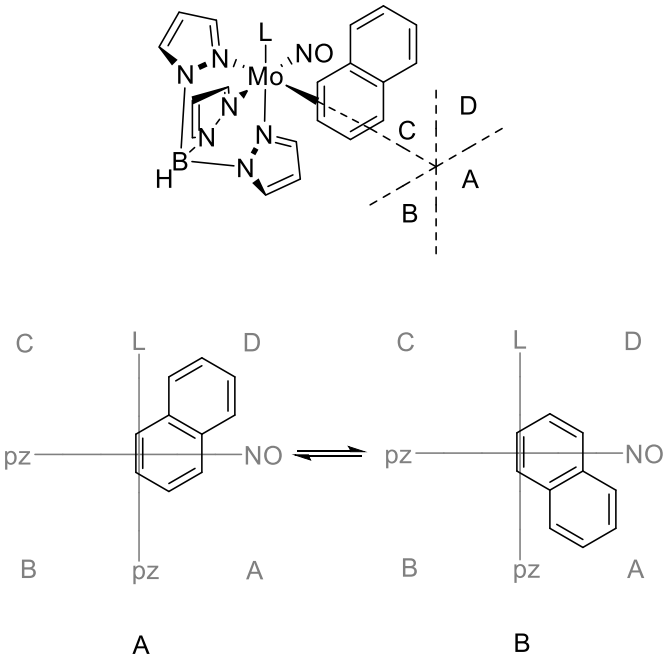

Figure 3: Quadrant analysis of ligand coordination and the impact of the steric profile of the ancillary ligand.

Due to the diastereomeric nature of A and B in Figure 2, we can assess the steric impact of the ancillary ligand on the ratio of observed coordination diastereomers. These analyses apply the coordinate system, proposed by Scott Meiere within the sterically similar {TpRe(MeIm)(CO)} fragment (Figure 3).[28-29] Studies on a variety of substituted alkenes established the steric profile of the quadrants to be C>>B>A>D for the rhenium system. Based on these results all proposed coordination diastereomers place the bulk of the uncoordinated ligand over the A and D

quadrants.[28] Molybdenum and rhenium complexes incorporating aromatic ancillary ligands (*e.g.*, MeIm, DMAP, py) also help to favor the A coordination isomer due to π-interactions with the uncoordinated naphthalene ring.[13-14]

A comparison between TpRe(L)(CO)(η^2-naphthalene), TpW(PMe_3)(NO)(η^2-naphthalene), and TpMo(L)(NO)(η^2-naphthalene) systems allows for a greater understanding of the steric impact of the ancillary ligand on the ratio of A and B coordination diastereomers (Figure 3), summarized in Table 3. The importance of sterics is demonstrated by comparing **II** with **III**-**VII**, in which the imposing steric profile of the phosphine results a dramatic change to the coordination preference of the rhenium center. While **III**-**VII** show a mixture of coordination diastereomers favoring the A isomer, **II** increases the steric crowding of quadrants C and D, such that not only is the B isomer favored, the A isomer is no longer observed (Table 3).[17-18, 21-22, 26] These results are also seen within the tungsten system, which relies solely on a PMe_3 ancillary ligand (**I**).[2, 10, 12]

Complex	Coordination Diasteromer Ratio (A:B)
TpMo(MeIm)(NO)(η^2-naphthalene) (**24**)	4 : 1
TpMo(DMAP)(NO)(η^2-naphthalene) (**26**)	2 : 1
TpMo(py)(NO)(η^2-naphthalene) (**28**)	4 : 1
TpMo(nic)(NO)(η^2-naphthalene) (**29**)	4 : 1
TpMo(3-pic)(NO)(η^2-naphthalene) (**30**)	4 : 1
TpMo(Im)(NO)(η^2-naphthalene) (**31**)	2 : 1
TpMo(pyr)(NO)(η^2-naphthalene) (**32**)	1.25 : 1
TpW(PMe_3)(NO)(η^2-naphthalene) (**I**)	B only
TpRe(PMe_3)(CO)(η^2-naphthalene) (**II**)	B only
TpRe(*t*-BuNC)(CO)(η^2-naphthalene) (**III**)	1.2 : 1
TpRe(py)(CO)(η^2-naphthalene) (**IV**)	3 : 1
TpRe(NH_3)(CO)(η^2-naphthalene) (**V**)	4 : 1
TpRe(MeIm)(CO)(η^2-naphthalene) (**VI**)	5 : 1
TpRe(DMAP)(CO)(η^2-naphthalene) (**VII**)	1.5 : 1

Table 3: Coordination diastereomer ratios of TpM(L)(CO/NO)(η^2-naphthalene) complexes (M = Re, W, or Mo).

However, upon analysis of the accumulated data we also see that sterics are not the only consideration in the ratio of resulting coordination diastereomers. This is clearly illustrated by comparing η^2-naphthalene complexes employing pyridine-based ancillary ligands within both rhenium and molybdenum systems. Pyridine rings with substitution at the 3- or 4-positions (**29**-**30** and **26**, **VII**, respectively) provides a nearly identical steric profile to the parent pyridine complexes (**28** and **IV**, Table 3), while providing a range of electronic profiles (Tables 1 and 2). Incorporation of an ERG on the pyridine ring (the amino group of DMAP), dramatically increases the electron density on the metal center.[12, 17] The more reducing **26** and **VII** are better able to stabilize the sterically less favorable B isomer than their less reducing analogs **28**-**30**, **IV**.[12, 14-15, 17] Interestingly, we see this effect across both rhenium and molybdenum systems, as **26** and **VII** produce B isomers that are twice as prevalent than when less donating pyridines (**28**-**30**, **IV**) are employed (Table 3).

2.7 Current Mo – Dearomatization: {TpMo(DMAP)(NO)}

As discussed in section 2.5, the {TpMo(MeIm)(NO)} dearomatization agent has been demonstrated to promote novel reactivity within PAHs. Moreover, the molybdenum system has distinguished itself from the current 3rd row tungsten system with the synthetic ease of liberating dearomatized products, while also providing a mechanism to recycle the molybdenum center to the η^2-aromatc precursor **3** in good yield (80-90 %).[11] Despite these advances within the {TpMo(MeIm)(NO)} framework, it is difficult to access an allylic naphthalene cationic species, which have been observed with previous osmium, rhenium, and tungsten dearomatization agents (Scheme 5).[10-11, 15, 30-32] This is a significant detraction to molybdenum based dearomatization, as access to the cationic allylic species allows for the addition of nucleophiles which are incompatible with acid, severely limiting the scope of transformations available for novel small molecule synthesis (Scheme 5). This is due to the instability of the **24-H** species, which is prone to oxidative

decomposition above 30 °C.[15] Due to the synthetic difficulties associated with a MeIm ancillary ligand, synthetic transformations to **26** and **27** were explored.

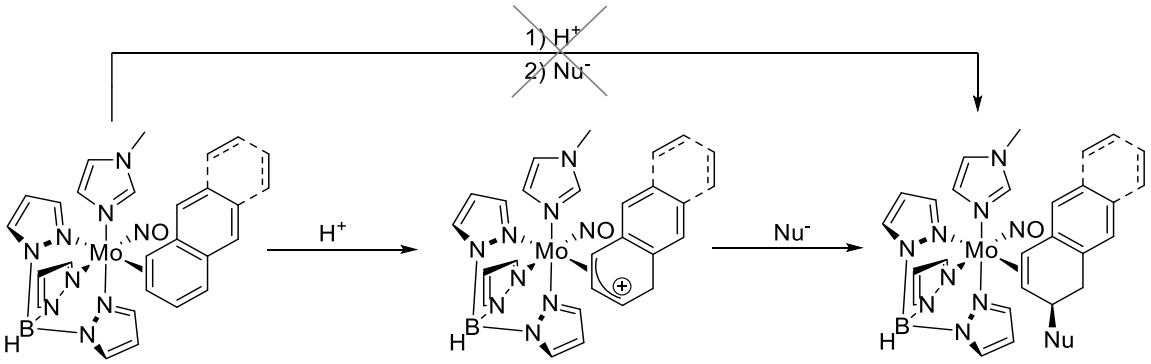

Scheme 5: Synthetic utility of accessing a stable allylic complex (**24-H**, **25-H**).

DMAP was chosen as a potential replacement for MeIm due to the similar electronic and steric profiles of the ligands, as discussed in section 2.6. Jeff Myers compared synthesis of the desired allylic species of **24-H** and **26-H**. Despite the electronic similarity of the DMAP and MeIm ligands under neutral conditions, the electron donation of the DMAP ligand can be modulated by interactions with the lone pair of the dimethylamino group. The ability to protonate this lone pair under highly acidic conditions reduces electron donation from the ligand (Scheme 6). Protonation effectively eliminates the donor ability of the amino group, which we propose shifts the potential approximately +0.1 V based on comparisons between **26** and **28** (Table 2). This shift in I/0 reduction potential stabilizes **26** from the oxidative decomposition seen with **24**, allowing access to the desired allylic species **26-H**, which is stable a room temperature (Scheme 6).[15]

Given the importance of accessing **24-H** and **26-H**, Jeff Myers applied the optimized conditions for transformations of **24** and **25** to **26** and **27**. These studies showed differences in reactivity between the two molybdenum systems, although both were able to access similar types of transformations.[15] Moreover, Jeff Myers demonstrated the applicability of the I_2 mediated recyclability of the {TpMo(DMAP)(NO)} fragment, with efficiency similar to that of the MeIm system.[15] Due to the synthetic advantages of an ancillary ligand which provides increased

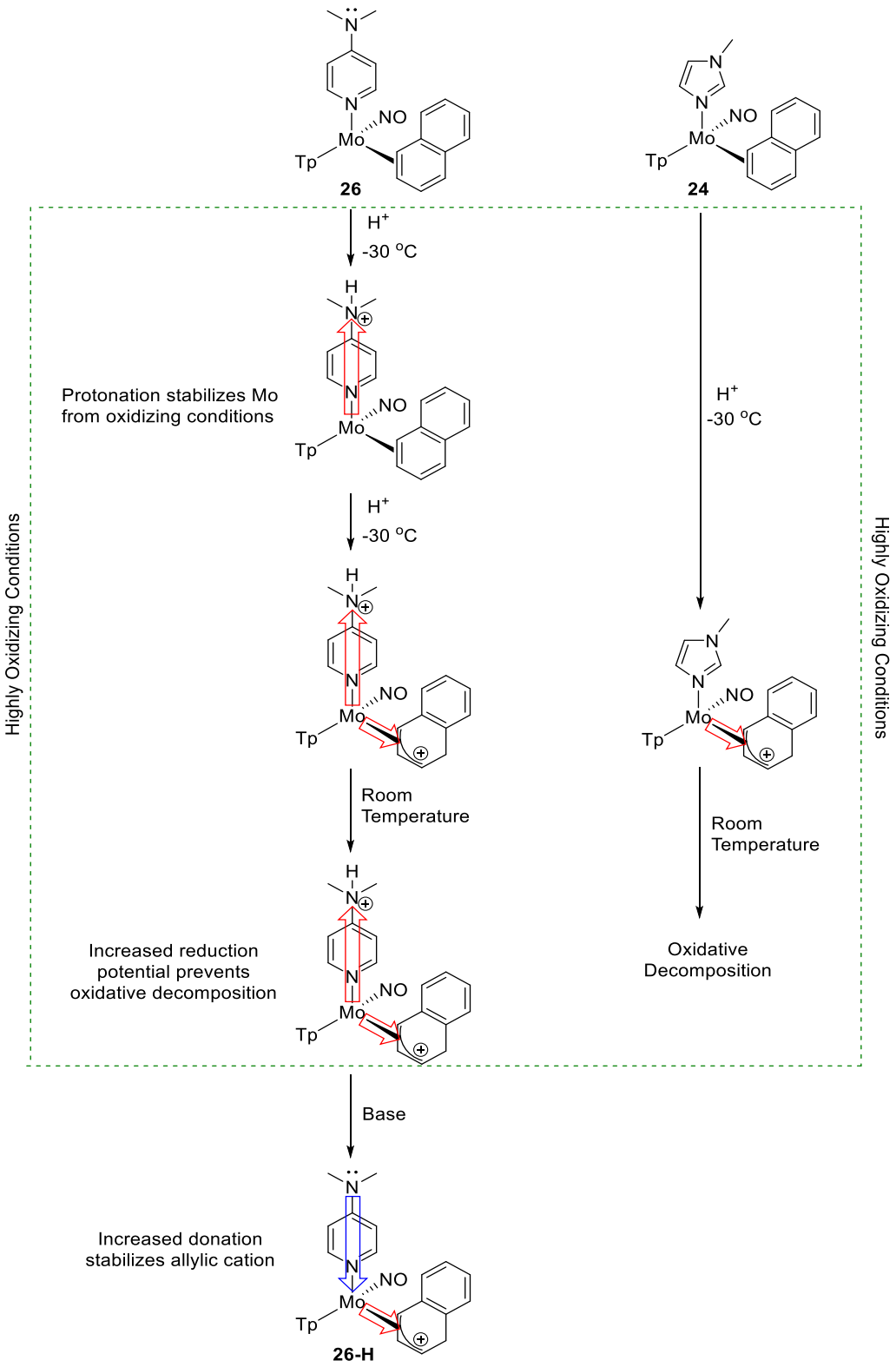

Scheme 6: {TpMo(DMAP)(NO)} Synthesis and stabilization of naphthalene allylic cation complexes (**26-H**).

stabilization under oxidative conditions, while providing similar steric and electronic properties, DMAP displaced MeIm as the ancillary ligand of choice for general molybdenum based dearomatization.

2.8 Conclusion

With the optimization of molybdenum – η^2-PAH complexes, and the syntheses of novel hydro-naphthalenes and anthracenes, the viability of molybdenum mediated dearomatization was established. Incorporation of DMAP as the ancillary ligand of choice allows access to cationic allylic species (**26-H**, **27-H**), which are stable at room temperature. The molybdenum bound PAH cores provide access to similar classes of reagents seen with previous 3rd row osmium, rhenium, and tungsten dearomatization agents, while the mild oxidation conditions required to liberate the organic products allow for the recyclability of the molybdenum metal center. Moreover, three separate synthetic pathways were optimized to access TpMo(L)(NO)(η^2-aromatic) complexes, with conditions amenable to the incorporation of a breadth of ancillary ligands. Also, the TpMo(DMAP)(NO)(X) precursor can be synthesized and stored *outside* of an inert atmosphere on a 170 g scale, with a 68% overall yield.[15]

Within the context of the three available synthetic pathways a variety of ancillary ligands were explored. These efforts yielded 5 new molybdenum – η^2-naphthalene complexes (**28**-**33**), demonstrating the increased tunability of the molybdenum ligand set in comparison to osmium and tungsten based dearomatization agents. The differences in reactivity noted between **24** and **25** compared to **26** and **27** indicate that subtle changes to the ancillary ligand result in appreciable changes to the reactivity of the dearomatized ligand. The breadth of η^2-PAH complexes allows for the possibility to access a range of novel hydro-naphthalene and anthracene products, while continued development of ancillary ligands may provide a means to increase the coordination scope of the 2nd row molybdenum dearomatization agent.

2.9 Experimental

General Methods

NMR spectra were obtained on 600 or 800 MHz spectrometers. Chemical shifts are referenced to tertramethylsilane (TMS) utilizing residual ^{1}H signals of the deuterated solvents as internal standards. Chemical shifts are reported in ppm and coupling constants (*J*) are reported in hertz (Hz). Infrared Spectra (IR) were recorded on a spectrometer as a glaze on a Horizontal Attenuated Total Reflectance (HATR) accessory, or as a glaze between two NaCl plates, with peaks reported in cm^{-1}. Electrochemical experiments were performed under a nitrogen atmosphere. Cyclic voltammetric data were recorded at ambient temperature at 100 mV/s unless otherwise noted, with a standard three electrode cell from +1.8 V to -1.8 V with a platinum working electrode, *N*,*N*-dimethylacetamide (DMA) or acetonitrile (MeCN) solvent, and tetrabutylammonium hexafluorophosphate (TBAH) electrolyte (~1.0 M). For CV data recorded in aqueous solutions, sodium triflate (NaOTf) was used as the electrolyte. All potentials are reported versus the normal hydrogen electrode (NHE) using cobaltocenium hexafluorophosphate ($E_{1/2}$ = -0.78 V, -1.75 V) or ferrocene ($E_{1/2}$ = 0.55 V) as an internal standard. Peak separation of all reversible couples was less than 100 mV. All synthetic reactions were performed in a glovebox under a dry nitrogen atmosphere unless otherwise noted. All solvents were purged with nitrogen prior to use. Deuterated solvents were used as received from Cambridge Isotopes. Compounds **1**-**3**, **7**-**9**, **15**, **20**, **22**, **24**-**28**, and **32** were prepared according to previous literature methods.[11-15] Compound **14** was not isolated and observed *in situ* during the synthesis of **28**.

Synthesis of TpMo(BuIm)(NO)(CO) (4)

$TpMo(NO)(CO)_2$ (5.15 g, 13 mmol), DMF (30 mL), and *N*-butylimidazole (5.1 mL, 38.8 mmol) were added to a 100 mL, 3-neck round bottom flask charged with a stir egg, reflux condenser, septum, and thermometer. The orange mixture was heated to reflux (154 °C) for 1 h, at which point the

green solution was cooled to room temperature. H_2O (200 mL) was added to the solution resulting in a green mixture, which was stirred at room temperature overnight (18 h). The green precipitate was then collected on a 150 mL fine frit, washed with Et_2O (3 X 50 mL) and desiccated overnight to yield (**4**) (56 %, 3.61 g, 7.35 mmol). ^{1}H NMR (acetone-d_6, δ): 7.89 (1H, d, Tp), 7.86 (1H, d, Tp), 7.83 (1H, d, Tp), 7.66 (1H, s), 7.65 (1H, d, Tp), 7.48 (1H, d, Tp), 7.42 (1H, d, Tp), 7.83 (1H, t, Im), 6.27 (1H, t, Tp), 6.24 (1H, t, Tp), 6.21 (1H, t, Tp), 4.12 (2H, t, butyl), 1.78 (2H, m, butyl), 1.30 (2H, m, butyl), 0.92 (3H, t, butyl). ^{13}C NMR (acetone-d_6, δ): 1.446, 142.8, 142.5, 140.6, 136.6, 136.3, 131.9, 120.9, 106.3, 106.3, 105.9, 47.9, 33.6, 20.2, 13.7. CV: $E_{p,a}$ = +0.18 V. IR: ν_{NO} = 1589 cm^{-1}; ν_{CO} = 1871 cm^{-1}; ν_{BH} = 2480 cm^{-1}.

Synthesis of TpMo(Im)(NO)(CO) (5)

$TpMo(NO)(CO)_2$ (2.06 g, 5.25 mmol), DMF (10 mL), and imidazole (1.06 g , 15.64 mmol), were added to a 3-neck round bottom flask charged with a stir egg, reflux condenser, septum, and thermometer. This orange mixture was heated to reflux (154 ^{o}C) for 3 h at which point the blue solution was cooled to room temperature. H_2O (30 mL) was added to the reaction mixture, resulting in a blue mixture, which was stirred at room temperature overnight (18 h). The blue precipitate was then collected on a 30 mL fine frit, washed with H_2O (3 X 20 mL), 10% EtOH in Et_2O (2 X 20 mL), and Et_2O (2 X 20 mL), and desiccated overnight to yield (**5**) (54 %, 1.24 g, 2.85 mmol). ^{1}H NMR (acetone-d_6, δ): 11.80 (1H, bs, NH), 7.90 (1H, d, Tp), 7.87 (1H, d, Tp), 7.84 (1H, d, Tp), 7.71 (1H, s, Im), 7.67 (1H, d, Tp), 7.47 (1H, d, Tp), 7.42 (1H, d, Tp), 7.28 (1H, s, Im), 6.91 (1H, s, Im), 6.27 (1H, t, Tp), 6.25 (1H, t, Tp), 6.21 (1H, t, Tp). ^{13}C NMR (acetone-d_6, δ): 144.61 (Im), 142.9 (Tp), 142.6 (Tp), 138.8 (Im), 136.2 (2C, Tp), 131.1 (Tp), 117.1 (Im), 106.9 (2C, Pz4), 106.8 (Pz4). CV: $E_{p,a}$ = +0.16 V. IR: ν_{NO} = 1585 cm^{-1}; ν_{CO} = 1871 cm^{-1}; ν_{BH} = 2484 cm^{-1}.

Synthesis of TpMo(Im)(NO)(Br) (6)

Compound **5** (1.0 g, 2.2 mmol) and DCM (5 mL) were added a solution of Br_2 in DCM (2.39 M, 0.46 mL, 1.1 mmol). The resulting green solution was stirred at room temperature for 5 min at which point hexanes was added inducing precipitation. This green precipitate was then collected on a 15 mL fine frit, washed with hexanes (2 X 5 mL), and desiccated for 15 min to yield (**6**) (99 %, 1.03 g, 2.19 mmol). CV: $E_{1/2}$ = -1.66 V, $E_{p,a}$ = +0.85 V.

Synthesis of TpMo(npam)(NO)(Br) (10)

TpMo(NO)$(Br)_2$ (1.026 g, 2.06 mmol) was added to a 25 mL Erlenmeyer flask charged with a stir bar. The solid was dissolved in DCM (15 mL), giving a red mixture. Zn^0 dust (0.753 g, 11.5 mmol) was added to the reaction mixture which was stirred for 10 min. Propylamine (1.0 mL, 12 mmol) was added drop-wise and the reaction mixture was stirred for an additional 10 min. The green mixture was filtered through a 15 mL medium frit with a 2 cm silica plug. DCM (20 mL) was used to wash the reaction flask and the silica plug. The dark green filtrate was evaporated to dryness, re-dissolved in DCM (4 mL), and precipitated by drop-wise addition into stirring Et_2O (100 mL). The product was collected on a 15 mL fine frit and dried *in vacuo* to give a dark green solid (**10**) (53%, 0.522 g, 1.09 mmol). CV: $E_{p,c}$ = -1.62 V, $E_{p,a}$ = +0.53 V. IR: ν_{NO} = 1616 cm^{-1}; ν_{BH} = 2488 cm^{-1}.

Synthesis of TpMo(aam)(NO)(Br) (11)

TpMo(NO)$(Br)_2$ (1.041 g, 2.09 mmol) was added to a 25 mL Erlenmeyer flask charged with a stir bar. The solid was dissolved in DCM (15 mL), giving a red mixture. Zn^0 dust (0.847 g, 12.9 mmol) was added to the reaction mixture which was stirred for 10 min. Allylamine (0.90 mL, 12 mmol) was added drop-wise and the reaction mixture was stirred for an additional 10 min. The mixture was filtered through a 15 mL medium frit with a 2 cm silica plug. DCM (30 mL) was used to wash the reaction flask and the silica plug. The green filtrate was evaporated to dryness, re-dissolved in DCM (4 mL), and precipitated by drop-wise addition into stirring hexanes (100 mL). The product

was collected on a 15 mL fine frit and dried *in vacuo* to give (**11**) (40 %, 0.398 g, 0.836 mmol). CV: $E_{p,c}$ = -1.60 V, $E_{p,a}$ = +0.46. IR: ν_{NO} = 1612 cm^{-1}; ν_{BH} = 2492 cm^{-1}.

Synthesis of TpMo(pyr)(NO)(Br) (12)

$TpMo(NO)(Br)_2$ (0.997 g, 2.00 mmol) was added to a 50 mL round bottom flask charged with a stir bar. The solid was dissolved in THF (40 mL), giving a red mixture. Zn^0 dust (0.769 g, 11.8 mmol) was added to the reaction mixture which was stirred for 10 min. Pyrrolidine (0.86 mL, 11 mmol) was added drop-wise and the reaction mixture was stirred for an additional 10 min. The dark green mixture was filtered through a 60 mL medium frit with a 4 cm silica plug. THF (50 mL) was used to wash the reaction flask and the silica plug. The emerald green filtrate was evaporated to dryness, re-dissolved in DCM (15 mL), and precipitated by drop-wise addition into stirring Et_2O (100 mL). The product was collected on a 15 mL fine frit and dried *in vacuo* to give (**12**) (56 %, 0.548 g, 1.12 mmol). CV: $E_{p,c}$ = -1.63 V, $E_{p,a}$ = +0.64 V. IR: ν_{NO} = 1585 cm^{-1}; ν_{BH} = 2492 cm^{-1}.

Synthesis of TpMo(mor)(NO)(Br) (13)

$TpMo(NO)(Br)_2$ (1.012 g, 2.03 mmol) was added to a 100 mL round bottom flask charged with a stir bar. The solid was dissolved in THF (40 mL), giving a red mixture. Zn^0 dust (0.947 g, 14.5 mmol) was added to the reaction mixture which was stirred for 10 min. *N*-Methylmorpholine (1.1 mL, 10 mmol) was added drop-wise and the reaction mixture was stirred for an additional 10 min. The olive green mixture was filtered through a 60 mL medium frit with a 4 cm silica plug. THF (100 mL) was used to wash the reaction flask and the silica plug. The dark green filtrate was evaporated to dryness, re-dissolved in DCM (6 mL), and precipitated by drop-wise addition into stirring Et_2O (100 mL). The product was collected on a 30 mL fine frit and dried *in vacuo* to give (**13**) (61 %, 0.644 g, 1.24 mmol). CV: $E_{p,c}$ = -1.56 V, $E_{p,a}$ = +0.57 V. IR: ν_{NO} = 1601 cm^{-1}; ν_{BH} = 2488 cm^{-1}.

Synthesis of TpMo(nic)(NO)(Br) (16)

Compound **23** (2.0 g, 3.78 mmol) and DCM (10 mL) were added a solution of Br_2 in DCM (19.3 M, 0.1 mL, 1.89 mmol). The resulting brown solution was stirred at room temperature for 5 min at which point hexanes (40 mL) were added inducing precipitation. The brown mixture was filtered through a 15 mL fine frit, washed with hexanes (2 X 5 mL), and desiccated for 15 min to yield (**16**) (38 %, 843 mg, 1.45 mmol). CV: $E_{1/2}$ = -1.25 V, $E_{p,a}$ = +0.83 V. IR: ν_{NO} = 1631 cm^{-1}; ν_{BH} = 2495 cm^{-1}.

Synthesis of TpMo(Fpy)(NO)(Br) (17)

TpMo(NO)$(Br)_2$ (0.497 g, 0.99 mmol) was added to a 100 mL round bottom flask charged with a stir bar. The solid was dissolved in THF (50 mL), giving a red mixture. Zn^0 dust (0.494 g, 7.55 mmol) was added to the reaction mixture which was stirred for 10 min. 4-Fluoropyridine hydrochloride (0.169 g, 1.26 mmol) was added and the reaction mixture was stirred for an additional 70 min. The dark green mixture was filtered through a 30 mL medium frit with a 3 cm silica plug. THF (100 mL) was used to wash the reaction flask and the silica plug. The dark green filtrate was concentrated to ~5 mL *in vacuo* and precipitated by drop-wise addition into stirring Et_2O (100 mL). The product was collected on a 15 mL fine frit and dried *in vacuo* to give (**17**) (24 %, 0.123 g, 0.238 mmol). CV: $E_{1/2}$ = -1.53 V, $E_{p,a}$ = +0.58 V. IR: ν_{NO} = 1616 cm^{-1}; ν_{BH} = 2511 cm^{-1}.

Synthesis of TpMo(HOpy)(NO)(Br) (18)

TpMo(NO)$(Br)_2$ (1.023 g, 2.05 mmol) was added to a 125 mL Erlenmeyer flask charged with a stir bar. The solid was dissolved in THF (100 mL), giving a red mixture. Zn^0 dust (0.919 g, 14.0 mmol) was added to the reaction mixture which was stirred for 10 min. 2-Hydroxypyridine (1.148 g, 12.1 mmol) was added and the reaction mixture was stirred for an additional 10 min. The dark green mixture was filtered through a 60 mL medium frit with a 4 cm silica plug. THF (100 mL) was used to wash the reaction flask and the silica plug. The dark green filtrate was concentrated to ~10 mL *in vacuo* and precipitated by drop-wise addition into stirring Et_2O (100 mL). The failed

precipitation resulted in the formation of a dark green oil, which was isolated by the evaporation of the Et_2O *in vacuo*. The oil was dissolved in 5 mL of DCM and re-precipitated in by drop-wise addition into stirring hexanes (100 mL). The product was collected on a 15 mL fine frit and dried *in vacuo* to give (**18**) (92 %, 0.969 g, 1.89 mmol). CV: $E_{p,c}$ = -1.60 V, $E_{p,a}$ = +0.17 V, +0.36 V. IR: ν_{NO} = 1601 cm^{-1}; ν_{BH} = 2511 cm^{-1}.

Synthesis of [TpMo(CN)(Br)]Na (21)

$TpMo(NO)(Br)_2$ (2.058 g, 4.13 mmol) was added to a 250 mL round bottom flask charged with a stir bar. The solid was dissolved in THF (100 mL), giving a red mixture. Zn^0 dust (1.633 g, 25.0 mmol) was added to the reaction mixture which was stirred for 10 min. NaCN (0.267 g, 5.45 mmol) was added and the reaction mixture was stirred for an additional 10 min. The dark green mixture was filtered through a 60 mL medium frit with a 4 cm silica plug. THF (50 mL) was used to wash the reaction flask and the silica plug. The dark green filtrate was concentrated to ~20 mL *in vacuo* and precipitated by drop-wise addition into stirring hexanes (200 mL). The product was collected on a 15 mL fine frit and dried *in vacuo* to give (**21**) (89 %, 1.721 g, 3.68 mmol). CV: $E_{1/2}$ = -1.54 V, $E_{p,a}$ = +0.58 V. IR: ν_{NO} =1608 cm^{-1}; ν_{BH} = 2509 cm^{-1}.

Synthesis of TpMo(nic)(NO)(CO) (23)

$TpMo(NO)(CO)_2$ (5.15 g, 13.0 mmol), DMF (50 mL), and (*S*)-nicotine (6.3 g, 39 mmol), were added to a 250 mL 3-neck round bottom flask charged with a stir egg, reflux condenser, septum, and thermometer. The orange mixture was heated to reflux (154 ^oC) for 1 h, at which point the red solution was cooled to room temperature. H_2O (150 mL) was added resulting in a red mixture, which was stirred at room temperature overnight (18 h). The red precipitate was then collected on a 30 mL fine frit, washed with 5% MeOH Et_2O (100 mL) and desiccated overnight to yield (**23**). (78 %, 5.34 g, 10.1 mmol). ^1H NMR (d^6-Acetone, δ): 8.32 (1H, m), 8.11 (1H, m), 7.96 (2H, m), 7.89 (1H, m), 7.77 (1H, m), 7.69 (1H, m), 7.52 (1H, s), 7.36 (1H, m), 7.25 (1H, m), 6.31 (1H, t), 6.28 (1H,

t), 6.27 (1H, t), 3.00 (2H, m), 2.07 (3H, s), 1.74 (2H, m), 1.55 (1H, m). CV: $E_{p,a}$ = +0.20 V. IR: ν_{NO} = 1593 cm^{-1}; ν_{CO} = 1874 cm^{-1}; ν_{BH} = 2480 cm^{-1}.

Synthesis of TpMo(nic)(NO)(η²-naphthalene) (29)

$TpMo(NO)(Br)_2$ (5.999 g, 12.0 mmol) was added to a 500 mL round bottom flask charged with a stir bar. The solid was dissolved in Et_2O (125 mL), giving a red mixture. Zn^0 dust (1.708 g, 26.1 mmol) was added to the reaction mixture which was stoppered and stirred for 10 min. (*S*)-Nicotine (2.1 mL, 13 mmol) was added drop-wise and the reaction mixture was stirred for an additional 90 min. Na^0 dispersion (6.658 g, 101 mmol) was prepared with washes in hexanes (3 X 30 mL) to remove the paraffin wax. The exposed sodium flakes were washed with Et_2O (20 mL) to remove residual hexanes. The exposed sodium flakes were added to the reaction mixture in Et_2O (20 mL), followed by the addition of naphthalene (16.364 g, 128 mmol). The reaction mixture was then stirred for an additional 27.5 h. The mixture was filtered through a 150 mL medium frit with a 5 cm silica plug. The column was eluted with Et_2O (150 mL), isolating a gold fraction, which was discarded. The bright red product band was eluted with Et_2O (500 mL), followed by 80 % Et_2O/ 20 % THF (300 mL). The red fraction was evaporated to dryness *in vacuo*, re-dissolved in DCM (12 mL), and precipitated by drop-wise addition into stirring pentane (100 mL). The product was collected on a 30 mL fine frit and dried *in vacuo* to give (**29**) (25 %, 1.89 g, 3.0 mmol). Partial characterization of the complex is given due to the fluxionality of the compound at ambient temperature. This compound was observed as a 4:1 ratio of diastereomers, the major having the unbound naphthalene ring proximal to the nicotine ligand and the minor having the unbound naphthalene ring distal to the nicotine ligand. ^{1}H NMR (acetone-d_6, δ): (Major diastereomer) 8.13 (broad d, *J* = 1.9, 1H, nicotine 6), 7.80 (broad singlet, 1H, nicotine 2), 7.32 (d, *J* = 8.3, 1H, nicotine 4), 6.84 (dd, *J* = 8.6, 6.1, 1H, nicotine 5), 6.44 (t, *J* = 2.1, 1H, Tp 4), 6.38 (t, *J* = 2.3, 1H, Tp 4), 6.06 (t, *J* = 2.1, 1H, Tp 4), 3.90 (broad singlet, 1H, naphthalene 3), 3.35 (m, 1H, nicotine 7), 3.12 (broad

singlet, 1H, naphthalene 4), 2.34-2.08 (m, 4H, nicotine methyl, nicotine 10b), 2.02-1.58 (m, 5H, nicotine 8a, 8b, 9a, 9b, 10a). (Minor diastereomer) 8.13 (broad peak overlapped with major, 1H, nicotine 6), 7.82 (broad s, 1H, nicotine 2), 7.30 (d, *J* = 8.3, 1H, nicotine 4), 6.45 (t, *J* = 2.1, 1H, Tp 4), 6.25 (t, *J* = 2.1, 1H, Tp 4), 6.05 (t, *J* = 1.9, 1H, Tp 4), 3.62 (ddd, *J* = 8.7, 5.1, 3.5, 1H, naphthalene 3), 3.49 (d, *J* = 8.8, 1H, naphthalene 4), 2.34-2.08 (m, 4H, nicotine methyl, nicotine 10b), 2.02-1.58 (m, 5H, nicotine 8a, 8b, 9a, 9b, 10a). CV: $E_{p,a}$ = -0.09 V. IR: ν_{NO} = 1585 cm^{-1}; ν_{BH} = 2480 cm^{-1}.

Synthesis of TpMo(3-pic)(NO)(η^2-naphthalene) (30)

$TpMo(NO)(Br)_2$ (5.997 g, 12.0 mmol) was added to a 250 mL round bottom flask charged with a stir bar. The solid was dissolved in THF (125 mL), giving a red mixture. Zn^0 dust (1.665 g, 25.5 mmol) was added to the reaction mixture which was stoppered and stirred for 10 min. 3-Picoline (1.2 mL, 12 mmol) was added drop-wise and the reaction mixture was stirred for an additional 90 min. Na^0 dispersion (3.673 g, 55.9 mmol) was prepared with washes in hexanes (3 X 30 mL) to remove the paraffin wax. The exposed sodium flakes were washed with THF (20 mL) to remove residual hexanes. The exposed sodium flakes were added to the reaction mixture in THF (5 mL), followed by the addition of naphthalene (16.369 g, 128 mmol). The reaction mixture was then stirred for an additional 20 min. The mixture was filtered through a 600 mL medium frit with a 9 cm silica plug. The column was eluted with Et_2O (50 mL), which gave a clear fraction that was discarded. The dark red product band was eluted with Et_2O (600 mL). The red fraction was evaporated to dryness *in vacuo*, re-dissolved in DCM (18 mL), and precipitated by drop-wise addition into stirring pentane (200 mL). The product was collected on a 30 mL fine frit and dried *in vacuo* to give (**30**) (26 %, 1.74 g, 3.1 mmol). Partial characterization of the complex is given due to the fluxionality of the compound as ambient temperature. This compound was observed as a 4:1 ratio of diastereomers, the major having the unbound naphthalene ring proximal to the picoline ligand and the minor having the unbound naphthalene ring distal to the picoline ligand.

^{1}H NMR (acetone-d_6, δ): (Major diastereomer) 8.14 (broad s, 1H, picoline 6), 7.75 (broad singlet, 1H, picoline 2), 6.38 (t, *J* = 2.1, 1H, Tp 4), 6.06 (t, *J* = 2.2, 1H, Tp 4), 3.82 (broad d, *J* = 7.9, 1H, naphthalene 4), 3.35 (broad dd, *J* = 7.5, 6.0, 1H, naphthalene 3). (Minor diastereomer) 6.45 (t, *J* = 2.1, 1H, Tp 4), 6.24 (t, *J* = 2.0, 1H, Tp 4), 3.60 (dd, *J* = 8.6, 5.2, 1H, naphthalene 3), 3.48 (d, *J* = 7.1, 1H, naphthalene 4). CV: $E_{p,a}$ = -0.09 V. IR: ν_{NO} = 1577 cm^{-1}; ν_{BH} = 2480 cm^{-1}.

Synthesis of TpMo(Im)(NO)(η^2-naphthalene) (31)

Compound **6** (2 g, 4.1 mmol), naphthalene (6.4 g, 49.9 mmol), Na/Hg amalgam (46 g, 200 mmol), and THF (120 mL) were added to a 250 mL round bottom flask charged with a stir bar. This mixture was stirred at room temperature for 24 h at which point the reaction mixture was decanted away from the mercury and concentrated to ~50 mL *in vacuo*. This solution was then loaded onto a 150 mL medium frit with 3 cm of silica. The product was eluted as an orange band with 1 : 1 Et_2O : Benzene (200 mL). This fraction was concentrated to ~20 mL *in vacuo* and slowly added to stirring hexanes (200 mL). The resulting orange mixture filtered through a 15 mL fine frit and desiccated to yield (**31**) (6 %, 130 mg, 0.242 mmol). Isolated as a 2 : 1 ratio of coordination diastereomers where the major has the unbound ring proximal to the ancillary ligand. ^{1}H NMR (acetone-d_6, δ): (Major isomer) 8.15 (1H, d, Pz3A/B), 8.00 (1H, d, Pz5C), 7.93 (1H, d, Pz5A/B), 7.80 (1H, d, Pz5A/B), 7.76 (1H, d, Pz3C), 7.28 (1H, bs, Im), 7.20 (1H, d, *J* = 7.4 Hz, H5), 7.12 (1H, bs, Im), 7.06 (1H, dd, *J* = 8.9 & 5.6 Hz, H3), 6.96 (1H, Pz3A/B), 6.90 (1H, t, *J* = 7.1 Hz, H6), 6.82 (1H, t, *J* = 7.0 Hz, H7), 6.64 (1H, bs, Im), 6.47 (1H, d, *J* = 8.8 Hz, H4), 6.39 (1H, t, Pz4C), 6.36 (1H, t, Pz4A/B), 6.13 (1H, d, *J* = 7.5 Hz, H8), 6.05 (1H, t, Pz4A/B), 4.64 (1H, BH), 3.70 (1H, d, *J* = 8.2 Hz, H1), 3.07 (1H, dd, *J* = 8.2 & 5.7 Hz, H2). (Minor isomer) 7.94 (1H, d, Pz3/5), 7.58 (1H, d, Pz3/5), 7.22 (1H, H5/8), 7.21 (1H, H5/8), 6.98 (1H, H7), 6.97 (1H, d, Pz3/5), 6.70 (1H, H8), 6.57 (1H, m, H3), 6.43 (1H, d, *J* = 9 Hz, H4), 6.39 (1H, t, Pz4), 6.24 (1H, t, Pz4), 3.47 (1H, dd, *J* = 8.6 & 5.3 Hz, H2), 3.22 (1H, d, *J* = 8.6 Hz, H1). ^{13}C NMR (acetone-d_6, δ): (Mix of isomers) 143.44, 143.12, 142.20, 142.13, 141.79, 141.59, 137.33,

136.97, 136.77, 135.57, 135.55, 134.75, 134.08, 132.63, 132.12, 128.81, 128.67, 128.39, 126.71, 126.46, 126.26, 125.48, 123.98, 123.67, 123.12, 122.98, 118.63, 117.73, 106.70, 106.54, 106.22, 106.00, 105.45, 79.22, 75.63, 72.52, 72.03, 69.72, 29.84. $E_{p,a}$ = -0.25 V. IR: ν_{NO} = 1579 cm^{-1}, ν_{BH} = 2483 cm^{-1}.

Synthesis of TpMo(pyr)(NO)(η^2-naphthalene) (33)

$TpMo(NO)(Br)_2$ (5.796 g, 11.6 mmol) was added to a 250 mL round bottom flask charged with a stir bar. The solid was dissolved in THF (125 mL), giving a red mixture. Zn^0 dust (1.635 g, 25.0 mmol) was added to the reaction mixture which was stoppered and stirred for 10 min. Pyrrolidine (1.0 mL, 12 mmol) was added drop-wise and the reaction mixture was stirred for an additional 90 min. Na^0 dispersion (3.792 g, 57.7 mmol) was prepared with washes in hexanes (3 X 30 mL) to remove the paraffin wax. The exposed sodium flakes were washed with THF (20 mL) to remove residual hexanes. The exposed sodium flakes were added to the reaction mixture in THF (40 mL), followed by the addition of naphthalene (16.702 g, 130.3 mmol). The reaction mixture was then stirred for an additional 18 h. The mixture was filtered through a 350 mL medium frit with a 7 cm silica plug. The column was eluted with Et_2O (50 mL), giving a gold band, which was discarded. The yellow product band was eluted with Et_2O (100 mL), followed immediately by a brown band giving both the product and decomposition products. This elution was evaporated to dryness *in vacuo*, re-dissolved in DCM (10 mL), and loaded onto a 5 cm silica plug in a 150 mL medium frit. The yellow product band was eluted with Et_2O (200 mL), which was evaporated to dryness *in vacuo*, re-dissolved in DCM (12 mL), and precipitated by drop-wise addition into stirring pentane (100 mL). The product was collected on a 60 mL fine frit and dried *in vacuo* to give (**33**) (2 %, 0.125 g, 0.232 mmol). This compound was observed as a 1.25:1 ratio of diastereomers, the major having the unbound naphthalene ring proximal to the pyrrolidine ligand and the minor having the unbound naphthalene ring distal to the pyrrolidine ligand. ^1H NMR (acetone-d_6, δ): (Major

diastereomer) 8.11 (d, *J* = 1.7, 1H, Tp 3/5), 7.99 (d, *J* = 2.1, 1H, Tp 3/5), 7.95-7.87 (m, 3H, 3 X Tp 3/5), 7.74 (d, *J* = 1.9, 1H, Tp 3/5), 7.26 (d, *J* = 7.7, 1H, naphthalene 8), 7.14-6.94 (m, 3H, naphthalene 5, 6, 7), 6.48 (d, *J* = 9.4, 1H, naphthalene 1), 6.35 (t, *J* = 2.1, 1H, Tp 4), 6.31 (t, *J* = 2.2, 1H, Tp 4), 6.30 (dd, *J* = 8.1, 4.5, 1H, naphthalene 2), 6.27 (t, *J* = 2.2, 1H, Tp 4), 3.86 (d, *J* = 8.3, 1H, naphthalene 4), 3.13 (dd, *J* = 8.3, 5.9, 1H, naphthalene 3), 2.84-2.69 (m, 4H, pyrrolidine 1), 1.77-1.52 (m, 4H, pyrrolidine 2). (Minor diasteromer) 8.01 (d, *J* = 2.1, 1H, Tp 3/5), 7.95-7.87 (m, 3H, 3 X Tp 3/5), 7.85 (d, *J* = 2.2, 1H, Tp 3/5), 7.79 (d, *J* = 2.1, 1H, Tp 3/5), 7.14-6.94 (m, 4H, naphthalene 5, 6, 7, 8), 6.41 (d, *J* = 8.9, 1H, naphthalene 1), 6.35 (t, *J* = 2.2, 1H, Tp 4), 6.30 (dd, *J* = 8.6, overlapped with major, 2H, Tp 4, naphthalene 2), 6.26 (t, *J* = 2.2, 1H, Tp 4), 6.16 (t, *J* = 2.2, 1H, Tp 4), 3.70 (dd, *J* = 8.3, 5.9, 1H, naphthalene 3), 3.19 (d, *J* = 8.3, 1H, naphthalene 4), 2.84-2.69 (m, 4H, pyrrolidine 1), 1.77-1.52 (m, 4H, pyrrolidine 2). CV: $E_{p,a}$ = -0.25 V. IR: ν_{NO} = 1550 cm^{-1}; ν_{BH} = 2480 cm^{-1}.

2.10 References

1. Graham, P. M.; Meiere, S. H.; Sabat, M.; Harman, W. D. *Organometallics* **2003,** *22*, 4364-4366.

2. Keane, J. M.; Harman, W. D. *Organometallics* **2005,** *24*, 1786-1798.

3. Graham, P. M.; Delafuente, D. A.; Liu, W.; Myers, W. H.; Sabat, M.; Harman, W. D. *J. Am. Chem. Soc.* **2005,** *127*, 10568-10572.

4. Graham, P. M.; Mocella, C. J.; Sabat, M.; Harman, W. D. *Organometallics* **2005,** *24*, 911-919.

5. Keane, J. M.; Chordia, M. D.; Mocella, C. J.; Sabat, M.; Trindle, C. O.; Harman, W. D. *J. Am. Chem. Soc.* **2004,** *126*, 6806-6815.

6. MacLeod, B. L.; Pienkos, J. A.; Myers, J. T.; Sabat, M.; Myers, W. H.; Harman, W. D. *Organometallics* **2014,** *33*, 6286-6289.

7. MacLeod, B. L.; Pienkos, J. A.; Wilson, K. B.; Sabat, M.; Myers, W. H.; Harman, W. D. *Organometallics* **2016,** *35*, 370-387.

8. Pienkos, J. A.; Knisely, A. T.; MacLeod, B. L.; Myers, J. T.; Shivokevich, P. J.; Teran, V.; Sabat, M.; Myers, W. H.; Harman, W. D. *Organometallics* **2014,** *33*, 5464-5469.

9. Welch, K. D.; Harrison, D. P.; Lis, E. C.; Liu, W.; Salomon, R. J.; Harman, W. D.; Myers, W. H. *Organometallics* **2007,** *26*, 2791-2794.

10. Strausberg, L.; Li, M.; Harrison, D. P.; Myers, W. H.; Sabat, M.; Harman, W. D. *Organometallics* **2013,** *32*, 915-925.

11. Myers, J. T.; Shivokevich, P. J.; Pienkos, J. A.; Sabat, M.; Myers, W. H.; Harman, W. D. *Organometallics* **2015,** *34*, 3648-3657.

12. Ha, Y.; Dilsky, S.; Graham, P. M.; Liu, W.; Reichart, T. M.; Sabat, M.; Keane, J. M.; Harman, W. D. *Organometallics* **2006,** *25*, 5184-5187.

13. Meiere, S. H.; Keane, J. M.; Gunnoe, T. B.; Sabat, M.; Harman, W. D. *J. Am. Chem. Soc.* **2003,** *125*, 2024-2025.

14. Mocella, C. J.; Delafuente, D. A.; Keane, J. M.; Warner, G. R.; Friedman, L. A.; Sabat, M.; Harman, W. D. *Organometallics* **2004,** *23*, 3772-3779.

15. Myers, J. T.; Dakermanji, S. J.; Chastanet, T. R.; Shivokevich, P. J.; Strausberg, L. J.; Sabat, M.; Myers, W. H.; Harman, W. D. *Organometallics* **2017,** *36*, 543-555.

16. McCleverty, J. A.; Seddon, D.; Bailey, N. A.; Joe' Walker, N. W. *J. C. S. Dalton* **1976,** 898-908.

17. Meiere, S. H.; Brooks, B. C.; Gunnoe, T. B.; Carrig, E. H.; Sabat, M.; Harman, W. D. *Organometallics* **2001,** *20*, 3661-3671.

18. Meiere, S. H.; Brooks, B. C.; Gunnoe, T. B.; Sabat, M.; Harman, W. D. *Organometallics* **2001,** *20*, 1038-1040.

19. Lis, E. C.; Delafuente, D. A.; Lin, Y.; Mocella, C. J.; Todd, M. A.; Liu, W.; Sabat, M.; Myers, W. H.; Harman, W. D. *Organometallics* **2006,** *25*, 5051-5058.

20. Gunnoe, T. B.; Sabat, M.; Harman, W. D. *J. Am. Chem. Soc.* **1998,** *120*, 8747-8754.

21. Gunnoe, T. B.; Sabat, M.; Harman, W. D. *J. Am. Chem. Soc.* **1999,** *121*, 6499-6500.

22. Gunnoe, T. B.; Sabat, M.; Harman, W. D. *Organometallics* **2000,** *19*, 728-740.

23. Chin, R. M.; Barrera, J.; Dubois, R. H.; Helberg, L. E.; Sabat, M.; Bartucz, T. Y.; Lough, A. J.; Morris, R. H.; Harman, W. D. *Inorg. Chem.* **1997,** *36*, 3553-3558.

24. Orth, S. D.; Barrera, J.; Sabat, M.; Harman, W. D. *Inorg. Chem.* **1993,** *32*, 594-601.

25. Orth, S. D.; Barrera, J.; Sabat, M.; Harman, W. D. *Inorg. Chem.* **1994,** *33*, 3026-3027.

26. Brooks, B. C.; Meiere, S. H.; Friedman, L. A.; Carrig, E. H.; Gunnoe, T. B.; Harman, W. D. *J. Am. Chem. Soc.* **2001,** *123*, 3541-3550.

27. Friedman, L. A.; Meiere, S. H.; Brooks, B. C.; Harman, W. D. *Organometallics* **2001,** *20,* 1699-1702.

28. Meiere, S. H.; Harman, W. D. *Organometallics* **2001,** *20*, 3876-3883.

29. Meiere, S. H.; Valahovic, M. T.; Harman, W. D. *J. Am. Chem. Soc.* **2002,** *124*, 15099-15103.

30. Winemiller, M. D.; Harman, W. D. *J. Org. Chem.* **2000,** *65*, 1249-1256.

31. Ding, F.; Valahovic, M. T.; Keane, J. M.; Anstey, M. R.; Sabat, M.; Trindle, C. O.; Harman, W. D. *J. Org. Chem.* **2004,** *69*, 2257-2267.

32. Valahovic, M. T.; Gunnoe, T. B.; Sabat, M.; Harman, W. D. *J. Am. Soc.* **2002,** *124*, 3309-3315.

Chapter 3

Exploration of a General Method for the Resolution of {TpMo*(L)(NO)}

3.1 Introduction:

Over the past 30 years π-basic dearomatization has provided a means for the facile synthesis of novel small molecules with a high degree of structural complexity. The synthetic power of this methodology is illustrated with the formation of new stereogenic centers within the cyclic framework afforded by aromatic ligands, enabling the creation of biologically interesting small molecule libraries. SAR studies have shown that greater biological activity is exhibited in structures with high fractions of saturation, as well the presence of chiral centers.[1] The chiral nature of biological systems results in reactivity which is heavily influenced by the chirality of the small molecules they interact with. Changes within the spatial orientation of bioactive molecules can result in the lack of biological response, or even harmful changes to reactivity.[2] Due to the importance of stereochemistry within the biological applications of small molecule synthesis, control of the absolute stereochemistry of the resulting chiral frameworks is paramount.

The chiral-at-metal complexes afforded by the [3-7]ligand motif established in the 2nd generation rhenium system, and incorporated into subsequent 3rd generation molybdenum and tungsten systems, allows for the possibility of *absolute* stereocontrol.[8-11] However, the syntheses of these systems, as outlined in Chapters 1 and 2, results in a racemic mixture of metal complexes (Scheme 1). The stereoselective nature of the ligand transformations employing these racemic mixtures provides *relative* control of the resulting stereocenters.[6-7, 10-25] However, the presence of both *R* and *S* forms of the metal center yields a racemic mixture of the resulting products (Scheme 1). In order to access the desired *absolute* stereocontrol, the racemic metal systems must be resolved.

3.2 Initial Attempts for Mo – Resolution: Chiral Ancillary Ligand {TpMo*(L*)(NO)}

Initial resolution attempts for chiral molybdenum dearomatization were based on the incorporation of a second stereogenic center at the ancillary ligand. With this strategy, the

addition of an enantiopure L* would transform the metal enantiomers into diastereomers, which could then be separated by physical means. Moreover, employing a chiral ancillary ligand also offered the possibility to influence the chiral nature of the metal center as the ancillary ligand is introduced to a prochiral complex (TpMo(NO)$(CO)_2$ or TpMo(NO)$(Br)_2$, Scheme 1). This method also offers a great deal of ligand choices, which fit well within the previously established tunable nature of molybdenum dearomatization agents (Chapter 2). Although there are a variety of commercially available chiral phosphines, the inability of {TpMo(PMe_3)(NO)} to produce dihapto-coordinate complexes, coupled with the larger steric profile and increased π-acidity of chiral phosphines compared to PMe_3, led us to look elsewhere. Looking back at ligands which have been shown to facilitate η^2-aromatic coordination (Chapter 2), we see that many hail from the pyridine family. Based on these data, *S*-nicotine was chosen as the ancillary ligand for molybdenum resolution; as it affords similar, if not moderately enhanced electronic donation compared to pyridine, while providing a negligible steric increase.

Initial attempts to incorporate the *S*-nicotine ancillary ligand were made via methods A and B (Scheme 1). However, while Method A consistently produced a species that fit the electronic profile of the desired product (as seen by CV monitoring of the reaction mixture), the product itself was not isolable using the established synthetic procedures. Moreover, while Method B did yield the desired product TpMo(nic)(NO)(CO) (**23**), which was subsequently oxidized to the Mo^{I} precursor TpMo(nic)(NO)(Br) (**16**), the results were not consistently reproducible.

In order to overcome these synthetic difficulties, Method C (Scheme 1) was employed, with the direct formation of TpMo(nic)(NO)(η^2-naphthalene) (**29**). The initial reduction conditions used THF as the solvent, however, due to the increased solubility of **29** compared to DMAP (**26**) and MeIm (**24**) analogs, the solvent was changed to Et_2O to improve chromatographic isolation.

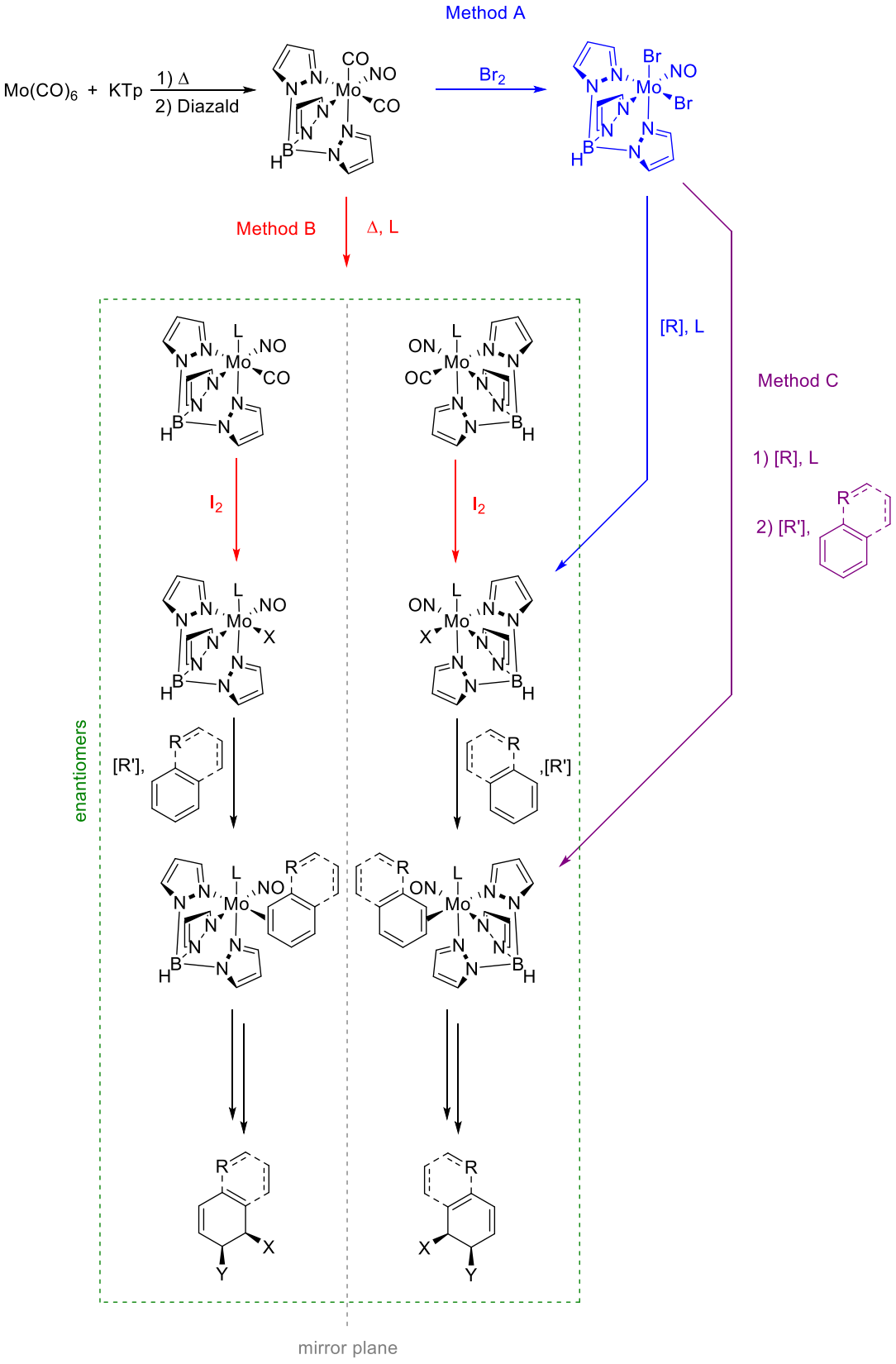

Scheme 1: The racemic synthesis of a molybdenum dearomatization agent.

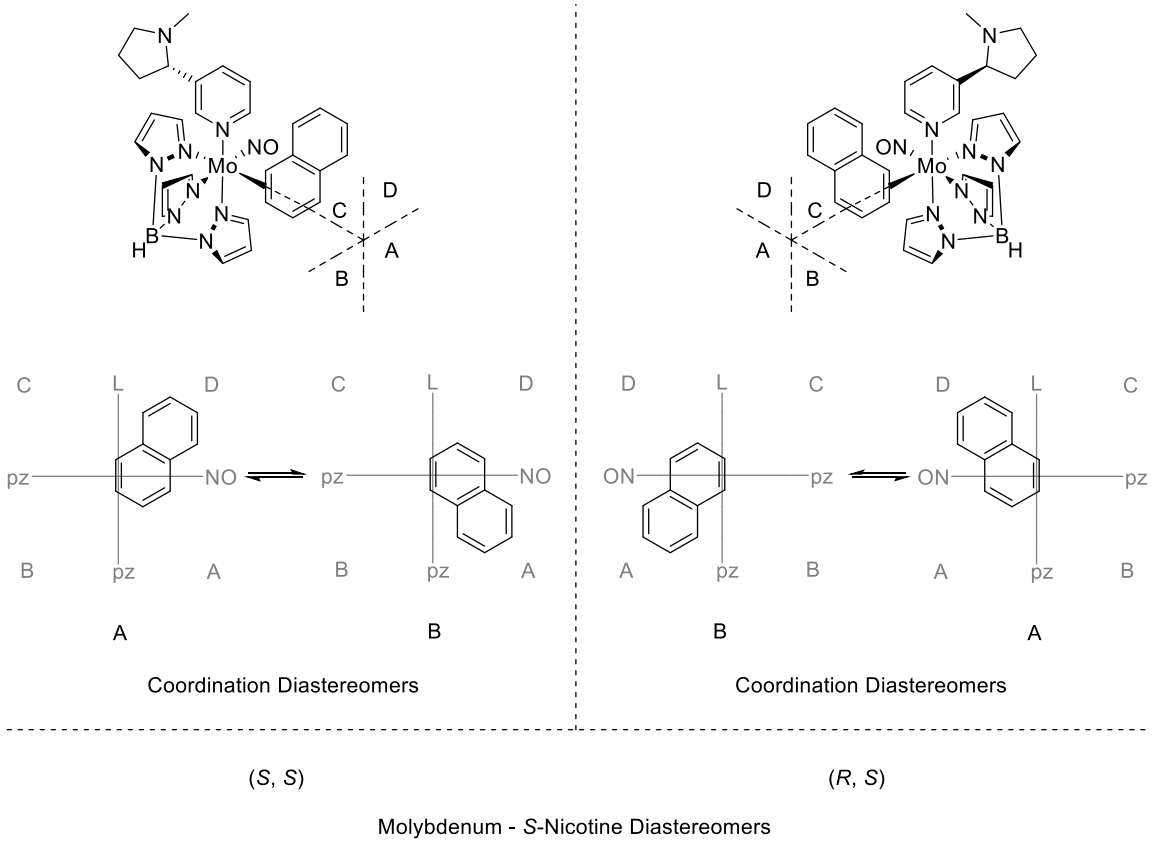

Figure 1: Molybdenum – *S*-nicotine diastereomers and coordination diastereomers of **29**.

^{1}H NMR analysis of **29** provided the same 4 : 1 ratio of A : B coordination diastereomers seen within the pyridine system **28** (Figure 1). At room temperature **29** produces broad signals for the protons of the coordinated naphthalene carbons (I and II in Figure 2A). These protons are easily identifiable on η^2-aromatic complexes, due to their upfield shift caused by electron donation from the molybdenum center, as well as the anisotropy of the nearby pyrazolyl rings.[3-9, 26-27] This signal broadening, which is only present in the major A isomer (I and II in Figure 2A), is due to rotation of the nicotine ligand on the NMR timescale. This is likely due to a higher barrier of rotation for the nicotine in the A coordination diastereomer, due to increased steric congestion in quadrant D, shared by nicotine and the uncoordinated naphthalene ring (Figure 1). The minor B isomer has a lower barrier of *S*-nicotine rotation due to the smaller steric profile of quadrant D (Figure 1), giving signal averaging of the *S*-nicotine rotamers (III and IV in Figure 2A).

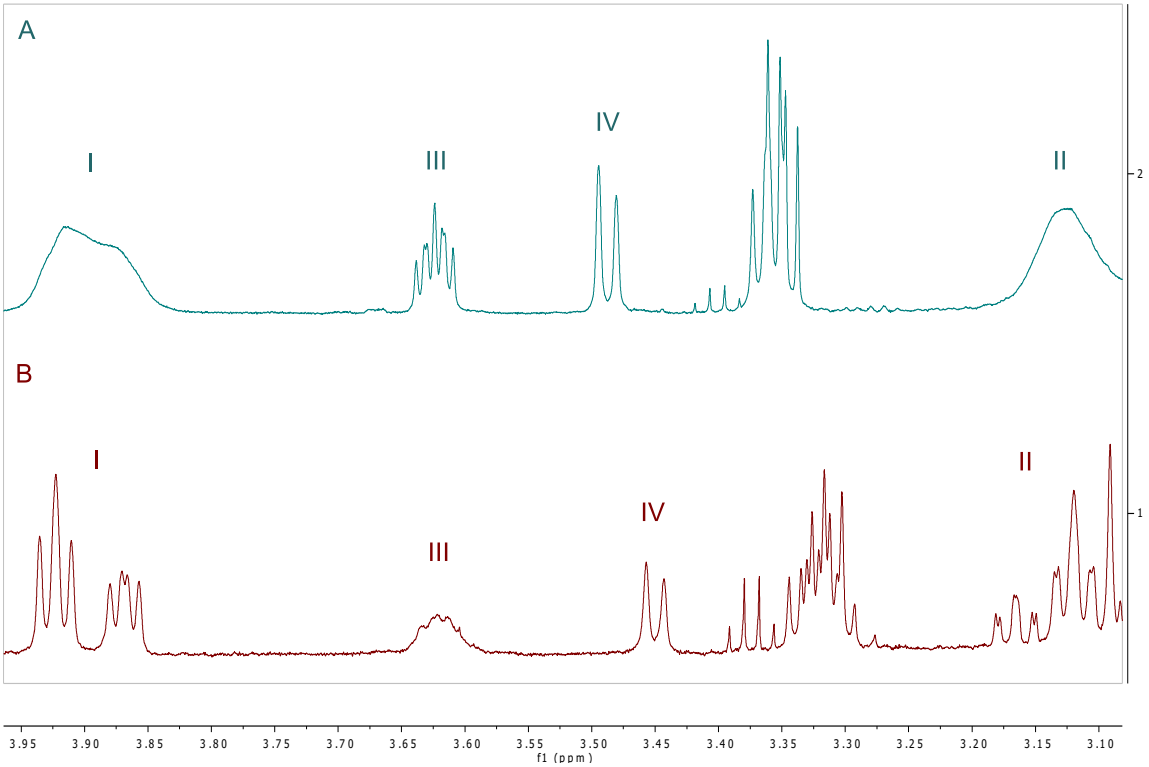

Figure 2: Coordinated protons of **29**, VT ^{1}H NMR resolution of rotamers shows 'chiral splitting' (1 = room temperature, 2 = -14^{o}C).

Dynamic ^{1}H NMR data shows the resolution of two rotamers upon cooling to -14 $^{\circ}$C from broad signals into two sets of signals for the I and II protons in a 1.7 : 1 ratio (Figure 2B). The ^{1}H NMR spectrum of **29** also shows increased splitting compared to all other η^{2}-naphthalene complexes isolated thus far. In the A isomer of **26** the naphthalene proton proximal to DMAP (I) is split into a doublet, while the proton distal to DMAP (II) is split into a doublet of doublets (Figure 3A). However, the low-temperature NMR spectrum of **29** shows the major A isomer split into an overlapping doublet of doublets for I, while II is split into an overlapping doublet of doublets of doublets (Figures 2B and 3B). The observed increase in splitting of I and II in **29** (Figures 2B and 3B) is likely coincidental overlap of metal diastereomers with similar chemical shifts (Figure 1). Furthermore, proton III in the NMR spectrum of **29** is split into a multiplet in contrast to the doublet of doublets observed for **26** (Figure 3A and B).

In order to obtain a better understanding of the spectral characteristics of **29**, without the increased spectroscopic challenges of the additional disatereomers produced by the incorporation of a 2nd stereogenic center, TpMo(3-pic)(NO)(η^2-naphthalene) (**30**) was synthesized. This model complex was used to determine if the additional splitting observed in **29** is due to the overlap of two (*R*, *S*) and (*S*, *S*) diastereomers (Figure 1). 3-Picoline was proposed as a model for *S*-nicotine, as it provided similar electronics with the coordination of a pyridine ring, and maintained substitution at the 3 position to mimic the sterics and NMR signal broadening observed with **29**. **30** proved to be a good model, giving a close match for the I and II naphthalene proton signals in **29** (Figure 3B and C). Like in the NMR spectrum of **29**, the signals for protons I and II of **30** were broadened, while the signals for protons III and IV remained sharp. Despite the broadening present in **30**, the signals for protons I and II display the expected doublet and doublet of doublets splitting patterns (Figure 3C). Moreover, III for **30** (Figure 3C) gives the expected doublet of doublets splitting pattern comparable to III in **26** (Figure 3A), while **29** produces a more complicated splitting pattern for III, consistent with overlap of molybdenum – *S*-nicotine diasteromers (Figure 3B). From these data we concluded that the additional 'splitting' observed in **29** (Figure 3B) is due to the formation of molybdenum – *S*-nictotine ((*R*, *S*),(*S*, *S*)) diastereomers is absent in **30** (Figure 3C). Due to the spectral complexity of 3-substituted pyridine ancillary ligands, and the lack of an easily isolable Mo*-L* diastereomer, resolution by chiral ancillary ligand was abandoned as a means for enantioenrichment of the molybdenum system.

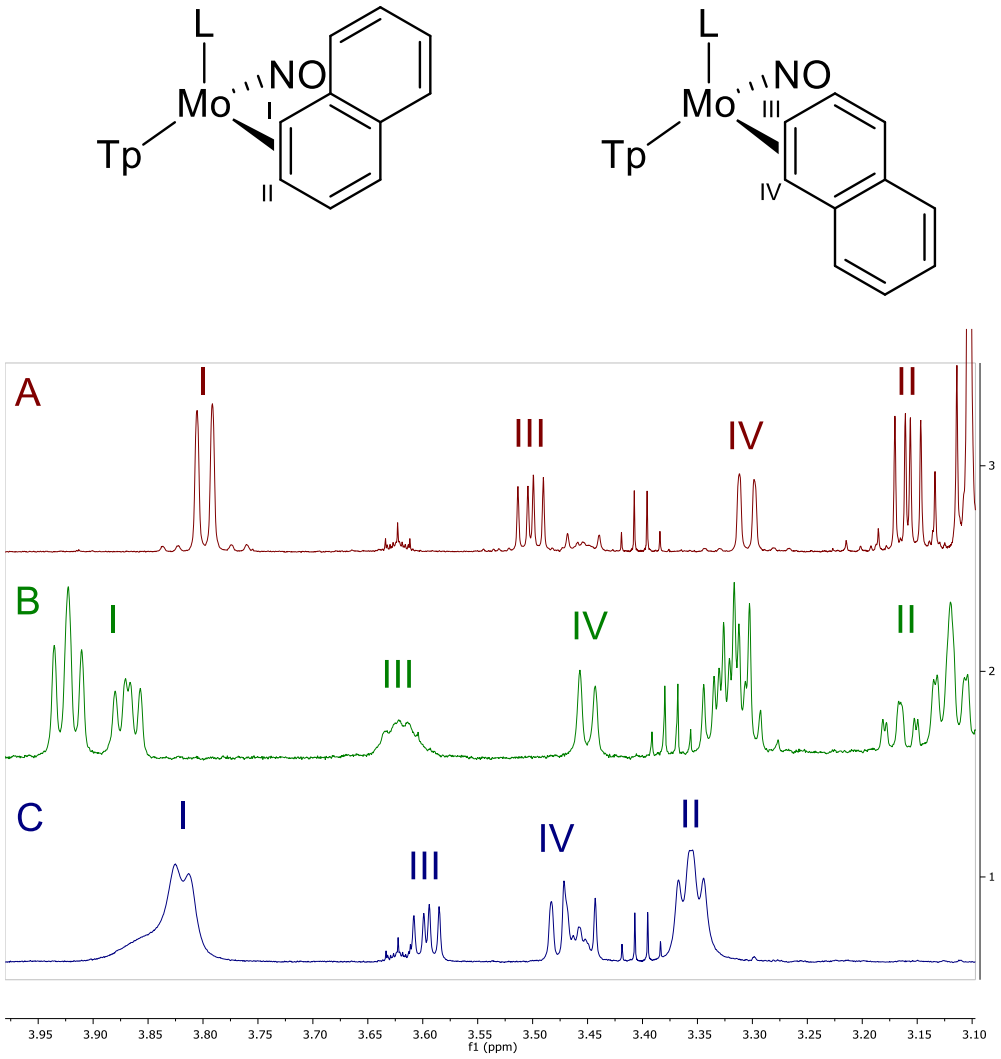

Figure 3: ^{1}H NMR signals of coordinated protons (I-IV) for **26**, **29**, and **30** (A, B, and C, respectively).

3.3 The Re – Resolution Method: Coordination of α-Pinene

The general method for resolution of the chiral {TpRe(MeIm)(CO)} fragment was accomplished by employing information gained from the steric trends of quadrant analyses (C>>B>A>D) within the context of the coordination of a variety of substituted alkene ligands. Studies involving the dihapto-coordination of tri-substituted alkenes showed that coordination occurred selectively, such that placement of alkyl substituents in quadrant C was limited.[9, 26] With this in mind, a general means of rhenium resolution was proposed by the dihapto-coordination of a tri-substituted chiral alkene. α-Pinene, commonly used for the preparation of hydroboration

agents, fit the desired profile, and is also relatively inexpensive and commercially available in both *R* and *S* forms.[9, 28]

Initial efforts to resolve the rhenium system employed *R*-α-pinene, which given the orientation of the double bond orthogonal to the CO to maximize backbonding, allows for eight possible coordination isomers (Figure 4).[26, 29-31] The geminal methyl bridgehead effectively blocks one face of the alkene from coordination, eliminating **III**, **IV**, **VII**, and **VIII**. Furthermore, placement of the ring in quadrant C is disfavored, eliminating **II** and **V**. This leaves two possible coordination isomers, one for each hand of the metal. However, **VI** places a methyl substituent in the C quadrant, while **I** only places a proton in the congested C quadrant. Due to the unfavorable steric interaction in **VI**, there is a thermodynamic bias favoring **I**, or the 'match' form, over **VI**, the 'mismatch' form (Figure 4).[9]

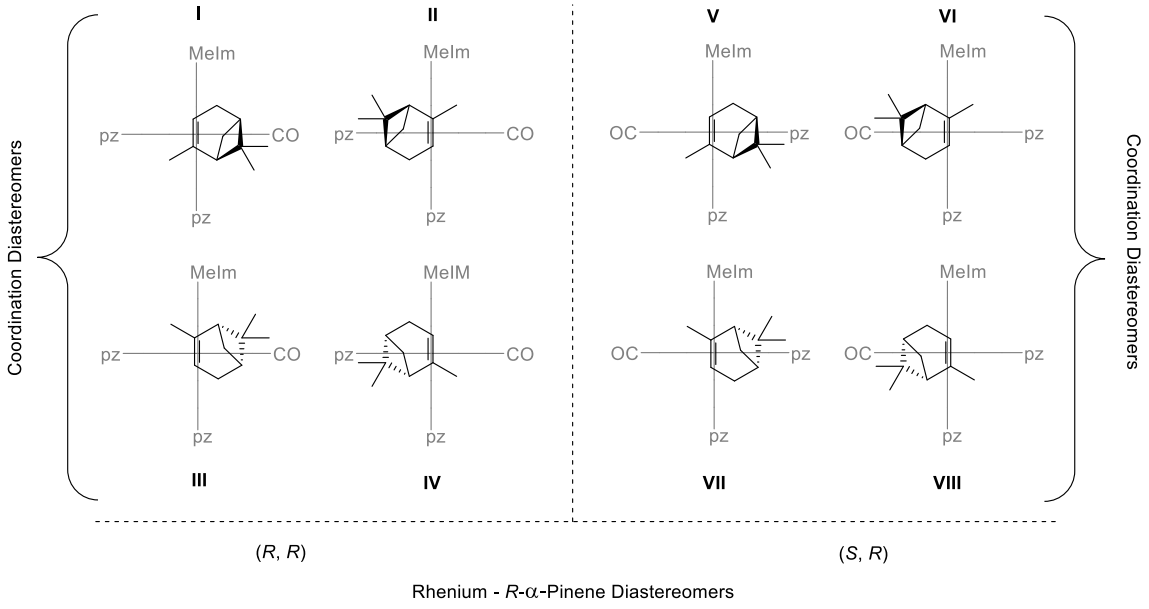

Figure 4: Possible coordination modes of TpRe(MeIm)(NO)(η²-*R*-α-pinene).

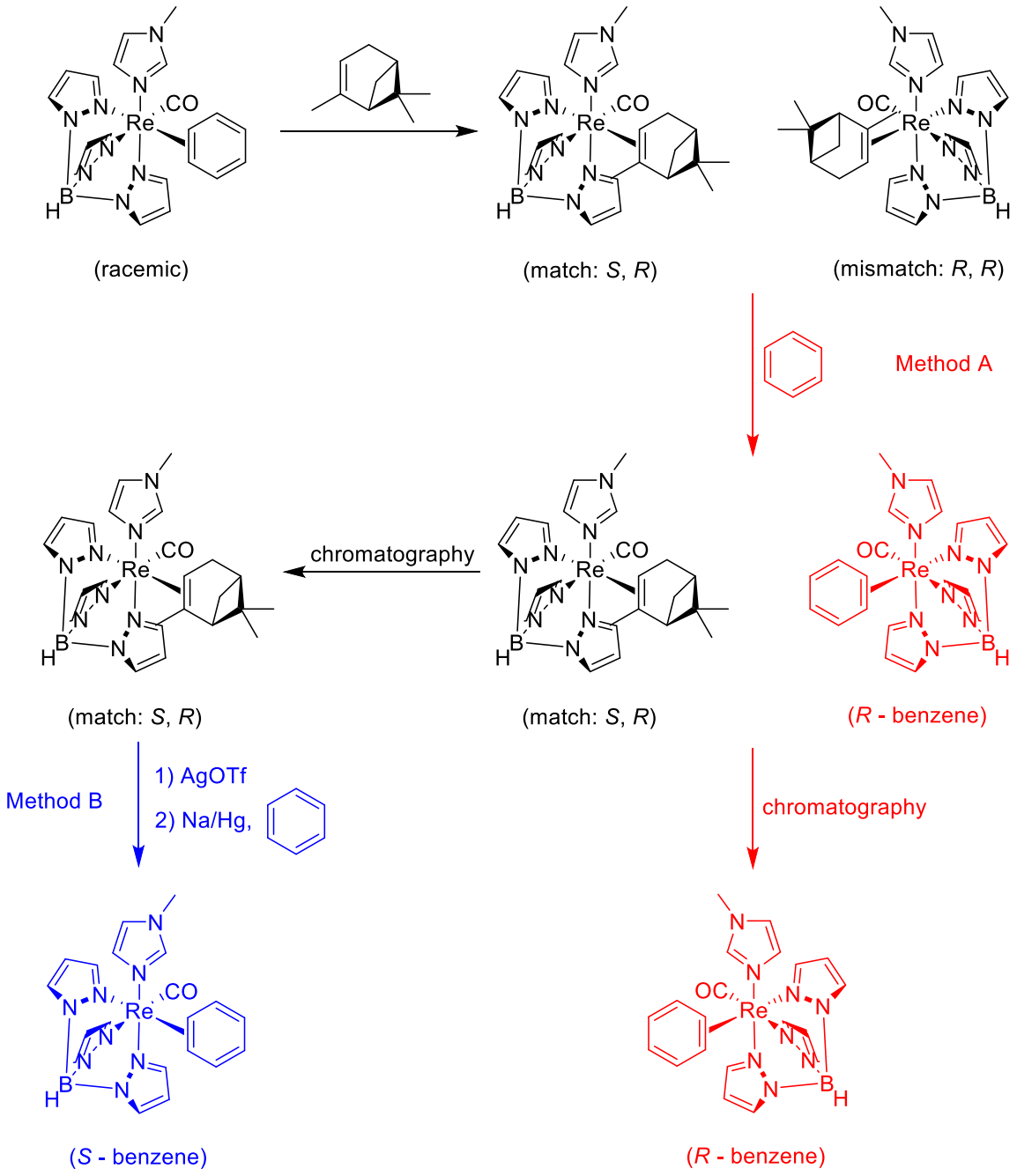

Scheme 2: Resolution of {TpRe*(MeIm)(CO)} by coordination of *R*-α-pinene.

Coordination of *R*-α-pinene results in the formation of both the match and mismatch isomers. However, due to the unfavorable steric interactions present in the mismatch complex, it is a more labile system than the match complex. The increased rate of substitution for the mismatch complex was used as the vehicle for the resolution of the rhenium system, as shown in

Method A (Scheme 2).[9] Match and mismatch complexes were synthesized by exchange from TpRe(MeIm)(CO)(η^2-benzene). The isolated mixture of was then stirred in benzene to generate *R*-TpRe(MeIm)(CO)(η^2-benzene), providing access to a variety of enriched rhenium complexes via benzene exchange (*vide supra*). Making use of the redox recyclability of the rhenium system, akin to that outlined for molybdenum in Chapter 2, *S*-TpRe(MeIm)(CO)(η^2-benzene) can be accessed by oxidation and reduction of the match α-pinene complex (Method B, Scheme 2).

With a resolution strategy in place, a method was required to test the stereochemical stability of the rhenium center throughout the exchange and redox processes. *S*-β-Pinene was used as the 'reporter' ligand for these studies. *S*-β-Pinene, like *R*-α-pinene, provides a 2nd chiral center which produces diastereomers upon coordination to the chiral rhenium center. However, unlike α-pinene it is a 2^{o} terminal alkene; and therefore lacks the methyl group that provides the thermodynamic bias used for the resolution process. The transfer of rhenium chirality to *R*-TpRe(MeIm)(CO)(η^2-benzene) and *S*-TpRe(MeIm)(CO)(η^2-benzene) was measured by exchange for *S*-β-pinene, yielding diastereomeric ratios (dr) of 19 : 1. Given the 97% ee of the *S*-β-pinene used for the exchanges, these drs correspond to maintaining 96% of the rhenium chirality.[9]

3.4 Application of α-Pinene Method to Mo – Resolution

Given the similarities between rhenium and molybdenum systems (tunable ligand set, recyclability), we sought to apply α-pinene coordination as a method for general molybdenum resolution. We approached this strategy expecting similar results to the rhenium system, and a similar means to access both hands of molybdenum. However, unlike rhenium, we had been unable to coordinate benzene with molybdenum, and therefore lacked the exchange pathway employed in the rhenium case. Instead we coordinated *R*-α-pinene by reduction, to give TpMo(DMAP)(NO)(η^2-*R*-α-pinene) (**34**). Given the relative synthetic ease, and focus on the DMAP

ancillary ligand, a one pot reduction from TpMo(NO)$(Br)_2$ to **34** was pursued (Method C, Scheme 1).

Initial reductions were carried out in THF, using the same conditions optimized for the synthesis of **26**. However, **34** gives increased solubility in non-polar solvents compared to previous TpMo(L)(NO)(η^2-naphtalene) complexes (**24**, **26**, **28**-**33**), and the reduction solvent was changed to Et_2O for ease of product isolation. Unexpectedly, the synthesis of **34** provided only one species in the ^{1}H NMR. 2D NMR analyses of the product are consistent with the anticipated matched product; however, signals consistent with the mismatched product were absent. This is due to the reduced efficacy of backbonding with 2nd row molybdenum, compared to 3rd row dearomatization agents (*vide supra*). Syntheses of **34** have yet to give a yield of greater than 50%. This result may indicate that the molybdenum system is stereochemically stable within the reduction conditions employed (giving a maximum yield of enantiopure **34** of 50% from racemic starting material). **34** provides an electronic profile which is similar to previous molybdenum dihapto-alkene and aromatic complexes (-0.17 V, ν_{NO} = 1548 cm^{-1}). The ^{1}H NMR spectrum shows a distinguishing feature of the coordinated methyl, which is placed in the 'Tp pocket' of quadrant B. The methyl signal is shifted upfield (0.60 ppm), due to a combined effect of increased electron density from molybdenum backdonation, as well as anisotropy due to the placement between pyrazolyl rings of the Tp ligand.[3, 5-7, 9, 26, 32] This methyl signal provides a convenient method for identification of the complex (*vide infra*).

3.5 Accessing Enriched TpMo(DMAP)(NO)(η^2-aromatic)

Following the effective resolution of the chiral molybdenum center by coordination of *R*-α-pinene, a procedure for exchanging the α-pinene ligand for an aromatic was required. The analogous rhenium match complex required redox chemistry to yield an η^2-aromatic complex (Method B, Scheme 2); however, with the well documented reduced backdonation of the 2nd row

molybdenum system, we decided to first try substitution similar to that of the rhenium mismatch complex (Method A, Scheme 2).

Initial tests for exchange of the α-pinene ligand were conducted in neat d^6-acetone to allow for ^{1}H NMR monitoring of the reaction progress. Moreover, conducting the experiment in neat d^6-acetone provided pseudo-1st order conditions for the exchange; and with past reports of the dissociative nature of ligand exchanges within our dearomatization agents, would allow for simplified rate information.[4, 6-7, 11, 27, 33-34] Reaction progress was easily monitored due to the unique spectroscopic signals of the coordinated methyl of both **34** and free *R*-α-pinene. When coordinated, the vinyl methyl appears as a singlet at 0.60 ppm, whereas the same methyl in free α-pinene is a quartet at 1.64 ppm. The ^{1}H NMR experiment showed the disappearance of the signal at 0.60 ppm over the course of 2 days, while signals matching TpMo(DMAP)(NO)(η^2-acetone) (**35**) became the dominant features. This result demonstrated that **34** substitutes (~2 days) at a rate similar to the rhenium mismatch complex (60 h).[9]

With the ability to exchange the resolving *R*-α-pinene ligand of **34**, the acetone experiment was repeated in THF, DME, benzene, and Et_2O (~100 mg **34** in 3 mL solvent), all with 10 molar equivalents of acetone. In THF, DME, and benzene **35** was produced in good yield (average 70 %) in the same time frame as the initial experiment in neat d^6-acetone. The Et_2O exchange also afforded **35** in good yield, although due to the heterogeneous nature of the exchange, the required time was increased to 6 days. Finally the exchange conditions were tested with a ligand of synthetic interest, naphthalene, which afforded **26** in good yield (80 %).

3.6 Mo – Racemization Studies: *S*-β-Pinene

With the ability to access multiple ligands (naphthalene, acetone) from **34**, racemization studies were performed to test the transfer of molybdenum chirality. These studies employed *S*-β-pinene as the chiral reporter ligand, using the exchange conditions established with

naphthalene (Method A, Scheme 3). Within these ^{1}H NMR experiments, we observed the disappearance of the 0.60 ppm signal associated with **34** over the course of 3 days. Upon analysis of TpMo(DMAP)(NO)(η^2-*S*-β-pinene) (**36**) we expected to see either one or two complexes; indicating the transfer of molybdenum chirality, or the loss of some portion of chirality through the exchange process. However, we once again were faced with a departure from the trends of 3rd row metal – η^2-pinene complexes, with the formation of four distinct isomers. These were categorized by the signal for the DMAP methyls, which is distinct in that it appears near 3 ppm, and gives a 6H integration (Figure 5). Full characterization was not carried out for **36**, due to the spectral complexity of 4 coordination isomers, which give a great deal of signal overlap; however, major spectral features (DMAP signals, β-pinene methyl signals, number of Tp triplets) gave integrations consistent with four complexes of η^2-*S*-β-pinene.

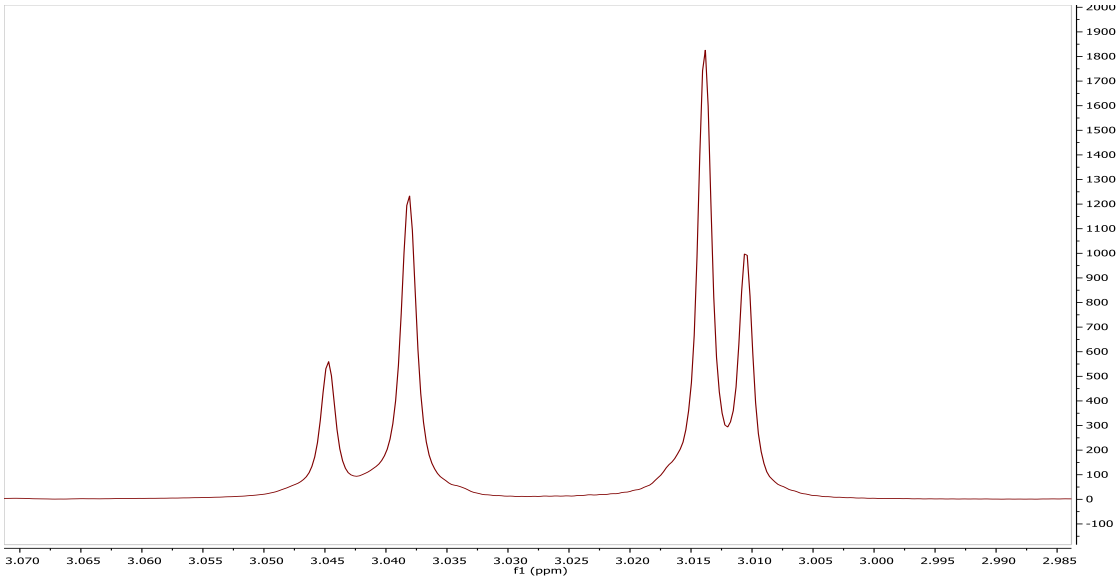

Figure 5: ^{1}H NMR signals for DMAP methyl groups of **36** isomers.

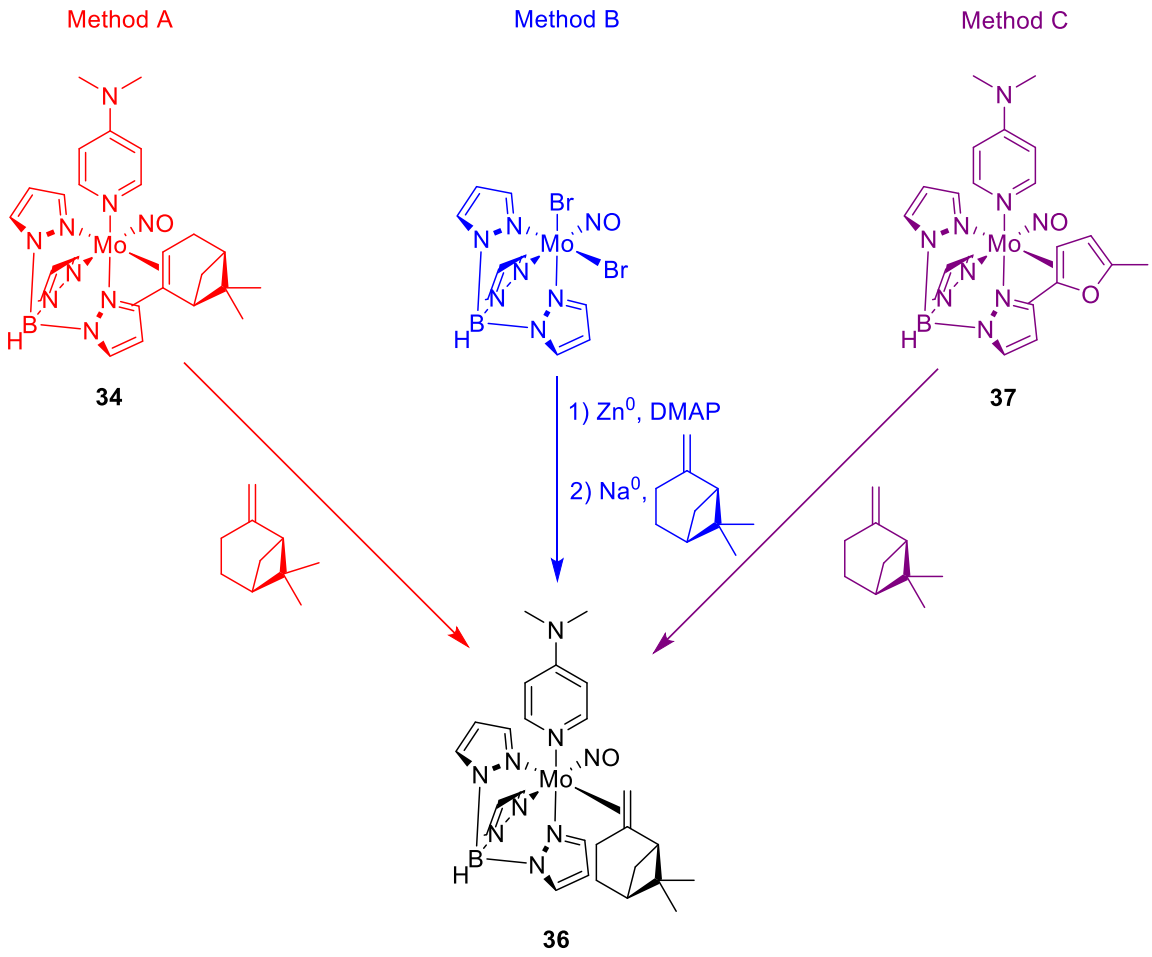

Scheme 3: Synthetic pathways to **36** to test for transfer of molybdenum chirality.

With this unexpected result, we sought to synthesize **36** from a racemic mixture. We took two approaches toward racemic **36**, one through the reduction conditions employed for **34**, and also by exchange from TpMo(DMAP)(NO)(η^2-2,5-dimethylfuran) (**37**) (Methods B and C, Scheme 3). In both cases **36** exhibited the same ratio of DMAP signals as the initial exchange from **34** (Figure 5). Based on these data we concluded that the 2nd row molybdenum center is more prone to racemization than 3rd row rhenium and tungsten systems.[9, 11] We believe that subtle changes to the sterics and electronics of the molybdenum system compared to 3rd row rhenium and tungsten systems affords the multiple coordination diastereomers observed with **36**, two for each hand of molybdenum (Figure 6).

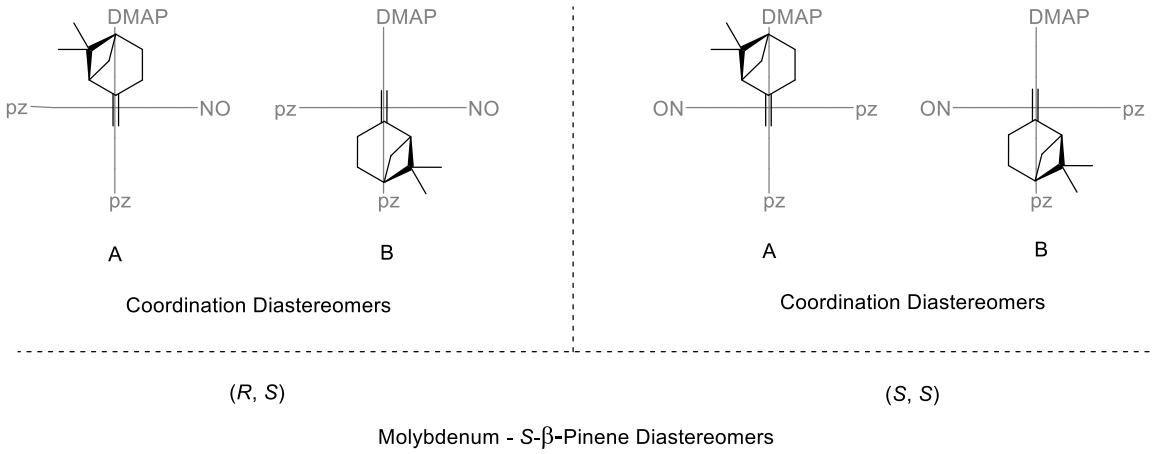

Figure 6: Proposed coordination isomers of **36**.

3.7 Mo – Racemization Studies: Exploration of a Reporter Ligand

Given the spectral complexity of **36**, we investigated replacement chiral reporter ligands before continuing our racemization studies. Ideally the reporter ligand would provide a single coordination diastereromer for each hand of the metal center, while giving no preference between *R*-TpMo(DMAP)(NO)(η^2-L*) and *S*-TpMo(DMAP)(NO)(η^2-L*). *R*-Fenchone, *S*-camphor, *S*-verbenone, and *R*-myternal were proposed as possible dihapto-chiral reporters (Figure 7), and were coordinated using the optimized exchange conditions from **34**.

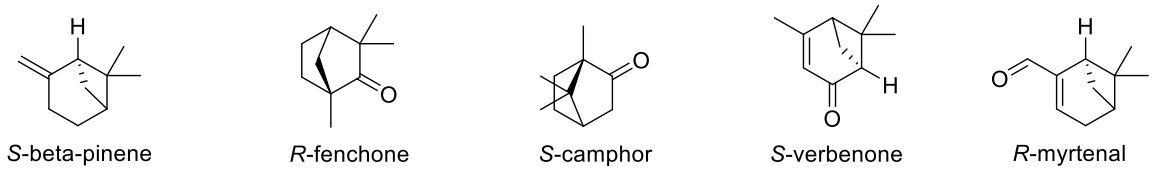

Figure 7: Chiral reporter ligands.

Of the chiral reporters illustrated in Figure 7, *R*-fenchone and *S*-camphor were the most appealing. Both ketones offer a single binding location, while giving a bulky ring structure similar to α- and β-pinene to promote coordination to a single face of the carbonyl. Moreover, coordination of *R*-fenchone and *S*-camphor would place the stereogenic center of the ligand in close proximity to the metal center, resulting in a greater difference in the chemical environments of the resulting diastereomers. While TpMo(DMAP)(NO)(η^2-*R*-fencone) (**38**) and

TpMo(DMAP)(NO)(η^2-*S*-camphor) (**39**) produced ^{1}H NMR spectra with less spectroscopic congestion than **36**, they still provided more than two DMAP signals (Figure 8A, B).

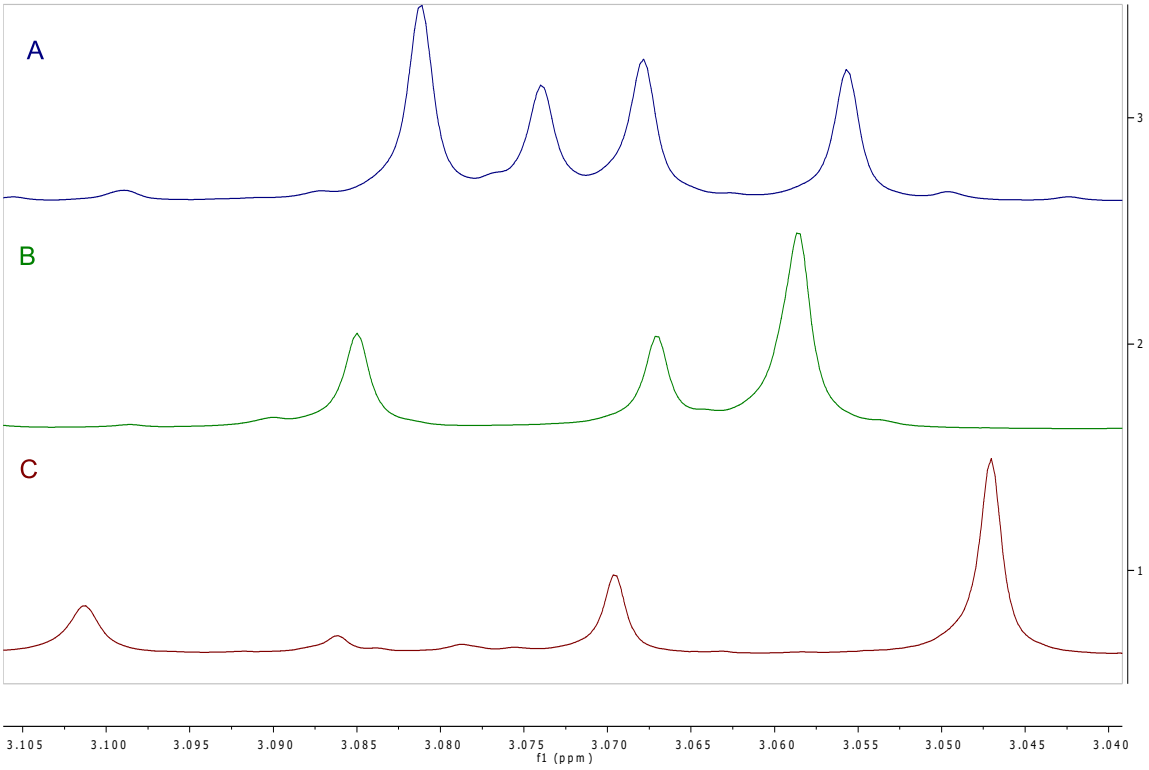

Figure 8: ^{1}H NMR signals for DMAP methyl groups of **38**, **39**, and **40** isomers (A, B, and C, respectively).

Due to the undesired multiple coordination isomers present in **38** and **39**, *S*-verbenone and *R*-myrtenal were investigated as *S*-β-pinene replacements. While the multiple coordination sites (carbonyl and alkene) were not ideal, we expected preferential coordination to the carbonyl. This is due to the same steric interactions present in **34**, as both ligands offered trisubstituted alkenes, which would be unlikely to compete with the sterically less hindered carbonyl position. Moreover, coordination through the carbonyl is likely kinetically preferred, as it is able to provide an initial κ^1-coordination mode by donation from the oxygen lone pairs.

S-Verbenone was thought to be the better option between the two, due to its increased sterics around the carbonyl compared to *R*-myrtenal, which we proposed to limit the number of coordination isomers. Moreover, the coordination through the *S*-verbenone carbonyl would

place the ligand's stereogenic center in closer proximity to the molybdenum center than *R*-myrtenal, allowing for easier differentiation of resulting diastereomers via NMR (*vide supra*). However, like **36**, **38**, and **39**, TpMo(DMAP)(NO)(η^2-*S*-verbenone) (**40**) produced more than the desired two coordination isomers (Figure 8C).

Exchange from **34** to TpMo(DMAP)(NO)(η^2-*R*-myrtenal) (**41**) gave another unexpected, but welcome result, with the formation of only two DMAP signals (Figure 9A). With this result **41** was also synthesized by exchange from racemic **37**, which produced the same signals, indicating that racemization of **34** continued within the exchange process. With this result in hand, characterization of **41** was carried out in order to determine the coordination mode of the ligand. CV is consistent with coordination at the aldehyde with $E_{p,a}$ = 0.40 V, which is comparable to other η^2-carbonyls (*e.g.*, **35** (0.27 V)), and more positive than η^2-alkenes (*e.g.*, **34** (-0.17 V)).[3, 27, 32] Moreover, ^{1}H NMR data is consistent with aldehyde coordination given the absence of the free aldehyde proton at ~10 ppm, which is shifted dramatically upfield by dihapto-coordination of the carbonyl to ~4 ppm (III in Figure 9B), while the alkene proton sees nearly no change in chemical shift (II in Figure 9B). Finally, the ^{13}C NMR is consistent with aldehyde coordination, with the absence of aldehyde signals at 190 ppm.

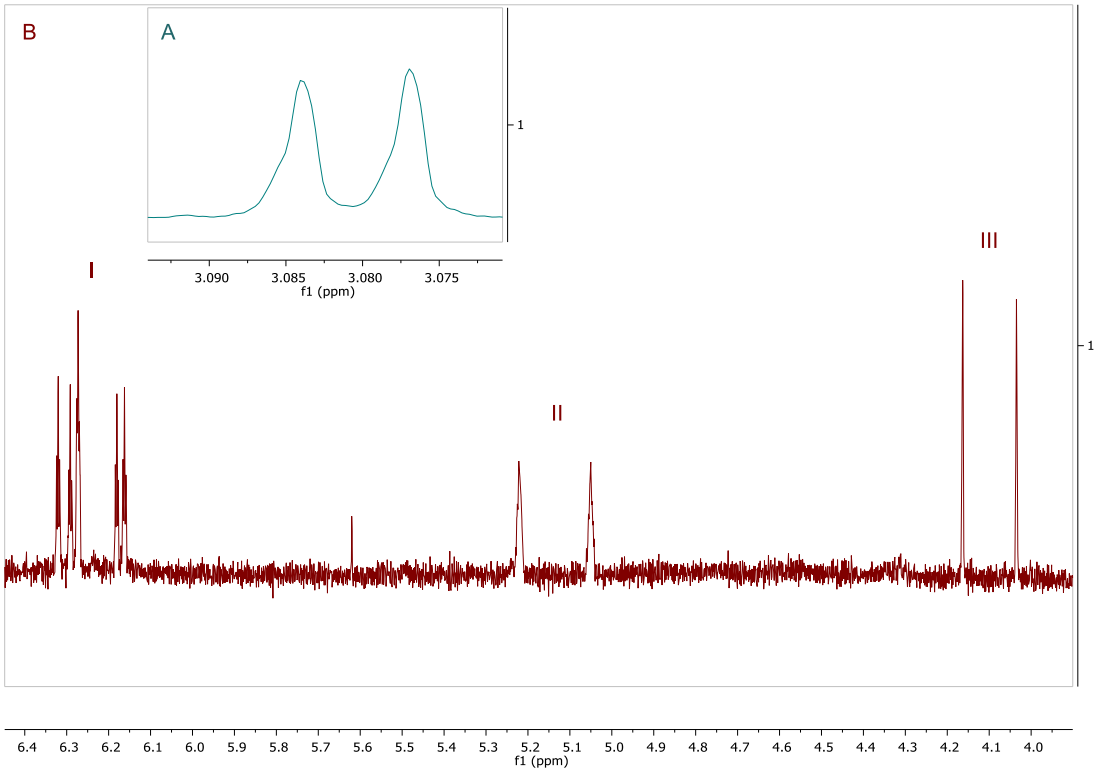

Figure 9: 1 : 1 dr ^{1}H NMR signals for **41**.

3.8 Mo – Racemization Studies: TpMo(DMAP)(NO)(η^2-α-Pinene) Exchange Conditions

With *R*-myrtenal established as a reliable chiral reporter ligand, the exchange conditions from **34** to **41** were probed for a means to overcome the racemization process. Initial experiments were focused on the solvent system of the exchange. Racemization studies within the rhenium system showed loss of enrichment in the redox pathway (Method B, Scheme 2) when carried out in benzene; however, racemization was prevented with the addition of THF as a cosolvent.[9] The importance of THF is its ability to act as a placeholder to stabilize the 5-coordinate intermediate following dissociation of the *R*-α-pinene ligand. With these data in mind, ether based exchanges (THF, DME, Et_2O) were scrutinized against those with benzene as the solvent; however, all cases gave the same 1 : 1 result of **41** diastereomers.

The effects of temperature were also tested as a means to increase the rate of substitution relative to the rate of racemization. Within these tests were elevated temperatures

(50, 100 °C), which resulted in decomposition. The opposite approach was also taken with reduced temperatures; however, running the exchanges at -30 °C gave no reaction progress over the course of > 30 days.

3.9 Mo – Racemization Studies: TpMo(L)(NO)(η²-α-Pinene) Exchange Conditions

Given the inability to transfer the resolution of **34** through exchange reactions we looked to probe the impact of the ancillary ligand on racemization. Given the range of ancillary ligands which afford η²-naphthalene complexes, we had a variety of options to apply to the α-pinene resolution strategy. MeIm was initially explored given the similar electronic profile to **34**, while also having a reactivity profile established by Jeff Myers (Chapter 2). Moreover, MeIm provides a slimmer steric profile than DMAP, which we reasoned may help to reduce the driving force for ligand migration within the proposed 5-coordinate intermediate (Scheme 4).

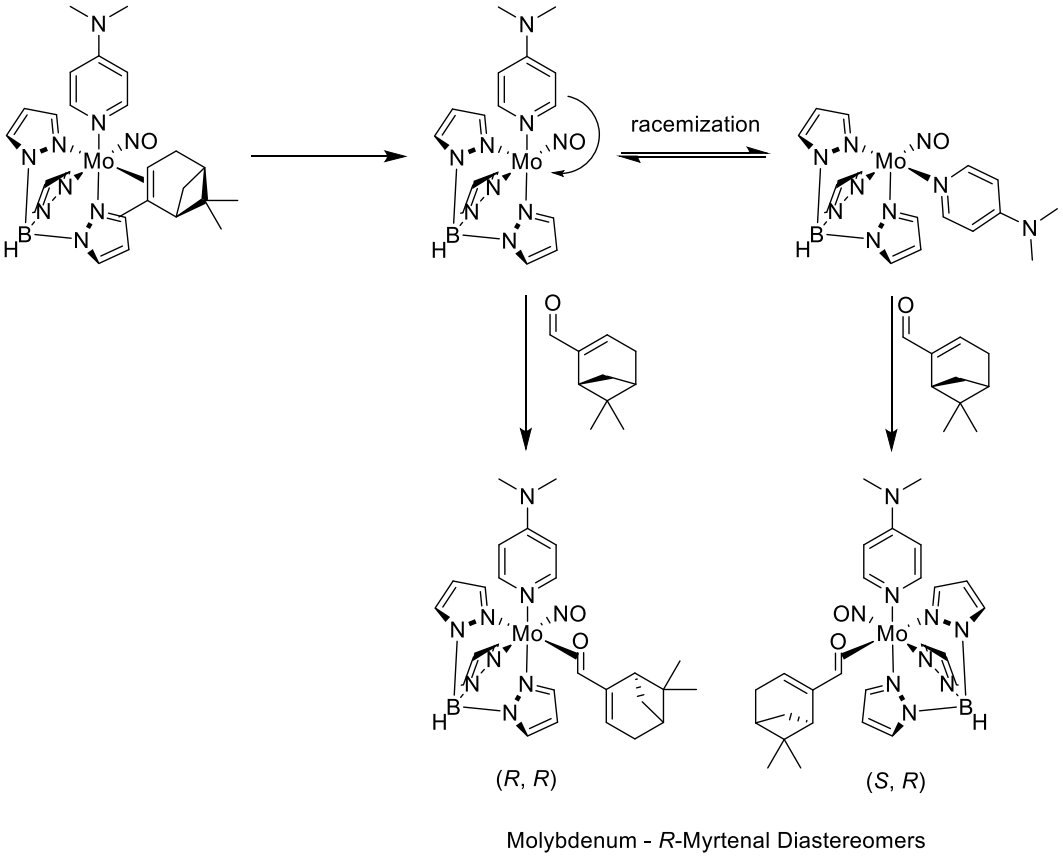

Scheme 4: Proposed racemization of {TpMo(DMAP)(NO)}.

TpMo(MeIm)(NO)(η^2-*R*-α-pinene) (**42**) was prepared via Methods B and C (Scheme 1) in low yields compared to that of **34** (10 %). **42** provided a spectroscopic profile similar to that of **34**, with the same convenient upfield methyl group (0.55 ppm) for ^{1}H NMR reaction monitoring. The slight decrease in reduction potential and steric profile within the {TpMo(MeIm)(NO)} fragment were manifested in a decreased rate of substitution for **42** relative to **34** (>10 days vs 3 days to completion, respectively). However, this was accompanied by a slight increase in the transfer of molybdenum chirality, with exchange to TpMo(MeIm)(NO)(η^2-*R*-myrtenal) (**43**) yielding a 2 : 1 diasteromer ratio. Although the {TpMo(MeIm)(NO)} fragment may provide enhanced stability of the chiral metal center, its slow rate of exchange limits the applicability of **42** for molybdenum resolution.

NH_3 was tested next due to its minimal steric profile, which we proposed to be a contributing factor in the racemization process. However, these attempts were hampered by the familiar synthetic difficulty of both {TpMo(NH_3)(NO)} and {TpRe(NH_3)(CO)} systems. Despite a variety of synthetic attempts using Methods A and C (Scheme 1), we were unable to identify any species consistent with the desired TpMo(NH_3)(NO)(η^2-α-pinene).

Keeping in mind the potential importance of sterics on the racemization process, we looked to incorporate F^- and CN^-, which give a reduced steric profile from DMAP, MeIm, and NH_3. Moreover, these ligands provide possible electronic benefits by increasing π-interactions with the molybdenum center. We reasoned that the tiny sterics, combined with possible π-donation from F^- or CN^-, would allow us to block the proposed migration of the ancillary ligand. Attempts to coordinate F^- proceeded through all three developed methods in Scheme 1. However, all attempts at F^- incorporation failed. This is likely due to the documented π-donor ability of the F^- ligand, which like NH_3, produces highly reducing complexes that are prone to oxidative decomposition.[4, 6, 35] Attempts to incorporate CN^- were more successful, likely due to the ability

of the ligand to act as both a π-acid or π-base, helping to stabilize a range of electronic environments. $[TpMo(CN)(NO)(Br)]^-$ (**21**) was prepared via Method A (Scheme 1) in yields comparable to other Mo^I species (89 %). However, coordination of α-pinene remained elusive via Methods A and C (Scheme 1). These synthetic difficulties may be due to the charge of the molybdenum species, giving **21** and the desired $[TpMo(CN)(NO)(\eta^2\text{-}\alpha\text{-pinene})]^-$ dramatically different physical properties compared to neutral **34** and **42**. Moreover, the charged complex would provide further synthetic difficulty due to incompatibility with the established chromatography-based work-up conditions of **34** and **42**.

Finally, pyridine was investigated as a means to overcome the molybdenum racemization issue. While pyridine does not offer any steric advantages over DMAP; the increased reduction potentials of pyridine complexes (Chapter 2), fit the extensive literature reports of Brunner, which show increased chirality transfer of chiral-at-metal systems with reduced electron density.[36-41] Synthesis of the desired $TpMo(py)(NO)(\eta^2\text{-}\alpha\text{-pinene})$ followed Method C (Scheme 1), which produced $TpMo(py)(NO)(\eta^2\text{-naphthalene})$ (**28**) in moderate yield (24 %). However, despite electrochemical glimpses of a species consistent with the desired product during reaction monitoring, $TpMo(py)(NO)(\eta^2\text{-}R\text{-}\alpha\text{-pinene})$ was never isolated. This is likely due to the sensitive nature of the complex, as the relatively high reduction potential of {TpMo(py)(NO)} may be unable to adequately stabilize the demanding sterics of the tri-substituted *R*-α-pinene ligand. We reason that $TpMo(py)(NO)(\eta^2\text{-}\alpha\text{-pinene})$ can be produced, however, was not isolated due to an increase in the substitution half-life of the complex from the relatively weak donation of the {TpMo(py)(NO)} fragment.

3.10 Mo – Racemization Studies: $TpMo(DMAP)(NO)(\eta^2\text{-}\alpha\text{-Pinene})$ Redox Conditions

With the inability to retain the resolution of **34** through exchange, the redox pathway established within the rhenium system was explored as an alternative (Method B, Scheme 2). This

pathway was effective within the rhenium system in the presence of a weakly coordinating cosolvent, and is compatible with the recyclability of the {TpMo(DMAP)(NO)} fragment, (*vide supra*). Moreover, we hoped that progressing through a Mo^{I}* (**20***) species would allow for increased transfer of metal chirality, consistent with the reports of Brunner.[36-41]

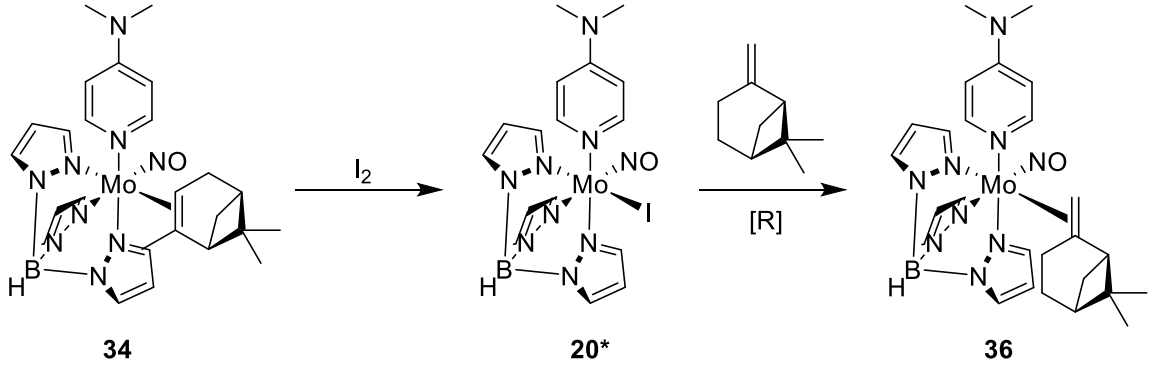

Scheme 5: Proposed redox scheme to overcome molybdenum racemization.

These efforts applied the oxidation procedure developed by Jeff Myers and gave **20*** in quantitative yield (Scheme 5). We looked to access a Mo^{0} species and assess the chirality transfer of the redox processes via ^{1}H NMR. Although we would have liked to test the dr of the complex using *R*-myrtenal, the strongly reducing conditions required are not compatible with the aldehyde functionality. Instead we used *S*-β-pinene, which is amenable to the highly reducing conditions, as our reporter ligand (Scheme 5). Unfortunately this resulted in the familiar ratio of 4 coordination isomers, shown by the ratio of DMAP methyl signals in Figure 5. Regrettably, this result does not allow us to determine if racemization occurs during *oxidation*, *reduction*, or *both*, only that complete racemization occurs. A final effort was made by oxidizing **34** to **20*** at reduced temperatures. Within this scenario we hoped that racemization occurs during the initial oxidation step of the redox process (Scheme 5), and that reduced temperatures would have a greater impact on the racemization rate than the rate of electron transfer. This again produced **20*** in good yield, but yielded the same ratio of diastereomers in **36**. Unfortunately, these data are not

conclusive, and we have yet to determine whether molybdenum resolution is maintained during the oxidation from **34** to **20***.

3.11 Mo – Racemization Studies: Redox Catalyzed Exchange of TpMo(DMAP)(NO)(η²-α-pinene)

Current work by Steven Dakermanji has provided hints into the chirality transfer process within the molybdenum system. While **34** was initially produced via Method C (Scheme 1), Steven Dakermanji produced **34'** via exchange from TpMo(DMAP)(NO)(η²-α,α,α-trifluorotoluene) (**I**) (Scheme 6, which will be discussed in greater detail in Chapter 4). This has given access to **34'** in higher yields (70 vs 40 % for exchange vs reduction, respectively), although the lack of a chromatographic work-up has resulted in a decrease in purity via the exchange method.

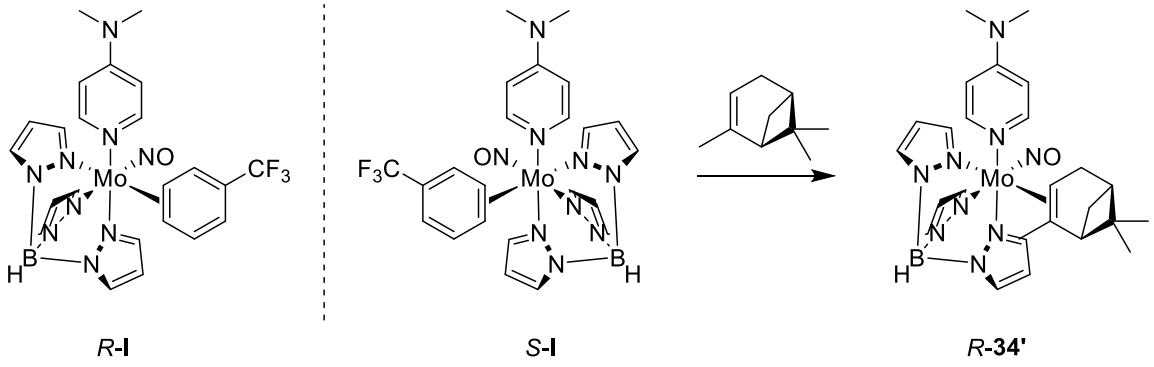

Scheme 6: Synthesis of **34** from TpMo(DMAP)(NO)(TFT) (**I**).

Steven Dakermaji has exchanged **34'** in neat *R*-myrtenal (~50 molar equivalents) yielding **41** with a 10 : 1 dr (Figure 10A), compared to the previously discussed 1 : 1 dr via **34** exchange with 10 molar equivalents of *R*-myrtenal (Figure 10B). Moreover, the rate of exchange was dramatically increased from ~3 days to <75 min. Interestingly, when **34'** was subjected to exchange conditions with 10 molar equivalents of *R*-myrtenal in an ethereal solvent, **41** was isolated with the same 1 : 1 dr and ~3 day substitution timeline as from **34**. Based on this surprising result the neat exchange of **34'** was applied to *S*-β-pinene, whose absence of lone pairs provides a more accurate model to aromatic systems. However, **34'** has reduced solubility in *S*-β-pinene compared to *R*-myrtental, producing a heterogeneous reaction mixture which

prevented direct exchange comparisons. Moreover, **36** produced from **34'** provided the same ratio of coordination isomers as our original experiments (Figure 5), indicating racemization during the exchange process.

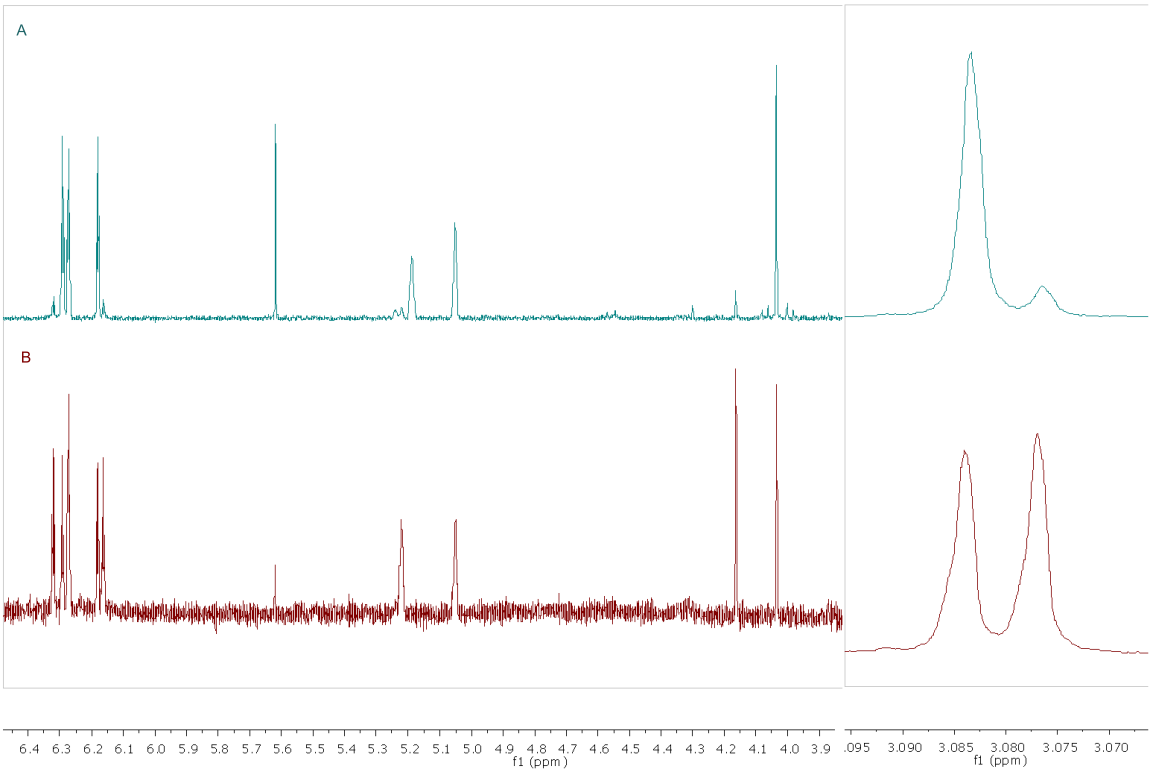

Figure 10: 10 : 1 dr ^{1}H NMR signals for **41** via Scheme 9.

Steven Dakermanji has gone on to test **34'** exchange conditions with the previously explored *R*-fenchone, which again pointed toward racemization, and also lacked the rate increase seen with *R*-myrtenal. Subsequent studies have shown exchanges from both **34'** and **26'** to have dramatically increased substitution rates when the exchange is carried out in neat *R*-mytrenal. We propose that this rate enhancement is due to the ability to access TpMo^{I}(DMAP)(NO)(κ^1-*R*-myrtenal) (**A**), which can isomerize to TpMo^{I}(DMAP)(NO)(η^2-*R*-myrtenal) (**B**) (Scheme 7). The ability to isomerize between κ^1- and η^2-myrtenal forms also produces a dramatic shift in reduction potential, allowing **B** to be reduced by **34** to form the product **41** with minimal chirality loss. The resulting **C** quickly loses the bulky α-pinene ligand, reforming the catalytic Mo^{I} species **A** (Scheme

7). We believe the ability to access the Mo^{I} – η^2-carbonyl from the initial κ^1-coordination mode is essential. For this reason rate enhancement, as well as chirality transfer, has only been observed in the coordination of sterically small carbonyls (*e.g.*, aldehydes and acetone).

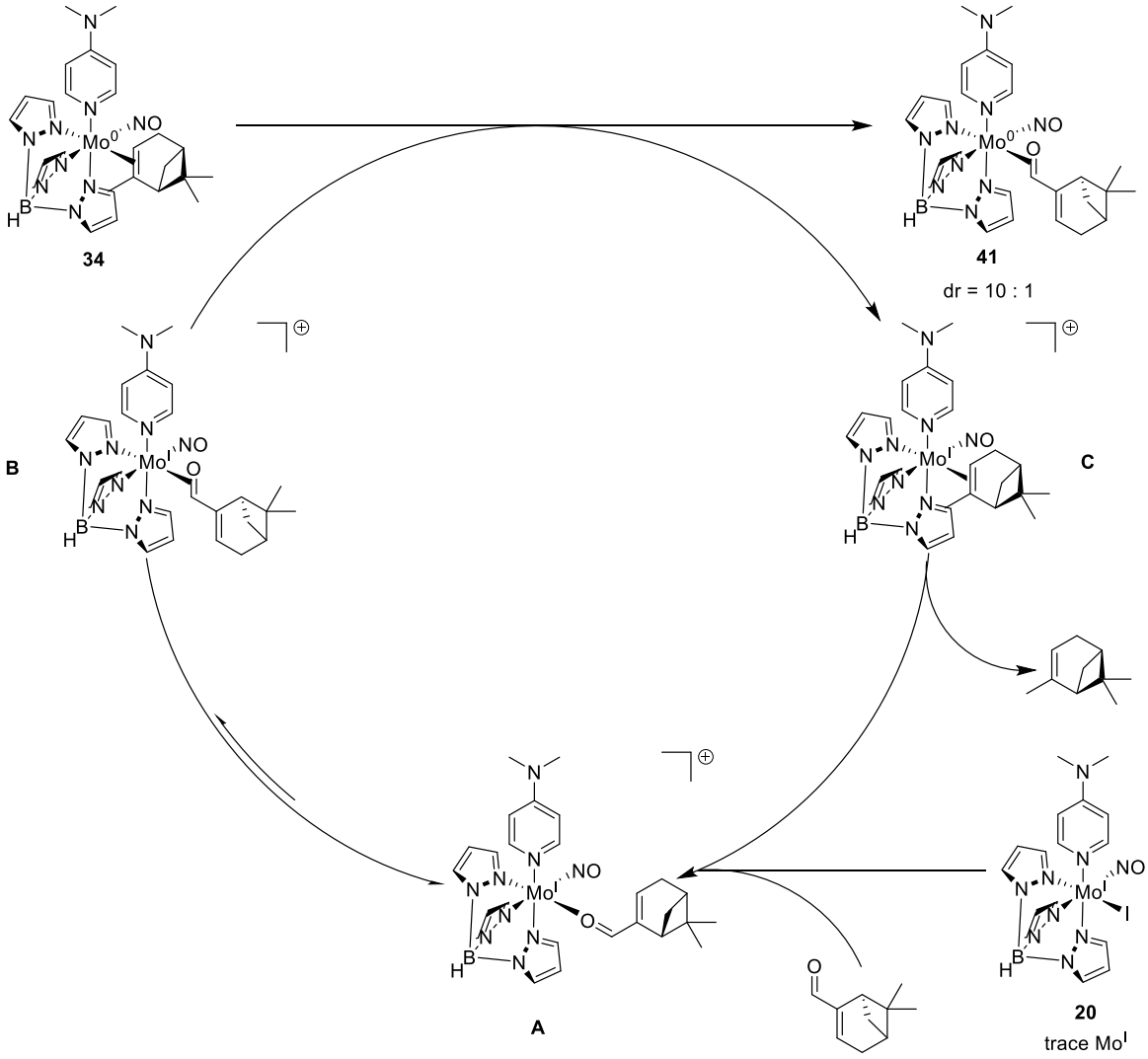

Scheme 7: Proposed redox catalyzed ligand exchange and molybdenum chirality transfer.

This proposed pathway has been supported by Steven Dakermanji with the addition of catalytic redox agents. Incorporation of the homogeneous reducing agent $CoCp_2$ (-0.78 V) inhibits the rate increase of the exchange process, while retaining the transfer of molybdenum chirality. Moreover, catalytic incorporation of a non-coordinating oxidant ($[Fe(Cp)_2]^+$, 0.55 V) provides the desired rate increase and enhanced stereochemical stability of the molybdenum center in both

high (~50 molar equivalents) and low (10 molar equivalents) concentrations of *R*-myrtenal. Work is ongoing to probe the proposed mechanism in order and collect more data on the effects of a catalytic oxidant on the exchange process.

These results support the trend reported by Brunner; that increased reduction potential also provides increased stereochemical stability of chiral-at-metal systems.[36-41] While our current results are difficult to apply to general resolution methods (due to the requirement of a Mo^{I} – η^2-carbonyl intermediate), they provide important insight into the chiral stability of molybdenum dearomatization agents. These results also suggest that we may maintain molybdenum resolution at the less reducing **20***, and that racemization of the complex likely occurs upon reduction to the less stereochemically robust Mo^{0}. With this in mind the ability to control the racemization process within the Mo^{I} to Mo^{0} reduction may provide a general route to molybdenum enantioenrichment.

3.12 Conclusion

The application of α-pinene resolution to 2nd row molybdenum dearomatization agents produced unexpected deviations from {TpRe(MeIm)(CO)}. These differences manifested themselves in terms of the number of coordination isomers for **34** and **36**, and also in the stereochemical stability of the 2nd row molybdenum center. The ability to access an enantiopure complex in **34**, which is also able to undergo ligand exchange, provides an excellent foundation for molybdenum resolution. However, the chiral metal center is prone to racemization.

Racemization studies of the exchange from **34** have resulted in the identification of a reliable chiral reporter ligand in *R*-myrtenal. Synthesis of **41** allows for a simple means of examining the level of enrichment of the molybdenum system via the resulting diastereomeric ratio. However, the examination of a range of {TpMo(L)(NO)} fragments resulted in the inability to overcome racemization. Recent work by Steven Dakermanji has demonstrated that a redox

catalyzed exchange employing *R*-myrtenal facilitates increased transfer of metal chirality, while also increasing the rate of substitution. The ability to dramatically increase the rate of exchange with catalytic, non-coordinating oxidants ($[FeCp_2]^+$) may allow for further investigations into the chiral stability of the {TpMo(MeIm)(NO)} fragment. Continued investigations and optimization of redox promoted exchange, in conjunction with enhancing the stereochemical stability of the electron-rich Mo^0 species are ongoing, and may deliver the elusive answer to overcoming molybdenum racemization.

3.13 Experimental

General Methods

NMR spectra were obtained on 600 or 800 MHz spectrometers. Chemical shifts are referenced to tertramethylsilane (TMS) utilizing residual ^1H signals of the deuterated solvents as internal standards. Chemical shifts are reported in ppm and coupling constants (*J*) are reported in hertz (Hz). Infrared Spectra (IR) were recorded on a spectrometer as a glaze on a Horizontal Attenuated Total Reflectance (HATR) accessory, or as a glaze between two NaCl plates, with peaks reported in cm^{-1}. Electrochemical experiments were performed under a nitrogen atmosphere. Cyclic voltammetric data were recorded at ambient temperature at 100 mV/s unless otherwise noted, with a standard three electrode cell from +1.8 V to -1.8 V with a platinum working electrode, *N*,*N*-dimethylacetamide (DMA) or acetonitrile (MeCN) solvent, and tetrabutylammonium hexafluorophosphate (TBAH) electrolyte (~1.0 M). For CV data recorded in aqueous solutions, sodium triflate (NaOTf) was used as the electrolyte. All potentials are reported versus the normal hydrogen electrode (NHE) using cobaltocenium hexafluorophosphate ($E_{1/2}$ = -0.78 V, -1.75 V) or ferrocene ($E_{1/2}$ = 0.55 V) as an internal standard. Peak separation of all reversible couples was less than 100 mV. All synthetic reactions were performed in a glovebox under a dry nitrogen atmosphere unless otherwise noted. All solvents were purged with nitrogen prior to use.

Deuterated solvents were used as received from Cambridge Isotopes. Compound **37** was prepared according to previous literature methods, and characterization of **20*** was consistent with literature reports of **20**.[6-7]

Synthesis of TpMo(DMAP)(NO)(I) (20*)

Compound **34** (0.510 g, 0.916 mmol), I_2 (0.190 g, 0.747 mmol), and Et_2O (50 mL) were added to a 100 mL round bottom flask charged with a stir bar giving a golden mixture, which turned green within 1 min. After 30 min the dark green mixture was evaporated to dryness *in vacuo*, and left under vacuum for 1 h to remove excess I_2. The solid was re-dissolved in DCM (4 mL), and precipitated by dropwise addition into stirring pentane (25 mL). The green mixture was filtered through a 15 mL fine frit, and the solid was desiccated to yield (**20***) (110 % (due to excess I_2, 0.596 g, 1.01 mmol).

Synthesis of TpMo(DMAP)(NO)(η^2-(*R*)-α-pinene) (34)

Na^0 dispersion (11.593 g, 176 mmol) was prepared with hexanes washes (3 X 30 mL) in a 500 mL round bottom flask, and the exposed Na^0 flakes were washed with benzene (25 mL) to remove residual hexanes. Compound **19** (7.448 g, 13.8 mmol), *R*-α-pinene (21.8 mL, 132 mmol), and benzene (125 mL) were added to the reaction flask and the reaction mixture was stirred overnight (18 h). The reaction mixture was loaded onto a 7 cm silica plug in a 600 mL medium frit. The column was eluted with Et_2O (400 mL), isolating a colorless fraction, which was discarded. The red product band was eluted with Et_2O (700 mL) followed by 80 % Et_2O/ 20 % THF (300 mL), which was evaporated to dryness *in vacuo*. The solid was re-dissolved in DCM (4 mL) and precipitated by drop-wise addition into stirring pentane (100 mL). The yellow mixture was filtered through a 15 mL fine frit, and the filtercake was washed with pentane (2 X 10 mL) and desiccated to give (**42**) (37 %, 3.038 g, 5.08 mmol) ^{1}H NMR (acetone-d_6, δ): 8.21 (d, *J* = 1.6, 1H, DMAP 2/6), 8.20 (d, *J* = 1.4, 1H, DMAP 2/6), 7.90 (d, *J* = 2.4, Tp 3/5), 7.85 (d, *J* = 2.3, 1H, Tp 3/5), 7.77 (d, *J* = 2.0, 1H, Tp

3/ 5), 7.73, (d, *J* = 2.2, 1H, Tp 3/5), 7.66 (d, *J* = 2.0, 1H, Tp 3/5), 7.11, (d, *J* = 1.8, 1H, Tp 3/5), 6.69 (d, *J* = 1.6, 1H, DMAP 3/5), 6.68 (d, *J* = 1.5, 1H, DMAP 3/5), 6.31 (t, *J* = 1.8, 1H, Tp 4), 6.31 (t, *J* = 1.8, 1H, Tp 4), 6.10 (t, *J* = 2.1, 1H, Tp 4), 3.08 (s, 6H, DMAP Me), 2.61 (d, *J* = 10.1, 1H), 2.50 (m, 2H, α-pinene CH_2) 2.24, (t, *J* = 5.67, 1H, α-pinene CH), 2.18, (m, 2H, α-pinene CH_2), 1.80 (m, 1H, α-pinene CH), 1.36, (s, 3H, α-pinene Me), 1.13 (s, 3H, α-pinene Me), 0.60 (s, 3H, α-pinene vinyl Me). ^{13}C NMR (acetone-d_6, δ): 159.0, 151.3, 145.0, 143.1, 141.5, 173.2, 136.3, 135.2, 108.3, 106.6, 106.0, 82.2, 68.4, 55.9, 42.9, 42.3, 39.1, 32.1, 31.1, 27.9, 27.8, 23.3. CV: $E_{p,a}$ = -0.17 V. IR: ν_{NO} = 1548 cm^{-1}; ν_{BH} = 2441 cm^{-1}.

Synthesis of TpMo(DMAP)(NO)(η^2-acetone) (35)

Compound **34** (97.4 mg, 0.163 mmol) was added to a 4 dram vial charged with a stir bar. The solid was dissolved in acetone (2.5 mL, 34 mmol), giving a brown solution, which was stirred for 2 d. The solution was precipitated by drop-wise addition to stirring pentane (25 mL). The resulting light brown mixture was left to stir for 5 min. The mixture was then filtered through a 15 mL fine fritted funnel, isolating a grey solid from a light yellow filtrate. The product was dried *in vacuo*, giving (**35**) (19 %, 13.1 mg, x mol). ^{1}H NMR (acetone-d_6, δ): 8.07 (1H, d, *J* = 2.1, Tp3/5), 7.91 (1H, d, *J* = 2.3, Tp3/5), 7.88 (1H, d, *J* = 2.5, Tp3/5), 7.84 (1H, d, *J* = 2.3, Tp3/5), 7.62 (1H, d, *J* = 1.5, DMAP2/6), 7.61 (1H, d, *J* = 1.5, DMAP2/6), 7.57 (1H, d, *J* = 1.9, Tp3/5), 7.32 (1H, d, *J* = 1.9, Tp3/5), 6.57 (1H, d, *J* = 1.5, DMAP 3/5), 6.56 (1H, d, *J* = 1.5, DMAP3/5), 6.35 (1H, t, *J* = 2.0, Tp4), 6.29 (1H, d, *J* = 2.2, Tp4), 6.15 (1H, d, *J* = 2.0, Tp4), 3.08 (6H, s, DMAP Me), 2.16 (3H, s, acetone Me), 0.91 (3H, s, acetone Me). ^{13}C NMR (acetone-d_6, δ): 155.7, 152.0, 143.7, 143.6, 143.3, 137.1, 136.3, 136.1, 107.3, 106.8, 106.5, 105.9, 102.039.3, 31.6, 27.2. CV: $E_{p,a}$ = +0.27 V. IR: ν_{NO} = 1574 cm^{-1}; ν_{BH} = 2480 cm^{-1}.

Synthesis of TpMo(DMAP)(NO)(η^2-(*S*)-β-pinene) (36)

Compound **34** (110.2 mg, 0.198 mmol) and *S*-β-pinene (0.32 mL, 2.05 mmol) were added to a 4 dram vial charged with a stir bar. The solid was dissolved in THF (3 mL), giving a red solution which was stirred for 3 d. The solution was precipitated by drop-wise addition to stirring pentane (25 mL). The resulting light brown mixture was left to stir for 5 min. The mixture was then filtered through a 15 mL fine fritted funnel, isolating a yellow solid which was desiccated giving (**36**) (79 %, 92.7 mg, 0.152 mmol). Partial characterization is given due to the spectral complexity of overlapping signals. Selected signals are matched in relative intensity between DMAP methyl signals and *S*-β-pinene methyl signals. ^{1}H NMR (acetone-d_6, δ): 3.07 (s, 6H, DMAP Me), 1.20 (S, 3H, pinene Me), 1.09 (s, 3H, pinene Me); 3.07 (s, 6H, DMAP Me), 1.22 (s, 3H, pinene Me), 1.11 (s, 3H, pinene Me); 3.04 (s, 6H, DMAP Me), 1.24 (s, 3H, pinene Me), 1.08 (s, 3H, pinene Me); 3.04 (s, 6H, DMAP Me), 1.04 (s, 3H, pinene Me), 0.86 (s, 3H, pinene Me). IR: ν_{NO} = 1557 cm^{-1}; ν_{BH} = 2425 cm^{-1}.

Synthesis of TpMo(DMAP)(NO)(η^2-(*R*)-fencone) (38)

Compound **34** (107.2 mg, 0.179 mmol) and *R*-fenchone (0.29 mL, 1.81 mmol) were added to a 4 dram vial charged with a stir bar. The solid was dissolved in THF (3 mL), giving a red solution which was stirred for 3 d. The solution was precipitated by drop-wise addition to stirring pentane (25 mL). The resulting light brown mixture was left to stir for 5 min. The mixture was then filtered through a 15 mL fine fritted funnel, isolating a yellow solid which was desiccated giving (**38**) (28 %, 30.7 mg, 0.05 mmol). Partial characterization is given due to the spectral complexity of overlapping signals. ^{1}H NMR (acetone-d_6, δ): (Major isomer) 8.34 (1H, d, *J* = 1.7, Tp 3/5), 7.89 (1H, d, *J* = 2.5, Tp 3/5), 7.84 (1H, d, *J* = 1.9, Tp 3/5), 7.45 (1H, d, *J* = 1.5, DMAP 2/6), 7.44 (1H, d, *J* = 1.5, DMAP 2/6), 6.52 (1H, d, *J* = 1.5, DMAP 3/5), 6.51 (1H, d, *J* = 1.5, DMAP 3/5), 6.33 (1H, t, *J* = 2.0, Tp 4), 6.26 (1H, d, *J* = 2.1, Tp 4), 6.15 (1H, d, *J* = 2.0, Tp 4), 3.06 (6H, s, DMAP Me), 1.75 (s, 3H, fenchone

Me), 1.05 (s, 3H, fenchone Me). (Mix of minor isomers) 8.18 (1H, d, *J* = 1.8, Tp 3/5), 7.57 (1H, d, *J* = 1.8, Tp 3/5), 7.47 (1H, d, *J* = 1.9, Tp 3/5), 7.25 (1H, d, *J* = 1.5, Tp 3/5), 6.58 (1H, d, *J* = 1.5, DMAP 3/5), 6.57 (1H, d, *J* = 1.5, DMAP 3/5), 6.57 (1H, d, *J* = 1.5, DMAP 3/5), 6.56 (1H, d, *J* = 1.5, DMAP 3/5), 6.35 (1H, t, *J* = 2.2, Tp 4), 6.34 (1H, d, *J* = 2.1, Tp 4), 6.28 (1H, d, *J* = 2.4, Tp 4), 6.20 (1H, t, *J* = 1.8, Tp 4), 6.18 (1H, d, *J* = 2.1, Tp 4), 6.14 (1H, d, *J* = 2.3, Tp4), 3.09 (6H, s, DMAP Me), 3.07 (s, 3H, DMAP Me) 1.06 (s, 3H, fenchone Me), 0.98 (s, 3H, fenchone Me), 0.97 (s, 3H, fenchone Me), 0.54 (s, 3H, fenchone Me). CV: $E_{p,a}$ = +0.31 V.

Synthesis of TpMo(DMAP)(NO)(η²-(*S*)-camphor) (39)

Compound **34** (104.0 mg, 0.187 mmol) and *S*-camphor (275.3 mg, 1.81 mmol) were added to a 4 dram vial charged with a stir bar. The solid was dissolved in THF (3 mL), giving a red solution which was stirred for 3 d. The solution was precipitated by drop-wise addition to stirring pentane (25 mL). The resulting light brown mixture was left to stir for 5 min. The mixture was then filtered through a 15 mL fine fritted funnel, isolating a yellow solid which was desiccated giving (**39**) (17 %, 19.5 mg, 0.032 mmol). Partial characterization is given due to the spectral complexity of overlapping signals. Selected signals are matched in relative intensity between DMAP methyl signals and *S*-camphor methyl signals. ^{1}H NMR (acetone-d_6, δ): (Mix of isomers) 3.10 (s, 6H, DMAP Me), 3.07 (s, 6H, DMAP Me), 3.05 (s, 6H, DMAP Me), 2.98 (s, 6H, DMAP Me), 1.07 (s, 3H, camphor Me), 1.04 (s, 3H, camphor Me), 0.96 (s, 3H, camphor Me), 0.95 (s, 3H, camphor Me), 0.92 (s, 3H, camphor Me), 0.89 (s, 3H, camphor Me), 0.87 (s, 3H, camphor Me), 0.83 (s, 3H, camphor Me), 0.83 (s, 3H, camphor Me), 0.80 (s, 3H, camphor Me), 0.80 (s, 3H, camphor Me), CV: $E_{p,a}$ = +0.29 V. IR: ν_{NO} = 1582 cm^{-1}; ν_{BH} = 2426 cm^{-1}.

Synthesis of TpMo(DMAP)(NO)(η²-(*S*)-verbenone) (40)

Compound **34** (112.2 mg, 0.187 mmol) and *S*-verbenone (0.28 mL, 1.82 mmol) were added to a 4 dram vial charged with a stir bar. The solid was dissolved in THF (3 mL), giving a red solution which

was stirred for 3 d. The solution was precipitated by drop-wise addition to stirring pentane (25 mL). The resulting light brown mixture was left to stir for 5 min. The mixture was then filtered through a 15 mL fine fritted funnel, isolating a yellow solid which was desiccated giving (**41**) (38 %, 43.4 mg, 0.071 mmol). Partial characterization is given due to the spectral complexity of overlapping signals. Selected signals are matched in relative intensity between DMAP methyl signals and *S*-verbenone methyl signals. ^{1}H NMR (acetone-d_6, δ): (Mix of isomers) 3.08 (s, 6H, DMAP Me), 3.07 (s, 6H, DMAP Me), 3.07 (s, 6H, DMAP Me), 3.06 (s, 6H, DMAP Me), 1.49 (s, 3H, verbenone Me), 1.48 (s, 3H, verbenone Me), 1.42 (s, 3H, verbenone Me), 1.27 (s, 3H, verbenone Me), 1.19 (s, 3H, verbenone Me), 1.15 (s, 3H, verbenone Me), 1.11 (s, 3H, verbenone Me), 1.07 (s, 3H, verbenone Me), 1.04 (s, 3H, verbenone Me), 0.96 (s, 3H, verbenone Me), 0.63 (s, 3H, verbenone Me).

Synthesis of TpMo(DMAP)(NO)(η^2-(*R*)-myrtenal) (41)

Compound **34** (106.9 mg, 0.192 mmol) and *R*-myrtenal (0.27 mL, 1.77 mmol) were added to a 4 dram vial charged with a stir bar. The solid was dissolved in THF (3 mL), giving a red solution which was stirred for 3 d. The solution was precipitated by drop-wise addition to stirring pentane (25 mL). The resulting light brown mixture was left to stir for 5 min. The mixture was then filtered through a 15 mL fine fritted funnel, isolating a yellow solid which was desiccated giving (**41**) (79 %, 92.7 mg, 0.152 mmol). ^{1}H NMR (acetone-d_6, δ): (Mix of isomers) 8.23 (d, *J* = 2.1, 1H, Tp 3/5), 8.07 (d, *J* = 1.8, 1H, Tp 3/5),7.71 (d, *J* = 2.1, Tp 3/5), 7.70 (d, *J* = 2.3, 1H, Tp 3/5), 7.69 (d, *J* = 1.6, 1H, DMAP 2/6), 7.68 (d, *J* = 1.4, 1H, DMAP 2/6), 7.69 (d, *J* = 2.4, 1H, Tp 3/5), 7.67, (d, *J* = 2.1, 1H, Tp 3/5), 7.66 (d, *J* = 2.4, 1H, Tp 3/5), 7.65 (d, *J* = 2.1, 1H, Tp 3/5), 7.64 (d, *J* = 1.6, 1H, DMAP 2/6), 7.63 (overlapped with DMAP 2/6, 1H, Tp 3/5), 7.62 (d, *J* = 1.4, 1H, DMAP 2/6), 7.54 (d, *J* = 1.8, 1H, Tp 3/5), 7.45 (d, *J* = 1.9, 1H, Tp 3/5), 7.44 (d, *J* = 1.9, 1H, Tp 3/5), 6.39 (m, 4H, DMAP 3/5), 6.21 (t, *J* = 2.2, 1H, Tp 4), 6.21 (t, *J* = 2.2, 1H, Tp 4), 6.19 (t, *J* = 2.0, 1H, Tp 4), 6.17 (t, *J* = 2.2, 1H, Tp 4), 6.09

(t, *J* = 2.0, 1H, Tp 4), 6.07 (t, *J* = 2.2, 1H, Tp 4), 5.31 (m, 1H, myrtenal alkene H), 5.12 (m, 1H, myrtenal alkene H), 4.25 (s, 1H, myrtenal aldehyde H), 4.13 (s, 1H, myrtenal aldehyde H), 3.01 (s, 6H, DMAP Me), 3.00 (s, 6H, DMAP Me), 2.79-2.45 (m, 8H, myrtenal), 2.18 (m, 1H, myrtenal CH) 2.14, (m, 1H, myrtenal CH), 1.53, (d, *J* = 9.1) 1H, myrtenal CH), 1.05 (d, *J* = 9.3, 1H, myrtenal CH), 1.39, (s, 3H, myrtenal Me), 1.19 (s, 3H, myrtenal Me), 0.97, (s, 3H, myrtenal Me), 0.73 (s, 3H, myrtenal Me). ^{13}C NMR (acetone-d_6, δ): (Mix of isomers) 157.0, 156.2, 155.8, 155.7, 151.7, 151.6, 144.2, 143.3, 143.3, 143.0, 142.3, 142.1, 136.9, 136.8, 136.6, 136.6, 136.4, 136.3, 117.0, 116.7, 107.6, 107.6, 107.0, 106.9, 106.3, 106.2, 106.2, 106.1, 100.1, 100.0, 42.4, 42.2, 42.2, 42.0, 39.4, 39.3, 38.9, 38.1, 33.0, 32.8, 32.6, 27.2, 27.1, 22.3, 22.0. CV: $E_{p,a}$ = +0.40 V. IR: ν_{NO} = 1578 cm^{-1}; ν_{BH} = 2445 cm^{-1}.

Synthesis of TpMo(MeIm)(NO)(η^2-(*R*)-α-pinene) (42)

Na^0 dispersion (11.593 g, 176 mmol) was prepared with hexanes washes (3 X 30 mL) in a 500 mL round bottom flask, and the exposed Na^0 flakes were washed with Et_2O (25 mL) to remove residual hexanes. Compound **2** (6.014 g, 12.0 mmol), *R*-α-pinene (21 mL, 132 mmol), and Et_2O (125 mL) were added to the reaction flask and the reaction mixture was stirred overnight (18 h). The reaction mixture was loaded onto a 5 cm silica plug in a 350 mL medium frit. The column was eluted with Et_2O (350 mL), isolating a colorless fraction, which was discarded. The bright yellow product band was eluted with Et_2O (1 L), which was evaporated to dryness *in vacuo*. The solid was re-dissolved in DCM (3 mL) and precipitated by drop-wise addition into stirring pentane (50 mL). The yellow mixture was filtered through a 15 mL fine frit, and the filtercake was washed with pentane (2 X 10 mL) and desiccated to give (**42**) (10 %, 0.666 g, 1.2 mmol) ^{1}H NMR (acetone-d_6, δ): 7.95 (s, 1H, MeIm H2), 7.86 (d, *J* = 2.1, Tp 3/5), 7.84 (d, *J* = 2.5, 1H, Tp 3/5), 7.77 (d, *J* = 1,.9, 1H, Tp 3/ 5), 7.69, (d, *J* = 2.3, 1H, Tp 3/5), 7.65 (d, *J* = 1.6, 1H, Tp 3/5), 7.24, (d, *J* = 1.8, 1H, Tp 3/5), 7.22 (t, *J* = 1.4, 1H, MeIm 3/4), 7.07 (t, *J* = 1.2, 1H, MeIm 3/4), 6.31 (t, *J* = 2.2, 1H, Tp 4), 6.27 (t, *J* = 1.9,

1H, Tp 4), 6.08 (t, *J* = 1.9, 1H, Tp 4), 3.89 (s, 3H, MeIm Me), 2.65 (d, *J* = 10.1, 1H), 2.46 (m, 2H, α-pinene CH_2), 2.21 (t, *J* = 5.67, 1H, α-pinene CH), 2.15, (m, 2H, α-pinene CH_2), 1.77 (m, 1H, α-pinene CH), 1.36, (s, 3H, α-pinene Me), 1.12 (s, 3H, α-pinene Me), 0.54 (s, 3H, α-pinene vinyl Me). CV: $E_{p,a}$ = -0.21 V. IR: ν_{NO} = 1543 cm^{-1}; ν_{BH} = 2427 cm^{-1}.

Synthesis of TpMo(MeIm)(NO)(η^2-(*R*)-myrtenal) (43)

Compound **42** (0.106 g, 0.190 mmol), *R*-myrtenal (0.27 mL, 1.77 mmol), and THF (3 mL) were added to a 4 dram vial charged with a stir pea, giving a yellow solution. After stirring for 20 d the solution was precipitated by addition of pentane (5 mL). The yellow mixture was filtered through a 15 mL fine frit, and the solid was desiccated to give (**43**) (31 %, 0.033 g, 0.059 mmol). The product exists as a 2 : 1 ratio of diastereomers. ^{1}H NMR (acetone-d_6, δ): (Major diastereomer) 8.05 (d, *J* = 1.8, 1H, Tp 3/5), 7.89 (m, 2H, MeIm 2H and Tp 3/5), 7.83 (d, *J* = 2.4, 1H, Tp 3/5), 7.81, (d, *J* = 2.1, 1H, Tp 3/5), 7.69 (d, *J* = 2.4, 1H, Tp 3/5), 7.43 (d, *J* = 2.1, 1H, Tp 3/5), 7.12 (t, *J* = 1.7, 1H, MeIm 3/4), 6.62 (t, *J* = 1.1, 1H, MeIm 3/4), 6.27 (t, *J* = 1.8, 1H, Tp 4), 6.26 (t, *J* = 2.4, 1H, Tp 4), 6.15 (t, *J* = 2.1, 1H, Tp 4), 5.02 (m, 1H, myrtenal vinyl H), 3.94 (s, 1H, myrtenal aldehyde H), 3.86 (s, 3H, MeIm Me), 2.74-2.41 (m, 4H, myrtenal), 2.11 (m, 1H, myrtenal CH), 1.49, (d, *J* = 9.0), 1.33, (s, 3H, myrtenal Me), 0.96, (s, 3H, myrtenal Me). (Minor diastereomer) 8.25 (d, *J* = 1.8, 1H, Tp 3/5), 7.91 (d, *J* = 2.3, 1H, Tp 3/5), 7.89 (m, 2H, MeIm 2H and Tp 3/5), 7.80 (d, *J* = 2.1, 1H, Tp 3/5), 7.78, (d, *J* = 1.7, 1H, Tp 3/5), 7.42 (d, *J* = 1.8, 1H, Tp 3/5), 7.10 (t, *J* = 1.7, 1H, MeIm 3/4), 6.53 (t, *J* = 1.4, 1H, MeIm 3/4), 6.31 (t, *J* = 2.1, 1H, Tp 4), 6.25 (t, *J* = 2.2, 1H, Tp 4), 6.13 (t, *J* = 2.0, 1H, Tp 4), 5.19 (m, 1H, myrtenal vinyl H), 4.07 (s, 1H, myrtenal aldehyde H), 3.85 (s, 3H, MeIm Me), 2.74-2.41 (m, 4H, myrtenal), 2.19 (m, 1H, myrtenal CH), 1.96, (s, 3H, myrtenal Me), 1.27 (d, *J* = 7.6), 1.18, (s, 3H, myrtenal Me).

3.14 References

1. Frank, B.; Humblet, J. *J. Med. Chem.* **2009,** *52*, 6752-6756.

2. Solomons, T. W. G.; Fryhle, C.; Snyder, S., *Organic Chemistry, 11th Edition*. 2012.

3. Graham, P. M.; Mocella, C. J.; Sabat, M.; Harman, W. D. *Organometallics* **2005,** *24*, 911-919.

4. Ha, Y.; Dilsky, S.; Graham, P. M.; Liu, W.; Reichart, T. M.; Sabat, M.; Keane, J. M.; Harman, W. D. *Organometallics* **2006,** *25*, 5184-5187.

5. Meiere, S. H.; Keane, J. M.; Gunnoe, T. B.; Sabat, M.; Harman, W. D. *J. Am. Chem. Soc.* **2003,** *125,* 2024-2025.

6. Mocella, C. J.; Delafuente, D. A.; Keane, J. M.; Warner, G. R.; Friedman, L. A.; Sabat, M.; Harman, W. D. *Organometallics* **2004,** *23*, 3772-3779.

7. Myers, J. T.; Dakermanji, S. J.; Chastanet, T. R.; Shivokevich, P. J.; Strausberg, L. J.; Sabat, M.; Myers, W. H.; Harman, W. D. *Organometallics* **2017,** *36*, 543-555.

8. Brooks, B. C.; Brent Gunnoe, T.; Dean Harman, W. *Coord. Chem. Rev.* **2000,** *206*, 3-61.

9. Meiere, S. H.; Valahovic, M. T.; Harman, W. D. *J. Am. Chem. Soc.* **2002,** *124*, 15099-15103.

10. Keane, J. M.; Harman, W. D. *Organometallics* **2005,** *24*, 1786-1798.

11. Lankenau, A. W.; Iovan, D. A.; Pienkos, J. A.; Salomon, R. J.; Wang, S.; Harrison, D. P.; Myers, W. H.; Harman, W. D. *J. Am. Chem. Soc.* **2015,** *137*, 3649-3655.

12. Graham, P. M.; Delafuente, D. A.; Liu, W.; Myers, W. H.; Sabat, M.; Harman, W. D. *J. Am. Chem. Soc.* **2005,** *127*, 10568-10572.

13. Harrison, D. P.; Zottig, V. E.; Kosturko, G. W.; Welch, K. D.; Sabat, M.; Myers, W. H.; Harman, W. D. *Organometallics* **2009,** *28*, 5682-5690.

14. Lis, E. C.; Salomon, R. J.; Sabat, M.; Myers, W. H.; Harman, W. D. *J. Am. Chem. Soc.* **2008,** *130*, 12472-12476.

15. MacLeod, B. L.; Pienkos, J. A.; Myers, J. T.; Sabat, M.; Myers, W. H.; Harman, W. D. *Organometallics* **2014,** *33*, 6286-6289.

16. MacLeod, B. L.; Pienkos, J. A.; Wilson, K. B.; Sabat, M.; Myers, W. H.; Harman, W. D. *Organometallics* **2016,** *35*, 370-387.

17. Pienkos, J. A.; Knisely, A. T.; MacLeod, B. L.; Myers, J. T.; Shivokevich, P. J.; Teran, V.; Sabat, M.; Myers, W. H.; Harman, W. D. *Organometallics* **2014,** *33*, 5464-5469.

18. Todd, M. A.; Sabat, M.; Myers, W. H.; Smith, T. M.; Harman, W. D. *J. Am. Chem. Soc.* **2008,** *130*, 6906-6907.

19. Welch, K. D.; Harrison, D. P.; Sabat, M.; Hejazi, E. Z.; Parr, B. T.; Fanelli, M. G.; Gianfrancesco, N. A.; Nagra, D. S.; Myers, W. H.; Harman, W. D. *Organometallics* **2009,** *28*, 5960-5967.

20. Ding, F.; Valahovic, M. T.; Keane, J. M.; Anstey, M. R.; Sabat, M.; Trindle, C. O.; Harman, W. D. *J. Org. Chem.* **2004,** *69*, 2257-2267.

21. Spera, M. L.; Chin, R. M.; Winemiller, M. D.; Lopez, K. W.; Sabat, M.; Harman, W. D. *Organometallics* **1996,** *15*, 5447-5449.

22. Valahovic, M. T.; Gunnoe, T. B.; Sabat, M.; Harman, W. D. *J. Am. Chem. Soc.* **2002,** *124*, 3309-3315.

23. Harman, W. D. *Chem. Rev.* **1997,** *97*, 1953-1978.

24. Winemiller, M. D.; Harman, W. D. *J. Org. Chem* **2000,** *65*, 1249-1256.

25. Myers, J. T.; Shivokevich, P. J.; Pienkos, J. A.; Sabat, M.; Myers, W. H.; Harman, W. D. *Organometallics* **2015,** *34*, 3648-3657.

26. Meiere, S. H.; Harman, W. D. *Organometallics* **2001,** *20*, 3876-3883.

27. Graham, P. M.; Meiere, S. H.; Sabat, M.; Harman, W. D. *Organometallics* **2003,** *22*, 4364-4366.

28. Dhokte, U. P.; Brown, H. C. *Tetrahedron Letters* **1994,** *35*, 4715-4718.

29. Brooks, B. C.; Meiere, S. H.; Friedman, L. A.; Carrig, E. H.; Gunnoe, T. B.; Harman, W. D. *J. Am. Chem. Soc.* **2001,** *123*, 3541-3550.

30. Friedman, L. A.; Meiere, S. H.; Brooks, B. C.; Harman, W. D. *Organometallics* **2001,** *20*, 1699-1702.

31. Gunnoe, T. B.; Sabat, M.; Harman, W. D. *J. Am. Chem. Soc.* **1999,** *121*, 6499-6500.

32. Lis, E. C.; Delafuente, D. A.; Lin, Y.; Mocella, C. J.; Todd, M. A.; Liu, W.; Sabat, M.; Myers, W. H.; Harman, W. D. *Organometallics* **2006,** *25*, 5051-5058.

33. Meiere, S. H.; Brooks, B. C.; Gunnoe, T. B.; Sabat, M.; Harman, W. D. *Organometallics* **2001,** *20*, 1038-1040.

34. Welch, K. D.; Harrison, D. P.; Lis, E. C.; Liu, W.; Salomon, R. J.; Harman, W. D.; Myers, W. H. *Organometallics* **2007,** *26*, 2791-2794.

35. Meiere, S. H.; Brooks, B. C.; Gunnoe, T. B.; Carrig, E. H.; Sabat, M.; Harman, W. D. *Organometallics* **2001,** *20*, 3661-3671.

36. Brunner, H. *Angew. Chem. Int. Ed.* **1971,** *10*, 249-260.

37. Brunner, H. *Ann. N Y Acad .Sci.* **1974,** *239*, 213-224.

38. Brunner, H. *Adv. Organomet. Chem.* **1980,** *18*, 151-206.

39. Brunner, H., Enantioselective synthesis of organic compounds with optically active transition metal catalysts in substoichiometric quantities. In *Topics in stereochemistry*, Wiley & sons New York: 1988; Vol. 18, p 129.

40. Brunner, H. *Angew. Chem. Int. Ed.* **1999,** *38*, 1194-1208.

41. Brunner, H. *Eur. J. Inorg. Chem.* **2001,** *2001*, 905-912.

Chapter 4

Application of

TpMo(DMAP)(NO)(η^2-α-pinene)

as an Exchange Reagent

4.1 Introduction

Prior to the development of TpMo(DMAP)(NO)(η^2-*R*-α-pinene) (**34**), the {TpMo(DMAP)(NO)} fragment lacked a general procedure to access diahpto-coordinated complexes by exchange. This deficiency has hampered the investigation of unique dihapto-coordinated ligands, which up to this point have been synthesized by reduction from Mo^{II} or Mo^{I} (*vide supra*). While these redox – based synthetic pathways have provided access to a variety of novel molybdenum complexes, they also provide synthetic challenges, including incompatibility with a range of functional groups (*vide supra*).

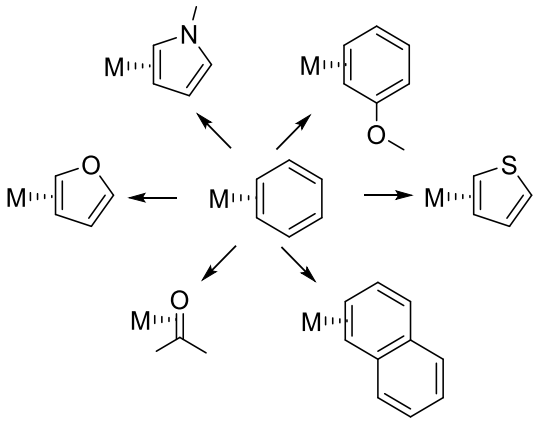

Scheme 1: Access to dihapto-aromatic complexes via benzene ligand exchange.

An alternate route to novel dihapto-complexes is ligand exchange, which has been utilized in previous 3rd row osmium, rhenium, and tungsten systems by exchange of the weakly coordinated M – η^2-benzene (Scheme 1).[1-5] However, initial molybdenum reports have shown a dramatically reduced coordination scope compared to previous heavy metal dearomatization agents, and as such the 2nd row molybdenum system lacked a dihapto-benzene complex to act as an exchange reagent. **34** has shown the ability to undergo ligand exchange, as demonstrated during the previously discussed racemization studies (Chapter 3); and we sought to utilize **34** as an exchange reagent to further probe the molybdenum coordination scope.

4.2 Accessing η^2-Aromatic Complexes via α-Pinene Exchange

We demonstrated the ability to isolate molybdenum dihapto-carbonyl and alkene complexes in Chapter 3. However, in order for an exchange pathway to have utility for dearomatization chemistry, we needed to access η^2-aromatic complexes from **34**. We began these attempts by the synthesis of the known complex TpMo(DMAP)(NO)(η^2-naphthalene) (**26**) (Scheme 2). Initial attempts employed ~100 mg of **34**, dissolved in 3 mL of THF, DME, or benzene, with 10 molar equivalents of naphthalene. Throughout these trials we were able to obtain **26** in consistent yields (40-70 %) with a simple precipitation into pentane.

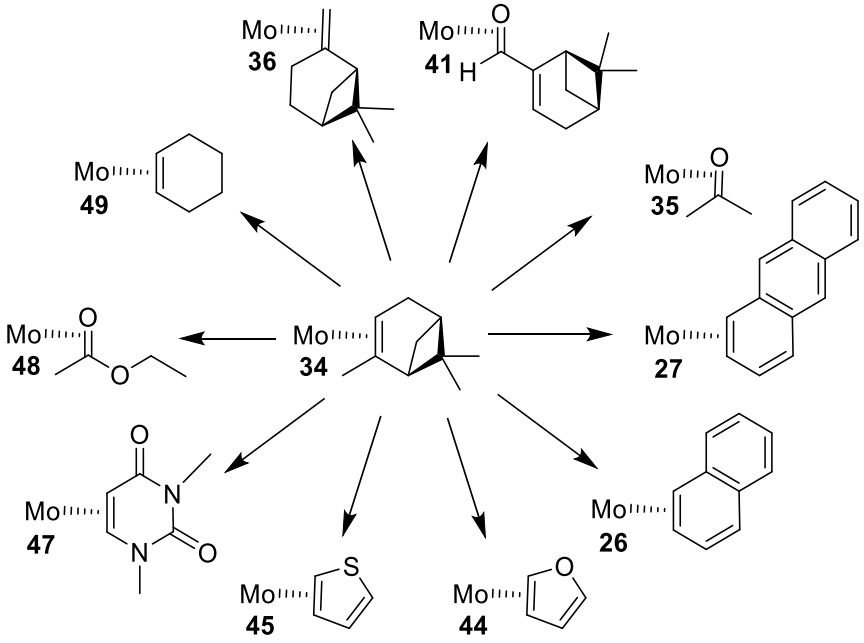

Scheme 2: Access to molybdenum – dihapto complexes via α-pinene ligand exchange.

TpMo(DMAP)(NO)(η^2-furan) (**44**) and TpMo(DMAP)(NO)(η^2-thiophene) (**45**) were synthesized by application of the exchange conditions from **34** to **26**. While these complexes had been reported with {TpMo(MeIm)(NO)}, they were shown to be equally amenable to coordination by exchange with the {TpMo(DMAP)(NO)} fragment. **44** and **45**, like **26**-**27** compared to **24**-**25**, are spectroscopically similar to their MeIm bearing cousins. For instance, **44** gives a 1.6 : 1 ratio of coordination diastereomers, in which the major isomer orients the oxygen atom away from

DMAP. The MeIm variant gives the same major isomer, although in a slightly more favorable 2 : 1 ratio.[6-7] In the case of thiophene, both **45** and the MeIm analog afford a 1 : 1 ratio of coordination diastereomers.[6-7]

Changes to the concentration of the incoming ligand were explored during initial exchange experiments. Once again, naphthalene was used as a model for these studies. Syntheses of **26** from **34** maintained the concentration of **34** (~100 mg/mL = ~0.167 M), while reducing the molar equivalents of naphthalene. These experiments show that naphthalene concentration has negligible impact on the substitution rate of **34**, or the yield of **26**. There was no significant change in yield when the molar equivalents of naphthalene were reduced from 10 to 3 (70 %), and only a slight drop in yield when reduced to a mere 1.6 molar equivalents (57 %). These data are consistent with the proposed dissociative nature of the exchange, in which dissociation of the α-pinene ligand is the rate determining step.[1-3, 8-10] This result is important for the coordination of expensive ligands, or where solubility is a concern (*e.g.*, anthracene).

In terms of extending the scope of aromatic coordination beyond the initial reports of naphthalene, anthracene, furan, and thiophene, exchange from **34** proved unsuccessful. Phenol, thiophenol, nitrobenzene, aniline, and anisole exchanges all resulted in decomposition. Within this range of incoming ligands, both low (~1 molar equivalent), and high (20 molar equivalents) ligand concentrations resulted in decomposition of the molybdenum complex. Phenol, thiophenol, nitrobenzene, and aniline exchanges all produced green mixtures, indicative of an oxidative decomposition pathway.

However, anisole exchanges produced a dark purple mixture, which we believe to be $TpMo(DMAP)_2(NO)$ (**46**). Formation of **46** is supported by similar electrochemical features when DMAP is used as the incoming ligand. The dark blue/purple color is consistent with κ^1-coordination through the nitrogen of the pyridine ring. The I/0 $E_{1/2}$ of -1.20 V is also consistent

with a ligand set incorporating 5 donors and NO^+ (*vide supra*). **46** is NMR silent, although we propose it to be a d^6, Mo^0 species, due to the reversible nature of the I/0 redox couple. Since both d^5 and d^6 states of **46** are chemically stable, and interconvert at the same electrochemical potential, they are able to rapidly convert between oxidation states in the presence of trace oxidant, erasing the NMR signal.

4.3 Accessing η^2-Carbonyl/Alkene Complexes via α-Pinene Exchange

While exchange from **34** proved unable to extend the molybdenum coordination scope within aromatic ligands, we employed the exchange reagent to access a range of dihapto-carbonyl complexes. Although dihapto-carbonyl complexes are far more common in the literature than dihapto-aromatic complexes, they are still relatively rare, especially within 2nd row metals.[2, 7, 11-14] Moreover, dihapto-carbonyl coordination is difficult to access by direct reduction, due to ligand incompatibility with the highly reducing conditions required. As discussed previously in Chapter 3, initial investigations with **34** provided TpMo(DMAP)(NO)(η^2-acetone) (**35**) and TpMo(DMAP)(NO)(η^2-*R*-myrtenal) (**41**) as examples of dihapto-coordinated ketones and aldehydes, respectively (Scheme 2). We looked to supplement these complexes by coordinating carbonyls with increased resonance stabilization, such as carboxylic acid, anhydride, amide, and ester functionalities.

Unfortunately, due to the electron-rich nature of the {TpMo(DMAP)(NO)} fragment, along with the relatively slow rate of exchange from **34**, the exchanges were prone to oxidative decomposition. The propensity for the molybdenum center to undergo oxidative decomposition upon dissociation of the *R*-α-pinene ligand was shown by the formation of Mo^I species when exposed to incoming ligands with weakly acidic protons (*e.g.*, phenol, pKa = 10). This made coordination of carboxylic acids (*e.g.*, benzoic acid, acetic acid) inaccessible, even under conditions employing 1 molar equivalent of the acid. Oxidation issues were also present in

attempted exchanges to acetic anhydride, which can access carboxylic acid functionality. The decomposition pathway appears to be operative through the proposed 5-coordinate Mo^0 intermediate (*vide supra*), as initial reaction points are qualitatively similar to successful exchanges. However, unlike successful cases, all carboxylic acid and anhydride exchanges turned green after stirring overnight. We associate this green color with Mo^I species, which is also supported by the lack of ^1H NMR signals, suggesting that the green color is derived from a paramagnetic complex. The application of exchanges to the less protic amide functionality also proved difficult. The attempted coordination of DMA and DMF resulted in exchanges dominated by the proposed decomposition product **46**, which was consistently observed in the CV, as well as in the dark blue color of attempted amide exchanges.

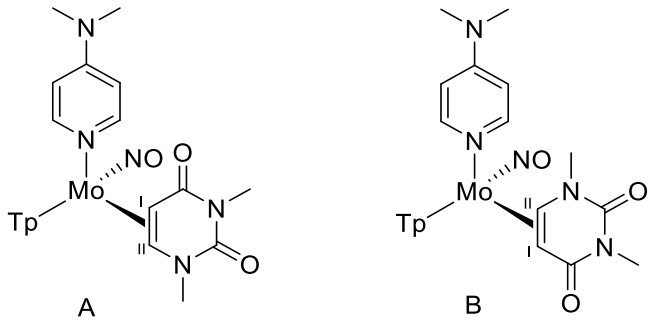

Figure 1: Coordination diastereomers of **47**.

We also attempted coordination of the biologically important cyclic amide uracil, which offers three potential coordination sites. Based on the difficulty in previous attempts to coordinate amide ligands, we expected coordination at the alkene, avoiding disruption of the amide stability. However, we were surprised to find these attempts met with the same oxidative decomposition observed with acids and anhydrides. A variety of different uracil concentrations were employed as a means to overcome the oxidation process, without success. These results illustrate the susceptibility of the {TpMo(DMAP)(NO)} fragment toward oxidation under the exchange conditions required from **34**. Given the relatively high pKa of 2^o amides (~15), any

exchange from **34** requires a completely aprotic environment. Employing the 3° *N*,*N*-dimethyl uracil derivative we eliminate the N-H bonds, and resulted in coordination through alkene (Figure 1). TpMo(DMAP)(NO)(η^2-*N,N*-dimethyl uracil) (**47**) provided the two coordination diastereomers illustrated in Figure 1 in a 1.5 : 1 ratio of A : B. In A, coordination shifts proton I from 5.4 ppm in the free ligand to 3.90 ppm and proton II from 7.4 to 2.76 ppm. The more dramatic change in the chemical in the chemical shift of proton II is due to placement in the anisotropic environment of the pyrazolyl rings. A similar trend is seen in B, in which proton II is shifted less dramatically to 4.70 (due to the absence of pyrazolyl anisotropy) and proton I is shifted from 5.4 to 2.38 ppm. Another spectroscopic feature of B is the chemical shift of the methyl group proximal to DMAP, which is shifted upfield to 2.60 ppm as it experiences anisotropy from the pyridine ring. Cyclohexene was also coordinated via **34** exchange. As in previous examples, TpMo(DMAP)(NO)(η^2-cyclohexene) (**49**) gave a similar spectroscopic profile to the MeIm analog produced by direct reduction (0.05 V).[7, 12]

Despite prior difficulties in molybdenum coordination of resonance stabilized carbonyls, we turned our attention toward the ester functionality. We reasoned that this would be our best chance of coordinating non-ketones or aldehydes, as esters are aprotic (avoiding the oxidative decomposition observed with carboxylic acids and anhydrides) and have less resonance stabilization than amides. However, despite these attributes dihapto-ester complexes are rare, with only a handful of literature reports, and to our knowledge no reports with 2nd row metals.[11-12] Coordination of ethyl acetate gives TpMo(DMAP)(NO)(η^2-EtOAc) (**48**), which is spectroscopically similar to the dihapto-carbonyls **35** and **41** (0.72 V). Coordination also provided new signals for the methylene protons of the ethyl group (3.84 and 3.77 ppm), which upon coordination to the chiral molybdenum center become diastereotopic. Also, as seen with **34**, **35**, and **37**, the methyl group of the coordinated ligand is placed into quadrant B to avoid the

unfavorable steric interactions of quadrant C, giving a single coordination diastereomer (Figure 2). The placement of the methyl group in quadrant B provides the familiar upfield shift to 0.78 ppm.

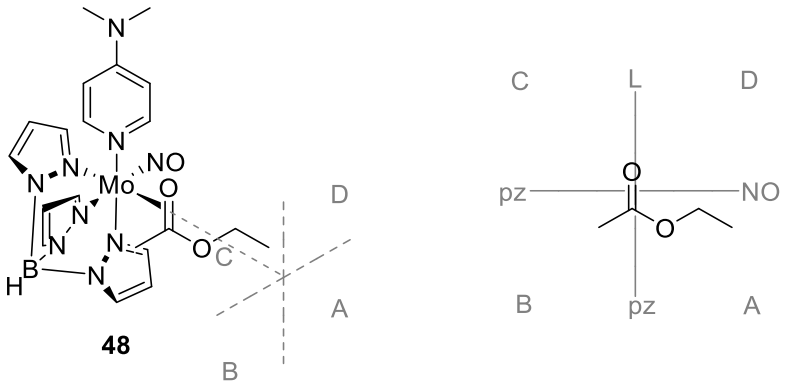

Figure 2: Dihapto-coordination of ethyl acetate (**48**).

4.4 Solvent Effects Influencing Coordination Diastereomer Ratio

Within the context of **34** exchanges, we explored coordination of the heterocyclic aromatic systems quinoline and isoquinoline. These complexes are accessible to previous 3rd row dearomatization agents, however, the number of possible coordination modes (Figure 3) provided a spectral mess. Given the reduced backdonation of the 2nd row molybdenum complex compared to previous 3rd row osmium, rhenium, and tungsten systems, we hoped that our {TpMo(DMAP)(NO)} fragment would be unable to sufficiently stabilize the higher energy coordination isomers (*vide supra*). Analysis of the quantity of resulting coordination isomers was conducted as described in Chapter 3, by the number of DMAP methyl signals. Despite the variety of coordination isomers available to TpMo(DMAP)(NO)(η^2-quinoline) (**50**), and their spectroscopically silent enantiomers (Figure 3A), only 5 were observed in the isolated product, with 3 predominant forms (Figure 4A). Similarly, the many coordination possibilities of TpMo(DMAP)(NO)(η^2-isoquinoline) (**51**) (Figure 3B) yielded 4 DMAP methyl signals, with once again 3 major isomers (Figure 4C). However, despite the relatively low number of isomers of **50**

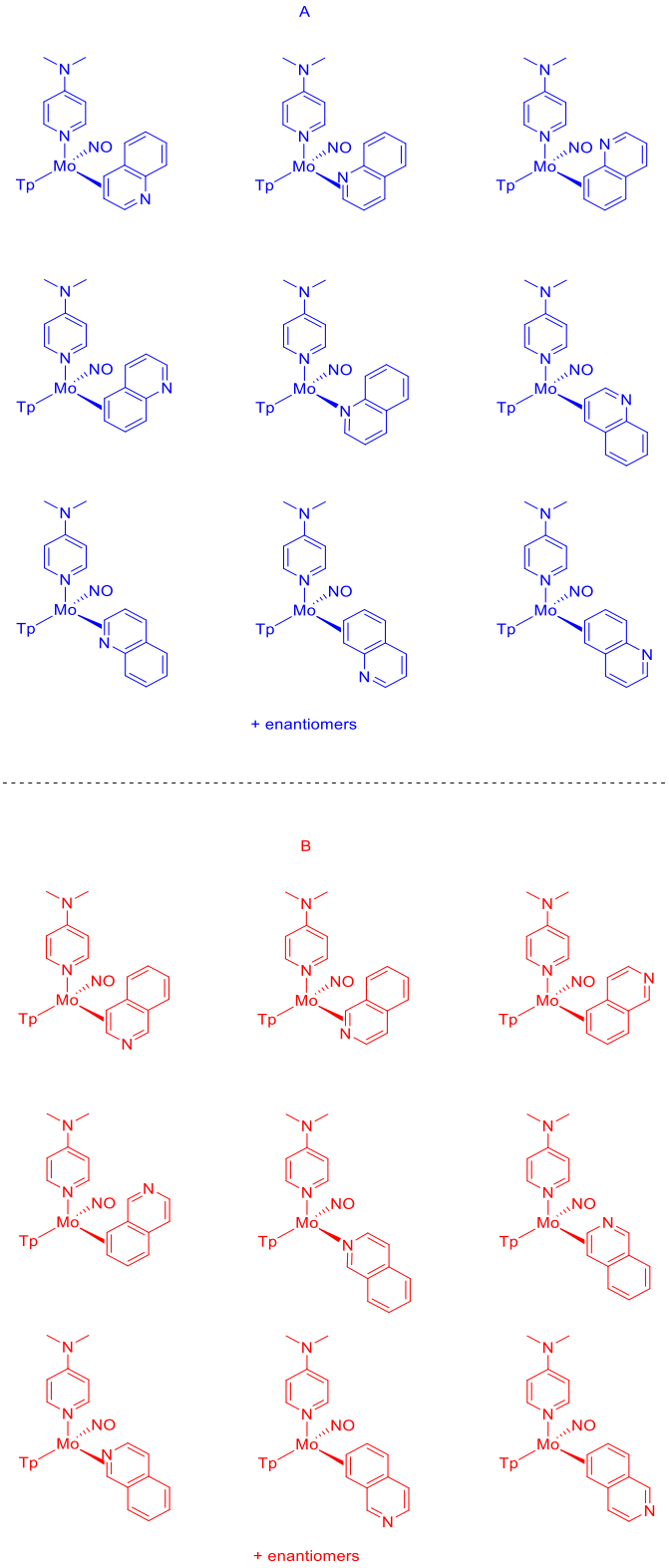

Figure 3: Possible coordination diastereomers of **50** (A) and **51** (B).

and **51**, the similar chemical environments produced within each system results in spectra with a great deal of overlap, making characterization difficult.

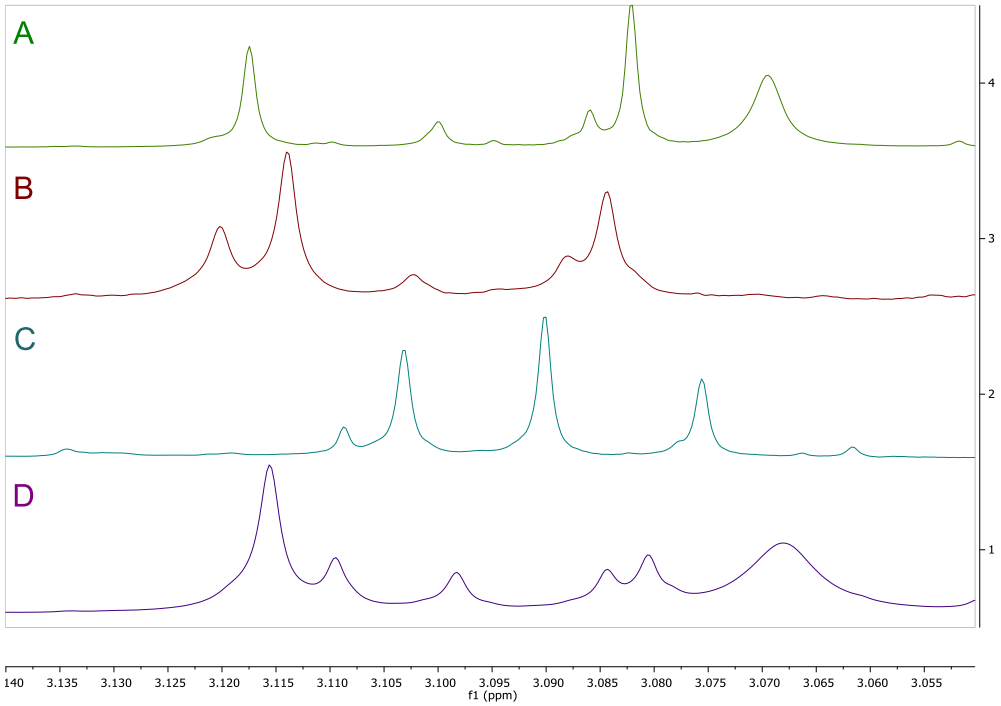

Figure 4: DMAP signals for coordination isomers of **50** (A and B) and **51** (C and D) from exchanges in THF (A and C) and xylenes (B and D).

We looked to simplify the spectra of **50** and **51** by providing enough energy to drive isomerization to thermodynamically preferred products. However, VT NMR experiments of **50** and **51** provided no change in the ratio of observed isomers, and continued heating above 50 °C resulted in decomposition. Based on these data we concluded that the observed product ratio is governed by thermodynamic preference.

We changed our strategy to focus on accessing the kinetically preferred isomers of **50** and **51**, by taking advantage of the increased solubility of **34** in non-polar solvents compared to other TpMo(DMAP)(NO)(η^2-ligand) complexes. We investigated a variety of organic solvents to give a homogenous solution of the initial **34** + ligand, while providing limited solubility to the resulting exchange product. We hoped that reducing the time the product was in solution would limit its

ability to isomerize, providing a ratio of coordination isomers governed by kinetic control. Analysis of the DMAP methyl signals shows the limited success of the kinetic solvent strategy. Each solvent provided a different ratio of coordination isomers for both **50** and **51**; with THF and xylenes having the biggest impact, as illustrated in Figure 4B and D, respectively. However, despite the ability to influence the ratio of coordination isomers by changes to the solvent system, the products still feature a great deal of spectral overlap preventing full characterization of **50** and **51**.

4.5 Current Mo – Exchange: TpMo(DMAP)(NO)(η^2-α,α,α-trifluorotoluene)

While **34** was the 1st molybdenum complex to be used a precursor, analogous to 3rd row dihapto-benzene complexes, it also provided a great deal of synthetic challenges. Due to the relatively slow rate of substitution, and susceptibility towards oxidative decomposition, other exchange complexes were investigated. TpMo(DMAP)(NO)(η^2-3,5-dimethylfuran) (**37**) was briefly employed, as discussed in Chapter 3, however, **37** has since been replaced by TpMo(DMAP)(NO)(η^2-α,α,α-trifluorotoluene) (**I**). **I** was initially synthesized by Jeff Myers, and was later optimized by Jacob Smith, who has also investigated its use as a molybdenum exchange reagent.

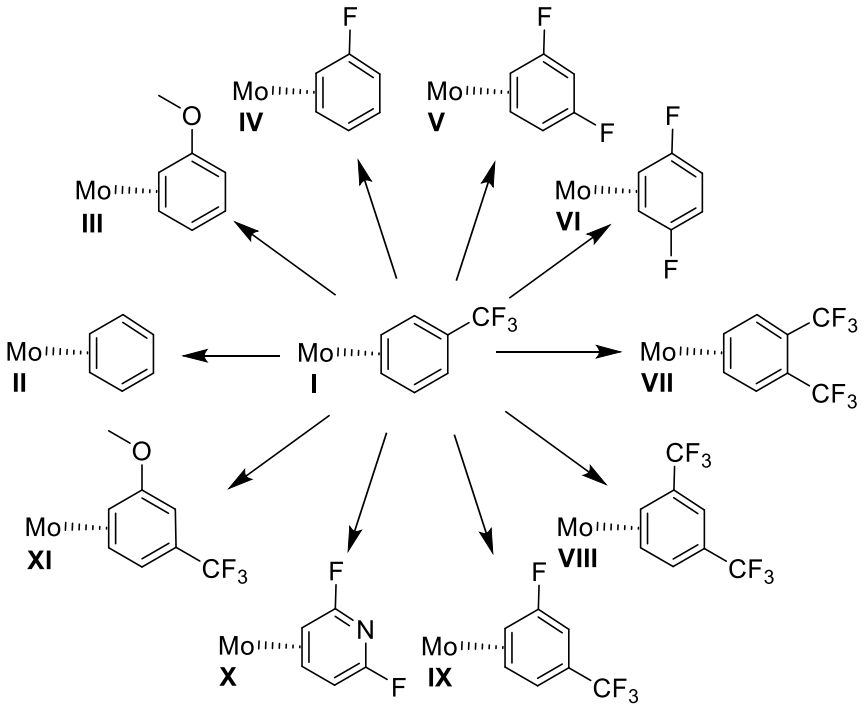

Scheme 3: Exchanges from **I** illustrating expanded molybdenum coordination scope.

Kinetic studies by Jacob Smith have shown that **I** exchanges at a much faster rate than **34** (3 h vs ~3 days). The shortened $t_{1/2}$ of **I** has also resulted in increased resistance towards oxidation, as well as access to new dihapto-molybdenum complexes (Scheme 3). Within these exchanges Jacob Smith has shown a difference in reactivity between molybdenum and tungsten dearomatization agents, as the more weakly donating molybdenum system allows for dihapto-coordination of the fluorinated aromatics **IV** and **IX**, which undergo C-F activation with {TpW(PMe_3)(NO)}.[3, 15] Moreover, Jacob Smith has shown the ability to coordinate benzene (**II**) and anisole (**III**), which were inaccessible from **34** (Scheme 3). The continued development of the molybdenum coordination scope is ongoing through the optimized **I** exchange conditions.

4.6 Conclusion

34 provided an important step forward in molybdenum based dearomatization chemistry as the 1st generation of exchange reagents. Through the optimized exchange conditions we were able to coordinate ligands that are incompatible with reduction from **20**, and yielded the 1st

example of a dihapto-coordinated ester by a 2nd row metal (**48**). Furthermore, the increased solubility of **34** compared to TpMo(DMAP)(NO)(η^2-aromatic) products has been demonstrated to impact the ratio of coordination isomers.

However, exchanges from **34** are also limited in scope, and are prone to oxidative decomposition due to the relatively long timeline required (~3 days). These drawbacks have led to the development of the current, more versatile **I**. **I** provides a much faster rate of exchange, which subsequently limits oxidative decomposition. Initial exploration of **I** as an exchange reagent has dramatically increased the coordination scope of the molybdenum system, and has provided access to a variety of dihapto-coordinate fluorinated aromatic complexes which are inaccessible to 3rd row dearomatization agents. The ongoing study of **I** to expand the coordination scope of aromatic systems offers the possibility to apply dearomatization chemistry to a variety of otherwise inaccessible biologically interesting cyclic cores.

4.7 Experimental

General Methods

NMR spectra were obtained on 600 or 800 MHz spectrometers. Chemical shifts are referenced to tertramethylsilane (TMS) utilizing residual ^{1}H signals of the deuterated solvents as internal standards. Chemical shifts are reported in ppm and coupling constants (*J*) are reported in hertz (Hz). Infrared Spectra (IR) were recorded on a spectrometer as a glaze on a Horizontal Attenuated Total Reflectance (HATR) accessory, or as a glaze between two NaCl plates, with peaks reported in cm^{-1}. Electrochemical experiments were performed under a nitrogen atmosphere. Cyclic voltammetric data were recorded at ambient temperature at 100 mV/s unless otherwise noted, with a standard three electrode cell from +1.8 V to -1.8 V with a platinum working electrode, *N*,*N*-dimethylacetamide (DMA) or acetonitrile (MeCN) solvent, and tetrabutylammonium hexafluorophosphate (TBAH) electrolyte (~1.0 M). For CV data recorded in aqueous solutions,

sodium triflate (NaOTf) was used as the electrolyte. All potentials are reported versus the normal hydrogen electrode (NHE) using cobaltocenium hexafluorophosphate ($E_{1/2}$ = -0.78 V, -1.75 V) or ferrocene ($E_{1/2}$ = 0.55 V) as an internal standard. Peak separation of all reversible couples was less than 100 mV. All synthetic reactions were performed in a glovebox under a dry nitrogen atmosphere unless otherwise noted. All solvents were purged with nitrogen prior to use. Deuterated solvents were used as received from Cambridge Isotopes. Characterization of **26-27** is consistent with previous literature reports.[16]

Synthesis of TpMo(DMAP)(NO)(η^2-furan) (44)

Compound **34** (106 mg, 0.177 mmol) and furan (0.14 mL, 1.93 mmol) were added to a 4 dram vial charged with a stir bar. The solid was dissolved in THF (3 mL), giving a red solution which was stirred for 3 d. The solution was precipitated by drop-wise addition to stirring pentane (25 mL). The resulting light brown mixture was left to stir for 5 min. The mixture was then filtered through a 15 mL fine fritted funnel, isolating a yellow solid which was desiccated giving (**44**) (71 %, 66.4 mg, 0.125 mmol). Present as a mix of isomers in a 1.6 : 1 ratio, with the major isomer having the furan oxygen distal to DMAP. ^{1}H NMR (acetone-d_6, δ): (Major isomer) 8.20 (d, *J* = 1.7, 1H, Tp 3/5), 7.92 (d, *J* = 2.1, 1H, Tp 3/5), 7.88 (d, *J* = 2.1, Tp 3/5), 7.86 (d, *J* = 2.1, 1H, Tp 3/5), 7.81 (bd, *J* = 5.7, 2H, DMAP 2/6), 7.26 (d, *J* = 1.3, 1H, Tp 3/5), 7.04, (d, *J* = 1.6, 1H, Tp 3/5), 7.64-7.59 (m, 3H, DMAP 3/5, furan H5), 6.33 (m, 1H, Tp 4), 6.25 (m, 1H, Tp 4), 6.16 (m, 2H, Tp 4, furan H4), 5.92 (t, *J* = 1.6, 1H, Tp 4), 5.77 (d, *J* = 4.5, 1H, furan H2), 3.67 (dd, *J* = 4.4, 2.8, 1H, furan H3), 3.07 (s, 6H, DMAP Me). (Minor isomer) 8.08 (d, *J* = 1.0, 1H, Tp 3/5), 7.91 (d, *J* = 1.9, 1H, Tp 3/5), 7.88 (d, *J* = 2.3, Tp 3/5), 7.86 (d, *J* = 2.1, 1H, Tp 3/5), 7.76 (bs, 2H, DMAP 2/6), 7.21 (d, *J* = 1.8, 1H, Tp 3/5), 7.03, (d, *J* = 1.5, 1H, Tp 3/5), 7.64-7.59 (m, 3H, DMAP 3/5, furan H5), 6.33 (m, 1H, Tp 4), 6.28 (d, *J* = 4.2, 1H, furan 2H), 6.25 (m, 2H, Tp 4, furan H4), 6.09 (m, 1H, Tp 4), 5.92 (t, *J* = 1.6, 1H, Tp 4), 3.21 (dd, *J* =

4.5, 2.8, 1H, furan H3), 3.07 (s, 6H, DMAP Me). CV: $E_{p,a}$ = -0.37 V. IR: ν_{NO} = 1573 cm^{-1}; ν_{BH} = 2479 cm^{-1}.

Synthesis of TpMo(DMAP)(NO)(η^2-thiophene) (45)

Compound **34** (109 mg, 0.182 mmol) and thiophene (0.14 mL, 1.75 mmol) were added to a 4 dram vial charged with a stir bar. The solid was dissolved in THF (3 mL), giving a red solution which was stirred for 3 d. The solution was precipitated by drop-wise addition to stirring pentane (25 mL). The resulting light brown mixture was left to stir for 5 min. The mixture was then filtered through a 15 mL fine fritted funnel, isolating a yellow solid which was desiccated giving (**45**) (79 %, 78 mg, 0.143 mmol). Present in a 1 : 1 mix of isomers. ^{1}H NMR (acetone-d_6, δ): (Mix of isomers) 8.45 (d, *J* = 1.4, 1H, Tp 3/5), 8.09 (d, *J* = 1.9, 1H, Tp 3/5), 7.95 (d, *J* = 2.2, 2H, DMAP 2/6), 7.92 (d, *J* = 2.5, Tp 3/5), 7.89 (d, *J* = 2.2, 1H, Tp 3/5), 7.85 (d, *J* = 2.3, 1H, Tp 3/5), 7.85 (d, *J* = 2.4, 1H, Tp 3/5), 7.80, (bs, 2H, DMAP 2/6), 7.45 (d, *J* = 2.3, 1H, Tp 3/5), 7.39 (d, *J* = 1.7, 1H, Tp 3/5), 7.00 (d, *J* = 2.1, 1H, Tp 3/5), 6.98 (d, *J* = 2.5, 1H, Tp 3/5), 6.71 (dd, *J* = 5.3, 2.6, 1H, thiophene H5), 6.65 (m, 4H, DMAP 3/5), 6.46 (dd, *J* = 5.5, 2.9, 1H, thiophene H5), 6.33 (t, *J* = 1.6, 2H, Tp 4), 6.31 (t, *J* = 1.9, 2H, Tp 4), 6.18 (dd, *J* = 5.1, 1.5, 1H, thiophene H4), 6.16 (dd, *J* = 5.3, 1.3, 1H, thiophene H4), 6.14 (t, *J* = 2.0, 2H, Tp 4), 4.39 (d, *J* = 7.1, 1H, thiophene H2), 3.95 (dd, *J* = 7.2, 2.9, 1H, thiophene H3), 3.89 (dd, *J* = 6.9, 1.4, 1H, thiophene H3), 3.56 (dd, *J* = 6.9, 3.0, 1H, thiophene H3), 3.08 (s, 6H, DMAP Me), 3.08 (s, 6H, DMAP Me). CV: $E_{p,a}$ = -0.38 V. IR: ν_{NO} = 1580 cm^{-1}; ν_{BH} = 2481 cm^{-1}.

Synthesis of TpMo(DMAP)$_2$(NO) (46)

Compound **34** (108.7 mg, 0.182 mmol) and DMAP (276.3 mg, 2.26 mmol) were added to a 4 dram vial charged with a stir bar. The solid was dissolved in THF (3 mL), giving a red solution which was stirred for 5 d. The solution was precipitated by drop-wise addition to stirring pentane (25 mL). The resulting blue mixture was left to stir for 5 min. The mixture was then filtered through a 15

mL fine fritted funnel, isolating a dark blue solid which was desiccated giving (**46**) (74 %, 78.6 mg, 0.134 mmol). CV: $E_{p,a}$ = +0.68 V, $E_{1/2}$ = -1.20 V.

Synthesis of TpMo(DMAP)(NO)(η²-*N*,*N*-dimethyl uracil) (47)

Compound **34** (110 mg, 0.184 mmol) and *N*, *N*-dimethyl uracil (254 mg, 1.81 mmol) were added to a 4 dram vial charged with a stir bar. The solid was dissolved in THF (3 mL), giving a red solution which was stirred for 3 d. The solution was precipitated by drop-wise addition to stirring pentane (25 mL). The resulting light brown mixture was left to stir for 5 min. The mixture was then filtered through a 15 mL fine fritted funnel, isolating a yellow solid which was desiccated giving (**47**) (200 % (impure with extra ligand), 245 mg). Present as a 1.5 : 1 ratio of coordination diasteromers, with the major isomer having the amide carbonyl oriented proximal to DMAP. ^{1}H NMR (acetone-d_6, δ): (Major isomer) 8.03 (d, *J* = 2.3, 1H, Tp 3/5), 7.99 (d, *J* = 2.5, 1H, Tp 3/5), 7.83 (m, 1H, Tp 3/5), 7.82 (d, *J* = 2.2, 1H, Tp 3/5), 7.72 (d, *J* = 2.1, 1H, Tp 3/5), 6.99 (d, *J* = 2.4, 1H, Tp 3/5), 6.41 (t, *J* = 2.3, 1H, Tp 4), 6.38 (1, *J* = 2.3, 1H, Tp 4), 6.11 (t, *J* = 2.1, 1H, Tp 4), 3.90 (d, *J* = 8.9, 1H, uracil alkene H), 3.29 (s, 3H, uracil Me) 3.07 (s, 6H, DMAP Me), 2.88 (s, 3H, uracil Me), 2.75 (d, *J* = 8.7, 1H, uracil alkene H). (Minor isomer) 8.44 (d, *J* = 2.1, 1H, Tp 3/5), 7.98 (d, *J* = 2.6, 1H, Tp 3/5), 7.84 (d, *J* = 2.3, Tp 3/5), 7.83 (m, 1H, Tp 3/5), 7.71 (bd, *J* = 5.7, 2H, DMAP 2/6), 7.15 (d, *J* = 2.0, 1H, Tp 3/5), 6.38 (t, *J* = 2.1, 1H, Tp 4), 6.27 (t, *J* = 2.1, 1H, Tp 4), 6.15 (t, *J* = 2.4, 1H, Tp 4), 4.68 (d, *J* = 8.4, 1H, uracil alkene H), 3.30 (s, 3H, uracil Me), 3.10 (s, 6H, DMAP Me), 2.62 (s, 3H, uracil Me), 2.39 (d, *J* = 8.6, 1H, uracil alkene H). CV: $E_{p,a}$ = +0.08 V.

Synthesis of TpMo(DMAP)(NO)(η²-ethyl acetate) (48)

Compound **34** (95.0 mg, 0.159 mmol), EtOAc (0.17 mL, 1.73 mmol), and THF (3 mL) were added to a 4 dram vial charged with a stir bar, giving a red solution which was stirred for 3 d. The solution was precipitated by drop-wise addition to stirring pentane (25 mL). The resulting light brown mixture was left to stir for 5 min. The mixture was then filtered through a 15 mL fine fritted

funnel, isolating a yellow solid which was desiccated giving (**48**) (42 %, 36 mg, 0.066 mmol). ^{1}H NMR (acetone-d_6, δ): 8.07 (d, *J* = 2.1, 1H, Tp 3/5), 8.02 (d, *J* = 1.8, 1H, Tp 3/5), 7.99 (d, *J* = 2.1, Tp 3/5), 7.95 (d, *J* = 2.3, 1H, Tp 3/5), 7.62 (d, *J* = 1.6, 1H, DMAP 2/6), 7.61 (d, *J* = 1.4, 1H, DMAP 2/6), 7.45 (d, *J* = 2.4, 1H, Tp 3/5), 7.09, (d, *J* = 2.1, 1H, Tp 3/5), 6.69 (d, *J* = 1.6, 1H, DMAP 3/5), 6.68 (d, *J* = 1.4, 1H, DMAP 3/5), 6.39 (t, *J* = 2.2, 1H, Tp 4), 6.34 (t, *J* = 2.2, 1H, Tp 4), 6.20 (t, *J* = 2.0, 1H, Tp 4), 3.84 (m, 1H, EtOAc CH_2), 3.77 (m, 1H, EtOAc CH_2), 3.00 (s, 6H, DMAP Me), 1.20 (t, *J* = 5.2, 3H, EtOAc Me), 0.78 (s, 3H, EtOAc Me). CV: $E_{p,a}$ = +0.72 V. IR: ν_{NO} = 1540 cm^{-1}; ν_{BH} = 2487 cm^{-1}.

Synthesis of TpMo(DMAP)(NO)(η^2-cyclohexene) (49)

Compound **34** (97 mg, 0.162 mmol) and cyclohexene (0.19 mL, 1.88 mmol) were added to a 4 dram vial charged with a stir bar. The solid was dissolved in THF (3 mL), giving a red solution which was stirred for 2 d. The solution was precipitated by drop-wise addition to stirring pentane (25 mL). The resulting light brown mixture was left to stir for 5 min. The mixture was then filtered through a 15 mL fine fritted funnel, isolating a yellow solid which was desiccated giving (**49**) (64 %, 56.3 mg, 0.104 mmol). ^{1}H NMR (acetone-d_6, δ): 8.04 (m, 3H, Tp 3/5, DMAP 2/6), 7.88 (d, *J* = 2.2, 1H, Tp 3/5), 7.4 (d, *J* = 2.4, Tp 3/5), 7.76 (d, *J* = 2.2, 1H, Tp 3/5), 7.55 (d, *J* = 2.1, 1H, Tp 3/5), 7.19, (d, *J* = 2.0, 1H, Tp 3/5), 6.65 (d, *J* = 1.6, 1H, DMAP 3/5), 6.64 (d, *J* = 1.6, 1H, DMAP 3/5), 6.29 (t, *J* = 2.1, 1H, Tp 4), 6.28 (t, *J* = 2.2, 1H, Tp 4), 6.11 (t, *J* = 1.9, 1H, Tp 4), 3.06 (s, 6H, DMAP Me), 2.74 (m, 1H, cyclohexene), 2.42 (m, 2H, cyclohexene), 2.20 (m, 3H, cyclohexene), 1.77 (m, 1H, cyclohexene), 2.74 (m, 2H, cyclohexene), 1.47 (m, 1H, cyclohexene), 1.37 (m, 1H, cyclohexene). CV: $E_{p,a}$ = -0.05 V.

Synthesis of TpMo(DMAP)(NO)(η^2-quinoline) (50)

Compound **34** (95 mg, 0.159 mmol) and quinoline (0.19 mL, 1.60 mmol) were added to a 4 dram vial charged with a stir bar. The solid was dissolved in THF (3 mL), giving a red solution which was stirred for 3 d. The solution was precipitated by drop-wise addition to stirring pentane (25 mL).

The resulting light brown mixture was left to stir for 5 min. The mixture was then filtered through a 15 mL fine fritted funnel, isolating a yellow solid which was desiccated giving (**50**) (32 %, 30 mg, 0.051 mmol). Partial characterization is given due to the spectral complexity of overlapping signals. ^{1}H NMR (acetone-d_6, δ): 3.90 (d, *J* = 7.8, 1H, quinoline), 3.51 (d, *J* = 8.2, 3.8, 1H, quinoline), 3.14 (d, *J* = 8.6, 6.6, 1H, quinoline), 3.12 (s, 6H, DMAP Me), 3.08 (s, 6H, DMAP Me), 3.07 (s, 6H, DMAP Me). IR: ν_{NO} = 1596 cm^{-1}; ν_{BH} = 2485 cm^{-1}.

Synthesis of TpMo(DMAP)(NO)(η^2-isoquinoline) (51)

Compound **34** (106 mg, 0.177 mmol) and isoquinoline (0.20 mL, 1.70 mmol) were added to a 4 dram vial charged with a stir bar. The solid was dissolved in THF (3 mL), giving a red solution which was stirred for 3 d. The solution was precipitated by drop-wise addition to stirring pentane (25 mL). The resulting light brown mixture was left to stir for 5 min. The mixture was then filtered through a 15 mL fine fritted funnel, isolating a yellow solid which was desiccated giving (**51**) (39 %, 41 mg, 0.069 mmol). Partial characterization is given due to the spectral complexity of overlapping signals. Selected signals are matched in relative intensity between DMAP methyl signals and protons on coordinated isoquinoline carbons. ^{1}H NMR (acetone-d_6, δ): 3.77 (d, *J* = 7.7, 1H, isoquinoline), 3.55 (dd, *J* = 8.1, 5.8, 1H isoquinoline), 3.11 (s, 6H, DMAP Me); 3.68 (d, *J* = 7.6, 1H, isoquinoline), 3.15 (dd, *J* = 7.9, 5.3, 1H isoquinoline), 3.10 (s, 6H, DMAP Me); 3.54 (d, *J* = 8.0, 1H, isoquinoline), 3.22 (dd, *J* = 8.0, 5.4, 1H isoquinoline), 3.08 (s, 6H, DMAP Me). IR: ν_{NO} = 1596 cm^{-1}; ν_{BH} = 2486 cm^{-1}.

4.8 References

1. Meiere, S. H.; Brooks, B. C.; Gunnoe, T. B.; Sabat, M.; Harman, W. D. *Organometallics* **2001,** *20*, 1038-1040.

2. Graham, P. M.; Meiere, S. H.; Sabat, M.; Harman, W. D. *Organometallics* **2003,** *22*, 4364-4366.

3. Welch, K. D.; Harrison, D. P.; Lis, E. C.; Liu, W.; Salomon, R. J.; Harman, W. D.; Myers, W. H. *Organometallics* **2007,** *26*, 2791-2794.

4. Harman, W. D. *Chem. Rev.* **1997,** *97*, 1953-1978.

5. Harman, W. D.; Taube, H. *J. Am. Chem. Soc.* **1987,** *109*, 1883-1885.

6. Meiere, S. H.; Keane, J. M.; Gunnoe, T. B.; Sabat, M.; Harman, W. D. *J. Am. Chem. Soc.* **2003,** *125*, 2024-2025.

7. Mocella, C. J.; Delafuente, D. A.; Keane, J. M.; Warner, G. R.; Friedman, L. A.; Sabat, M.; Harman, W. D. *Organometallics* **2004,** *23*, 3772-3779.

8. Meiere, S. H.; Valahovic, M. T.; Harman, W. D. *J. Am. Chem. Soc.* **2002,** *124*, 15099-15103.

9. Keane, J. M.; Harman, W. D. *Organometallics* **2005,** *24*, 1786-1798.

10. Ha, Y.; Dilsky, S.; Graham, P. M.; Liu, W.; Reichart, T. M.; Sabat, M.; Keane, J. M.; Harman, W. D. *Organometallics* **2006,** *25*, 5184-5187.

11. Graham, P. M.; Mocella, C. J.; Sabat, M.; Harman, W. D. *Organometallics* **2005,** *24*, 911-919.

12. Lis, E. C.; Delafuente, D. A.; Lin, Y.; Mocella, C. J.; Todd, M. A.; Liu, W.; Sabat, M.; Myers, W. H.; Harman, W. D. *Organometallics* **2006,** *25*, 5051-5058.

13. Meiere, S. H.; Ding, F.; Friedman, L. A.; Sabat, M.; Harman, W. D. *J. Am. Chem. Soc.* **2002,** *124*, 13506-13512.

14. Meiere, S. H.; Harman, W. D. *Organometallics* **2001,** *20*, 3876-3883.

15. Liu, W.; Welch, K.; Trindle, C. O.; Sabat, M.; Myers, W. H.; Harman, W. D. *Organometallics* **2007,** *26*, 2589-2597.

16. Myers, J. T.; Dakermanji, S. J.; Chastanet, T. R.; Shivokevich, P. J.; Strausberg, L. J.; Sabat, M.; Myers, W. H.; Harman, W. D. *Organometallics* **2017,** *36*, 543-555.

Chapter 5

Investigation of a Dual Bidentate Molybdenum Dearomatization Agent

5.1 Introduction

The stereochemical instability of the chiral molybdenum center when proceeding through the proposed 5-coordinate $TpMo^0(DMAP)(NO)$ intermediate has limited the applicability of a general method for molybdenum resolution. Thus, far efforts to transfer chirality through a 5-coordinate Mo^0 intermediate, either through exchange or reduction from the purported **20*** have been unsuccessful. We explored an alternative ligand set as a means to overcome the propensity of the molybdenum center to racemize. The proposed ligand set featured two bidentate ligands in place of the combination of Tp and L, while maintaining NO^+ as a means to achieve the desired electrochemical potential. We reasoned that a ligand set featuring two bidentate ligands would provide a higher barrier to racemization (through the proposed migration of L, Chapter 3), as migration of one arm of a bidentate ligand would necessitate a change in the geometry of the other, non-migratory arm. With this strategy in place, we began to explore alternatives to Tp and L (Figure 1).

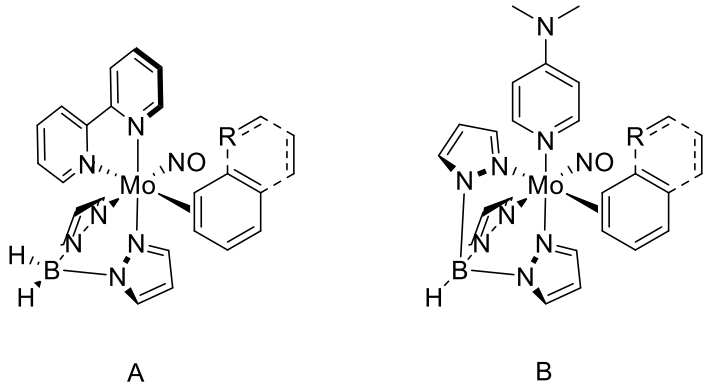

Figure 1: Comparison of proposed dual bidentate ligand set (A) with the established Tp – based ligand set (B).

5.2 Bis(pyrazolyl)borate (Bp) Complexes

While a bidentate based ligand set required changes to the established ligand motif of previous rhenium, tungsten, and molybdenum based dearomatization chemistry; given the difficulty in establishing a suitable replacement for the 1st generation osmium system, we hoped

to make the changes as small as possible. With that goal in mind we looked to maintain the steric and electronic characteristics of the {TpM(L)(CO/NO)} fragments by employing the bidentate ligand dihydridobis(pyrazolyl)borate (Bp, **52**). Bp was introduced by Trofimenko early in the history of scorpionate chemistry, and like Tp provides a negative charge to balance the NO^+.[1] **52** also coordinates in a non-planar fashion, which provides a similar steric profile to the pyrazolyl rings cis to the dihapto-coordination site of the {TpMo(DMAP)(NO)} fragment (Figure 1). This geometry avoids the unfavorable sterics illustrated in the previous polypyridal rhenium complexes. The non-planar coordination of the Bp ligand allows the incorporation of a bipyridal – based ligand as the 2nd bidentate ligand (Figure 1A), producing a complex which we expected to provide similar steric and electronic properties as the established molybdenum dearomatization agents (Figure 1B).

We envisioned the synthesis of **III** as similar to that employed for TpMo(DMAP)(NO)(I) (**20**) (Scheme 1). In the proposed synthesis we would generate $[BpMo(CO)_4]^-$ (**53**) *in situ*, isolating the neutral **I**, analogous to $TpMo(NO)(CO)_2$. Coordination of the bipyridine (bpy) ligand would then proceed through thermolysis to give **II**, which could undergo oxidation with Br_2 or I_2 to provide a dearomatization precursor **III** (Scheme 1).

Despite the straightforward nature of the proposed synthesis, we were met with synthetic difficulties from the start. These difficulties began with the synthesis of the bidentate ligand **52**. While Trofimenko reported the ligand in 1967, **52** was synthesized and reacted *in situ* and isolated as a metal complex.[1] Efforts to isolate **52** in a manner similar to that of KTp resulted in an impure mixture, yielding a viscous oil. Optimization of **52** was achieved by careful control of the reaction temperature, which was kept under 125 ^oC until hydrogen evolution ceased. The resulting mixture was then purified by crystallization from a dioxane and anisole solution, which consistently produced clean **52** with 88 % yield on a 100 g scale.

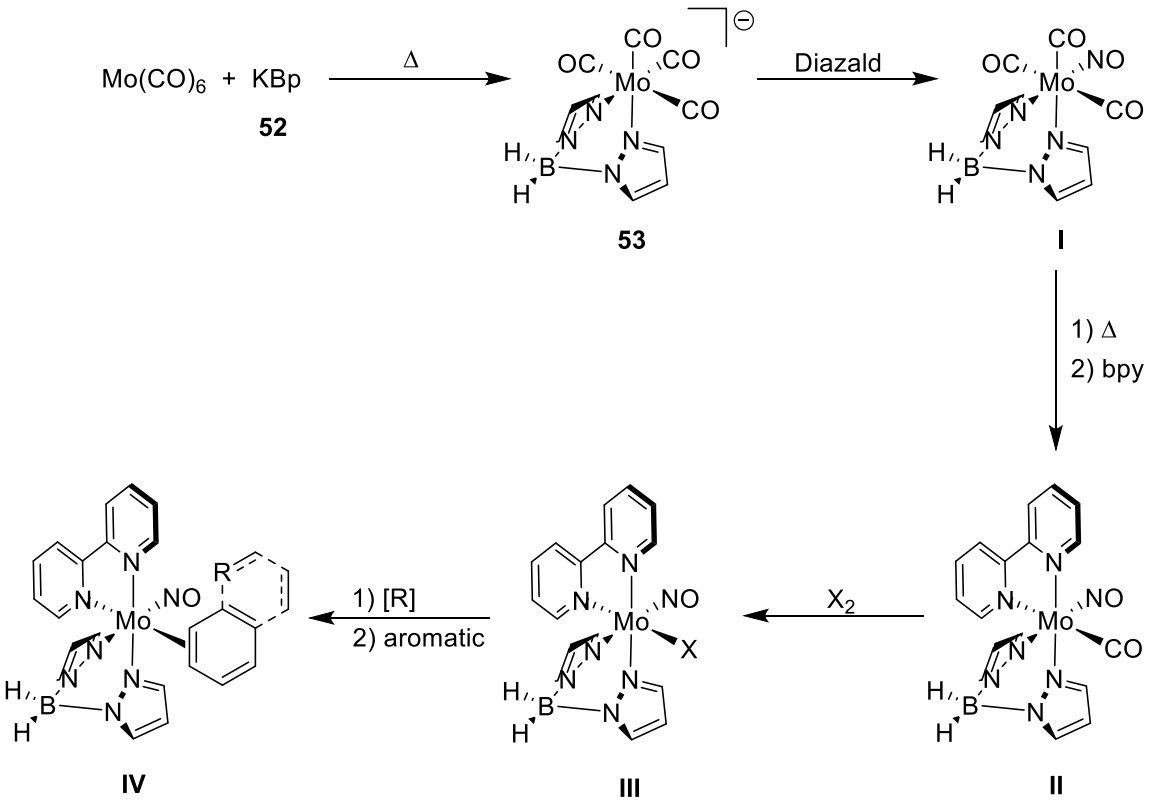

Scheme 1: Proposed synthesis of a molybdenum dearomatization agent featuring two bidentate ligands (**IV**).

Coordination of **52** proceeded by thermolysis of $Mo(CO)_6$ in THF, analogous to Tp coordination, and we looked to generate the nitrosylated complex **I** by addition of Diazald®. These efforts continuously yielded products lacking a NO stretch in the IR. Moreover, the isolated products appeared to decompose in air over time, changing from tan to dark brown. We proposed that unreacted Diazald®, or a byproduct formed upon the addition of the nitrosylating agent was responsible for the decomposition of the product. We looked to isolate $[BpMo(CO)_4]^-$ (**53**), and test nitrosylation conditions on the resulting complex. However, we found that this product also degraded as a solid in air over time, and concluded that while less electron rich than $[TpMo(CO)_3]^-$, **53** was also vulnerable to air oxidation (*vide infra*).

Due to the instability of the tetracarbonyl **53** in air, synthesis and isolation were conducted in the glovebox. **53** provided limited solubility in THF, and we reasoned that the heterogeneous nature of the reaction mixture may be the problem with the nitrosylation process.

DMF and DMSO were explored as potential alternatives to THF for a one-pot synthesis of **I**, which were also unsuccessful. Due to our inability to introduce a nitrosyl to **53** we contemplated an alternative synthesis for our proposed bidentate based dearomatization agent **IV**.

5.3 2,2'-Bipyridal Complexes

Faced with the synthetic difficulties of Bp complexes, we proposed an alternative synthesis of **IV**. In the new pathway, the bipyridine ligand would be introduced initially, and the bidentate scorpionate **52** would be coordinated by thermolysis of the nitrosylated molybdenum bipyridine product (**V** in Scheme 2). Introduction of bpy followed previous literature reports via thermolysis of $Mo(CO)_6$, producing $bpyMo(CO)_4$ (**54**).

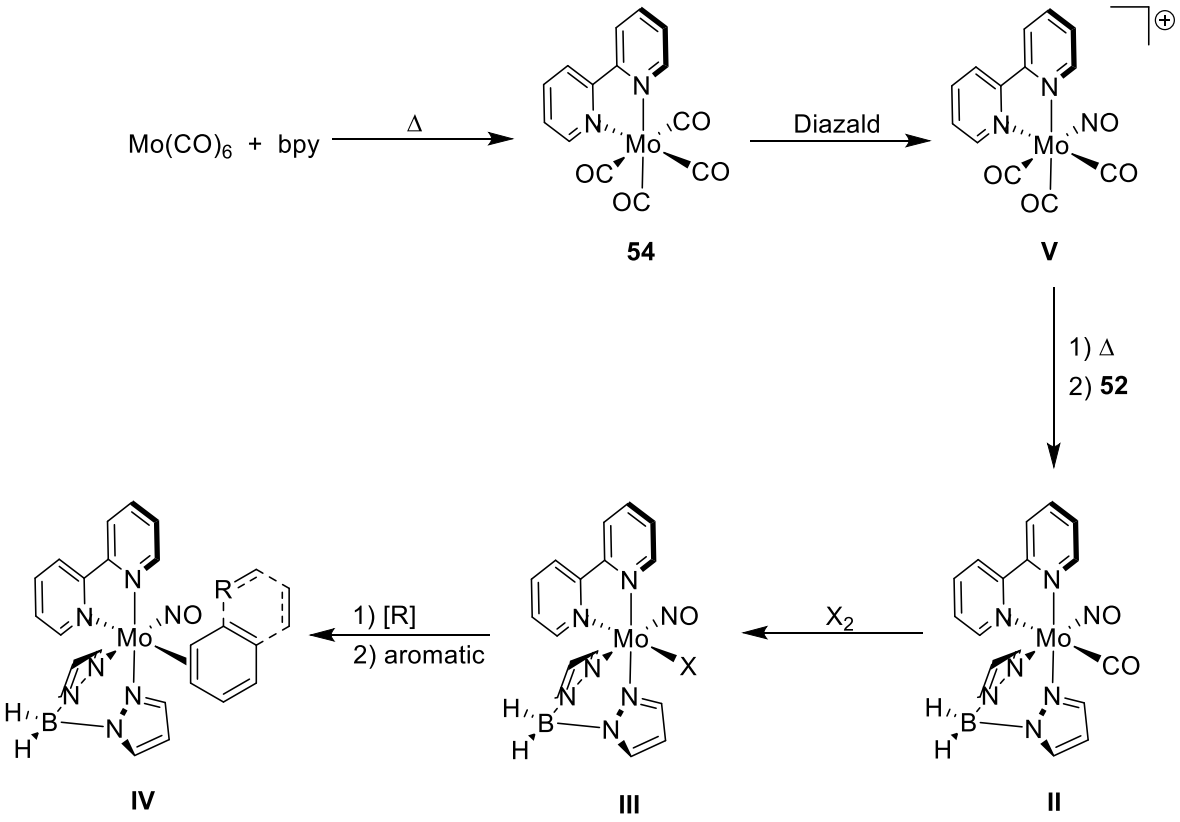

Scheme 2: Alternate synthetic pathway to **IV**.

However, **54** also proved to be unreactive towards Diazald®. Despite this challenge, **54** is air stable, and showed no signs of decomposition upon exposure to Diazald®. These changes are

likely due to the increased reduction potential of **54** vs **53**, as the bpy ligand provides reduced electron donation as well as a neutral molybdenum complex. The eventual introduction of NO^+ followed a literature report for nitrosylation of bpyMo(MeIm)$(CO)_3$ (**55**).[2] We were able to reproduce **55**, giving $[bpyMo(MeIm)(NO)(CO)_2]^+$ **56** in good yield, and decided to once again amend the proposed synthesis of **IV**, outlined in Scheme 3.

Within Scheme 3 we proposed that thermolysis of **57** would preferentially cleave the Mo – MeIm bond, providing a coordination site for the 2nd bidentate ligand. We employed the thermolysis conditions optimized for TpMo(DMAP)(NO)(CO) (**22**), as **56** provided an electrochemical profile similar to TpMo$(NO)(CO)_2$.[3] Monitoring the reaction by CV revealed a species that was consistent with the desired product, providing a reversible couple at 0.50 V. However, attempts to isolate the product via water precipitation, as in TpMo(L)(NO)(CO) syntheses, were unsuccessful. The reaction mixture remained homogeneous, even when stirred in water overnight. Organic solvents (*e.g.*, Et_2O, THF, toluene, and xylenes) were explored as alternatives to water precipitation; however, these solvents were also unsuccessful, giving either homogeneous solutions or viscous oils which no longer provided the desired electrochemical signature. Given the difficulty of product isolation from DMF, we conducted the thermolysis xylenes and toluene, similar to initial the thermolysis conditions for the synthesis of TpMo(MeIm)(NO)(CO) (**1**).[4] However, the longer reaction times required of the lower boiling solvents (110 and 138 vs 154 ^oC for toluene and xylenes vs DMF, respectively) resulted in decomposition.

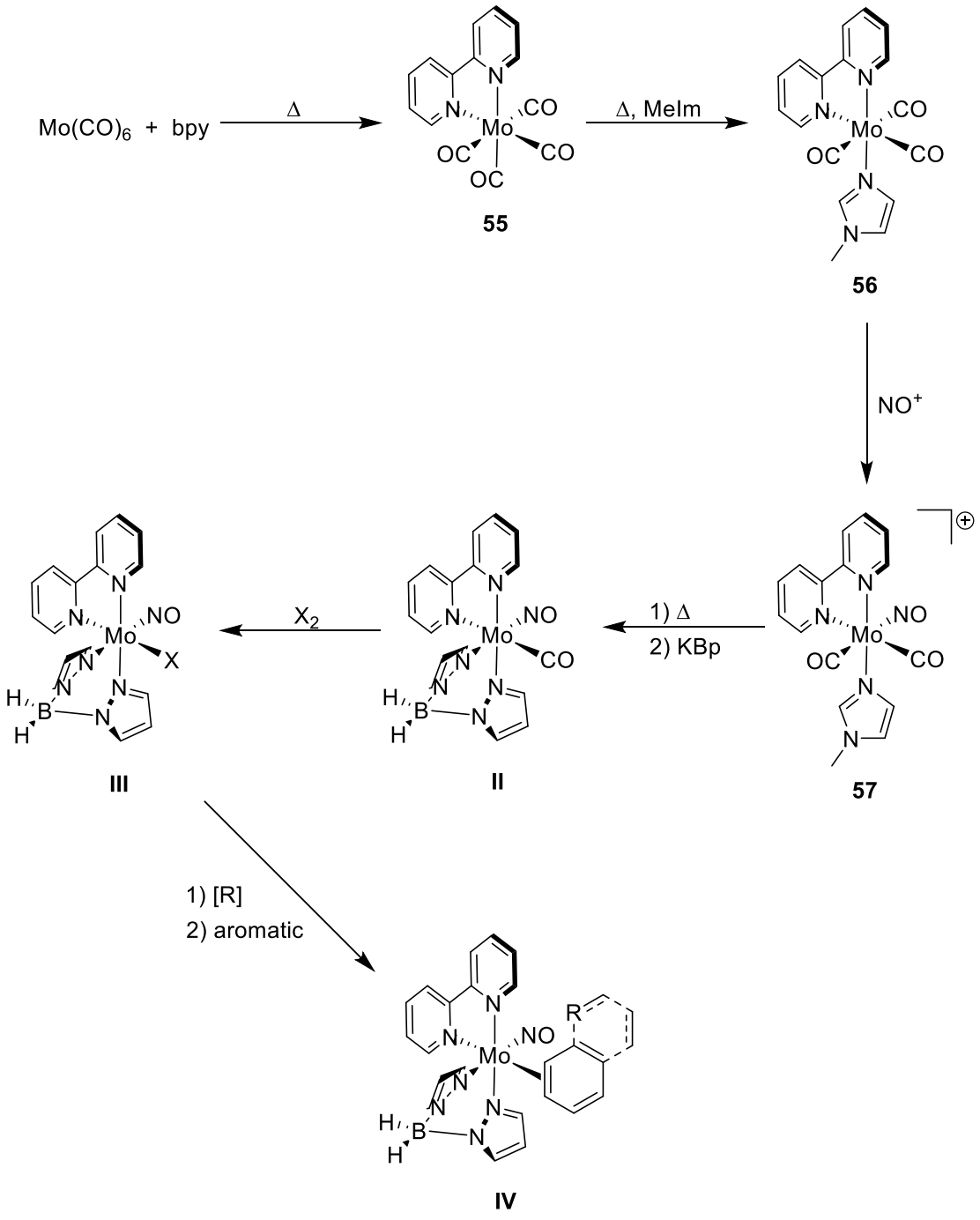

Scheme 3: Alternate synthetic pathway to **IV**, with incorporation of literature reports of **56** and **57**.

5.4 Polypyridal Molybdenum Complexes

Due to the synthetic difficulties associated with **52**, and its resulting molybdenum complexes, we decided to explore alternative bidentate ligands. We began this investigation with

the addition of a 2nd bpy, despite the associated steric difficulties of polypyridal metal systems as dearomatization agents (*vide supra*). These efforts simply substituted bpy for **52**, as illustrated in Scheme 5, isolating $[bpy_2Mo(NO)(CO)]^+$ (**57**). **57** provided similar electronics to the TpMo(L)(NO)(CO) analogs **1**, **4**-**5**, **22**-**23** (0.65 V, ν_{NO} = 1584, ν_{CO} = 1874). The reduced electron density of **57** is due to the reduced donation and increased π-acidity of the conjugated polypyridal systems, as well as the net positive charge of the complex. ^{1}H NMR of **57** showed the presence of both possible isomers illustrated in Figure 2, favoring the *trans* form B by 1 : 2 (A : B). This was a surprising result given the strong trans-effect of the NO^+ and CO ligands.[5] Although this produced the undesired achiral B form as the major isomer, we hoped the bpy ligands would undergo a rearrangement during the oxidation process.

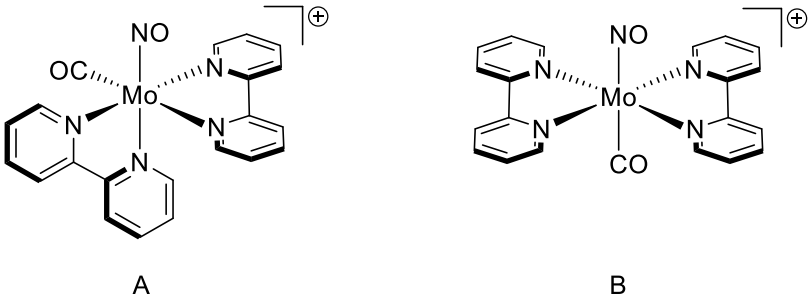

Figure 2: Coordination isomers of **57**.

Oxidation of **57** with Br_2 produced $bpy_2Mo(NO)(Br)$ (**58**) in good yield (86 %) (Scheme 4). However, the resulting Mo^I complex was much more electron deficient (-0.49 V) than TpMo(L)(NO)(X) precursors (< -1.2 V). Despite the relatively high reduction potential and unfavorable sterics associated with the polypyridal molybdenum complex, we attempted reduction to a dihapto-cyclopentene complex. Initial attempts used Mg^o, Zn^o, and Zn/Hg amalgam reducing agents as a means to take advantage of the increased reduction potential of **58** compared with TpMo(L)(NO)(Br) (L = MeIm (**2**) or DMAP (**19**)). However, these reducing agents proved too mild, giving no reaction; while the highly reducing nature of Na^o yielded decomposition.

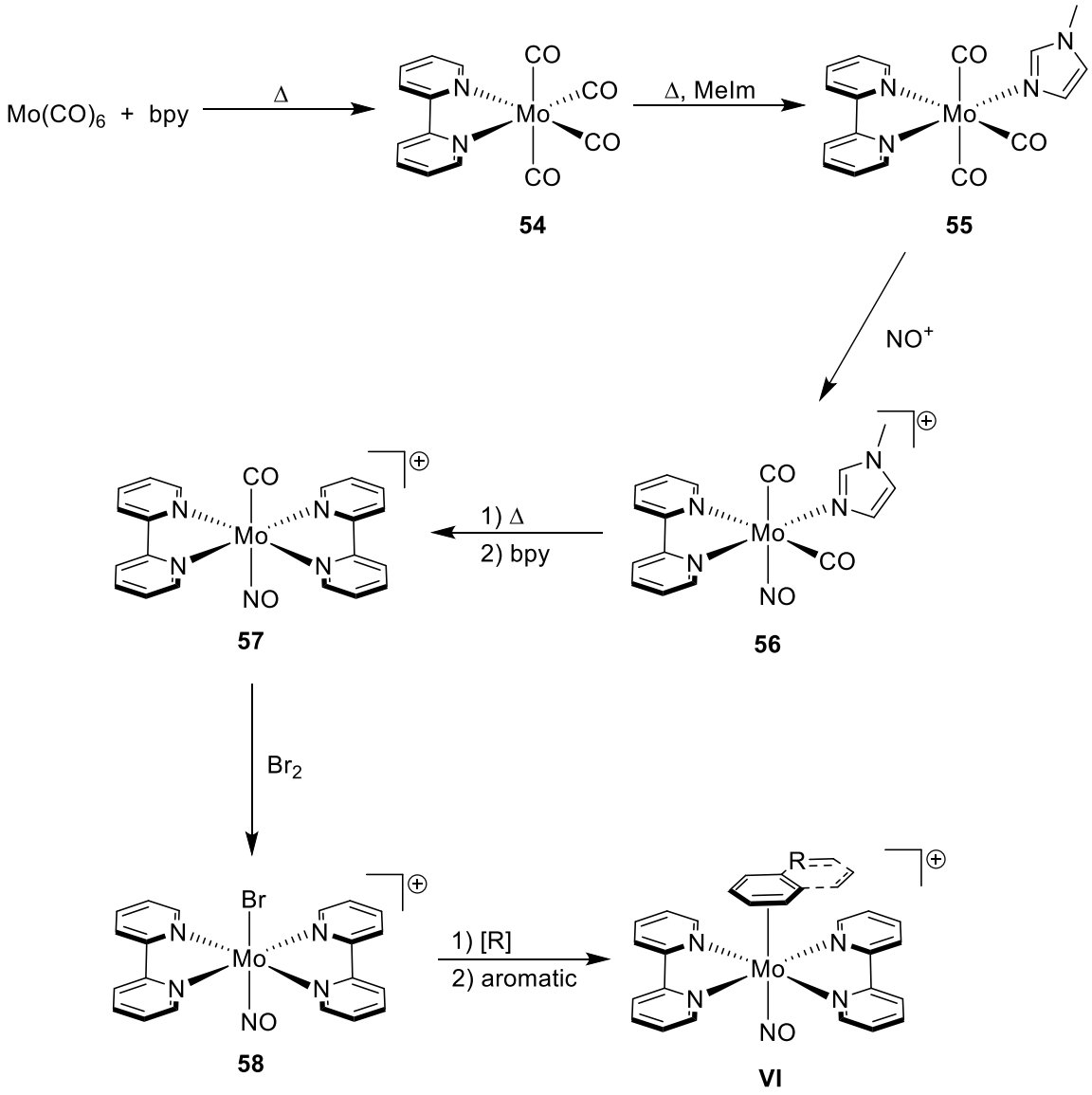

Scheme 4: Proposed synthesis of a polypyridal molybdenum dearomatization agent (**VI**).

Next, we explored ampy as the 2nd bidentate ligand, which would provide increased electron donation from the amino group, while the lack of conjugated π systems would also serve to reduce π-acidity. Initial attempts to introduce ampy proceeded via thermolysis of **56** according to Method A in Scheme 5. However, these attempts were unsuccessful and yielded a range of decomposition products. With this result we sought to introduce ampy initially by thermolysis of $Mo(CO)_6$, and then follow the synthetic procedure outlined in Scheme 6 Method B.

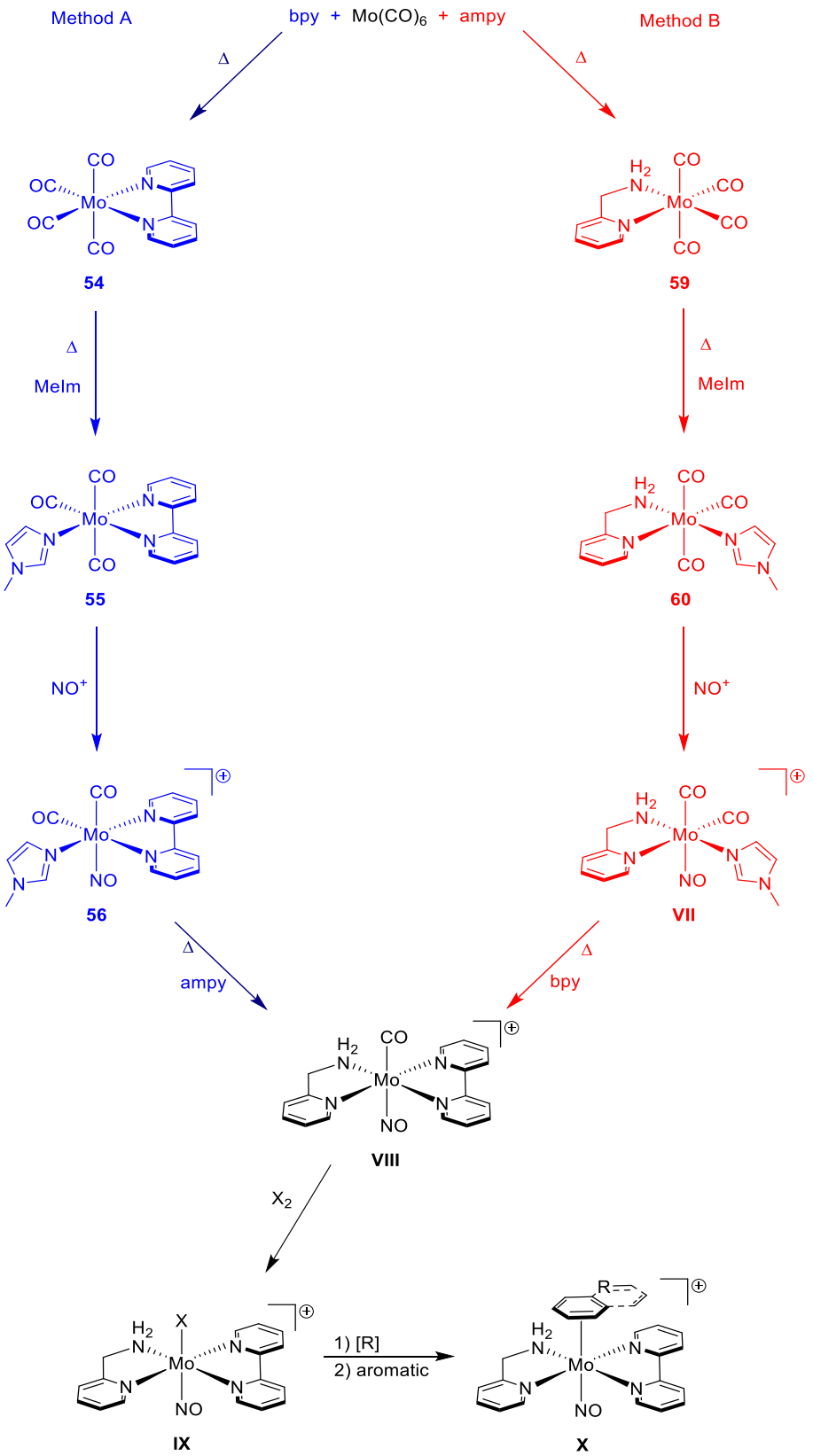

Scheme 5: Proposed synthesis of a mixed polypyridal molybdenum dearomatization agent (**X**).

ampyMo(CO)$_4$ (**59**) was produced in good yield (86 %), and gave a more electron rich complex than **54** (0.72 vs 0.82, Table 1). The addition of MeIm to produce ampyMo(MeIm)(CO)$_3$ (**60**) also proceeded in good yield (82 %), and again featured a lower reduction potential than **55** (0.10 vs 0.24 V). However, the incorporation of an asymmetric ligand provides more potential coordination isomers, and ^{1}H NMR analysis of **60** showed the presence of all 3 possible isomers (Figure 3). Once again, we hoped that the isomers would funnel to a thermodynamic preference in subsequent synthetic steps.

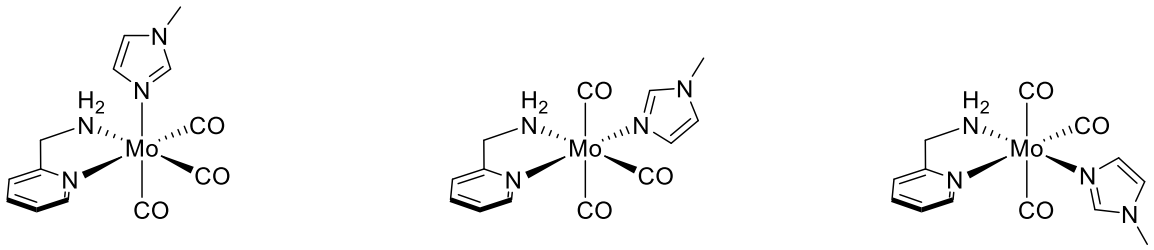

Figure 3: Coordination isomers of **60**.

Efforts to nitrosylate **60** gave only decomposition. Alternative nirtosylating agents were explored, with $NOPF_6$ and Diazald® also giving decomposition. This is likely due to the decreased steric protection and reduction potentials of **60** compared to **55**. Given the inability to nitrosylate **60**, and the decomposition of **56** via thermolysis in the presence of ampy, the synthesis of **X** was abandoned.

While **58** proved too electron deficient to allow for dihapto-coordination, a minor change from NO^+ to CO would likely provide the correct electronics (*vide supra*). With a new target in mind we proposed a synthesis for **XII** in Scheme 6.

Complex	d^5/d^6 Reduction Potential (V)
$[BpMo(CO)_4]^-$ (**53**)	0.62
$bpyMo(CO)_4$ (**54**)	0.82
$ampyMo(CO)_4$ (**59**)	0.72
$bpyMo(MeIm)(CO)_3$ (**55**)	0.24
$ampyMo(MeIm)(CO)_3$ (**60**)	0.10
TpMo(MeIm)(NO)(CO) (**1**)	0.22
TpMo(DMAP)(NO)(CO) (**22**)	0.27
$[bpy_2Mo(NO)(CO)]^-$ (**57**)	0.65
$[bpy_2Mo(CO)_2$ (**61**)	0.15
$[bpy_2Mo(NO)(Br)]^-$ (**58**)	-0.50
TpMo(py)(NO)(Br) (**14**)	-1.23
TpMo(MeIm)(NO)(Br) (**2**)	-1.53
TpMo(DMAP)(NO)(Br) (**19**)	-1.53
$TpW(PMe_3)(NO)(Br)$	-1.33

Table 1: Reduction potential for molybdenum bidentate complexes and their {TpMo(L)} analogs.

$Bpy_2Mo(CO)_2$ (**61**) was isolated in good yield (71 %), producing a species with electronic characteristics similar to **1**, **4**-**5**, **22**-**23** (Table 1). ^1H NMR showed that once again the incorporation of 2 bpy ligands favored the undesired *trans* orientation. Unfortunately, attempts to isolate **61** with Br_2 and I_2 were unsuccessful, and instead produced a mix of starting material and decomposition products.

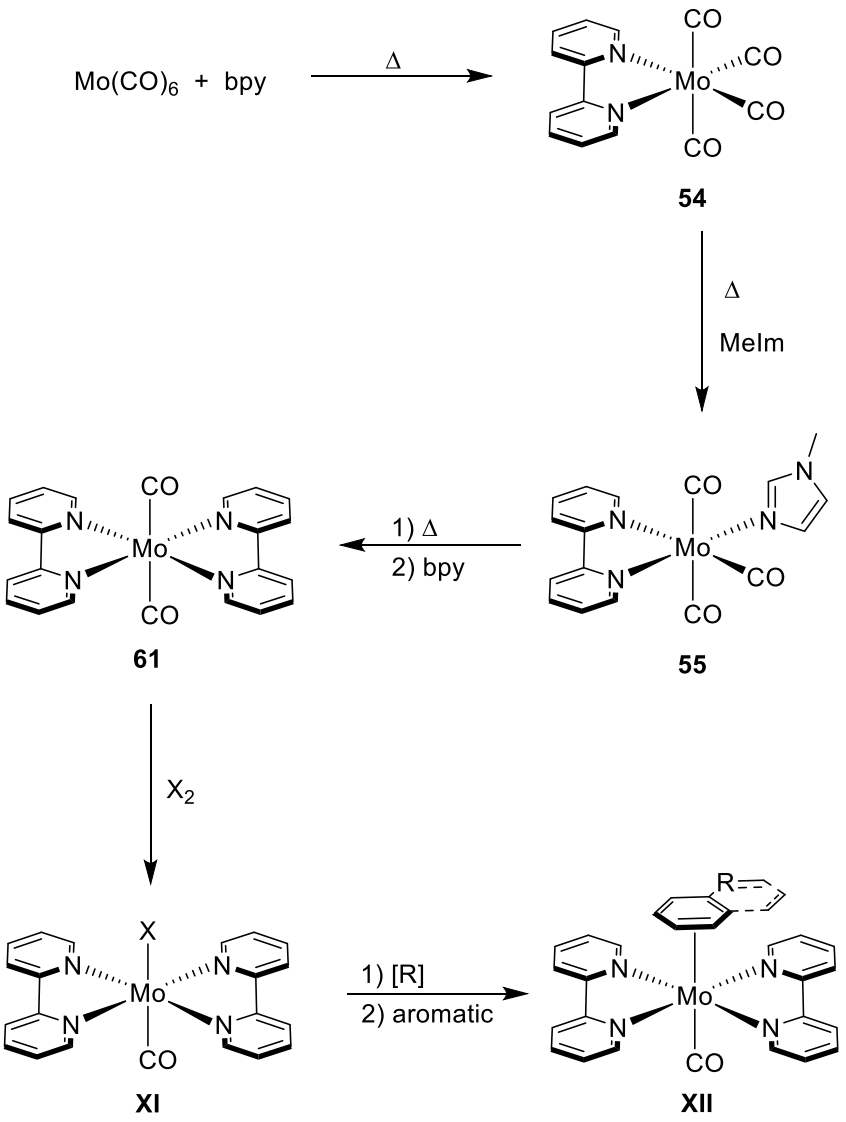

Scheme 6: Proposed polypyridal molybdenum dearomatization agent featuring a CO π-acid (**XII**).

5.5 Conclusion

Efforts to produce a dual bidentate molybdenum dearomatization agent highlighted the narrow steric and electronic window that such complexes operate within. The investigation of a variety of bidentate ligands produced a range of complexes with similar electronics to the established {TpMo(DMAP)(NO)} fragment (Table 1). However, none of these molybdenum systems proved effective as a dearomatization agent. The steric problems, which were inherent with polypyridal rhenium complexes, were illustrated with the reduced backbonding capabilities

of the 2nd row molybdenum center, which proved ineffective for the dihapto-coordination of alkenes.[6-10] Given the ineffectiveness of bidentate molybdenum complexes, we returned to a more familiar ligand set incorporating a tridentate scorpionate ligand.

5.6 Experimental

General Methods

NMR spectra were obtained on 600 or 800 MHz spectrometers. Chemical shifts are referenced to tertramethylsilane (TMS) utilizing residual ^{1}H signals of the deuterated solvents as internal standards. Chemical shifts are reported in ppm and coupling constants (*J*) are reported in hertz (Hz). Infrared Spectra (IR) were recorded on a spectrometer as a glaze on a Horizontal Attenuated Total Reflectance (HATR) accessory, or as a glaze between two NaCl plates, with peaks reported in cm^{-1}. Electrochemical experiments were performed under a nitrogen atmosphere. Cyclic voltammetric data were recorded at ambient temperature at 100 mV/s unless otherwise noted, with a standard three electrode cell from +1.8 V to -1.8 V with a platinum working electrode, *N*,*N*-dimethylacetamide (DMA) or acetonitrile (MeCN) solvent, and tetrabutylammonium hexafluorophosphate (TBAH) electrolyte (~1.0 M). For CV data recorded in aqueous solutions, sodium triflate (NaOTf) was used as the electrolyte. All potentials are reported versus the normal hydrogen electrode (NHE) using cobaltocenium hexafluorophosphate ($E_{1/2}$ = -0.78 V, -1.75 V) or ferrocene ($E_{1/2}$ = 0.55 V) as an internal standard. Peak separation of all reversible couples was less than 100 mV. All synthetic reactions were performed in a glovebox under a dry nitrogen atmosphere unless otherwise noted. All solvents were purged with nitrogen prior to use. Deuterated solvents were used as received from Cambridge Isotopes. Compounds **54-56** were prepared according to previous literature methods.[2]

Synthesis of KBp (52)

Pyrazole (100 g, 1.47 mol) and KBH_4 (34.92 g, 0.647 mol) were added to a 1 L round bottom flask charged with a stir bar. The flask was fitted with a reflux condenser with an attached N_2 line and was placed into an oil bath preheated to 120 ^oC where it was stirred until H_2 evolution ceased (8 h). The apparatus was removed from the oil bath and toluene was added to the white reaction mixture (400 mL). The mixture was placed in an ice bath for 16 h, and was filtered through a 350 mL medium frit. The white solid was recrystallized from anisole/pentane and desiccated to give (**52**) (88 %, 106.05 g, 0.57 mol) ^1H NMR (DMSO-d_6, δ): 7.32 (d, *J* = 1.9, 2H, H3/5), 7.20 (d, *J* = 1.5, 2H, H3/5), 5.92 (t, *J* = 1.8, 2H, H4).

Synthesis of [BpMo(CO)$_4$]K (53)

Compound **53** (16.89 g, 90.8 mmol) $Mo(CO)_6$ (21.78 g, 82.5 mmol), and THF (150 mL) were added to a 250 mL round bottom flask charged with a stir bar which was fitted with a vigreaux column. The reaction mixture was refluxed for 6 h, and then was allowed to cool to room temperature and then filtered through a 60 mL fine frit. The green solid was washed with hexanes (50 mL) and desiccated to give (**53**) (8 %, 2.63 g, 6.67 mmol). ^1H NMR (DMSO-d_6, δ): 7.32 (d, *J* = 1.9, 2H, H3/5), 7.22 (d, *J* = 1.7, 2H, H3/5), 5.92 (t, *J* = 1.8, 2H, H4). CV: $E_{p,a}$ = +0.62 V. IR: ν_{CO} = 2269, 2205 cm^{-1}, ν_{BH} = 2370 cm^{-1}.

Synthesis of [bpy$_2$Mo(NO)(CO)]PF$_6$ (57)

Compound **56** (3.63 g, 6.42 mol) and bpy (4.44 g, 28.4 mol) were added to a 250 mL round bottom flask charged with a stir bar, and fitted with a vigreaux column. The solids were dissolved in xylenes (125 mL), and refluxed overnight (16 h). After cooling to room temperature the hexanes were added to the reaction mixture (150 mL), and the dark green mixture was left to stir for 3 h. A dark green solid was isolated by filtration through a 30 mL fine frit. The solid was washed with Et_2O (3 X 20 mL) and desiccated to give (**57**) (78 %, 3.06 g, 5.01 mmol). ^1H NMR (acetone-d_6, δ):

9.28 (d, *J* = 4.1, 1H, H6), 9.17 (d, *J* = 5.4, 1H, H6), 8.88 (d, *J* = 7.49, 1H, H6), 8.76 (t, *J* = 6.75, 1H, H4/5), 8.73 (d, *J* = 8.22, 1H, H6), 8.49 (t, *J* = 7.49, 1H, H4/5), 8.22 (t, *J* = 7.49, 1H, H4/5), 8.19 (t, *J* = 8.81, 1H, H4/5), 7.93 (t, *J* = 5.43, 1H, H4/5), 7.82 (t, *J* = 6.02, 1H, H4/5), 7.50 (m, 4H, H3). CV: $E_{p,a}$ = +065 V. IR: ν_{CO} = 1874 cm^{-1}; ν_{NO} = 1584 cm^{-1}.

Synthesis of $bpy_2Mo(NO)(Br)$ (58)

Compound **57** (503 mg, 0.824 mmol) and DCM (10 mL) were added to a 50 mL Erlenmeyer flask charged with a stir bar. A solution of Br_2 in DCM (1.765 M, 0.25 mL, 0.438 mmol) was added to the reaction mixture, giving a color change to red. After stirring for 5 min Et_2O was added to the reaction mixture (30 mL), and a brown solid was isolated by filtration through a 15 mL fine frit was washed with Et_2O (2 X 10 mL) and desiccated giving (**58**) (51 %, 281 mg, 0.424 mmol). CV: $E_{p,a}$ = +1.07 V, $E_{1/2}$ = -0.50, -1.23 V. IR: ν_{NO} = 1612 cm^{-1}.

Synthesis of $ampyMo(CO)_4$ (59)

$Mo(CO)_6$ (4.98 g, 18.9 mmol), ampy (2 mL, 19.4 mmol), and THF (50 mL) were added to a 100 mL round bottom flask charged with a stir bar and reflux condenser with an attached N_2 line. The reaction mixture was refluxed for 3 h, and was then cooled to room temperature. The reaction mixture was slowly poured into stirring hexanes (400 mL) and a yellow solid was isolated by filtration through a 60 mL fine frit. The solid was washed with hexanes (2 X 50 mL) and desiccated to give (**59**) (86 %, 5.099 g, 16.1 mmol). ^{1}H NMR (acetone-d_6, δ): 8.84 (d, *J* = 5.4, 1H, pyridine H6), 7.91 (td, *J* = 7.8, 1.6, 1H, H5), 7.55 (dq, *J* = 7.9, 1H, H4), 7.38 (ddd, *J* = 6.4, 1H, H43), 4.37 (t, *J* = 5.8, 2H, CH_2), 4.22 (bs, 2H, NH_2). CV: $E_{p,a}$ = +0.72 V.

Synthesis of $ampyMo(MeIm)(CO)_3$ (60)

Compound **59** (10.04 g, 31.8 mmol), MeIm (4 mL, 50 mmol), and toluene (100 mL) were added to a 250 mL round bottom flask charged with a stir bar and reflux condenser with attached N_2 line. The reaction mixture was refluxed for 4 h, turning red after 1 h or reflux. The reaction mixture

was cooled to room temperature then slowly added to stirring hexanes (600 mL). The red solid was isolated by filtration through a 60 mL fine frit, was washed with hexanes (3 X 50 mL), and desiccated to give (**60**) (82 %, 9.66 g, 26.1 mmol). Present as a mix of isomers (2 : 1) for major signals. ^{1}H NMR (acetone-d_6, δ): (Major isomer) 8.99 (d, *J* = 4.8, 1H, pyridine H6), 7.91 (td, *J* = 7.8, 1.6, 1H, H5), 7.84 (td, *J* = 7.5, 1.7, 1H, H4), 7.55 (s, 1H, MeIm H2), 7.43 (m, 1H, H3), 7.00 (bs, 1H, MeIm H3/4), 6.88 (bs, 1H, MeIm 3/4), 4.37 (t, *J* = 5.9, 2H, CH_2), 4.22 (bs, 2H, NH_2), 3.71 (s, 3H, MeIm Me). (Minor isomer) 8.84 (d, *J* = 5.3, 1H, pyridine H6), 7.54 (s, 1H, MeIm H2), 7.43 (m, 1H, H3), 7.38 (td, *J* = 6.5, 1.9, 1H, H5), 7.32 (td, *J* = 6.4, 2.1, 1H, H4), 6.98 (t, *J* = 1.1, 1H, MeIm H3/4), 6.52 (t, *J* = 1.6, 1H, MeIm 3/4), 4.19 (m, 4H, CH_2, NH_2), 3.69 (s, 3H, MeIm Me). CV: $E_{1/2}$ = +0.10 V.

Synthesis of bpy$_2$Mo(CO)$_2$ (61)

$Mo(CO)_6$ (1.68 g, 6.36 mmol), bpy (2.14 g, 13.7 mmol), and xylenes (20 mL) were added to a 50 mL round bottom flask charged with a stir bar and vigreaux column. The reaction mixture was refluxed for 2 d, and was then left to cool before being slowly added to stirring hexanes (300 mL). The product was isolated by filtration through a 30 mL fine frit, was washed with hexanes (2 X 20 mL), and desiccated to give (**61**) (71 %, 1.37 g, 2.95 mmol). Present in an 8 : 1 ratio of trans : cis oriented bpy ligands. ^{1}H NMR (acetone-d_6, δ): (Major isomer) 9.13 (d, *J* = 4.5, 4H, H4/5), 8.48 (dt, *J* = 8.3, 1.0, 4H, H6), 8.13 (dd, *J* = 7.7, 2.0, 4H, H3), 7.58 (dd, *J* = 5.3, 1.0, 4H, H4/5). (Minor isomer) 9.51 (bs, 2H, H6), 8.61 (dt, *J* = 8.3, 1.0, 2H, H4/5), 8.36 (d, *J* = 8.1, 2H, H6), 8.21 (dd, *J* = 7.6, 1.7, 2H, H4/5), 7.67 (dd, *J* = 6.4, 1.0, 1H, H4/5), 7.14 (bs, 2H, H3), 7.07 (dd, *J* = 5.9, 1.1, 2H, H4/5). CV: $E_{p,a}$ = +0.15 V, $E_{1/2}$ = -1.17, -2.13 V. IR: ν_{CO} = 1755, 1697 cm^{-1}.

5.7 References

1. Trofimenko, S. *J. Am. Chem. Soc.* **1967,** *89*, 3165-3170.

2. Dilsky, S.; Palomaki, P. K. B.; Rubin, J. A.; Saunders, J. E.; Pike, R. D.; Sabat, M.; Keane, J. M.; Ha, Y. *Inorg. Chim. Acta* **2007,** *360*, 2387-2396.

3. Myers, J. T.; Dakermanji, S. J.; Chastanet, T. R.; Shivokevich, P. J.; Strausberg, L. J.; Sabat, M.; Myers, W. H.; Harman, W. D. *Organometallics* **2017,** *36*, 543-555.

4. Mocella, C. J.; Delafuente, D. A.; Keane, J. M.; Warner, G. R.; Friedman, L. A.; Sabat, M.; Harman, W. D. *Organometallics* **2004,** *23*, 3772-3779.

5. Crabtree, R. H., *The organometallic chemistry of the transition metals*. John Wiley & Sons: 2009.

6. Brooks, B. C.; Brent Gunnoe, T.; Dean Harman, W. *Coord. Chem. Rev.* **2000,** *206*, 3-61.

7. Gunnoe, T. B.; Meiere, S. H.; Sabat, M. *Inorg. Chem.* **2000,** *39*, 6127-6130.

8. Helberg, L. E.; Barrera, J.; Sabat, M.; Harman, W. D. *Inorg. Chem.* **1995,** *34*, 2033-2041.

9. Helberg, L. E.; Gunnoe, T. B.; Brooks, B. C.; Sabat, M.; Harman, W. D. *Organometallics* **1999,** *18*, 573-581.

10. Helberg, L. E.; Orth, S. D.; Sabat, M.; Harman, W. D. *Inorg. Chem.* **1996,** *35*, 5584-5594.

Chapter 6

Development of Next Generation Group 6 Dearomatization with Incorporation of the Tunable Tz Scorpionate Ligand

6.1 Introduction

With our inability to produce a bidentate dearomatization agent we began to look for alternatives for the next generation of dearomatization agents. We envisioned a means to increase the stereochemical stability of the metal center, and avoid racemization, by reversibly manipulating the electron density of the complex. Moreover, the ability to reversibly influence the electron density at the metal center would likely serve as a means to modulate reactivity patterns of dihapto-coordinated ligands allowing for liberation of dearomatized ligands without oxidation of the metal complex.

With this goal in mind we looked to keep a similar ligand set to previous dearomatization agents, and once again build upon a scorpionate foundation. Previous efforts have thoroughly investigated Tp ligand sets for both tungsten and molybdenum complexes, leaving little room for further elaboration.[1-6] Past efforts with the 2nd most prevalent scorpionate hydrotris(pyrazolyl)methane (Tpm, Figure 1) with tungsten and molybdenum frameworks proved unsuccessful. The difficulties in building a dearomatization agent on a Tpm foundation are reduced donation compared to Tp.[1] Furthermore, the neutral charge of Tpm results in complexes which bare a net positive charge due to the presence of the NO^+ ligand, which is required to establish the correct electronics within group 6 complexes (*vide supra*).

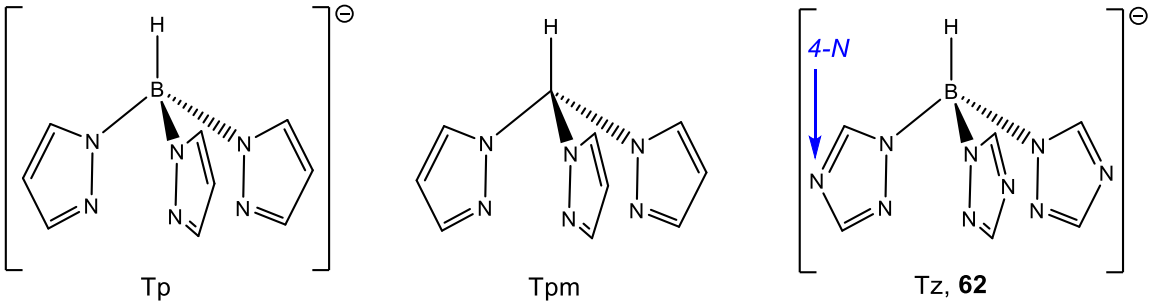

Figure 1: Scorpionates applied to dearomatization chemistry.

When surveying the scorpionate literature we found reports of hydrotris(1,2,4-triazolyl)borate (Tz, **62**, Figure 1), which like Tp provides a negative charge.[7-8] With the

adoption of Tz (**62**) as the foundation for future group 6 tungsten and molybdenum dearomatization agents, we envisioned the syntheses of dearomatization agents of the {TzM(L)(NO)} (M = W or Mo, L = σ-donor) variety. With our new target established we began to investigate the literature regarding Tz and its transition metal complexes.

6.2 The Scorpionate Ligand Tris(1,2,4-triazolyl)borate (Tz)

Despite the initial report of **62** alongside Tp by Trofimenko in 1966; it was largely ignored for nearly 25 years.[7-8] Meanwhile, Tp became well established within organometallic chemistry, as evidenced by thousands of publications.[7-13] Like the case of **52**, the initial reports of **62** were for *in situ* synthesis, with isolation as a metal complex.[7-8] It was not until 1991 that a detailed synthesis for the free ligand was reported by Lobbia et al.[14] In the 25 years since Tz resurfaced in the literature, there has been only modest progress in the exploration of Tz complexes with transition metals. This may be due to the conclusion by Lobbia et al. in 1991 that the insolubility of the metal complexes reported therein were likely due to coordination polymers, made possible due to the *exo*-oriented nitrogen (4-N, Figure 1);[15-16] a property which often relegated Tz transition-metal complexes as 'unsuitable of further characterization.'[14]

The few literature reports of Tz complexes do little but establish that the triazole-based scorpionates are less electron-donating than their more famous pyrazole cousins as a result of the additional nitrogen in each ring.[16-20] This was exciting as it meant that we might see changes to the reactivity produced by Tz – dearomatization agents, and also that the majority of the complexes en route to dearomatization would be new additions to the organometallic community. Tz complexes offer possible advantages over Tp; including increased water solubility, giving a dramatic change compared to our previous dearomatization agents. Additionally, the triazolyl rings can be electronically modulated in ways not possible for pyrazole-based scorpionates. For example, Robinson et al. have recently

published a computational study that explores the potential to access carbene scorpionates via the alkylation of the triazolyl 4-N positions, thereby increasing the electron-donating ability of the carbene scorpionate to levels similar to Tp.[21]

We envisioned the ability to modulate the electron density at the metal center of Tz complexes by taking advantage of interactions with the 4-N lone pairs of the triazolyl rings. This could be achieved through solvent interactions, such as hydrogen bonding, as well as by protonation, alkylation, or coordination to a transition metal or other Lewis acid (Figure 2). The ability to modulate the electron density of our metal centers may also allow for modification of reactivity patterns within dearomatization chemistry; and the possibility to liberate our novel dearomatized products without the need to oxidize the metal, especially important for application to tungsten dearomatization (*vide supra*).

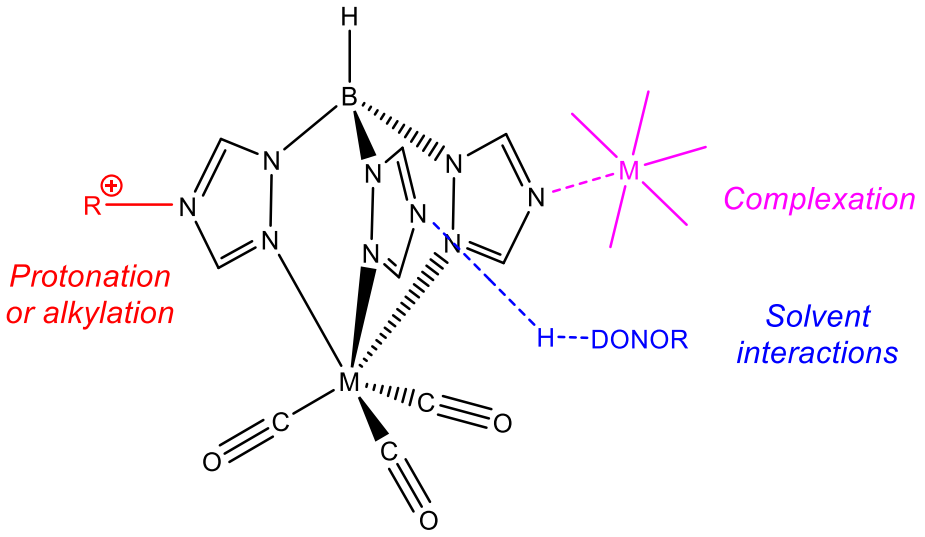

Figure 2: Possible means to modulate electron density at the metal center by interactions with 4-N lone pairs.

Initial attempts to synthesize **62** followed previous literature procedures,[7, 14, 20] however, either the reported yields were too low for our use as a general ligand synthesis or we were unable to reproduce the reported yields. Met with unexpected difficulty in ligand synthesis, we adapted our synthesis from the original Tp procedure published by Trofimenko,

where the molten reaction mixture of triazole and KBH_4 was heated to 190 ^oC until H_2 evolution ceased.[8] However, isolation and recrystallization from toluene was not amenable to **62**, yielding a thick oil with a range of products. One common problem with the synthesis of **62**, as adopted from KTp, was the presence of a yellow product after extended heating above 200 ^oC. During our purification efforts we discovered a dramatic change in the solubility of **62** compared to Tp, in that it is sparingly soluble in acetone; and we employed acetone trituration as a means to purify **62**, however, the presence of undesired side products severely limited yield (~40 %).

The synthesis of **62** was optimized by Alex Heyer, who investigated a variety of temperatures, reaction times, and ratios of 1,2,4-triazole : BH_4^-. Through these efforts we concluded that an increase in molar equivalents of triazole (5 : 1 triazole : BH_4^-) were required in order to sufficiently solubilize the borohydride and intermediate products. The scorpionate product was then isolated via distillation of the excess molten triazole under reduced pressure (using a modified rotary evaporator), followed by crystallization of the product from acetone. The new synthetic procedure proved to be scalable, and we consistently produce **62** on a 160 g (2/3 mole) scale with 80% yield and high purity.

6.3 Exploration of a Tz Dearomatization Agent: {TzM(L)(NO)} (M = Mo or W)

With the establishment of a suitable synthesis for **62**, we turned our attention to its application within group 6 dearomatization agents. We envisioned synthetic pathways similar to those outlined in Chapter 2, as illustrated in Scheme 1. Given the relative obscurity of Tz transition metal complexes, and the predominance of classical scorpionate complexes within our synthetic scheme, we looked to compare the properties of Tp and Tz group 6 complexes en route to our proposed dearomatization agent (**III**, Scheme 1).

We faced differences in reactivity between scorpionate ligands upon coordination to our group 6 metals. Initial coordination of **62** to tungsten and molybdenum proceeded through thermolysis of the appropriate $M(CO)_6$, however, treatment of the $[TzM(CO)_3]^-$ (M = Mo (**63**) or W(**64**)), generated *in situ*, with Diazald® resulted in decomposition. As in the case of our bidentate molybdenum complexes, we isolated **63** and **64** to probe nitrosylation conditions. We found that both **63** and **64** were amenable to nitrosylation via the *in situ* synthesis of NO^+ with HCl (aq) and $NaNO_2$, which we applied from the nitrosylation conditions for **56** in Chapter 2.[22] However, the resulting orange solid, thought to be $[HTzMo(NO)(CO)_2]^+$, was insoluble in most organic solvents (*e.g.*, THF, DCM, acetone) and water. When this complex was treated with base, solubility in water and organic solvents greatly improves. Based on this observation, we hypothesize that protonation of one or more of the 4-N nitrogens on the Tz ligand caused this dramatic change in solubility. By replacing HCl (aq) with acetic acid, we recovered an orange solid consistent with $TzM(NO)(CO)_2$ (M = Mo (**65**) or W(**66**)). Thus, treating Tz complexes with HCl (aq) could prove to be a valuable tool for their isolation and purification, much in the way amines are routinely purified as HCl salts in organic synthesis. We were then able to apply these conditions to a one-pot synthesis of **65** and **66**, so that similar to the syntheses of $TpM(NO)(CO)_2$ (M = Mo (**67**) or W(**68**)), the tricarbonyl species is not isolated. Despite the fact that we no longer needed to isolate **63**-**64** for our dearomatization synthesis, we decided to compare the characteristics of both scorpionates prior to introduction of NO^+, and synthesized $[TpM(CO)_3]^-$ (M = Mo (**69**) or W (**70**)) according to procedures by Trofimenko.[23]

With consistent syntheses of **63**-**66** in place we were able to compare properties of Tp and Tz classical scorpionate complexes. ^1H NMR spectra of the complexes **63**-**64** and **69**-**70** gave the expected sets of signals (two singlets for Tz, and two doublets and a doublet-of-doublets for Tp), for $[LM(CO)_3]^-$ complexes with C_3 symmetry. Complexes of the form

$LM(NO)(CO)_2$ (**65**-**68**) displayed a 2:1 ratio of ring protons for both Tz and Tp complexes due to their mirror symmetry.

Complex	d^5/d^6 Reduction Potential (V)	ν_{NO} (cm^{-1})	ν_{CO} (cm^{-1})
$[TzMo(CO)_3]^-$ (**63**)	0.22	n/a	1773, 1905
$[TzW(CO)_3]^-$ (**64**)	0.17	n/a	1772, 1905
$[TpMo(CO)_3]^-$ (**69**)	0.02	n/a	1761, 1894
$[TpW(CO)_3]^-$ (**70**)	-0.07	n/a	1750, 1882
$TzMo(NO)(CO)_2$ (**65**)	1.30	1654	1910, 2010
$TzW(NO)(CO)_2$ (**66**)	1.26	1636	1884, 1994
$TpMo(NO)(CO)_2$ (**67**)	1.18	1642	1898, 2001
$TpW(NO)(CO)_2$ (**68**)	1.12	1624	1874, 1986
$TzMo(NO)(Cl)_2$ (**71**)	n/a	1699	n/a
$TpMo(NO)(Br)_2$	n/a	1699	n/a
TzMo(DMAP)(NO)(Cl) (**72**)	-1.25	1654	n/a
TpMo(py)(NO)(Br) (**14**)	-1.23	--	n/a
TpMo(MeIm)(NO)(Br) (**2**)	-1.53	1610	n/a
TpMo(DMAP)(NO)(Br) (**19**)	-1.53	1613	n/a

Table 1: Reduction potentials and IR stretches for selected group 6 Tp and Tz complexes.

Comparison of **63** vs **69** and **64** vs **70** showed that across both molybdenum and tungsten metal centers Tz provided a less electron rich complex than Tp, consistent with previous literature reports.[16-20] **63**-**66** showed the expected decrease in electron density at the metal center, when compared to **67**-**70** (Table 1). Both NO and CO stretching frequencies increase by approximately 10 cm^{-1}, and I/0 reduction potentials (Figure 3) become 0.15 – 0.25 V more positive, consistent with a more electron-deficient metal in the Tz systems. These findings are also consistent with calculations of Lu et al.[24]

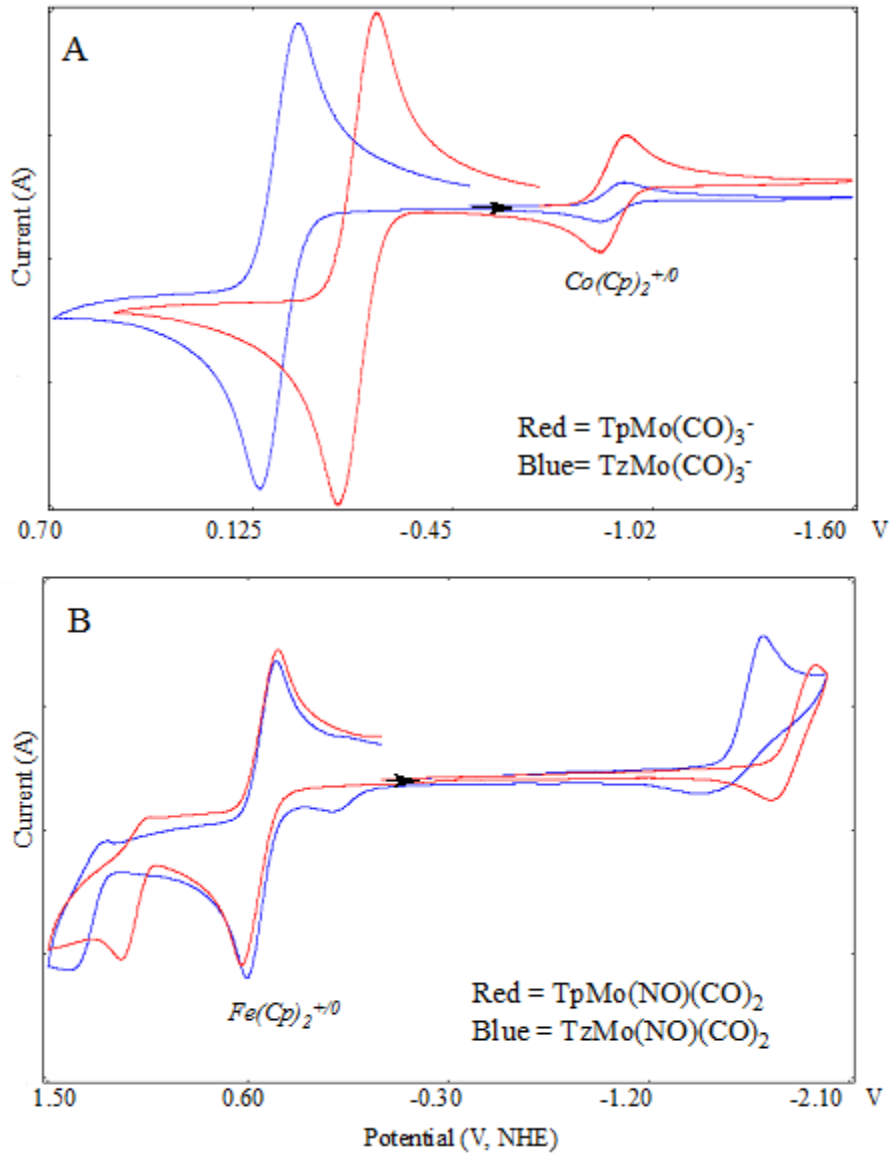

Figure 3: Comparison of cyclic voltammograms of scorpionate complexes $[LMo(CO)_3]^-$ (A) and $LMo(NO)(CO)_2$ (B) with the presence of internal standards cobalicinium hexafluorophosphate (A) and ferrocene (B).

We looked to apply **67** to the same thermolysis conditions optimized for TpMo(DMAP)(NO)(CO) (**22**) in Chapter 2 (Scheme 1).[6] These conditions in the presence of DMAP produced a species consistent with TzMo(DMAP)(NO)(CO) (0.60 V), within the same 5 h timeframe for the synthesis of **22**.[5] However, unlike **22** we were unable to isolate the desired product by water precipitation. The addition of water gave either a homogeneous blue

solution, or an oil which no longer contained the desired electrochemical signals. Once again, we searched for an alternative

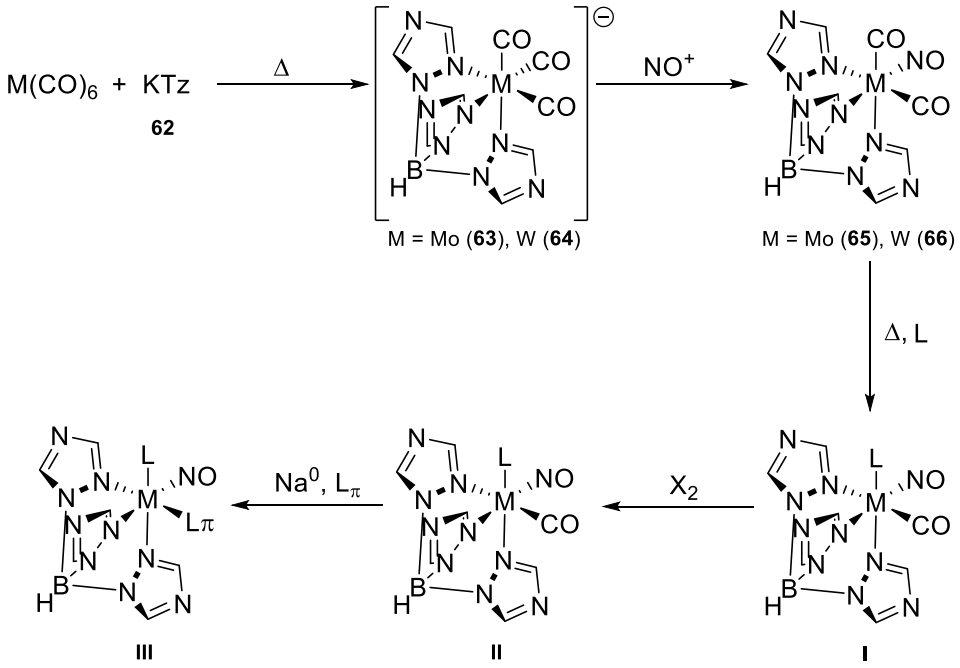

Scheme 1: Proposed synthesis of dihapto-complexes (**III**) for group 6 tungsten and molybdenum Tz complexes.

to DMF for the reflux solvent (*e.g.*, toluene, xylenes), but were faced with the same isolation problems as the initial DMF attempts. We then explored *p*-dioxane and *n*-butanol, however, these resulted in the lack of the desired CV signals. Finally, we explored sulfolane as a DMF alternative, which we heated to similar temperatures (~160 ^{o}C). In this case we were able to isolate a blue/green solid by precipitation with Et_2O. However, the isolated solid proved insoluble in water, and common organic solvents. Solubility tests with >20 solvents resulted in colorless solutions and a dark blue/green solid. While the insolubility of the solid isolated from thermolysis of **65** prevented characterization, we propose that the insolubility is due to the formation of coordination polymers. The insoluble nature of the solid is consistent with physical properties of complexes reported by Lobbia et. al., and the propensity of Tz transition metal complexes to form coordination polymers is well documented.[14-15, 25-35]

In an effort to avoid the possible coordination polymers which accompany thermolysis in sulfolane, we returned to our initial conditions of refluxing in DMF to liberate a CO from **65**. We also looked to overcome the isolation issues from DMF by reacting **I** *in situ* with I_2 or Br_2 to produce **II**. Both I_2 and Br_2 appear to produce **II**, as the reaction mixture yields the appropriate signals at -1.28 V, along with several side products. However, isolation of **II** from DMF also proved inaccessible by precipitation from water, as well as a variety of organic solvents. Due to the difficulties in product isolation from DMF, and the proposed coordination polymers isolated from sulfolane, we decided to abandon the strategy shown in Scheme 1.

With the possible formation of coordination polymers at elevated temperatures, we returned to the familiar redox pathway (Scheme 2). However, oxidation of **65**-**66** with Br_2 gave no reaction. This is likely due to the more electronegative metal centers for the Tz complexes, compared to their Tp analogs (**65**-**66** vs. **67**-**68**); as indicated by the increase in the I/0 reduction potential, as well as an increase in CO and NO stretching frequencies (Table 1). We sought to overcome this difficulty in the oxidation of **65**-**66** with the use of a stronger oxidant, pursuing oxidation by Cl_2 (g) (+1.36 V vs Br_2 (+1.07 V)) to a mixture of **65** or **66** in DCM. Chlorination of **65** resulted in the precipitation of $TzMo(NO)(Cl)_2$ (**71**) as a solid in good yield (81 %). Characterization of the 16 e^- **71** proved difficult due to its limited solubility in non-coordinating solvents. We were unable to obtain reliable NMR or CV data on the complex, however, IR provides a ν_{NO} = 1699 cm^{-1}, a match for the analogous $TpMo(NO)(Br)_2$. Surprisingly, when we applied the same reaction conditions to the more reducing **66** we were unable to consistently obtain the desired product.

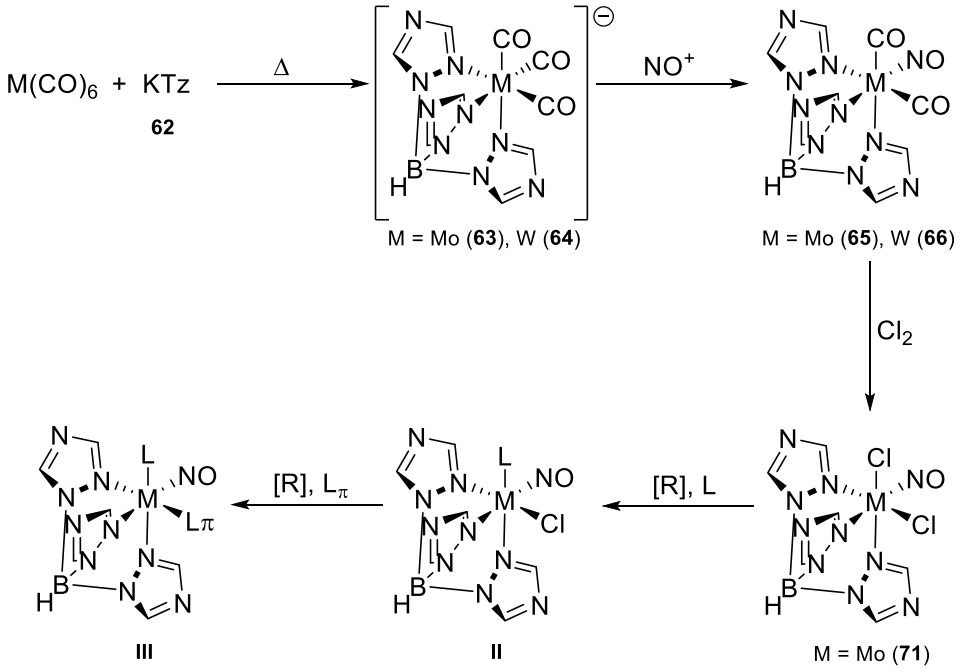

Scheme 2: Proposed synthesis of **III** via redox reactions.

Continuing with Scheme 2, we looked to introduce DMAP via Zn^0 reduction of **71**, by applying the conditions optimized for TpMo(DMAP)(NO)(Br) (**19**). Once again we were met by synthetic challenges due to the limited solubility of our Tz complexes. **71** proved insoluble in both DCM and THF, our solvents of choice for Zn^0 reductions of $TpMo(NO)(Br)_2$ to TpMo(L)(NO)(Br) (Chapter 2). Interestingly, solubility of **71** was dramatically increased upon the addition of DMAP. We believe that this is due to coordination of DMAP to the 16 e^- Mo^{II} complex, resulting in a change to the solubility properties of the complex. However, these solubility changes are accompanied by changes to the reduction potential, which shifts negative in the proposed 7-coordinate species (**V** in Scheme 3). We believe that **V** can reduce **71**, or disproportionate another **V**, producing a variety of decomposition products, as illustrated by the large number of products observed electrochemically in the isolated solid.[1, 4] Moreover, upon the addition of DMAP to the reaction mixture a gas is evolved, which we propose to be nitric oxide, liberated from a high oxidation state molybdenum species.

However, within the various decomposition products we see signals that are consistent with our desired product TzMo(DMAP)(NO)(Cl) (**72**) (-1.25 V).

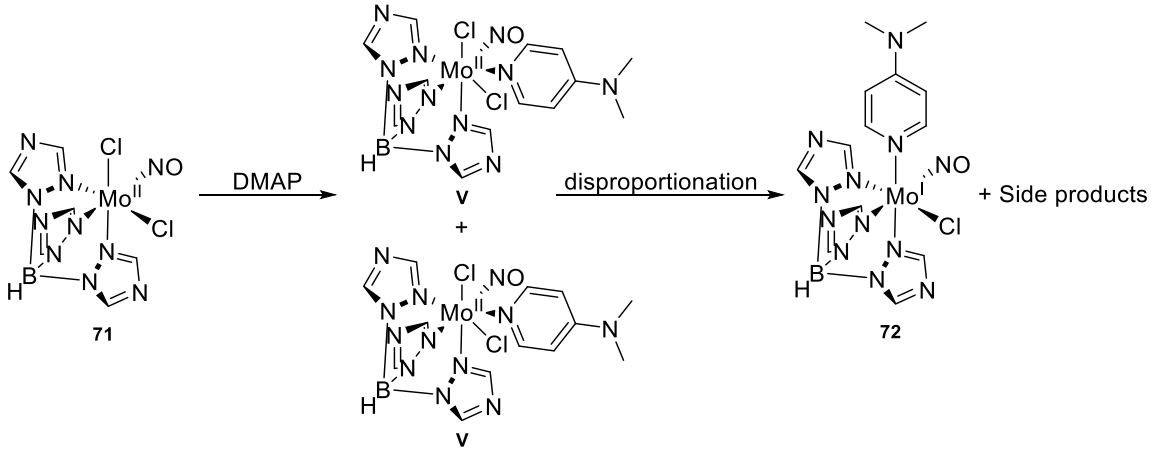

Scheme 3: Proposed disproportionation during the synthesis of **72**.

In an attempt to overcome the possible disproportionation of **V** we looked to increase the solubility of **71** by changing solvents from DCM/THF. We reasoned that if we could increase the solubility of **71**, we may be able to adequately pre-reduce it (as is the case with $TpMo(NO)(Br)_2$), thereby making a 7-coordinate species less likely (19 e^- vs 18 e^- for **V**). With this in mind we investigated a variety of solvents (*e.g.*, acetone, MeOH, EtOAc, DMF, DMA), without success. Acetone, MeOH, and EtOAc proved ineffective at solubilizing **71**, while DMA and DMF reacted with **71** and evolved gas.

With the inability to circumvent decomposition by changing the solvent, we explored alternatives to Zn^0 as our reducing agent. The use of Mg^0 and Na^0 gave no change, and complete loss of **72** signals, respectively. We then explored sodium naphthalenide and anthracenide (-2.81 V) as homogeneous reducing agents; which like Na^0 resulted in over-reduction, and complete loss of signals for **72**. Finally we employed $CoCp_2$, which like sodium naphthalenide and anthracenide is a homogeneous reducing agent, although more mild (-0.78

V). However, $CoCp_2$ gave no change in reactivity compared to Zn^0, and like other mild reducing agents appears to be hampered by the low solubility of **71**.

Given our inability to avoid the possible disproportionation of **V**, we looked to purify **72**, and attempt the subsequent reduction to **III** (Scheme 2). Initial efforts focused on reprecipitation and recrystallizations of crude **72**, employing a range of organic solvents, with limited success. These purification efforts did increase the purity of **72**, however, with a dramatic loss of yield, resulting in a mixture which was merely less impure. We then employed extraction as a means to take advantage of the ability to change the physical properties of **72** via protonation (*vide supra*), which also proved ineffective.

Finally, we investigated chromatographic purification methods. Silica column conditions were optimized for the isolation of pure **72** from >7 different bands. **72** gave the electrochemical signals identified earlier (-1.25 V (I/0)), and ν_{NO} = 1654 cm^{-1} which are consistent with the proposed Mo^{I} complex. Moreover, these data fit the trends seen between Tz and Tp complexes illustrated in Table 1, with shifts of +0.18 V and +41 cm^{-1} compared to **19**. However, the chromatographic purification of **72** gave a low mass recovery of the pure complex, reducing the yield from **71** to < 20 %. Furthermore, because the initial impure mixture of **72** is air sensitive the chromatography must be conducted in the glovebox, making large scale purification difficult.

With the purification of **72** completed, we began to explore conditions for **III**, which were initially focused on the coordination of naphthalene. However, like the initial reductions of **19** to TpMo(DMAP)(NO)(η^2-naphthalene) (**26**), these attempts resulted in the over-reduction of **72**. Given the difficulty of the synthesis and purification of **72**, we changed our focus from naphthalene to cyclopentene, to avoid the formation of an *in situ* homogenous reducing agent (sodium naphthalenide, *vide supra*). These attempts provided glimpses of a

potential product by CV reaction monitoring (0.20 V), although thus far we have been unable to isolate the desired product.

6.4 pH Modulation of Group 6 Tz Complexes

Despite our current inability to isolate **III**, we sought to demonstrate the potential to modulate the electronics of the metal center by interactions with the lone pair of the triazolyl 4N (Figure 2). The $[LM(CO)_3]^-$ complexes **63**-**64** are ideally suited to explore the effects of protonation of the scorpionate, owing to the presence of a reversible I/0 ($E_{1/2}$) wave in the CV, as well as clear ν_{CO} stretches in the IR. Initial studies involved measuring this reduction potential in solvents with varying abilities to engage in hydrogen bonding with the *exo*-lone pairs of the 4-N triazolyl rings (Figure 2). A redox-active reference compound was included *in situ* that did not possess the ability to be a H bond acceptor ($Fe(Cp)_2$ or $[Co(Cp)_2]^+$). The effects of weak acids (diisopropylammonium triflate, pKa = 11.0; *N*-methylmorpholinium triflate, pKa = 7.4; and acetic acid, pKa = 4.8) in MeCN solutions were also explored. In all of these cases, no statistically significant change within either Tp or Tz framework was observed.

It was not until stronger acids were employed that notable changes were recorded in the electrochemical behavior of the Tz complexes. The introduction of DPhAT (diphenylammonium triflate, pKa = 0.78), to an MeCN solution of **63** or **64**, resulted in a positive shift of ~0.2 V in the reduction potential, while maintaining its reversible character (blue scan, Figure 4). Addition of acid to the solution gave an initial broadening of both the cathodic and anodic waves. These signals sharpen when the amount of acid is raised to three molar equivalents, and remain unchanged up to 10 molar equivalents (blue scan, Figure 4). Addition of a bulky base, such as trimethylamine (TEA), appears to cleanly deprotonate the complex, and the reversible couple shifts back to its original value (purple scan, Figure 4). The reversible nature of the protonation and resulting modulation of the reduction potential ($E_{1/2}$) occurs for

both molybdenum and tungsten metal centers (**63**-**64**, Table 2). This effect can also be demonstrated with stronger acids, such as HCl (aq) or triflic acid (pKa = -14). The effects of protonation can also be measured through the stretching frequencies of the CO ligands, as demonstrated in experiments by Alex Heyer (Table 2). These data also support the conclusions made with electrochemistry as the CO stretches of **63**-**64** are shifted by +18 and +13 cm^{-1}, indicating reduced backdonation from the metal center. Protonation of **63**-**64** with the strong acids DPhAT (pKa = 0.8), HCl (aq), or triflic acid (MeCN, pKa = -14), increases the π-acidic nature of the Tz scorpionate and protects the metal from oxidative decomposition (Figure 4). The protonated species can survive highly oxidizing conditions, including the presence of >10 molar equivilents of triflic acid in an MeCN solution.

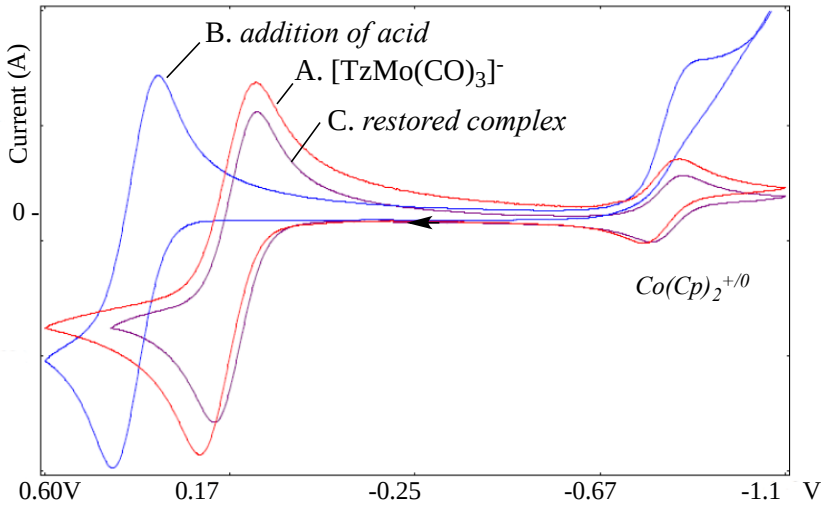

Figure 4: Cyclic voltammagrams demonstrating the reversible modulation of the electrochemical Behavior of **63** upon protonation/deprotonation with DPhAT/TEA. Red: initial solution of 3 (~0.02 M). Blue: addition of 10 eq of DPhAT; purple: addition of an excess of TEA.

In dramatic contrast, treatment of **69**-**70** with 1 molar equivalent of DPhAT completely and irrevocably destroys the complex (Figure 5). This result is also supported by IR experiments conducted by Alex Heyer, in which large shifts observed for **69**-**70** (~150 cm^{-1}), indicate a dramatic change to the metal complex (Table 2). These IR data, combined with the loss of CV

signal upon exposure to acid, indicate that **69**-**70** undergo some irreversible decomposition pathway. **69**-**70**, which do not have basic nitrogens accessible, suffer complete decomposition upon exposure to one molar equivalent of the acid DPhAT (0.17 M, Figure 5), and the original complex cannot be resurrected by the addition of base (TEA). This feature of Tz is significant, as it enables the syntheses of complexes that offer similar electronic properties to Tp analogs, while also protecting the metal from potential oxidative decomposition pathways in acidic environments.

Complex	d^5/d^6 Reduction Potential (V)	d^5/d^6 Reduction Potential + acid(V)	ν_{CO} (cm^{-1})	ν_{CO} + acid (cm^{-1})
$[TzMo(CO)_3]^-$ (**63**)	0.22	0.43	1773, 1905	1791, 1918
$[TzW(CO)_3]^-$ (**64**)	0.17	0.38	1772, 1905	1791, 1918
$[TpMo(CO)_3]^-$ (**69**)	0.02	n/a	1761, 1894	1908, 2014
$[TpW(CO)_3]^-$ (**70**)	-0.07	n/a	1750, 1882	1914, 2006

Table 2: The effects of acid on $[LM(CO)_3]^-$ complexes (L = Tz or Tp, M = Mo or W).

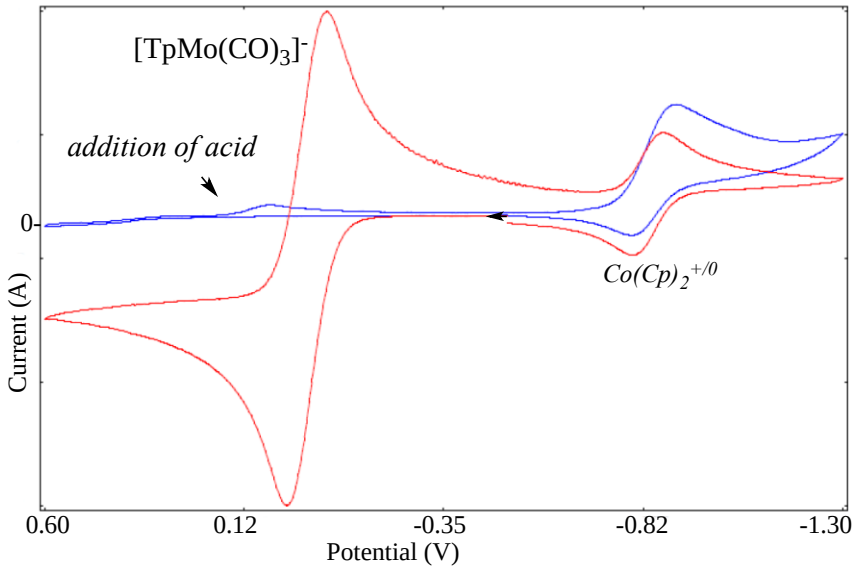

Figure 5: Cyclic voltammagrams demonstrating the decomposition of **69** upon treatment with one molar equivalent of DPhAT in the presence of a cobaltocenium hexafluorophosphate internal standard. Red = initial scan; blue = addition of 1 eq DPhAT.

Further reactivity differences between Tp and Tz analogs were realized in aqueous media. Only the $[TzM(CO)_3]^-$ complexes (**63**-**64**) gave sufficient water solubility for these tests,

so unfortunately no direct comparison with the Tp complexes was possible. However, upon changing the solvent from MeCN to water **63**-**64** showed loss of the full reversibility of the I/0 redox couple at the original 100 mV/s scan rate. Reversibility was restored by increasing the scan rate to 200 mV/s. Treatment of the complexes with one molar equivalent of triflic acid precipitated the neutral compound [HTzM(CO)$_3$] giving the subsequent reduction in current (blue scan, Figure 6). In contrast, the treatment of **63** with NaOH (aq) resulted in a dramatic increase in current when compared to the initial red scan (purple scan, Figure 6). Following the bulk electrolysis of **63** (0.8 V vs NHE, pH = 9) a gas was collected. Analysis of the gas by GC-TCD identified the gas as CO, with little or no CO_2 detected. Based on this result the current increase is likely due to the rapid, multi-electron oxidation of **63** under basic aqueous conditions, accompanied by the loss of CO. The tungsten complex **64** also appeared to undergo decomposition under basic aqueous conditions, although without the current increase seen with molybdenum (**63**).

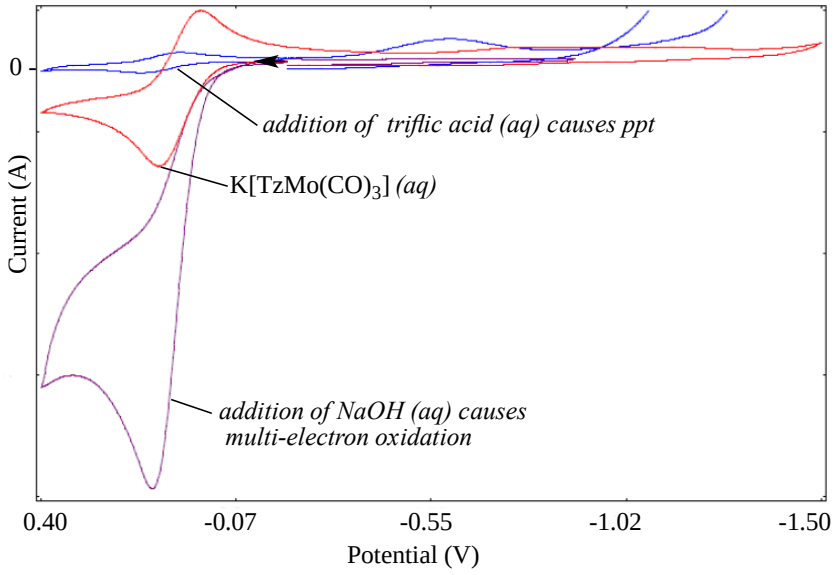

Figure 6: Red: Cyclic voltammagrams of **63** (~0.02 M) in aqueous solution. Blue: addition of HOTf $_{(aq)}$ causes precipitation and loss of current; purple: addition of NaOH $_{(aq)}$ results in irreversible multi-electron oxidation.

6.5 Exploration of Alternative Tz Dearomatization Agents: {TzM(L)(CO)}$^-$ (M = Mo or W)

Given our current lack of success in producing a dihapto-complex from reduction of **72**; and the reduced electron donation from the Tz ligand in comparison to Tp, we proposed a group 6 dearomatization agent featuring Tz and CO in place of Tp and NO^+ ({TzM(L)(CO)}$^-$). Within this context our ancillary ligand would be a weak σ-donor, or perhaps even a moderate to strong π-acid in order to provide the correct electrochemical potential for π-basic dearomatization. Given our ability to access **63**-**64** in good yields, we outlined potential synthetic pathways from the anionic tricarbonyl complexes (Schemes 4 and 5).

We were unable to draw a parallel to Scheme 2, as **63**-**64**, like **69**-**70**, form 7-coordinate M^{II} species when subjected to oxidation by I_2 or Br_2.[8, 20, 23] Therefore our initial attempts focused on the thermolysis of **63**-**64** to liberate CO and coordinate L (Scheme 4). Within this synthetic pathway we proposed two possible means of accessing **VIII**, depending on the identity of L. If we wished to incorporate L ≠ CO (*e.g.*, isonitrile, pyridine, PMe_3, $P(OMe)_3$) we would proceed via Method A, with ligand incorporation to give **VI**, followed by redox reactions to **VIII**. However, if we wished to incorporate L = CO we would proceed via Method B, in which the initial CO is replaced with a weakly coordinating ligand Y (Scheme 4). **IX** would then be exposed to the desired dihapto-coordinated ligand, displacing Y and yielding **VIII**. Unfortunately CO proved difficult to liberate from **63**-**64**, and gave either no reaction or decomposition.

Given the high temperatures required for Scheme 4, we proposed that we could reduce the temperature, and avoid subsequent decomposition by oxidation of **63**-**64** during the thermolysis (Scheme 5). While we are unable to oxidize the tricarbonyl species with a halogen,

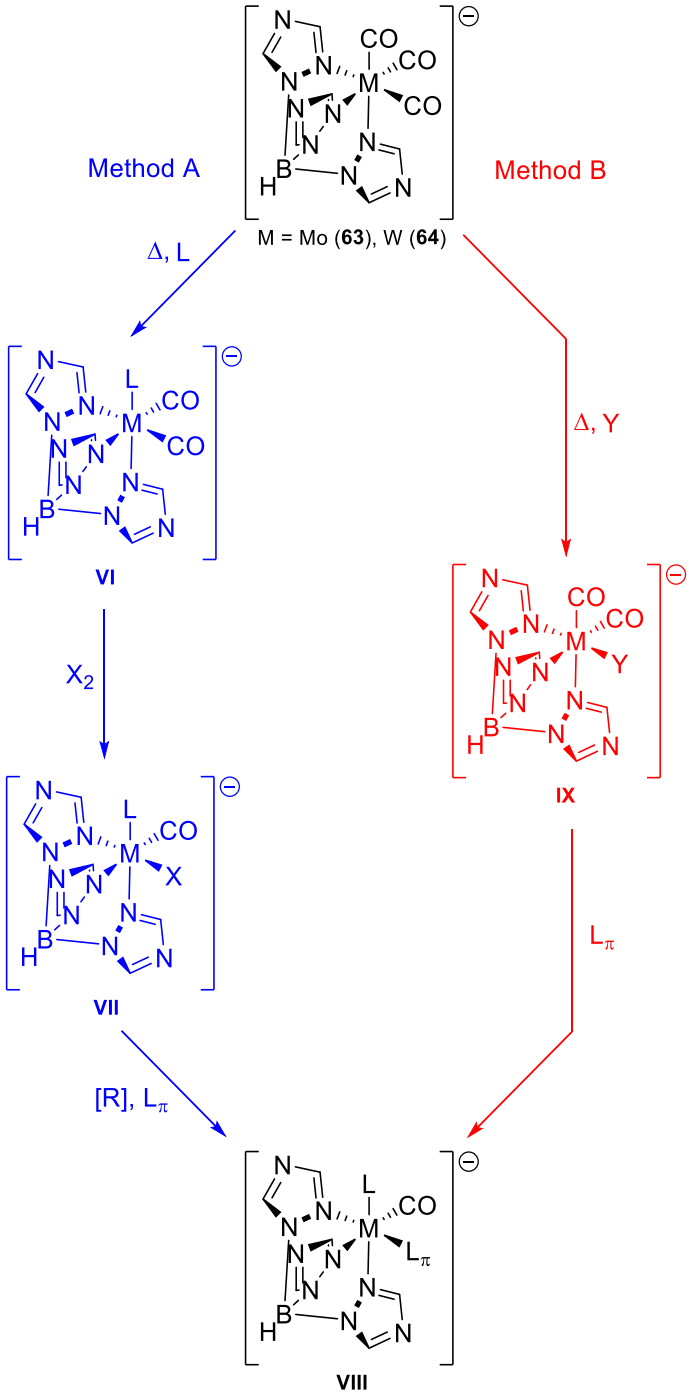

Scheme 4: Proposed synthesis of group 6 tungsten and molybdenum dearomatization agents $\{TzM(L)(CO)\}^-$ (**VIII**) by thermolysis of **63**-**64**.

we proposed $[FeCp_2]^+$ as the oxidizing agent. $[FeCp_2]^+$ is strong enough (0.55 V) to oxidize both **65** and **66**, while also providing an innocent, non-coordinating product in $FeCp_2$.

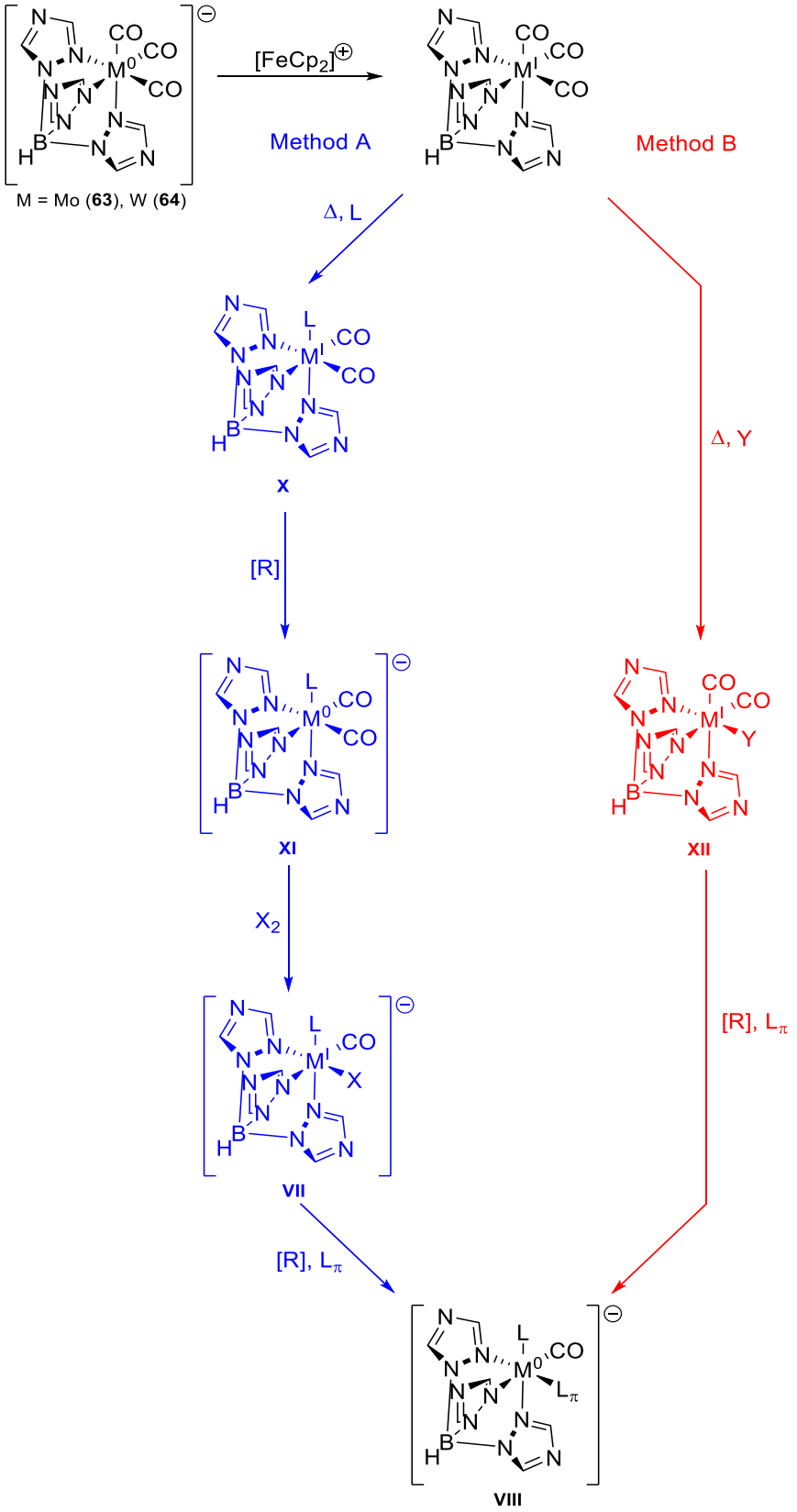

Scheme 5: Proposed synthesis of **VIII** via tandem oxidation/thermolysis of **63**-**64**.

Once again, we envisioned two pathways within Scheme 5, depending on the identity of the ancillary ligand (Method A L ≠ CO, Method B L = CO). Initial attempts of the oxidation/ thermolysis in low boiling solvents (*e.g.*, THF, MeOH, EtOAc, acetone (56-77 ^{o}C)) produced only the oxidized form of **63** and **64** ($TzM^{I}(CO)_3$). Increasing the temperature to 101 ^{o}C with *p*-dioxane produced decomposition. While this result showed that dioxane acts as a poor ligand for **X** or **XII**, it also meant that we are able to liberate a CO from $TzM^{I}(CO)_3$ at 100 ^{o}C. Based on this result, we changed solvents from dioxane to pyridine, which affords a higher reflux temperature (115 ^{o}C), as well as a more stabilizing ligand. After refluxing **63** in pyridine with $[FeCp_2]^+$ for 3 h, our reaction mixture underwent a color change to green/brown. We were able to isolate a green solid in good yield (85 %) by precipitation with Et_2O, leaving ferrocene in the orange filtrate. The green solid is consistent with $TzMo(py)(CO)_2$ (**73**), with ν_{CO} = 1896, 1741 cm^{-1}, and a I/0 potential of -1.28 V. Interestingly the I/0 reduction is not reversible, indicating that pyridine likely dissociates from **73** upon reduction to Mo^0. With this result it may be possible to coordinate dihapto-ligands with the $\{TzMo(CO)_2\}^-$ fragment, as **73** provides a close electrochemical match for TpMo(L)(NO)(X) complexes (**2**-**3**, **6**-**21**, Table 3). Furthermore, optimization of these reaction conditions for **64** to produce $TzW(py)(CO)_2$, would likely result in a slightly more electron rich complex (~-1.3 V), which is nearly an exact match for $TpW(PMe_3)(NO)(Br)$ (-1.33 V, Table 3).[1, 36]

Complex	d^5/d^6 Reduction Potential (V)
$[TzMo(CO)_3]^-$ (**63**)	0.22
$[TzW(CO)_3]^-$ (**64**)	0.17
TpMo(MeIm)(NO)(CO (**1**)	0.22
TpMo(DMAP)(NO)(CO) (**22**)	0.27
$TzMo(py)(CO)_2$ (**73**)	-1.28
TpMo(py)(NO)(Br) (**14**)	-1.23
TpMo(MeIm)(NO)(Br) (**2**)	-1.53
TpMo(DMAP)(NO)(Br) (**19**)	-1.53
$TpW(PMe_3)(NO)(Br)$	-1.33

Table 3: Comparison of reduction potentials for $\{TzM(L)(CO)\}^-$ and {TpM(L)(NO)} dearomatization agents (M = Mo or W).

6.6 Conclusion

We have reported a large-scale synthesis for **62** (160 g) that maintains or improves on the yield and purity previously reported.[14] Complexes of the form $K[LM(CO)_3]$ and $LM(NO)(CO)_2$ were synthesized for both Tp and Tz, and their physical and chemical properties were compared. Owing to their more electron-deficient nature, Tz complexes showed significant differences in reactivity compared to their Tp analogs. Tz complexes also show spectroscopic changes from their Tp analogs, that are similar to those of Tpm,[37] but with the advantage maintaining the overall charge of the complex. Moreover, the Tz complexes have tunable chemical, electrochemical, and solubility properties resulting from their acid-base activity. Significantly, their ability to be reversibly protonated results in greater stability to oxidative reaction conditions (by about 0.40 V compared to Tp), as well as dramatic solubility differences. These desirable characteristics have provided a proof of concept that if we are able to access a group 6 – Tz based dearomatization agent that we can effectively and predictably control electron density at the metal center through interactions with the 4-N lone pairs of the triazolyl rings. The ~+0.20 V shift observed upon protonation is likely sufficient to

liberate a range of dihapto-coordinate ligands, while offering a means to influence reactivity patterns in systems which are sufficiently reducing to maintain dihapto-coordination.

Incorporation of Tz to group 6 tungsten and molybdenum dearomatization agents has seen limited success. The syntheses of our initially proposed {TzM(L)(NO)} fragments were met with a great deal of synthetic difficulty due to the increased reduction potentials of the complexes, and their dramatically different solubility properties compared to our established {TpM(L)(NO)} fragments. We were able to successfully synthesize a possible precursor for dihapto-coordination with molybdenum (**72**); however, thus far it has been unable to produce isolable dihapto-complexes, and its low yield and intensive purification requirements make it unappealing for an alternative to {TpMo(DMAP)(NO)}.

However, by replacing NO^+ for CO with the proposed $\{TzM(L)(CO)\}^-$ active fragment we have avoided the synthetic difficulties associated with **72**. We have prepared a precursor to the potential dearomatization agent $\{TzMo(CO)_2\}^-$ in **73**, whose electrochemical potential is a close match for TpMo(py)(NO)(Br) (**14**), from which coordination of naphthalene was achieved (**28**). Continued tuning of L from CO to a weaker π-acid may give access to a $\{TzMo(L)(CO)\}^-$ fragment with a reduction potential similar to that of our current molybdenum dearomatization agent {TpMo(DMAP)(NO)}. The reduction of **73** and similar complexes may result in successful formation of a dihapto-aromatic complex. Furthermore, the synthesis of a tungsten analog to **73** would likely provide a near match to the current tungsten – dihapto-aromatic precursor $TpW(PMe_3)(NO)(Br)$. It remains to be seen whether we will be able to access a new generation of dearomatization chemistry, and whether our ability to reduce electron density will enable us to stabilize the resulting group 6 metal centers from spatial rearrangement.

6.7 Experimental

General Methods

NMR spectra were obtained on 600 or 800 MHz spectrometers. Chemical shifts are referenced to tertramethylsilane (TMS) utilizing residual ^{1}H signals of the deuterated solvents as internal standards. Chemical shifts are reported in ppm and coupling constants (*J*) are reported in hertz (Hz). Infrared Spectra (IR) were recorded on a spectrometer as a glaze on a Horizontal Attenuated Total Reflectance (HATR) accessory, or as a glaze between two NaCl plates, with peaks reported in cm^{-1}. Electrochemical experiments were performed under a nitrogen atmosphere. Cyclic voltammetric data were recorded at ambient temperature at 100 mV/s unless otherwise noted, with a standard three electrode cell from +1.8 V to -1.8 V with a platinum working electrode, *N*,*N*-dimethylacetamide (DMA) or acetonitrile (MeCN) solvent, and tetrabutylammonium hexafluorophosphate (TBAH) electrolyte (~1.0 M). For CV data recorded in aqueous solutions, sodium triflate (NaOTf) was used as the electrolyte. All potentials are reported versus the normal hydrogen electrode (NHE) using cobaltocenium hexafluorophosphate ($E_{1/2}$ = -0.78 V, -1.75 V) or ferrocene ($E_{1/2}$ = 0.55 V) as an internal standard. Peak separation of all reversible couples was less than 100 mV. All synthetic reactions were performed in a glovebox under a dry nitrogen atmosphere unless otherwise noted. All solvents were purged with nitrogen prior to use. Deuterated solvents were used as received from Cambridge Isotopes. Compounds **67-70** were prepared according to previous literature methods,[32, 33] and characterization of **62-63** is consistent with the findings reported by Shiu *et al.*[26]

Synthesis of KTz (62)

A mixture of 1,2,4-triazole (250 g, 3.62 mol) and KBH_4 (43.4g, 0.804 mol) was added to a 1 L round bottom flask and placed in an oil bath preheated to 125 °C. The flask was fitted with a N_2 line and

a cold-finger condenser containing dry-ice/acetone. The 1,2,4-triazole melted over 10 min and dissolved the KBH_4, giving a colorless molten solution and H_2 evolution (CAUTION!). The oil bath temperature was then slowly increased to 200 °C over the course of 15 min, with continuous H_2 evolution. The molten solution was allowed to stir at 200 °C for 2 h. The N_2 line was then removed and the excess 1,2,4-triazole was removed *in vacuo* for 20 min, until the molten solution became a white solid, and triazole began to deposit on the cold finger. The reaction mixture was then removed from the oil bath and allowed to cool to room temperature. The resulting solid was washed with acetone (4 x 200 mL) and desiccated giving (**62**) (168.17 g, 82%).

Synthesis of [TzMo(CO)$_3$]K (63)

Compound **62** (69.58 g, 0.237 mol), $Mo(CO)_6$ (68.98 g, 0.261 mol), and MeOH (700 mL) were added to a 2 L round bottom flask charged with a stir bar, giving a yellow mixture. The flask was fitted with a reflux condenser and was placed in a heating mantle. The reaction mixture was refluxed overnight (16 h), giving a bright yellow mixture, which was removed from heat and cooled to room temperature. The mixture was filtered through a 600 mL fine frit, and the filtercake was washed with MeOH (2 x 250 mL) followed by Et_2O (3 x 250 mL). The yellow solid (**63**) was collected and desiccated (87%, 89.71 g, 0.206 mol).

Synthesis of [TzW(CO)$_3$]K (64)

Compound **62** (38.61 g, 0.151 mol), $W(CO)_6$ (51.85 g, 0.147 mol), and diglyme (250 mL) were added to a 1 L round bottom flask charged with a stir bar, giving a yellow mixture. The flask was fitted with a reflux condenser and was placed in a heating mantle. The reaction mixture was refluxed overnight (16 h), giving a bright yellow mixture, which was removed from heat and cooled to room temperature. The mixture was filtered through a 350 mL fine frit and the filtercake was washed with MeOH (2 x 150 mL) followed by Et_2O (3 x 150 mL) and the product (**64**) was desiccated and collected. (88%, 67.65 g, 0.129 mol). ^{1}H NMR (DMSO-d_6, δ): 8.15 (s, 3H); 8.61

(s, 3H). ^{13}C NMR (DMSO-d_6, δ): 148.5, 154.5. CV: $E_{1/2}$ = -0.07 V. IR: ν_{CO} = 1684, 1856 cm^{-1}; ν_{BH} = 2481 cm^{-1}.

Synthesis of TzMo(NO)(CO)$_2$ (65)

Compound **62** (50.17 g, 0.197 mol), Mo(CO)$_6$ (49.93 g, 0.189 mol), and MeOH (500 mL) were added to a 1 L round bottom flask charged with a stir bar, giving a yellow mixture. The flask was fitted with a reflux condenser and was placed in a heating mantle. The reaction mixture was refluxed overnight (14 h), giving a bright yellow mixture, which was removed from heat and cooled to room temperature. The mixture was then poured into a 1 L Erlenmeyer flask, in an ice bath, and charged with $NaNO_2$ (14.51 g, 0.210 mol) and a stir bar. Acetic acid (50 mL, 0.874 mol) was added to the stirring solution, giving a color change to orange and the evolution of gas. After stirring for 30 min, the mixture was filtered through a 600 mL medium frit, and the product (**65**) was washed with H_2O (5 x 400 mL) followed by Et_2O (3 x 400 mL) and then desiccated. (83%, 62.75 g, 0.158 mol). ^{1}H NMR (DMSO-d_6, δ): 8.90 (s, 2H); 8.75 (s, 2H); 8.85 (s, 1H); 8.73 (s, 1H). ^{13}C NMR (DMSO-d_6, δ): 150.5, 150.6, 156.1, 156.3. CV: $E_{p,a}$ = +1.30 V. IR: ν_{NO} = 1654 cm^{-1} ν_{CO} = 1910, 2010 cm^{-1}; ν_{BH} = 2533 cm^{-1}.

Synthesis of TzW(NO)(CO)$_2$ (66)

Compound **62** (44.37 g, 0.174 mol), W(CO)$_6$ (58.77 g, 0.167 mol), and DMF (500 mL) were added to a 1 L round bottom flask charged with a stir bar, giving a yellow mixture. The flask was fitted with a reflux condenser and was placed in a heating mantle. The reaction mixture was refluxed overnight (16 h), giving a bright yellow mixture, which was removed from heat and cooled to room temperature. The mixture was then poured into a 2 L Erlenmeyer flask, charged with $NaNO_2$ (12.11 g, 0.176 mol) and a stir bar, and placed in an ice bath. Acetic acid (50 mL, 0.847 mol) was added to the stirring solution, giving a color change to orange and evolution of gas. After stirring for 30 min, the mixture was filtered through a 600 mL medium frit, and the filtercake was washed

with H_2O (5 X 400 mL) followed by Et_2O (3 X 400 mL). The orange solid was desiccated giving (**66**) (79%, 68.99 g, 0.1342 mol). Anal. Found: C, 19.95; H, 1.39; N, 28.54. $C_8H_7BN_{10}O_3W$ calc.: C, 19.78; H, 1.45; N, 28.83. ^{1}H NMR (DMSO-d_6, δ): 8.73 (s, 1H); 8.75 (s, 2H); 8.85 (s, 1H); 8.90 (s, 2H). ^{13}C NMR (DMSO-d_6, δ): 150.1, 150.1, 156.1, 156.4. CV: $E_{p,a}$ = +1.26 V. IR: ν_{NO} = 1636 cm^{-1} ν_{CO} = 1884, 1994 cm^{-1}; ν_{BH} = 2550 cm^{-1}.

Synthesis of TzMo(NO)(Cl)$_2$ (71)

Compound **65** (100.05 g, 0.251 mol) and DCM (1 L) were added to a 3 L multi-neck round bottom flask charged with a stir bar, giving an orange mixture. The flask was fitted with a reflux condenser and attached N_2 line, and the apparatus was purged with N_2 for 10 min. A Teflon® cannula was connected to a Cl_2 (g) source and was attached to the apparatus through a septum, being fully submerged in the DCM mixture. Cl_2 (g) (CAUTION!) was flowed through the reaction mixture for 30 min, resulting in a color change from orange to brown to olive green. The Cl_2 (g) line was replaced for an N_2 line, which was flowed through the reaction mixture for 1 h. Hexanes (1.5 L) were added to further precipitate the product, and the green mixture was stirred for 1 h. The reaction mixture was filtered through a 600 mL fine frit, and the filtercake was washed with hexanes (3 X 200 mL). The green solid was desiccated giving (**71**) (81 %, 74.71 g, 0.181 mol). IR: ν_{NO} = 1699 cm^{-1}.

Synthesis of TzMo(DMAP)(NO)(Cl) (72)

Compound **71** (10.232 g, 24.8 mmol), DMAP (6.392g, 52.3 mmol), and DCM (100 mL) were added to a 500 mL round bottom flask charged with a stir bar, giving a green mixture which evolved gas. After stirring for 1 h the reaction mixture was filtered through a silica plug in a 150 mL medium frit, and the reaction flask and silica plug were washed with 250 mL of DCM. The dark green filtrate was concentrated *in vacuo* to ~25 mL, and was precipitated by slow addition into 500 mL

of stirring Et_2O. The resulting green mixture was stirred for 10 min, then filtered through a 60 mlL fine frit. The green solid was redissolved in x mL of DCM, and was loaded onto a silica column. The bright green product band was eluted with 60 % Et_2O/ 40 % THF (2 L). The green fraction was concentrated *in vacuo* to ~5 mL, and was precipitated by slow addition into 100 mL of stirring Et_2O. After stirring for 10 min the mixture was filtered through a 15 mL fine frit, and the filtercake was washed with Et_2O (3 X 10 mL). The bright green solid was desiccated giving (**72**) (16 %, 1,98 g, 3.97 mmol). CV: $E_{1/2}$ = -1.25 V; $E_{p,a}$ = -1.25 V. IR: ν_{NO} = 1654 cm^{-1}.

Synthesis of TzMo(py)$(CO)_2$ (73)

Compound **63** (4.03 g, 9.26 mmol), $[FeCp_2](PF_6)$ (3.143 g, 9.50 mmol), and 40 mL pyridine were added to a 100 mL round bottom flask fitted with a vigreaux column, giving a green mixtue. The reaction mixture was refluxed for 3 h, and after cooling to room temperature was precipitated by slow addition into 200 mL of stirring Et_2O. After stirring for 15 min the mixture was filtered through a 30 mL fine frit. The green solid was washed with Et_2O (3 X 30 mL) and desiccated giving (**73**) (85 %, 3.12 g, 7.87 mmol). CV: $E_{p,c}$ = -1.28 V; $E_{p,a}$ = +1.03 V. IR: ν_{CO} = 1896, 1741 cm^{-1}.

Electrochemical Studies

Electrochemical studies were carried out for complexes **63-64** and **69-70** with the following general procedure. Stock solutions of 0.02 M $[LM(CO)_3]^-$ and 1.0 M tetrabutylammonium hexafluorophosphate in MeCN were prepared, along with 0.1 M DPhAT in MeCN. The concentration of complex was held constant by adding 1 mL of the (complex + electrolyte) solution to the CV cell, and adding variable amounts of acid and solvent until a final volume of 2 mL was reached. For example, the introduction of 0.5 eq of DPhAT solution is obtained by adding (0.1 mL x N) DPhAT solution then adding (1 mL – (0.10 mL x N)) of MeCN to reach the final 2 mL volume. Through these additions, the effects of acid were tested from 0 – 5 eq of

DPhAT (0 – 0.067 M DPhAT vs 0.0067 M **63-64**, **69-70**). All runs were performed in the presence of cobaltocenium hexafluorophosphate as an internal standard.

6.8 References

1. Ha, Y.; Dilsky, S.; Graham, P. M.; Liu, W.; Reichart, T. M.; Sabat, M.; Keane, J. M.; Harman, W. D. *Organometallics* **2006,** *25*, 5184-5187.

2. Harman, W. D.; Trindle, C. *J. Comp. Chem.* **2005,** *26*, 194-200.

3. Meiere, S. H.; Keane, J. M.; Gunnoe, T. B.; Sabat, M.; Harman, W. D. *J. Am. Chem. Soc.* **2003,** *125*, 2024-2025.

4. Mocella, C. J.; Delafuente, D. A.; Keane, J. M.; Warner, G. R.; Friedman, L. A.; Sabat, M.; Harman, W. D. *Organometallics* **2004,** *23*, 3772-3779.

5. Myers, J. T.; Dakermanji, S. J.; Chastanet, T. R.; Shivokevich, P. J.; Strausberg, L. J.; Sabat, M.; Myers, W. H.; Harman, W. D. *Organometallics* **2017,** *36*, 543-555.

6. Myers, J. T.; Shivokevich, P. J.; Pienkos, J. A.; Sabat, M.; Myers, W. H.; Harman, W. D. *Organometallics* **2015,** *34*, 3648-3657.

7. Trofimenko, S. *J. Am. Chem. Soc.* **1966,** *88,* 1842-1844.

8. Trofimenko, S. *J. Am. Chem. Soc.* **1967,** *89*, 3170-3177.

9. Trofimenko, S., *Scorpionates: The Coordination Chemistry of Polypyrazolylborate Ligands*. Imperial College Press: 1999.

10. Ritter, S. K. *Chemical & engineering news* **2003,** *81*, 40-43.

11. Trofimenko, S *Polyhedron* **2004,** *23*, 197-203.

12. Schwalbe, M.; Andrikopoulos, P. C.; Armstrong, D. R.; Reglinski, J.; Spicer, M. D. *Eur. J. Inorg. Chem.* **2007,** *2007*, 1351-1360.

13. Pettinari, C., *Scorpionates II: Chelating Borate Ligands: Dedicated to Swiatoslaw Trofimenko*. World Scientific: 2008.

14. Lobbia, G. G.; Bonati, F.; Ceccih, P. *Synth. React. Inorg. and Met.-Org. Chem.* **1991,** *21*, 1141-1151.

15. Youm, K.-T.; Kim, M. G.; Ko, J.; Jun, M.-J. *Angew. Chem. Int. Ed.* **2006,** *45*, 4003-4007.

16. Macleod, I. T.; Tieknik, E. R. T.; Young, C. G. *J Organomet. Chem.* **1996,** *506*, 301-306.

17. Kumar, M.; DePasquale, J.; White, N. J.; Zeller, M.; Papish, E. T. *Organometallics* **2013,** *32*, 2135-2144.

18. Lobbia, G. G.; Pellei, M.; Pettinari, C.; Santini, C.; Skelton, B. W.; Somers, N.; White, A. H. *J. C. S. Dalton* **2002,** *11*, 2333-2340.

19. Shiu, K.-B.; Guo, W.-N.; Peng, S.-M.; Cheng, M.-C. *Inorg. Chem.* **1994,** *33*, 3010-3013.

20. Shiu, K.-B.; Lee, J. Y.; Yu, W.; Ming-Chu, C.; Sue-Lein, W.; Fen-Ling, L. *J. Organomet. Chem.* **1993,** *453*, 211-219.

21. Robinson, L.; Cooke, D. J.; Elliott, P. I. P.ligand tuning *J. Organomet. Chem.* **2011,** *696*, 2580-2583.

22. Dilsky, S. *J. Organomet. Chem.* **2007,** *692*, 2887-2896.

23. Trofimenko, S. *J. Am. Chem. Soc.* **1969,** *91*, 588-595.

24. Lu, D.; Tang, H. *Phys. Chem. Chem. Phys.* **2015,** *17*, 17027-17033.

25. Effendy; Gioia Lobbia, G.; Marchetti, F.; Pellei, M.; Pettinari, C.; Pettinari, R.; Santini, C.; Skelton, B. W.; White, A. H. *Inorg. Chim. Acta* **2004,** *357*, 4247-4256.

26. Janiak, C. *J. Chem. Soc. Chem. Commun.* **1994,** *4*, 545-547.

27. Janiak, C. *Chemische Berichte* **1994,** *127*, 1379-1385.

28. Janiak, C.; Hemling, H. *J. C. S. Dalton* **1994,** *20*, 2947-2952.

29. Janiak, C.; Scharmann, T. G. *Polyhedron* **2003,** *22*, 1123-1133.

30. Janiak, C.; Scharmann, T. G.; Albrecht, P.; Marlow, F.; Macdonald, R. *J. Am. Chem. Soc.* **1996,** *118*, 6307-6308.

31. Janiak, C.; Scharmann, T. G.; Bräuniger, T.; Holubová, J.; Nádvorník, M. *Zeitschrift fur Anorganische und Allgemeine Chemie* **1998,** *624*, 769-774.

32. Janiak, C.; Scharmann, T. G.; Green, J. C.; Parkin, R. P. G.; Kolm, M. J.; Riedel, E.; Mickler, W.; Elguero, J.; Charamunt, R. M.; Sanz, D. *Chem. Eur. J.* **1996,** *2*, 992-1000.

33. Janiak, C.; Scharmann, T. G.; Günther, W.; Girgsdies, F.; Hemling, H.; Hinrichs, W.; Lentz, D. *Chem. Eur. J.* **1995,** *1*, 637-644.

34. Janiak, C.; Scharmann, T. G.; Hemling, H.; Lentz, D.; Pickardt, J. *Chemische Berichte* **1995,** *128*, 235-244.

35. Janiak, C.; Temizdemir, S.; Scharmann, T. G.; Schmalstieg, A.; Demtschuk, J. *Zeitschrift fur Anorganische und Allgemeine Chemie* **2000,** *626*, 2053-2062.

36. Graham, P. M.; Meiere, S. H.; Sabat, M.; Harman, W. D. *Organometallics* **2003,** *22*, 4364-4366.

37. Trofimenko, S. *J. Am. Chem. Soc.* **1970,** *92*, 5118-5126.

Concluding Remarks

The goal of this research was to access a viable route to dearomatization chemistry with a 2nd row molybdenum fragment. With this goal in mind we revisited previous attempts to establish molybdenum dearomatization agents with a {TpMo(L)(NO)} ligand set. We successfully optimized previous procedures to access dihapto-aromatic complexes with a range of ancillary ligands. Through this work we have demonstrated the adjustable nature of the molybdenum system, allowing for the tuning of the sterics and electronics for an array of dihapto-naphthalene complexes. Manipulations of the dihapto-coordinated PAH cores have shown that changes to the ancillary are manifested in subtle changes to the reactivity patterns of the coordinated ligand.

Within the investigation of a variety of ancillary ligand options, we settled on DMAP as our ligand of choice. The {TpMo(DMAP)(NO)} fragment has provided access to all of the aromatic systems of the initial {TpMo(MeIm)(NO)} fragment, and additionally provides a means of stabilization from oxidative conditions via protonation of the lone pair on the amino group. This additional stabilization has provided access to stable allylic cationic species, which are inaccessible to the MeIm variant, allowing for incorporation of acid-sensitive nucleophiles. The molybdenum dearomatization agent has shown the ability to undergo liberation of dearomartized organic products with a weak oxidant, providing for increased yields of the product compared to the 3rd row tungsten species. Both {TpMo(DMAP)(NO)} and {TpMo(MeIm)(NO)} provide sufficient electrochemical stability for redox-based recycling of the metal center. Furthermore, synthesis of the precursor to molybdenum dearomatization (TpMo(DMAP)(NO)(I)) has been optimized to give a 68 % yield on 170 g scale *outside of an inert atmosphere*. The ability to produce our 2nd row molybdenum dearomatization agent inexpensively, on a large scale, and without special air-sensitive techniques provides greater applicability of our dearomatization methods to a wide audience.

Following the development of molybdenum dearomatization, we investigated a method to resolve the racemic metal center, and provide a means to control the *absolute* stereochemistry of additions to dihapto-coordinated aromatic ligands. Application of the rhenium – *R*-α-pinene resolution method to {TpMo(DMAP)(NO)} resulted in the isolation of a single diastereomer. The TpMo(DMAP)(NO)(η^2-*R*-α-pinene) complex was able to undergo ligand exchange with selected aromatics, and a range of carbonyl species. However, racemization studies employing *S*-β-pinene proved complicated. This led to the exploration of a range of chiral aldehydes and ketones, and the eventual adoption of *R*-myrtenal as our 'reporter' ligand. Unfortunately, racemization studies showed the chiral molybdenum center to be stereochemically unstable, resulting in complete racemization of the {TpMo(DMAP)(NO)} fragment. Application of α-pinene resolution to the {TpMo(MeIm)(NO)} fragment showed a modest increase in chirality transfer. Unfortunately this stability was accompanied by a slow exchange rate of the pinene ligand, limiting its synthetic utility. Recently our lab has discovered the ability to dramatically increase the rate of exchange, while also in maintaining metal resolution to TpMo(DMAP)(NO)(η^2-*R*-myrtenal) in the presence of catalytic, non-coordinating oxidant. Investigations into this increase in the rate of exchange and stereochemical stability of molybdenum species in the presence of catalytic oxidant are ongoing. These studies may result in the ability to overcome racemization of the molybdenum center, and allow for *absolute* control of stereochemistry for molybdenum dearomatization.

With our inability to overcome racemization of {TpMo(L)(NO)} fragments, we explored new ligand sets as a means to increase the stereochemical stability of the molybdenum center. These efforts were focused on a motif set featuring two bidentate ligands. Within this context a mixture of Bp, bpy, and ampy complexes were explored. Like initial efforts to develop an alternative to osmium – based dearomatization with rhenium complexes, we were able to mimic

the electronics of previous molybdenum dearomatization agents. However, these complexes proved too sterically bulky for dihapto-coordination.

Our efforts turned to a dearomatization agent featuring Tz, rather than Tp scorpionate. We reasoned that a dearomatization agent with the reduced donation of the triazole based scorpionate would increase the stability of the chiral molybdenum center, following the reports of Brunner. Furthermore, the ability to modulate electron donation by interactions with the *exo* 4-N lone pair of the triazolyl rings would allow for changes to the reactivity patterns of dihapto-coordinated ligands, and the possible means to liberate dearomatized products without oxidation of the metal complex.

We were able to synthesize the Tz ligand in high yield and purity (80 %) on a large scale (160 g). The syntheses of classical scorpionate complexes allowed us to compare the reactivity of Tz and Tp complexes. Within these studies we demonstrated the ability to reversibly protonate the Tz ligand, providing a +0.20 V shift in electrochemical potential. This positive shift stabilized Tz complexes to highly oxidizing environments, while their Tp analogs decomposed.

Syntheses of {TzM(L)(NO)} complexes were met with synthetic difficulty. Changes to the reduction potential and physical properties proved incompatible with our optimized Tp procedures. While we were able to synthesize a possible dearomatization precursor in TzMo(DMAP)(NO)(Cl), were have been unable to isolate any dihapto-complexes. Furthermore, the low yields and laborious synthesis of the Tz complex limit its appeal as an alternative to Tp – based group 6 dearomatization chemistry.

However, preliminary investigation into a $\{TzM(L)(CO)\}^-$ dearomatization agent shows promise. We have proposed syntheses for these possible dearomatization agents from $[TzM(CO)_3]^-$ complexes, which can be synthesized in high yields. Moreover, initial results show that these species provide a close electrochemical match to current {TpM(L)(NO)}

dearomatization agents. The continued investigation into Tz – based dearomatization offers the allure of a dearomatization agent which can undergo reversible changes to its reactivity, and provide stability from highly oxidizing conditions. Moreover, the ability to dramatically reduce electron donation may provide a means to overcome the racemization of chiral molybdenum frameworks.

Appendix

^{1}H NMR (d^{6}-acetone) of Compound 4

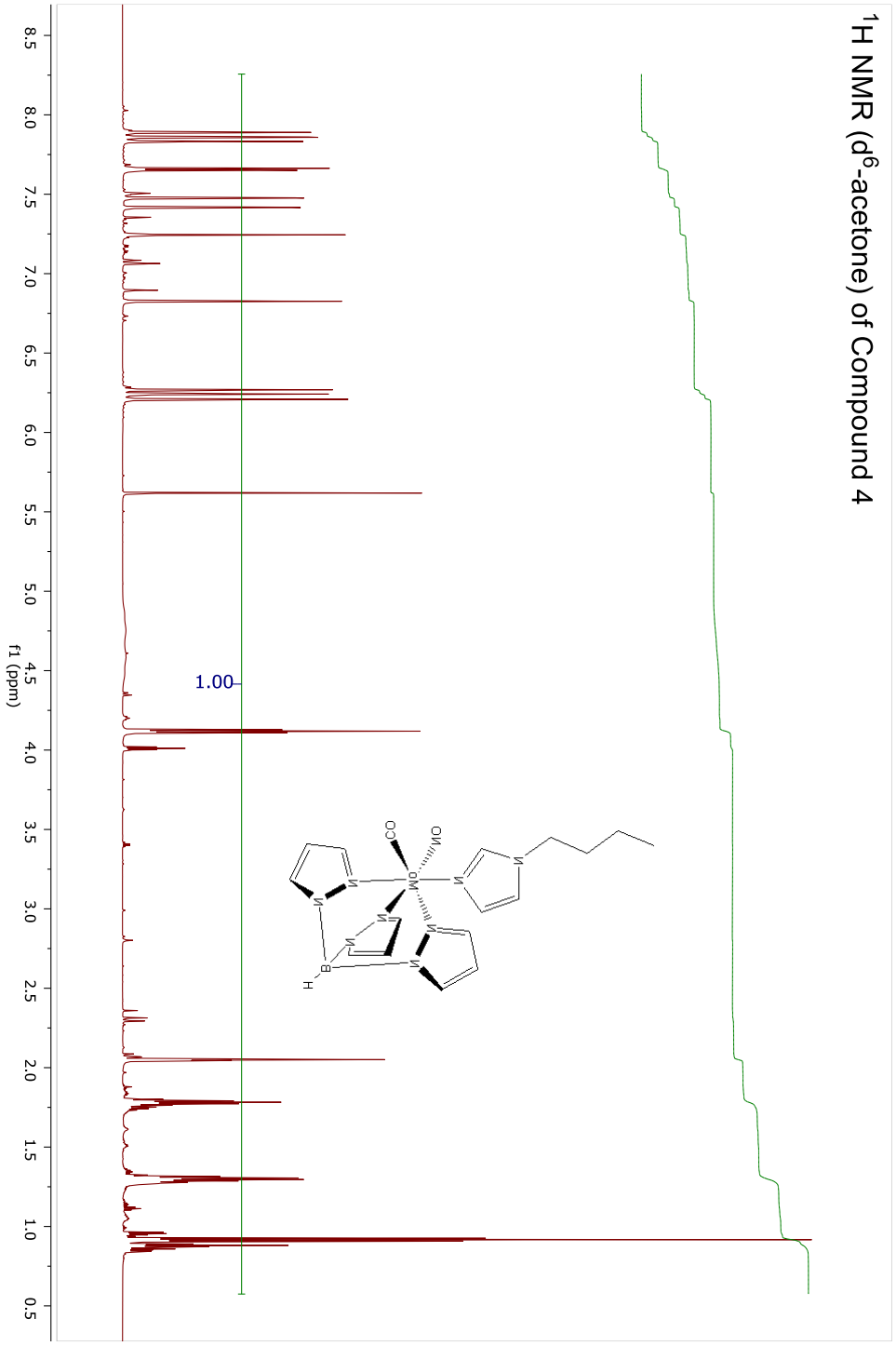

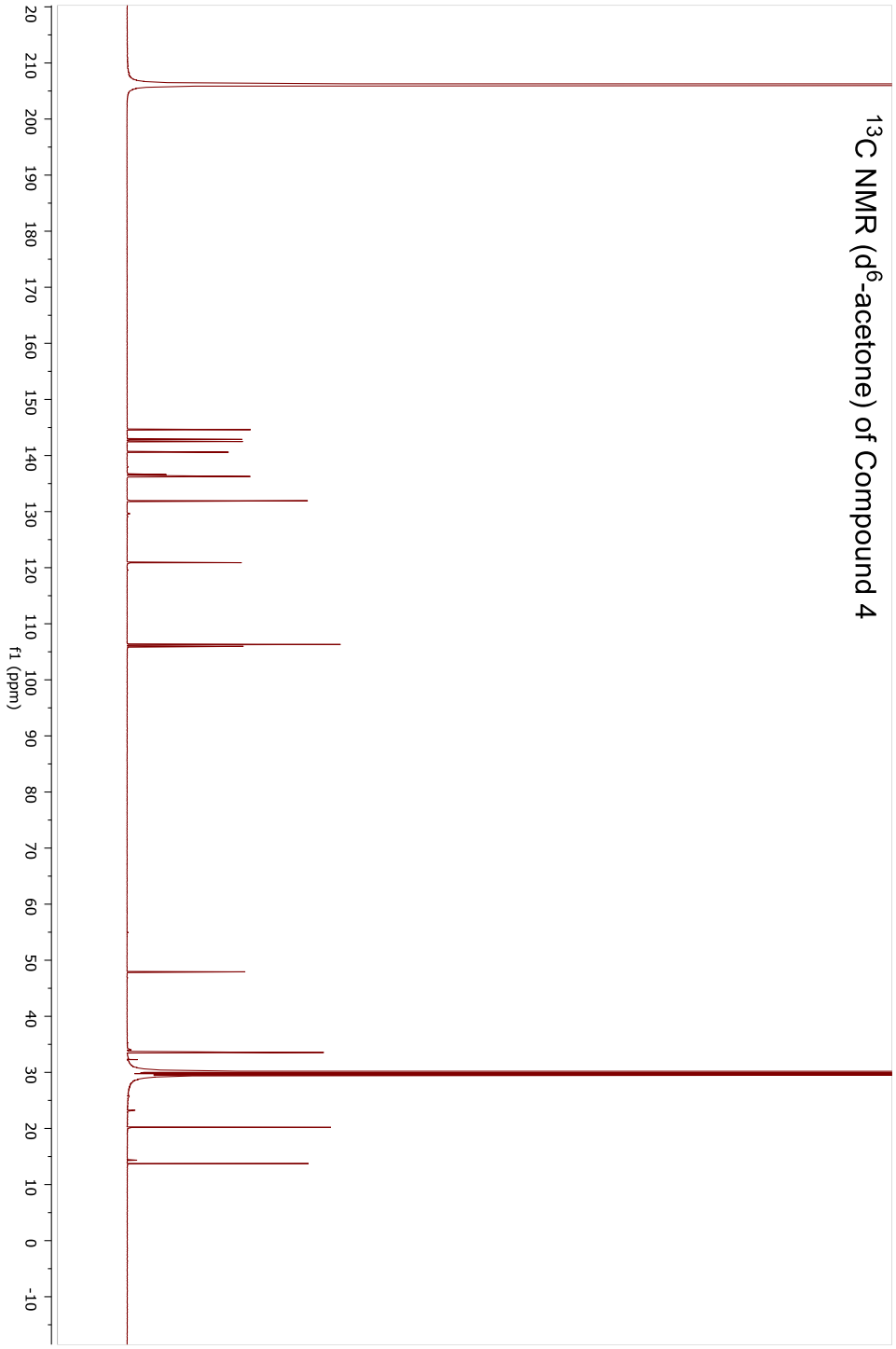
^{13}C NMR (d^6-acetone) of Compound 4
f1 (ppm)
220
210
200
190
180
170
160
150
140
130
120
110
100
90
80
70
60
50
40
30
20
10
0
-10

^{1}H NMR (d^6-acetone) of Compound 5

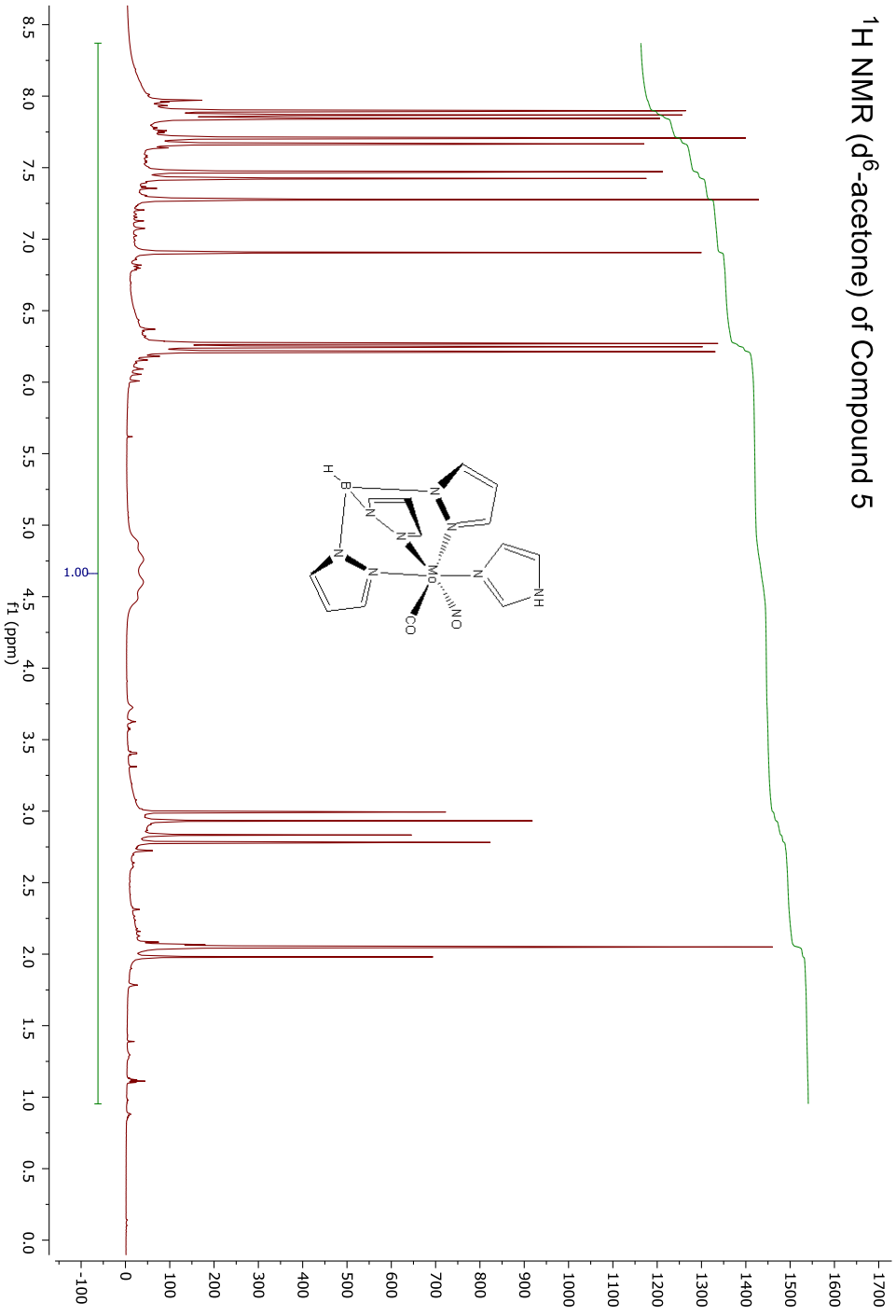

^{13}C NMR (d^6-acetone) of Compound 5

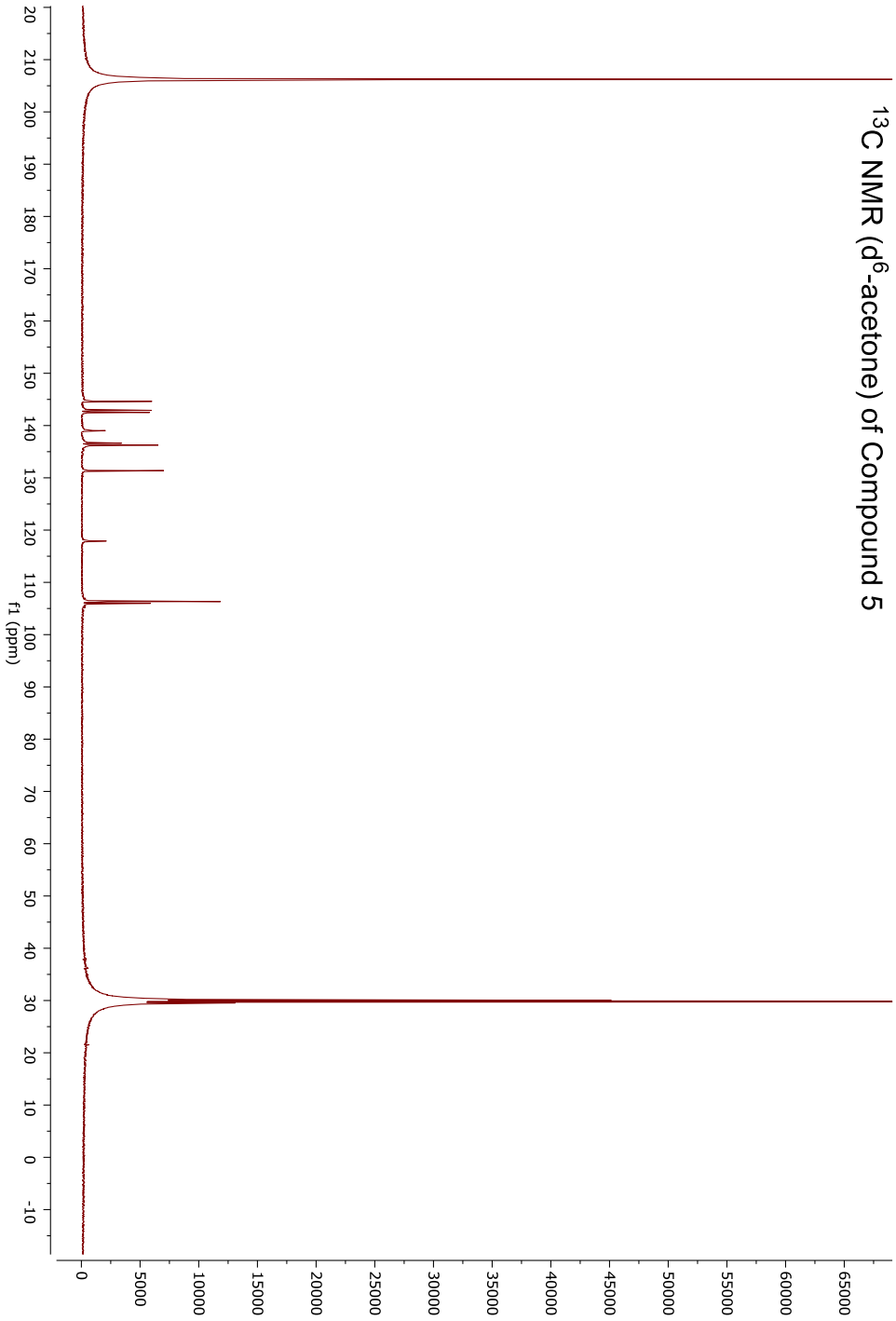

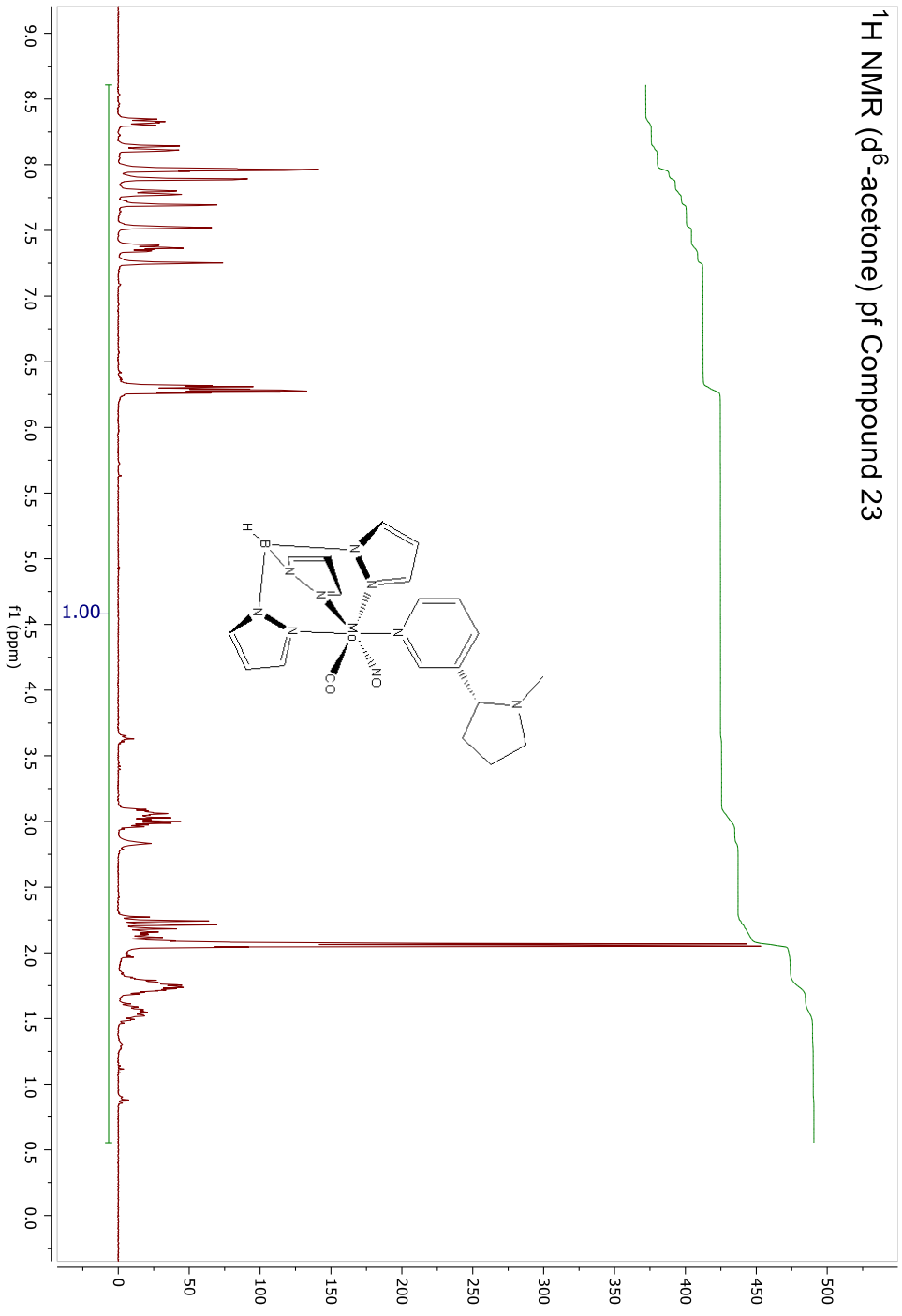
^{1}H NMR (d^6-acetone) pf Compound 23
1.00
f1 (ppm)
9.0
8.5
8.0
7.5
7.0
6.5
6.0
5.5
5.0
4.5
4.0
3.5
3.0
2.5
2.0
1.5
1.0
0.5
0.0
0
50
100
150
200
250
300
350
400
450
500

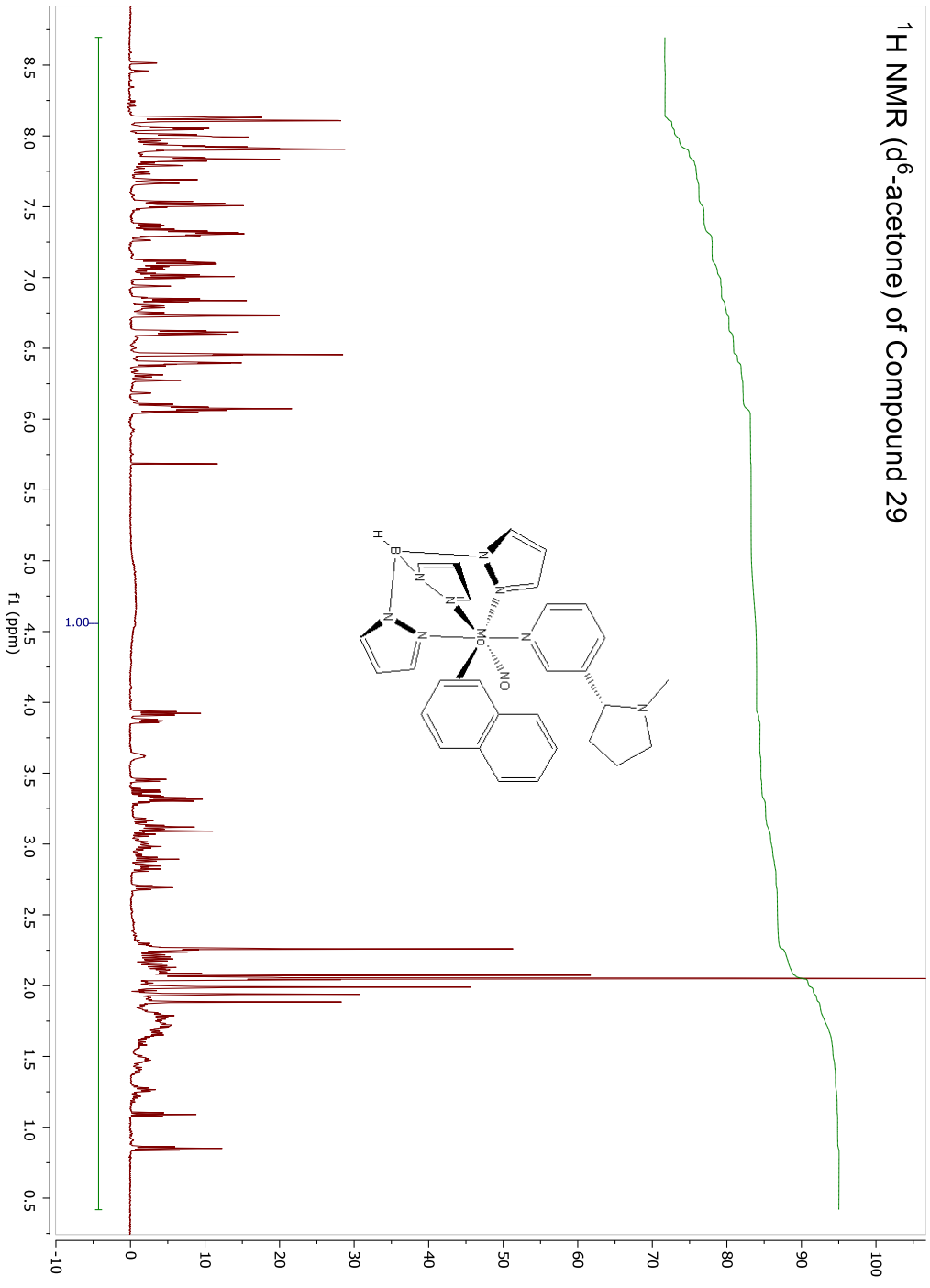
^{1}H NMR (d^6-acetone) of Compound 29
f1 (ppm)
1.00
8.5
8.0
7.5
7.0
6.5
6.0
5.5
5.0
4.5
4.0
3.5
3.0
2.5
2.0
1.5
1.0
0.5
-10
0
10
20
30
40
50
60
70
80
90
100
H
B
N
Mo
NO

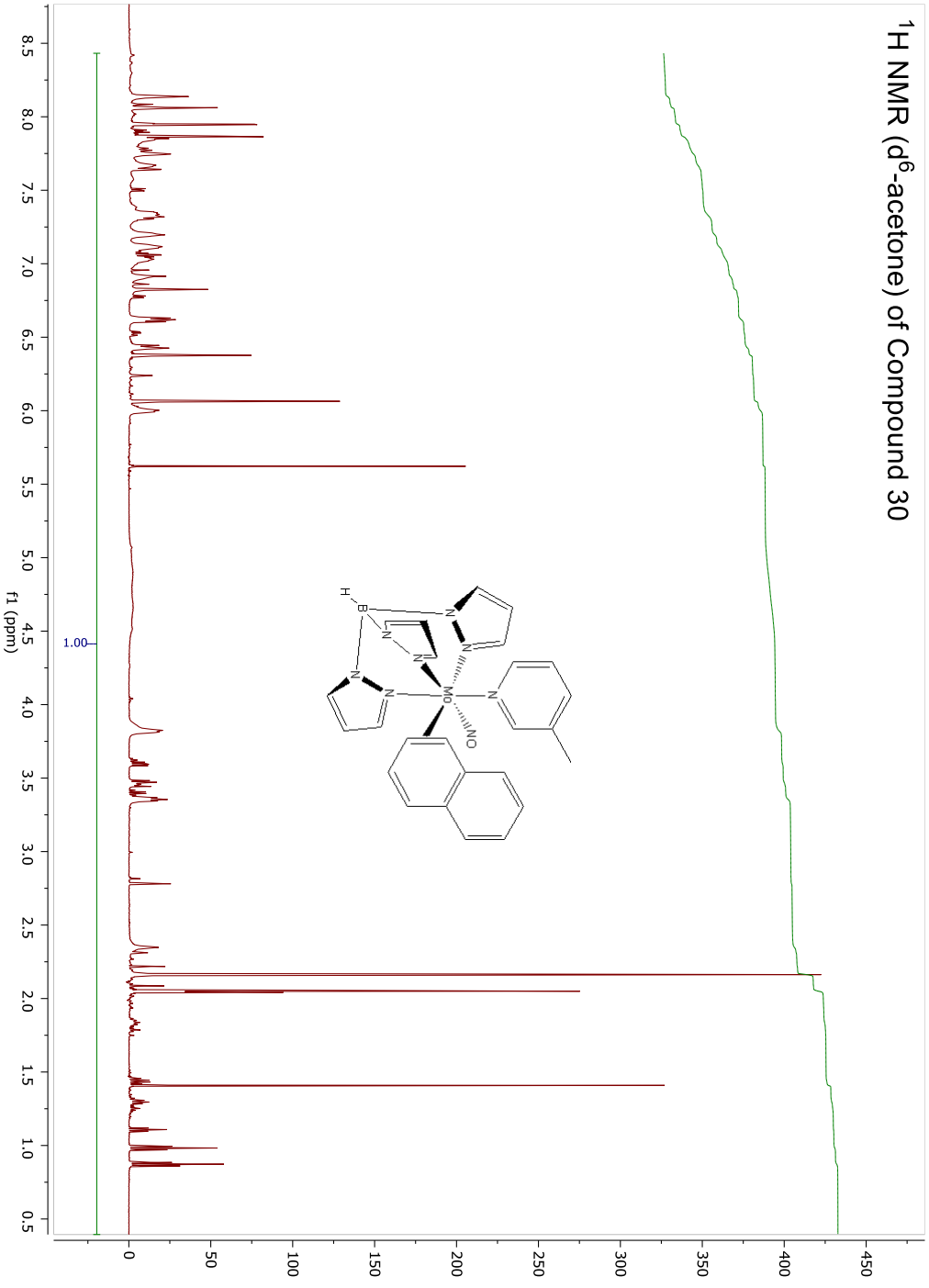
^{1}H NMR (d^6-acetone) of Compound 30
f1 (ppm)
1.00
8.5
8.0
7.5
7.0
6.5
6.0
5.5
5.0
4.5
4.0
3.5
3.0
2.5
2.0
1.5
1.0
0.5
0
50
100
150
200
250
300
350
400
450
H
B
N
Mo
NO

^{1}H NMR (d^6-acetone) of Compound 31

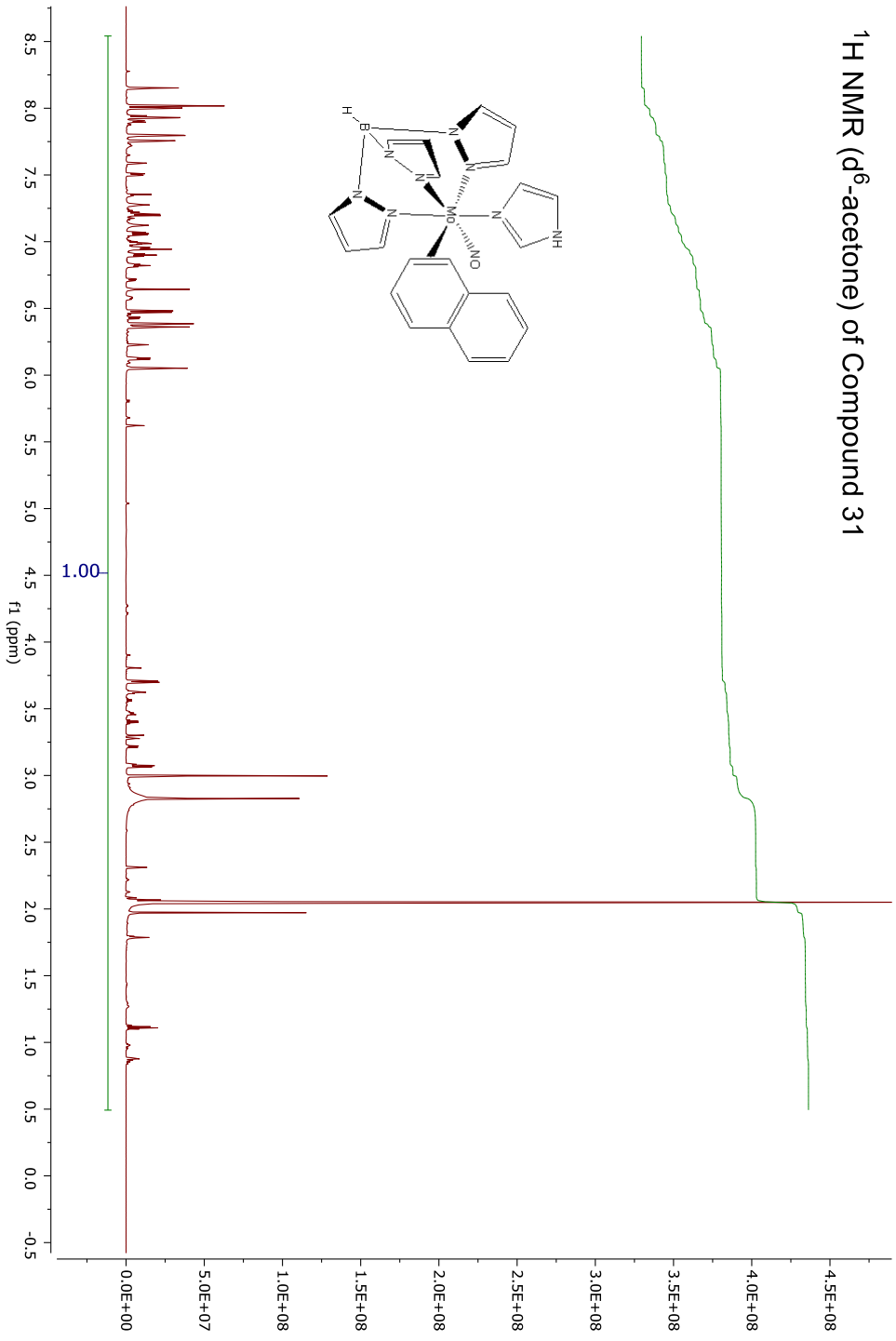

^{13}C NMR (d^6-acetone) of Compound 31

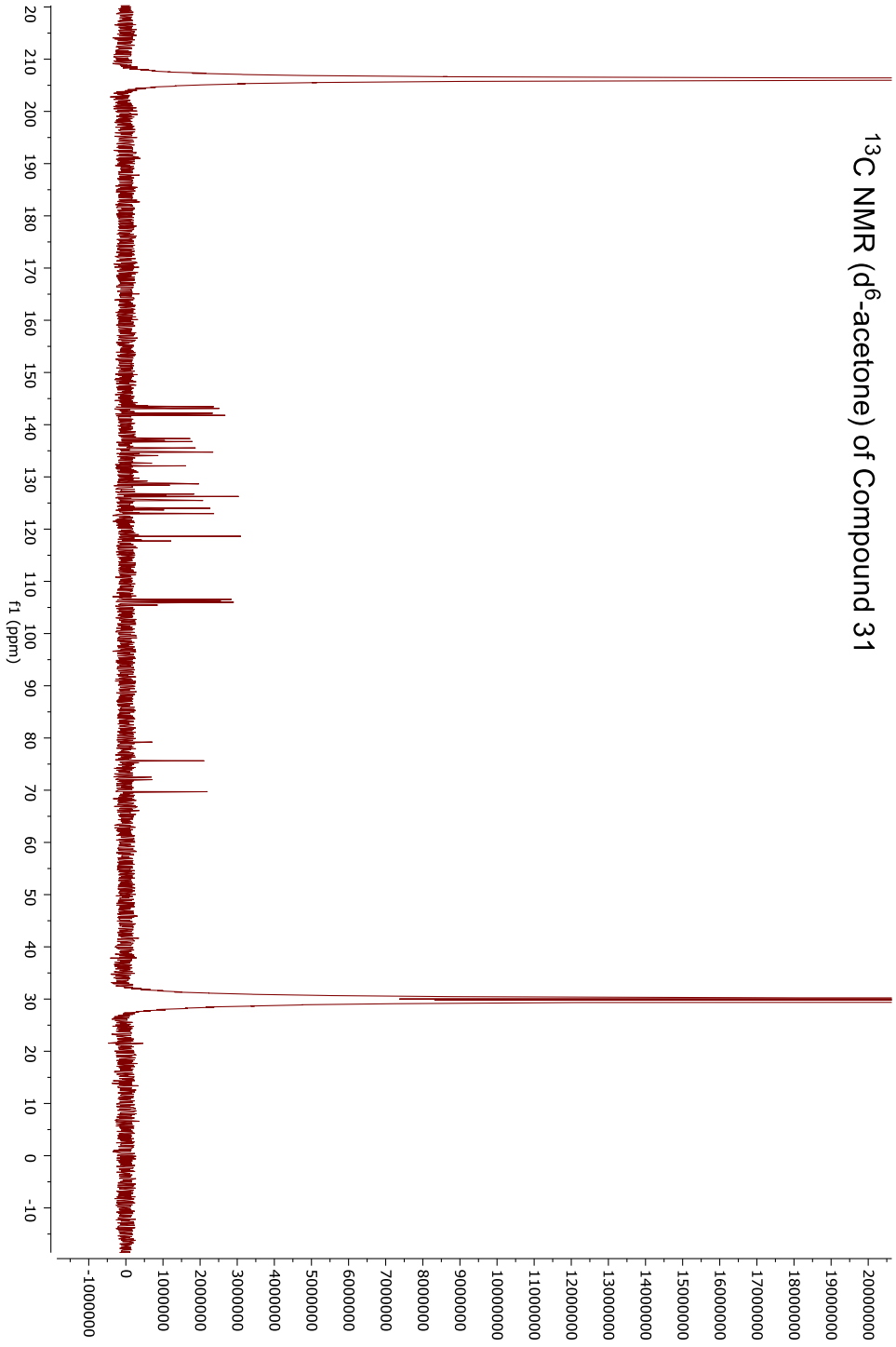

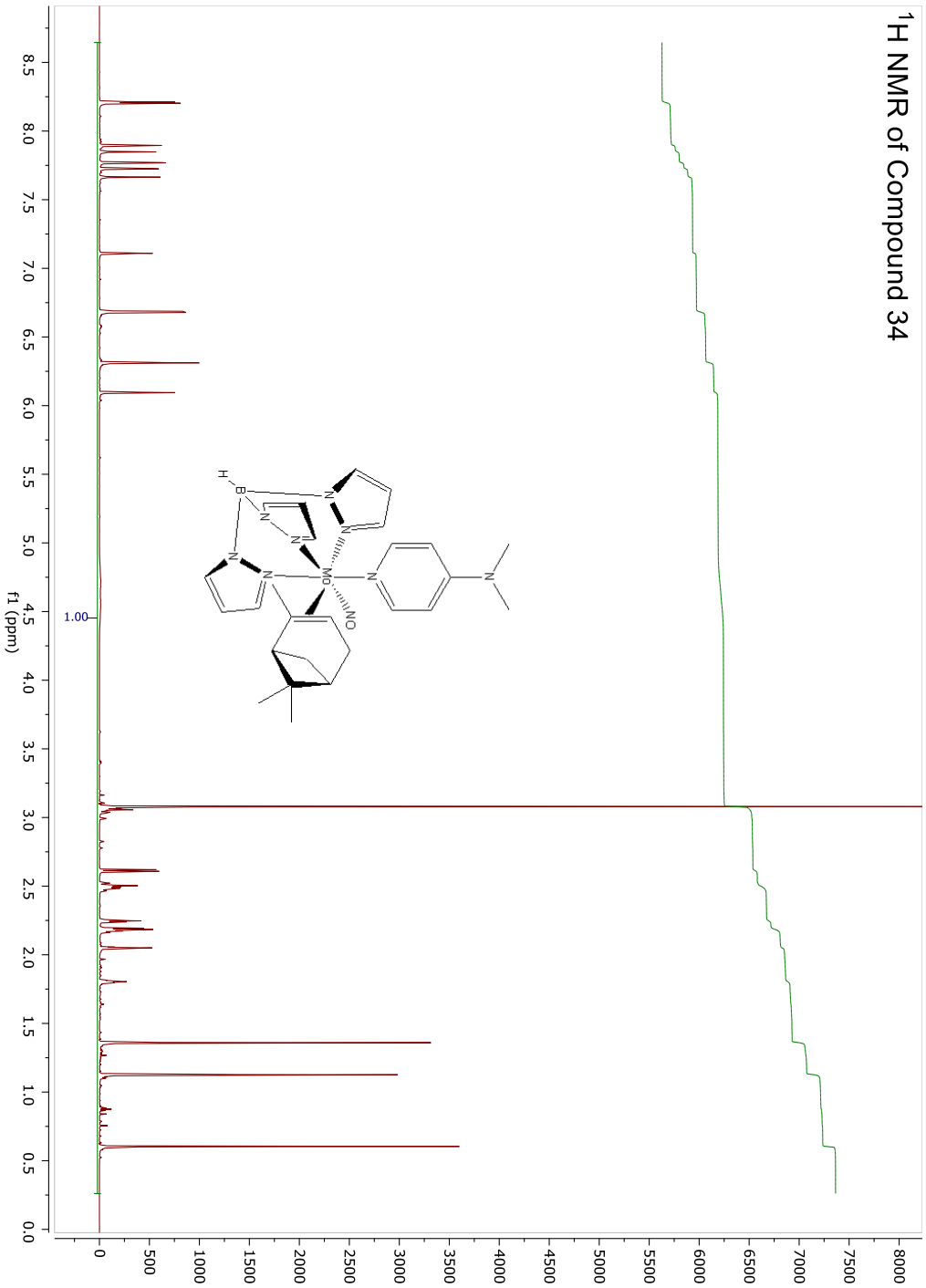
1H NMR of Compound 34
f1 (ppm)
1.00
Mo
NO
B
H
N

^{13}C NMR (d^6-acetone) of Compound 34

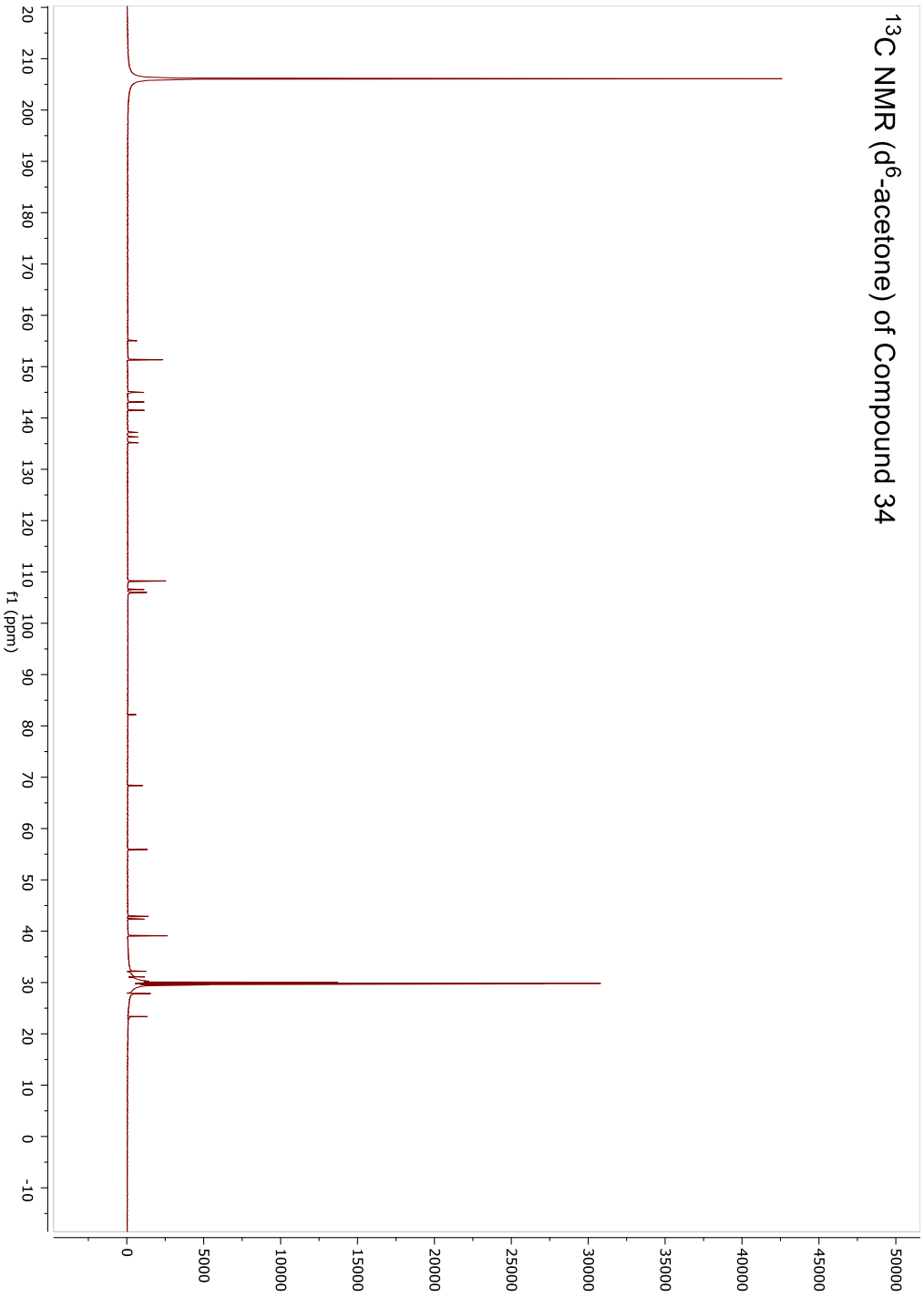

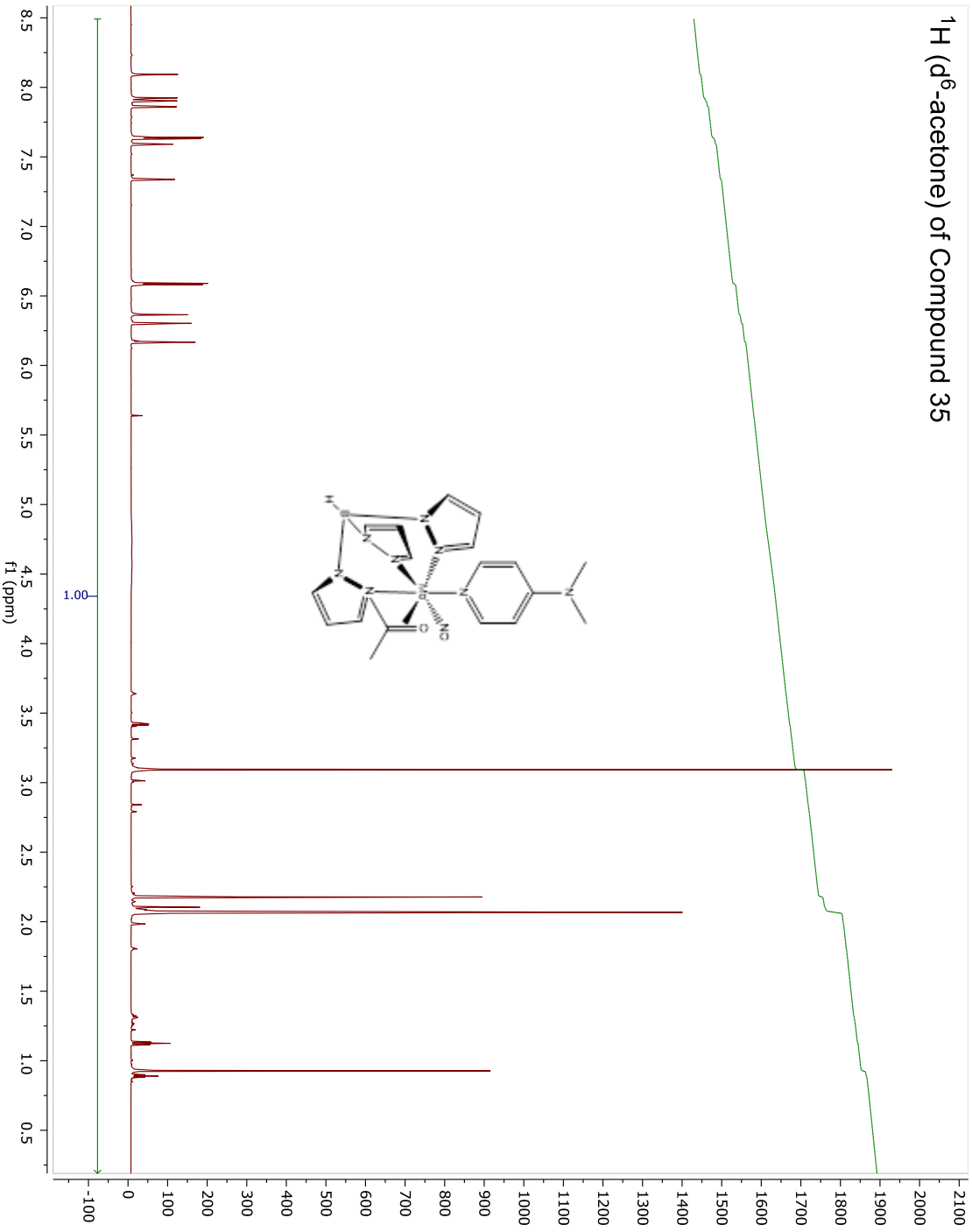
^{1}H (d^6-acetone) of Compound 35
f1 (ppm)
1.00

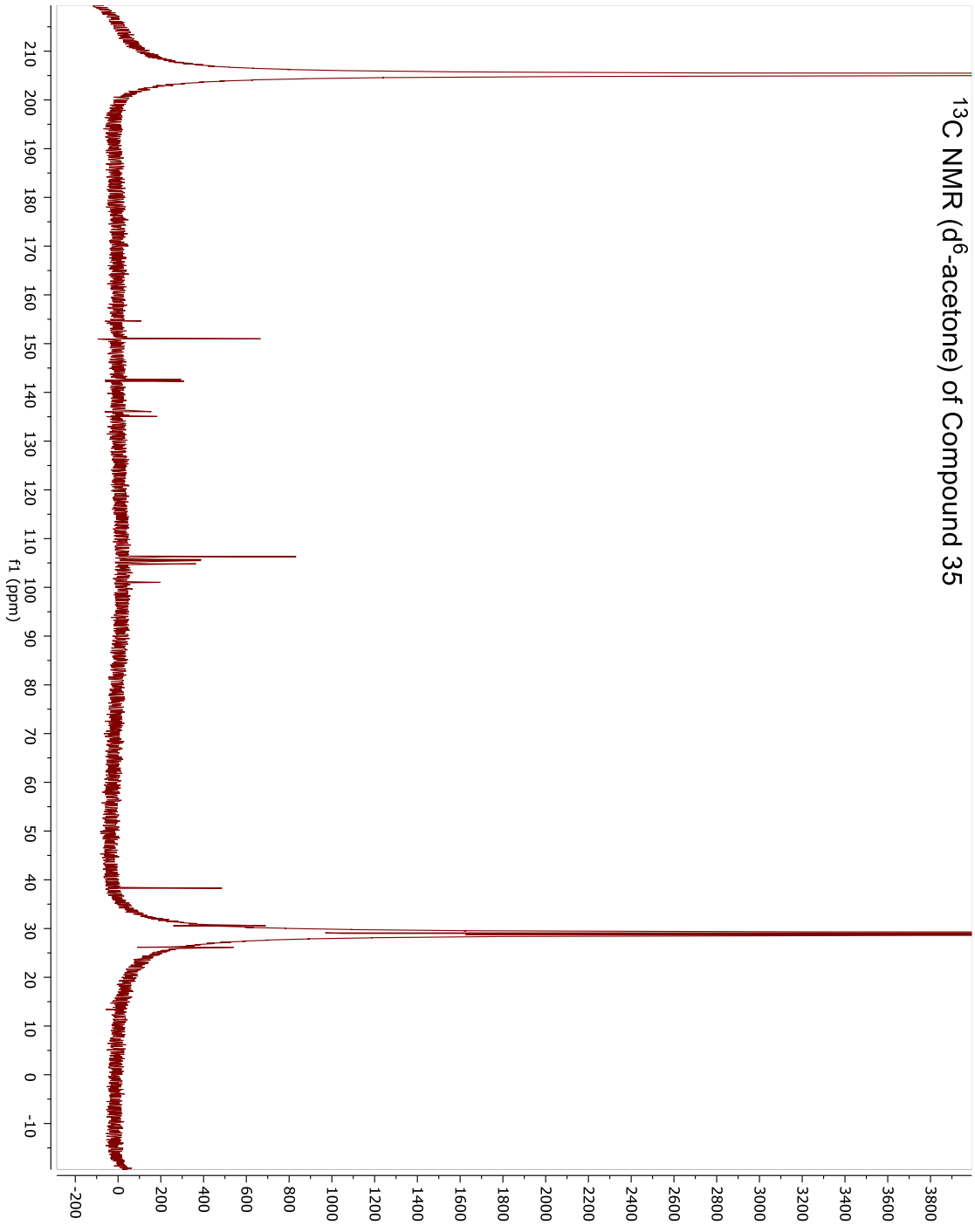
^{13}C NMR (d^6-acetone) of Compound 35
f1 (ppm)

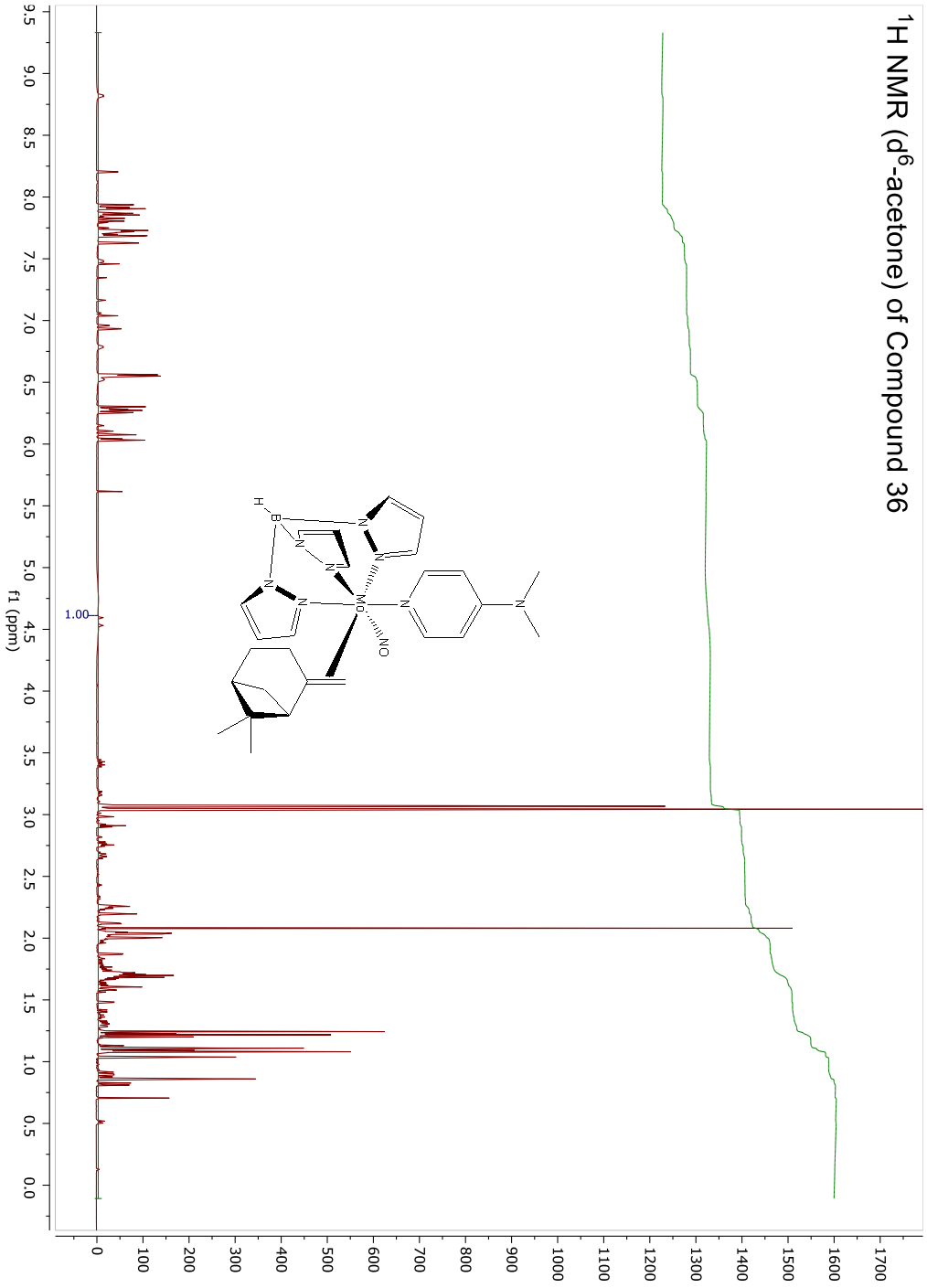
^{1}H NMR (d^6-acetone) of Compound 36
f1 (ppm)
1.00

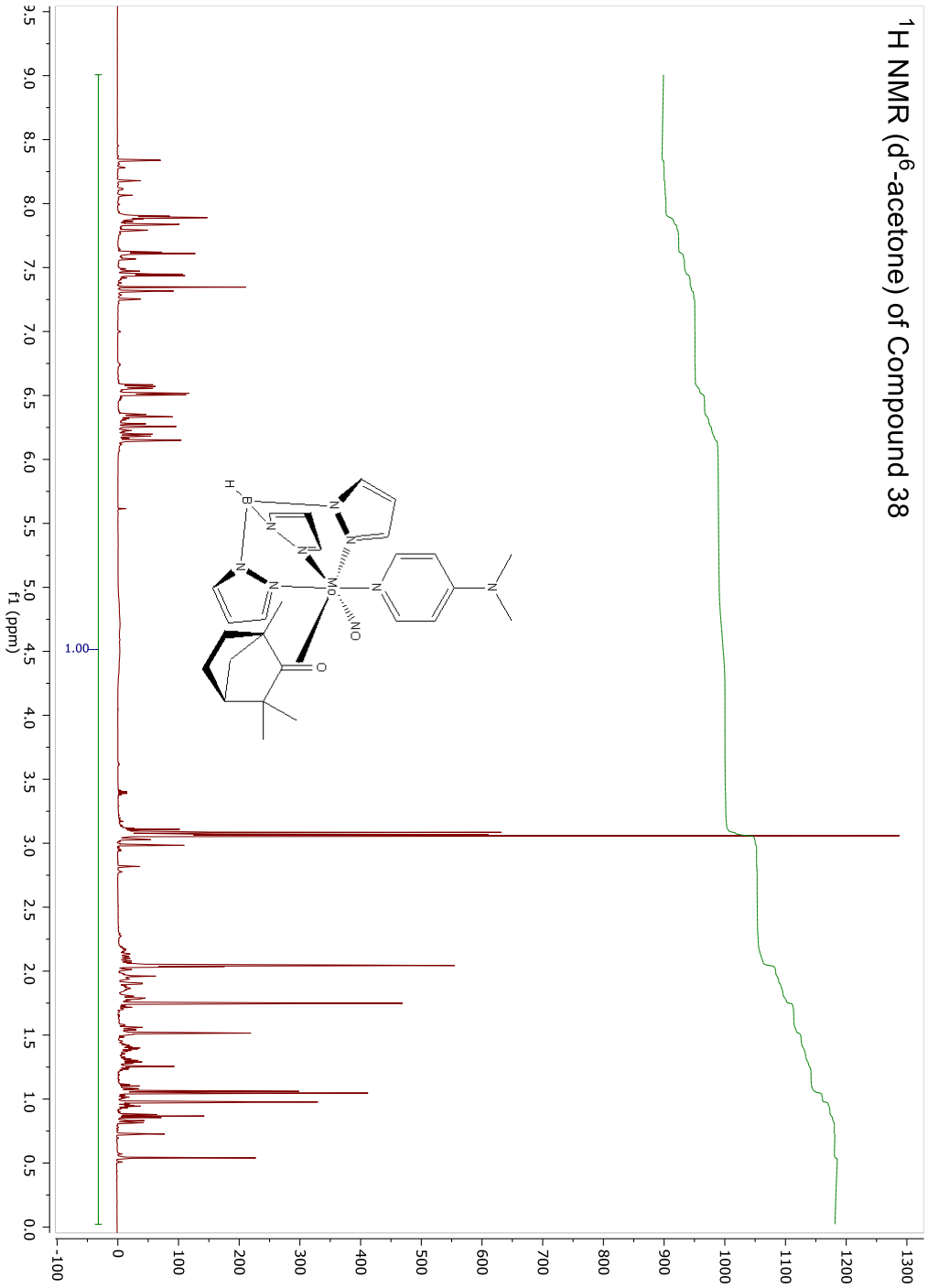
^{1}H NMR (d^6-acetone) of Compound 38
f1 (ppm)
1.00
H
B
N
Mo
NO
O

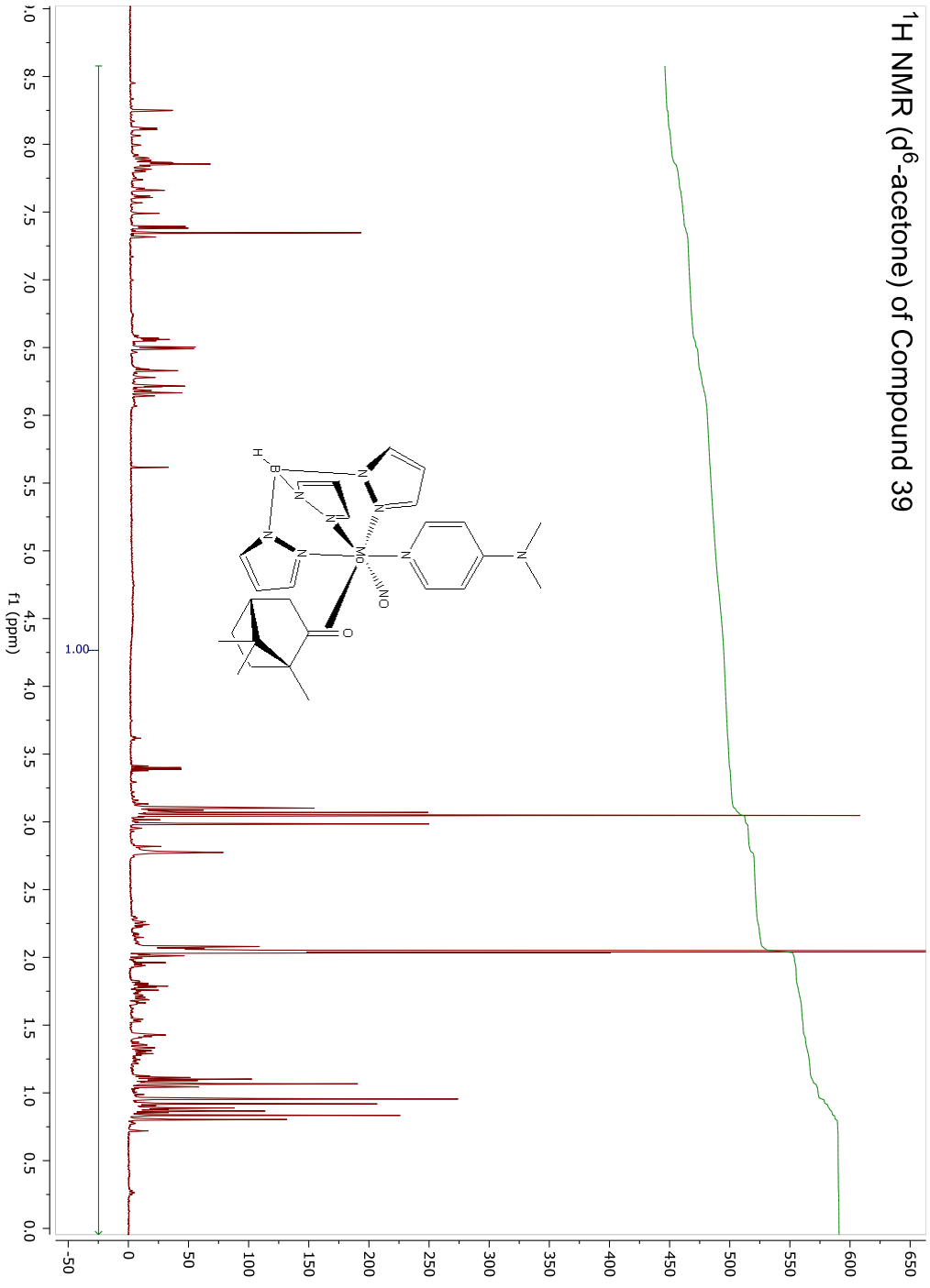
^{1}H NMR (d^6-acetone) of Compound 39
f1 (ppm)
1.00
H
B
N
Mo
NO
O

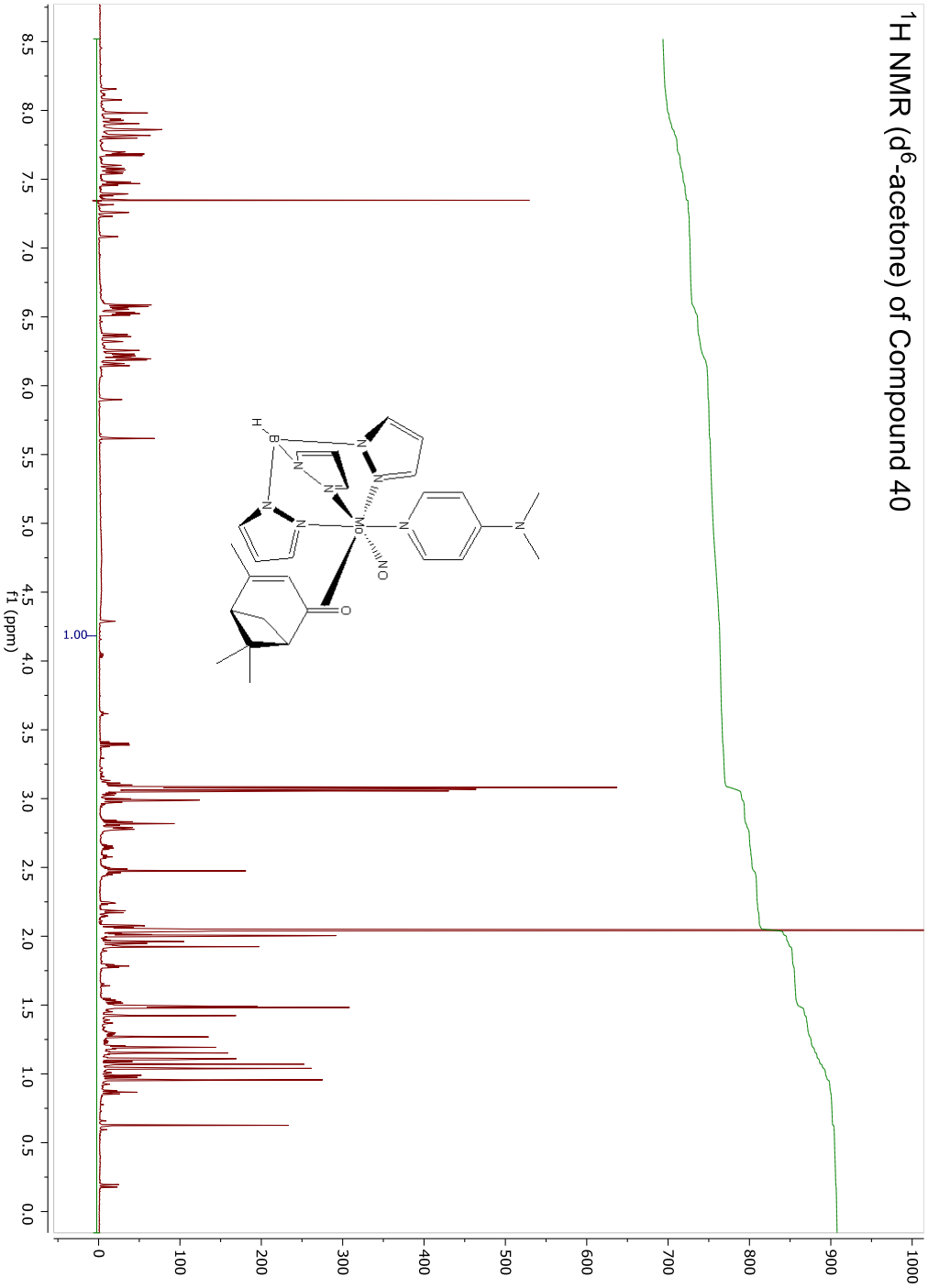
^{1}H NMR (d^6-acetone) of Compound 40
f1 (ppm)
1.00
H
B
N
Mo
N
O
O

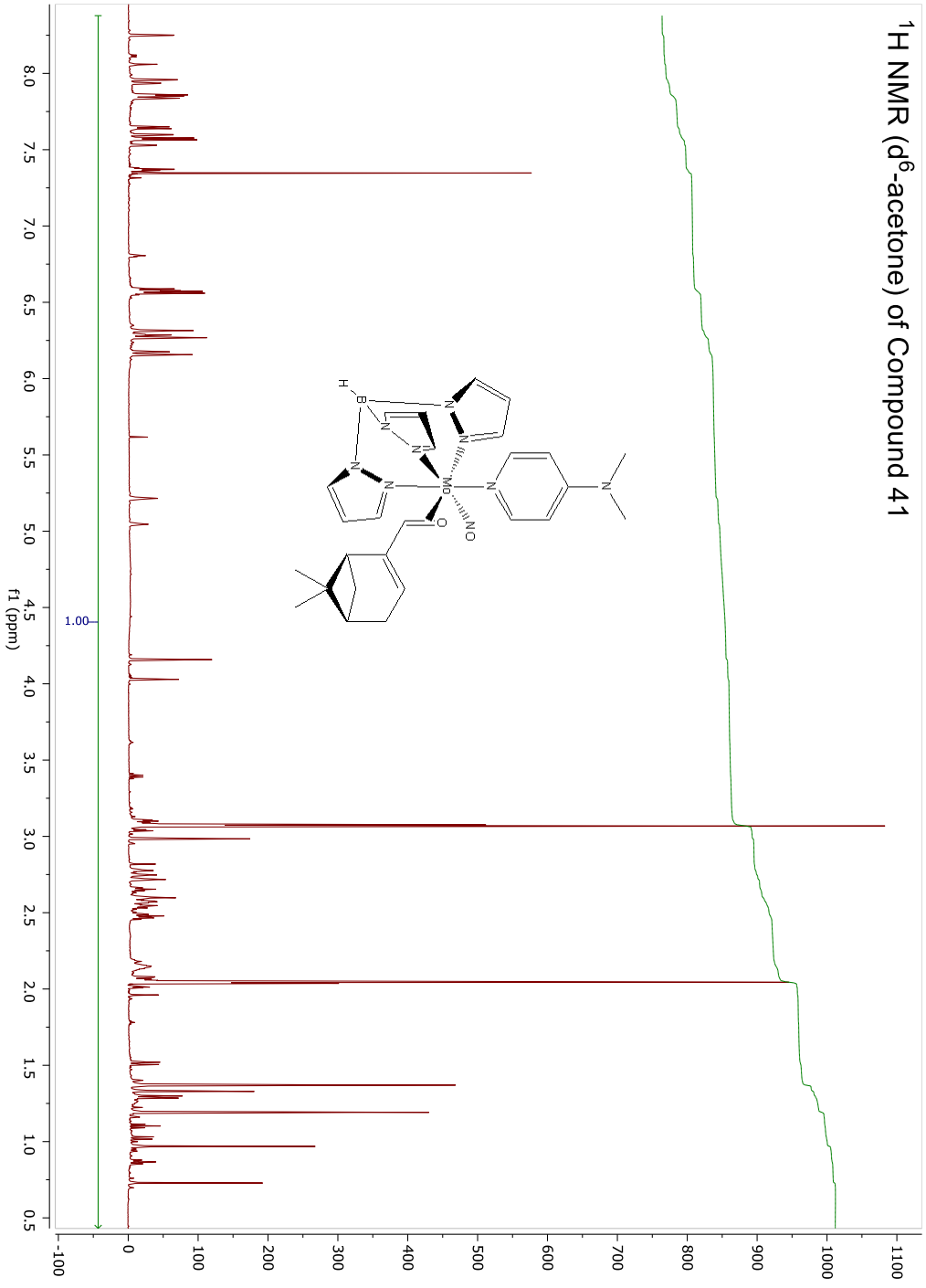
^{1}H NMR (d^6-acetone) of Compound 41
f1 (ppm)
1.00

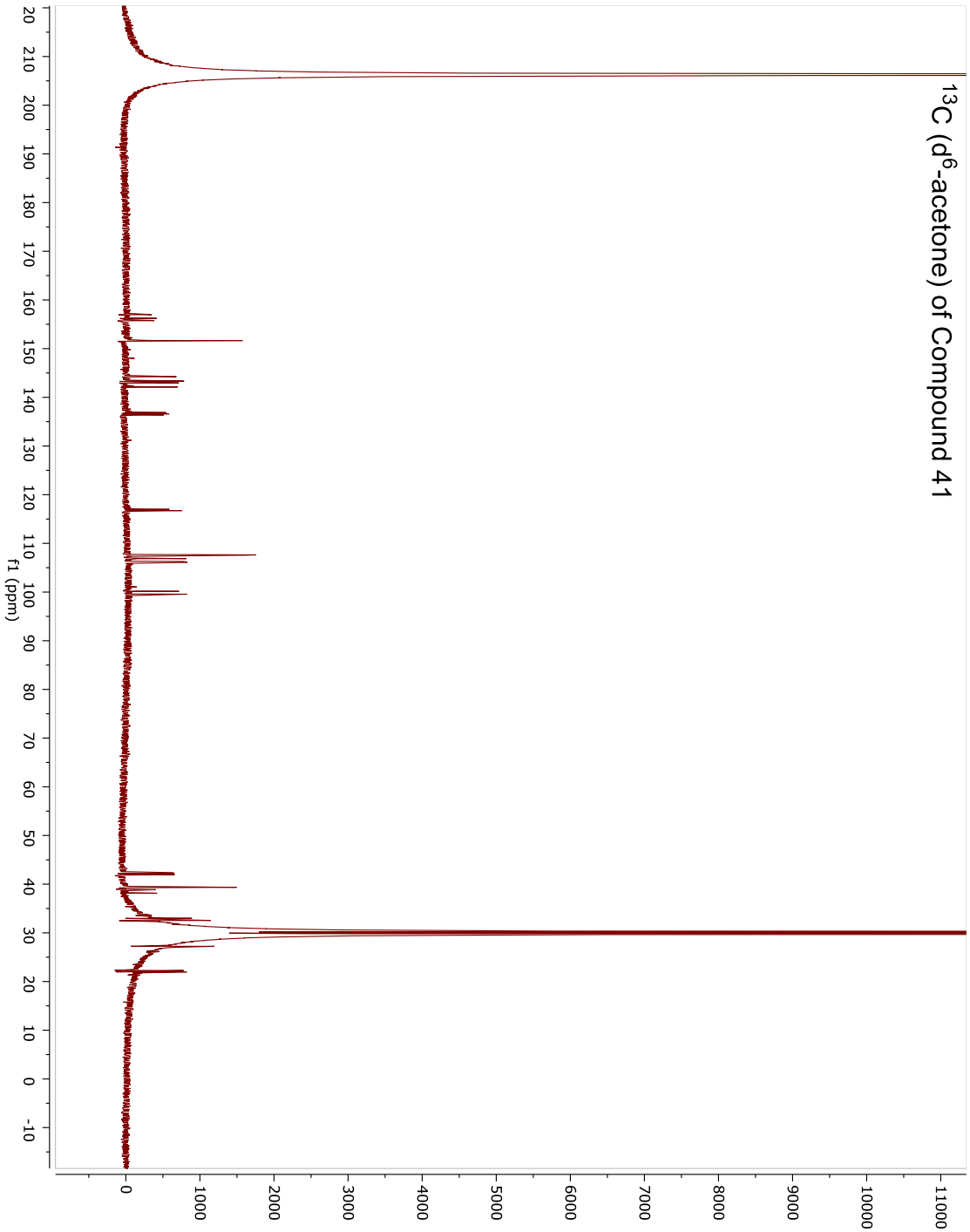
^{13}C (d^6-acetone) of Compound 41
f1 (ppm)
20 210 200 190 180 170 160 150 140 130 120 110 100 90 80 70 60 50 40 30 20 10 0 -10
0 1000 2000 3000 4000 5000 6000 7000 8000 9000 10000 11000

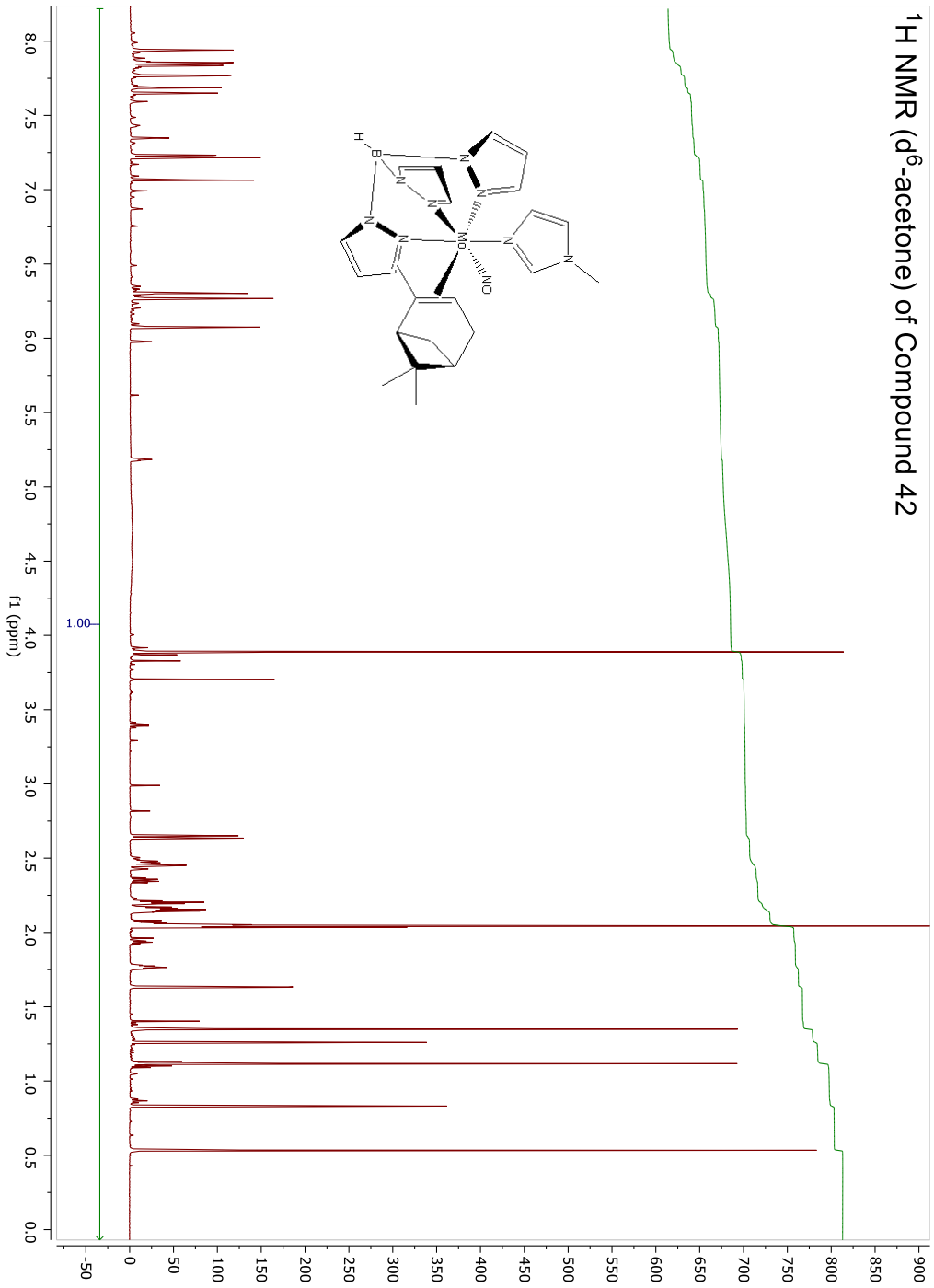
^{1}H NMR (d^6-acetone) of Compound 42
f1 (ppm)
1.00
H
B
N
Mo
NO

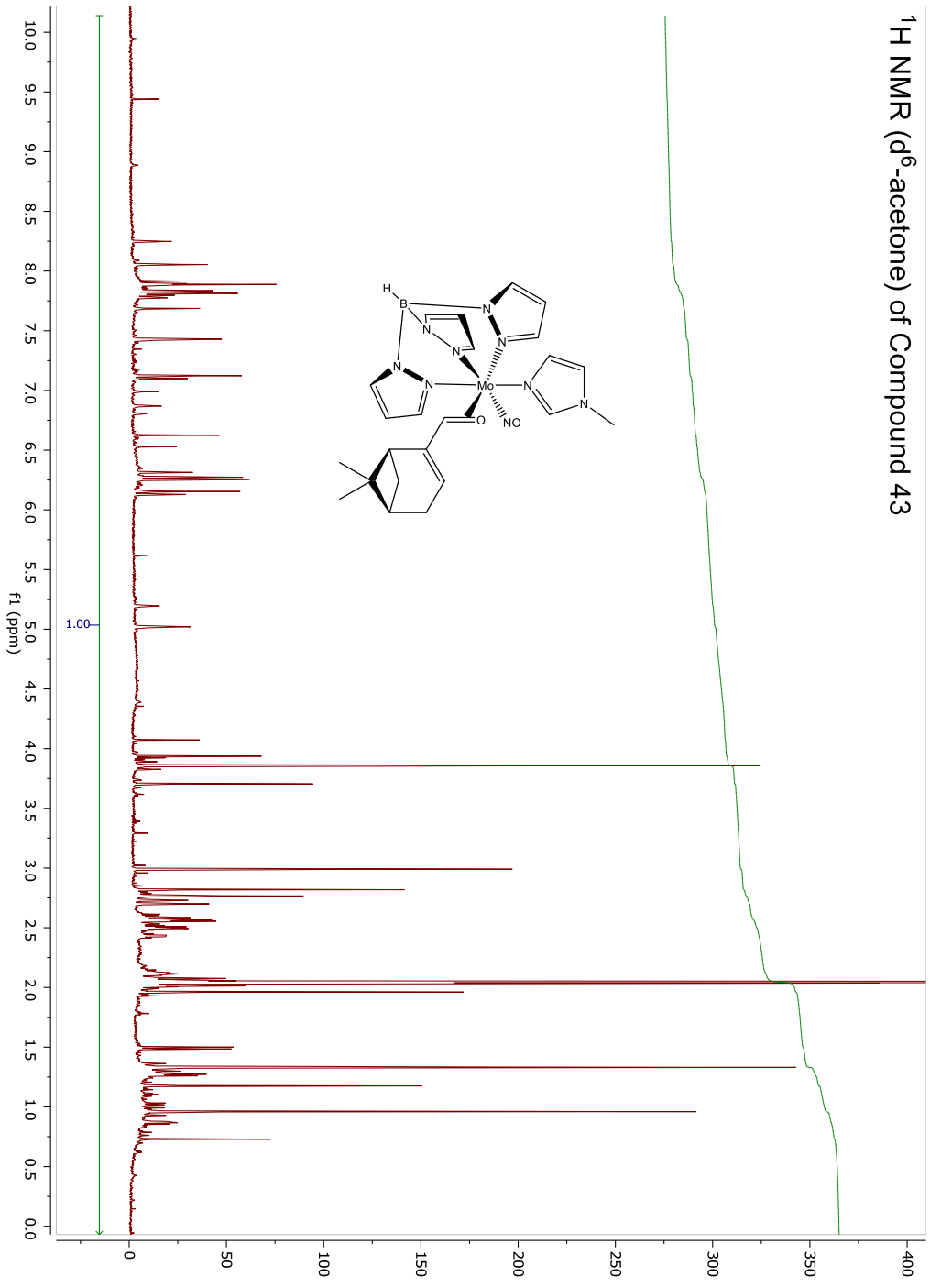
^{1}H NMR (d^6-acetone) of Compound 43
f1 (ppm)
1.00
H
B
N
Mo
O
NO

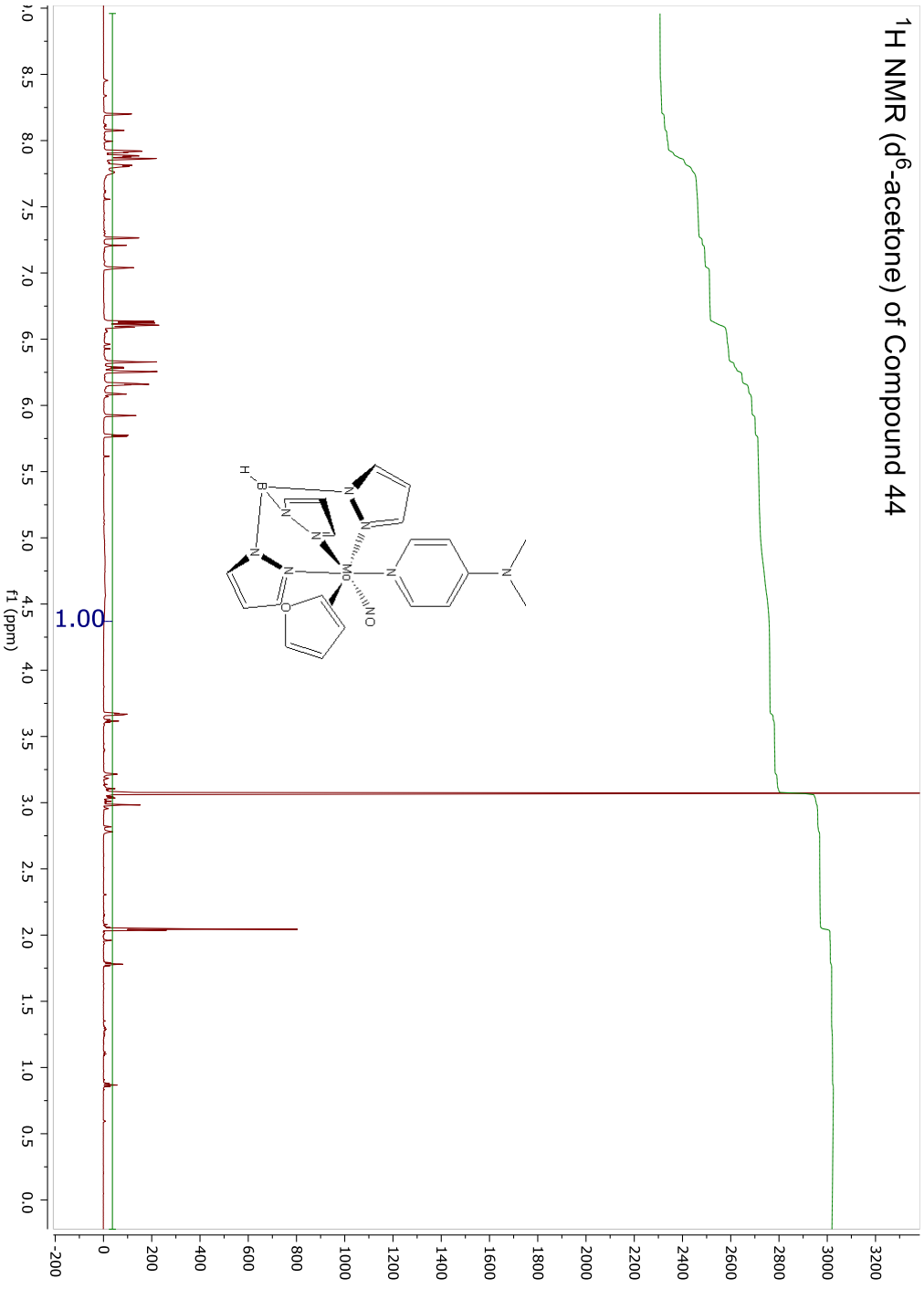
^{1}H NMR (d^6-acetone) of Compound 44
1.00
f1 (ppm)

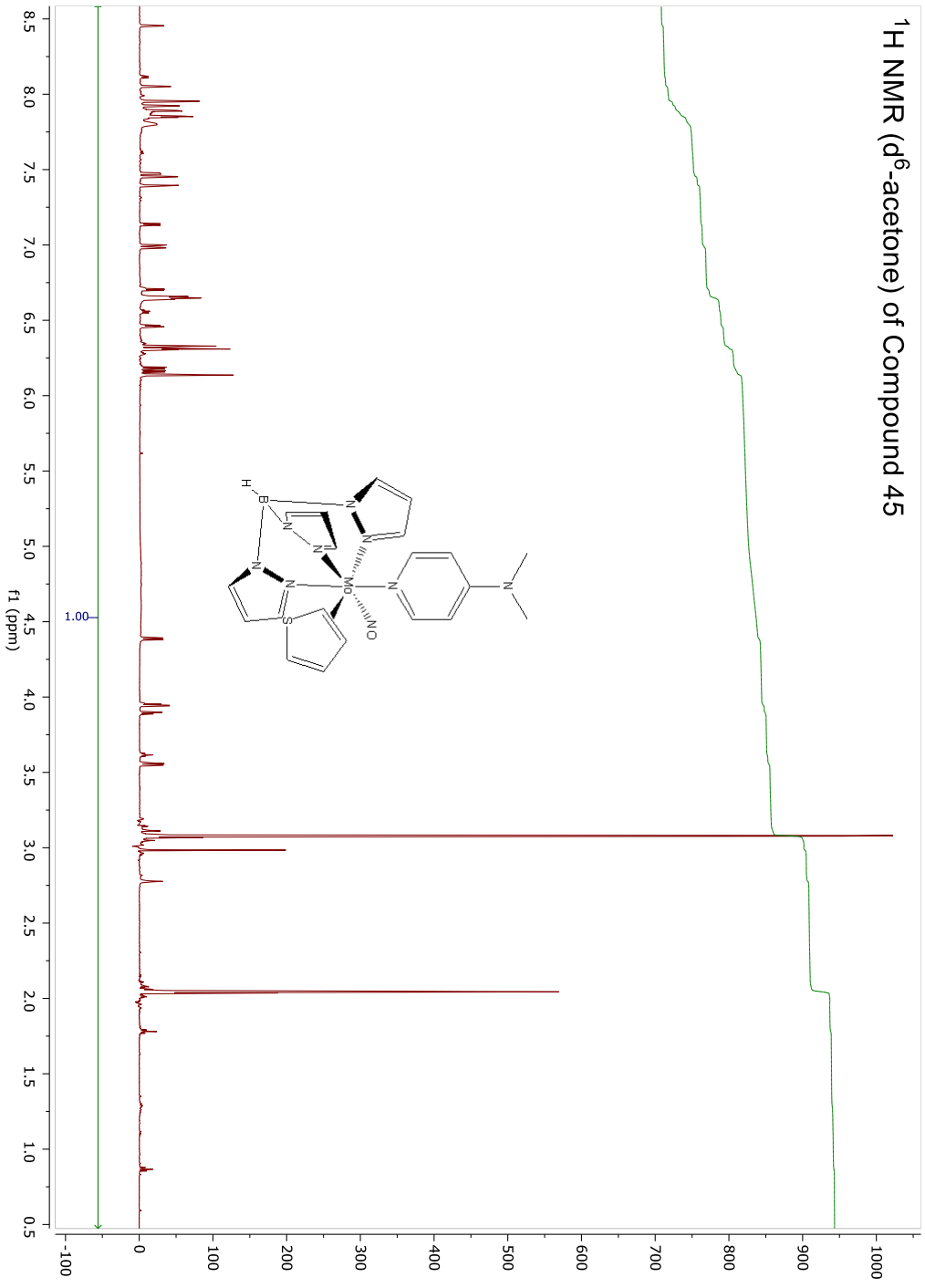
^{1}H NMR (d^6-acetone) of Compound 45
f1 (ppm)
1.00
H
B
N
Mo
O
S

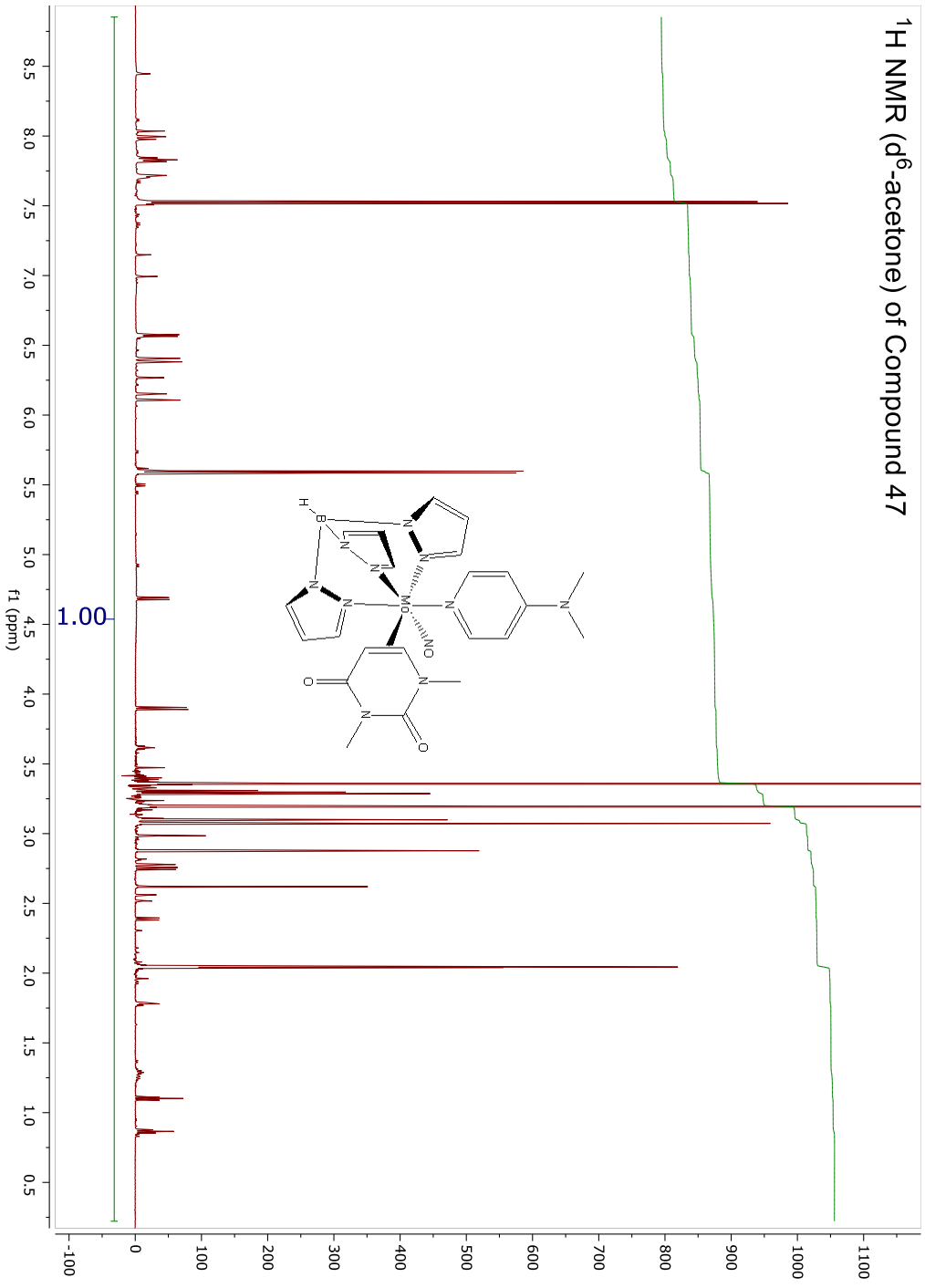
^{1}H NMR (d^6-acetone) of Compound 47
1.00
f1 (ppm)
8.5
8.0
7.5
7.0
6.5
6.0
5.5
5.0
4.5
4.0
3.5
3.0
2.5
2.0
1.5
1.0
0.5
-100
0
100
200
300
400
500
600
700
800
900
1000
1100

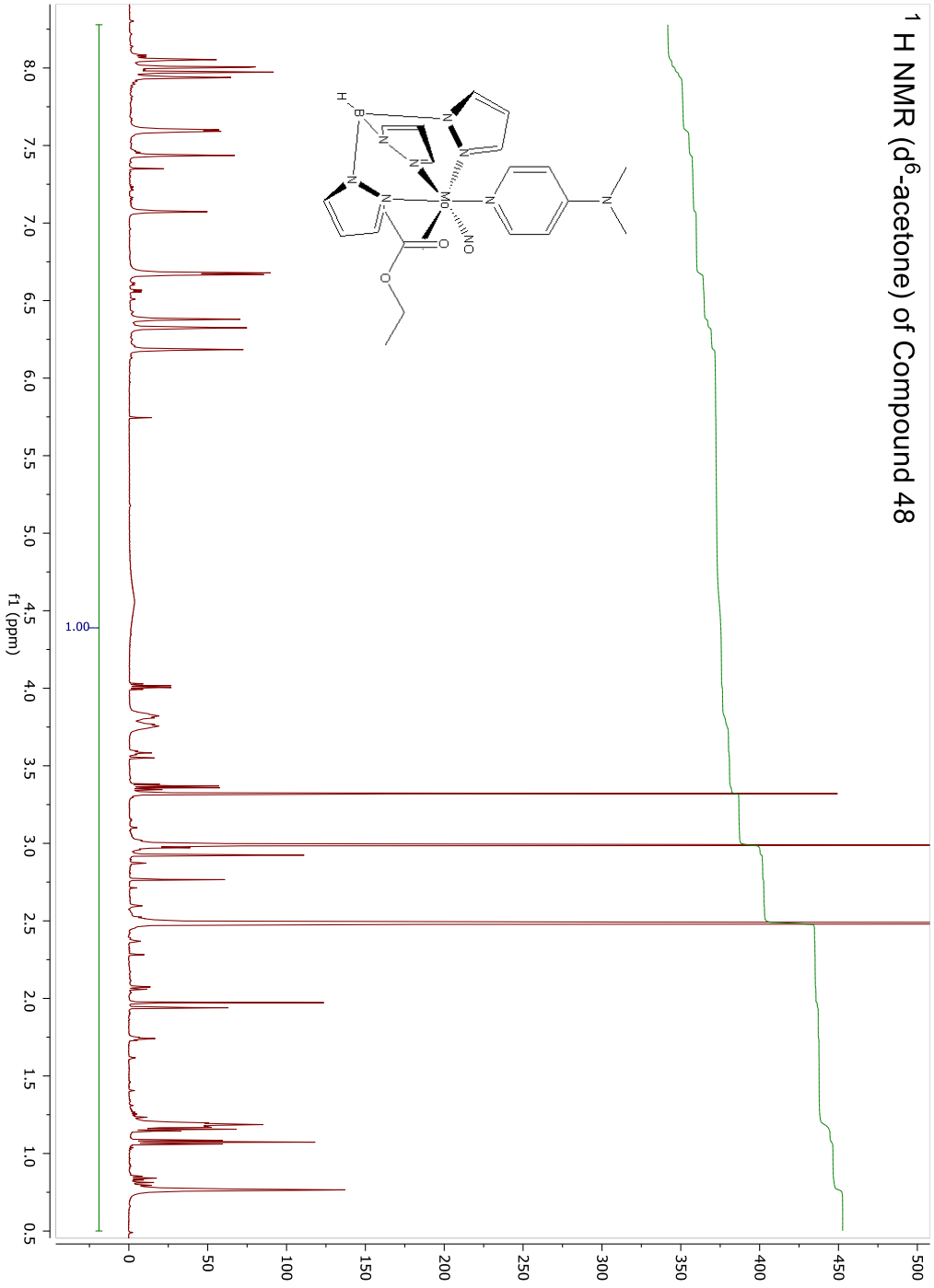
1 H NMR (d6-acetone) of Compound 48
f1 (ppm)
1.00

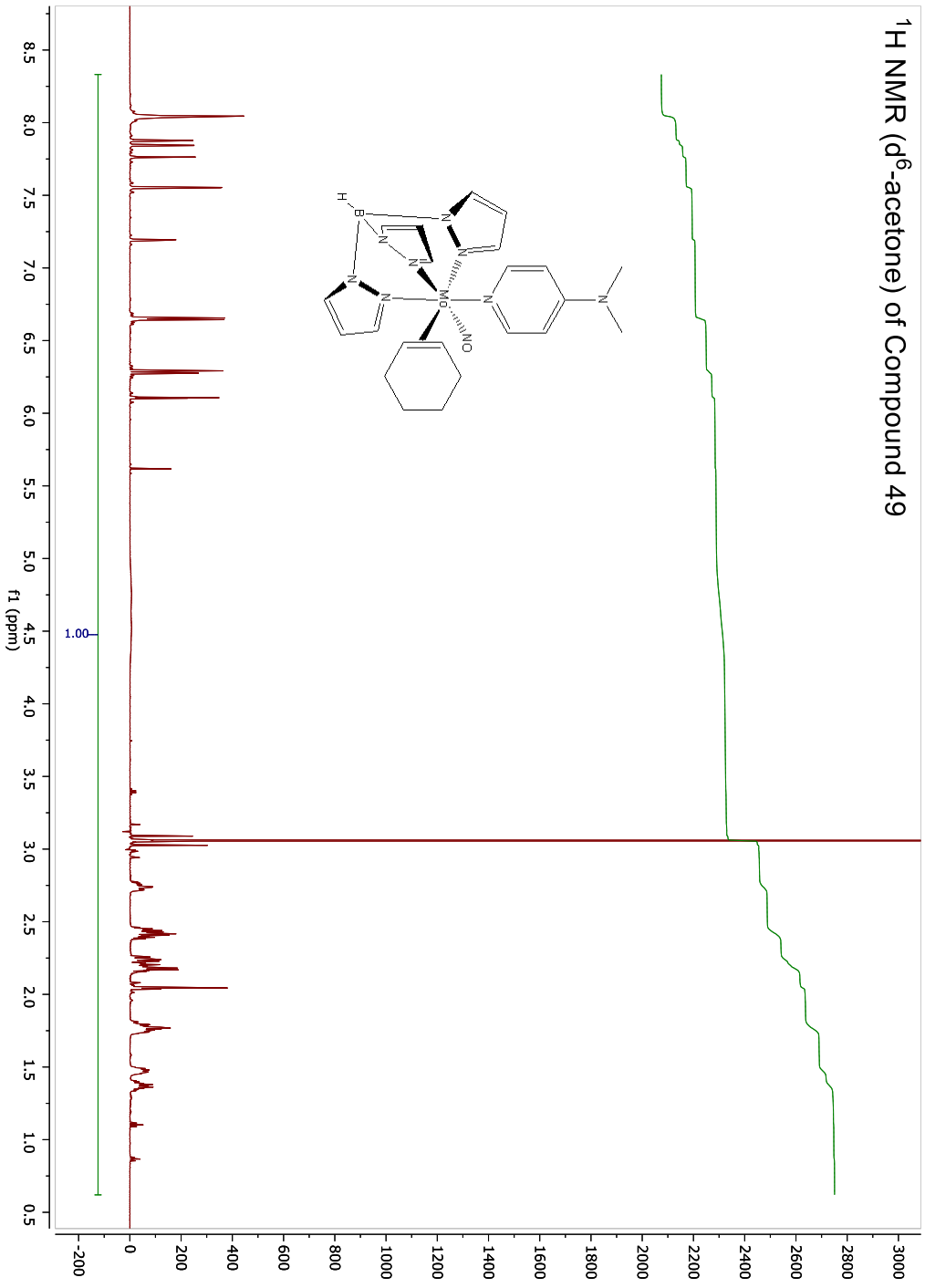
^{1}H NMR (d^6-acetone) of Compound 49
f1 (ppm)
1.00
H
B
N
Mo
NO

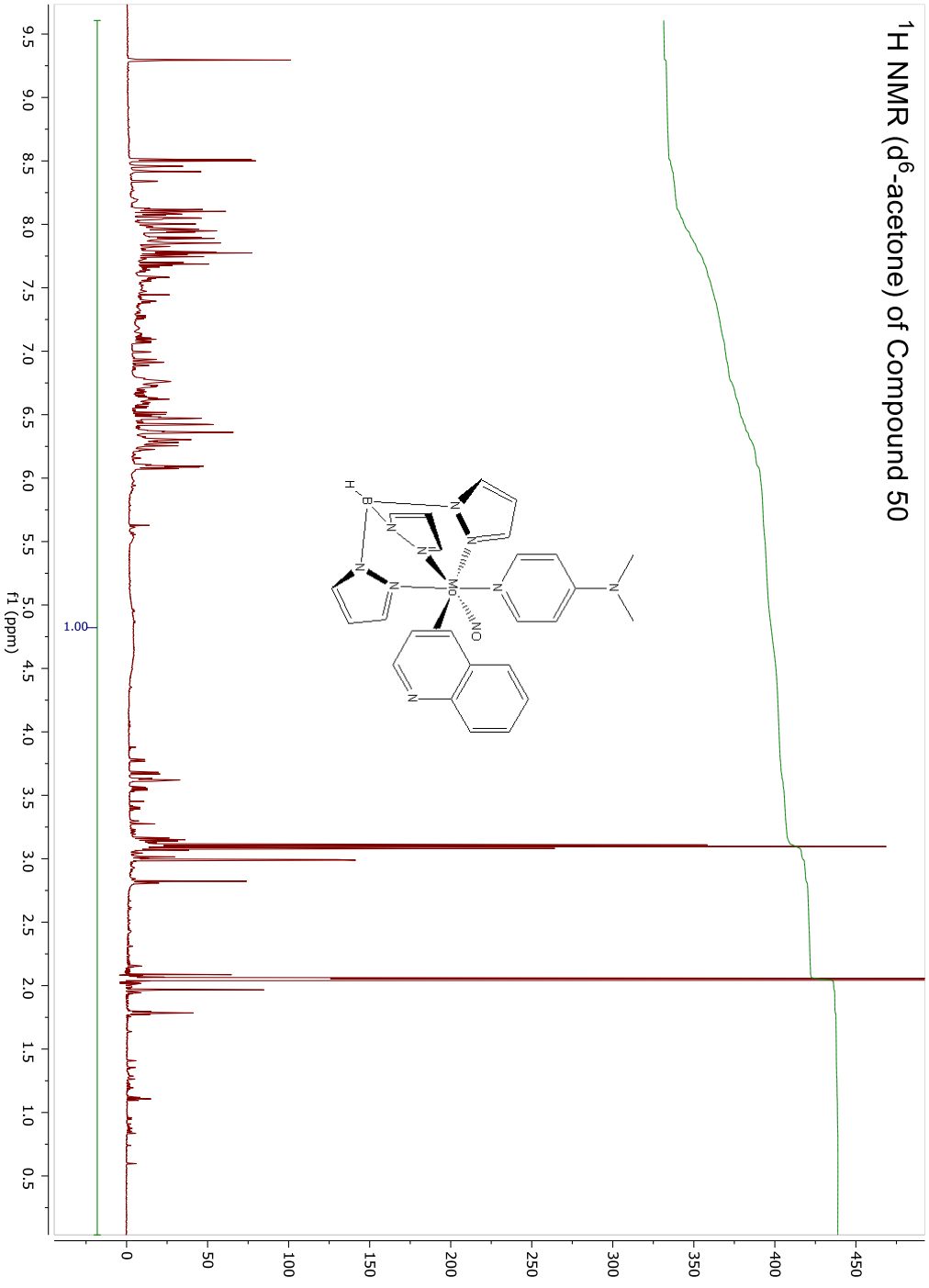
^{1}H NMR (d^6-acetone) of Compound 50
f1 (ppm)
1.00
H
B
N
Mo
O

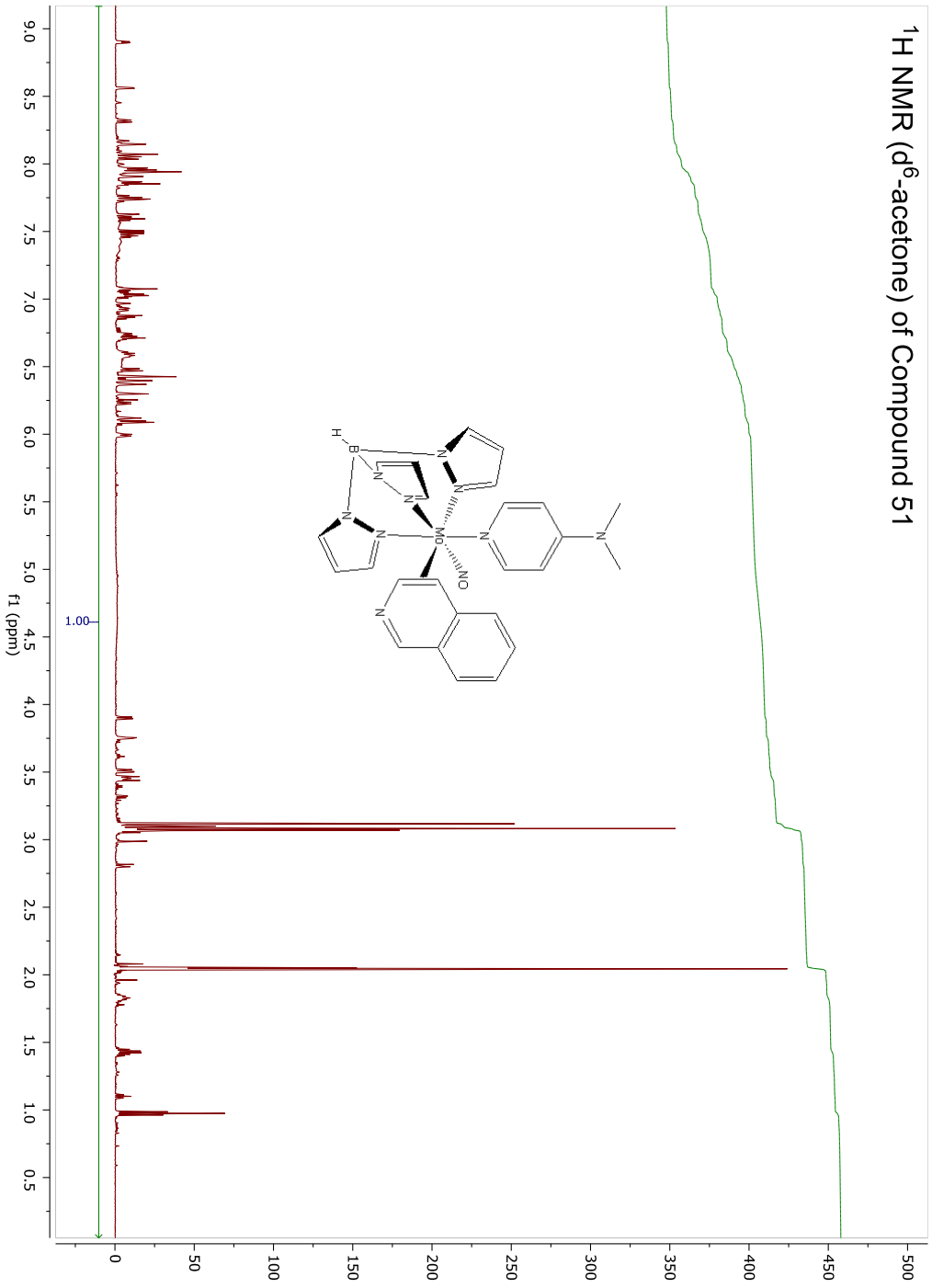
^{1}H NMR (d^6-acetone) of Compound 51
f1 (ppm)
1.00
Mo
NO
B
H
N

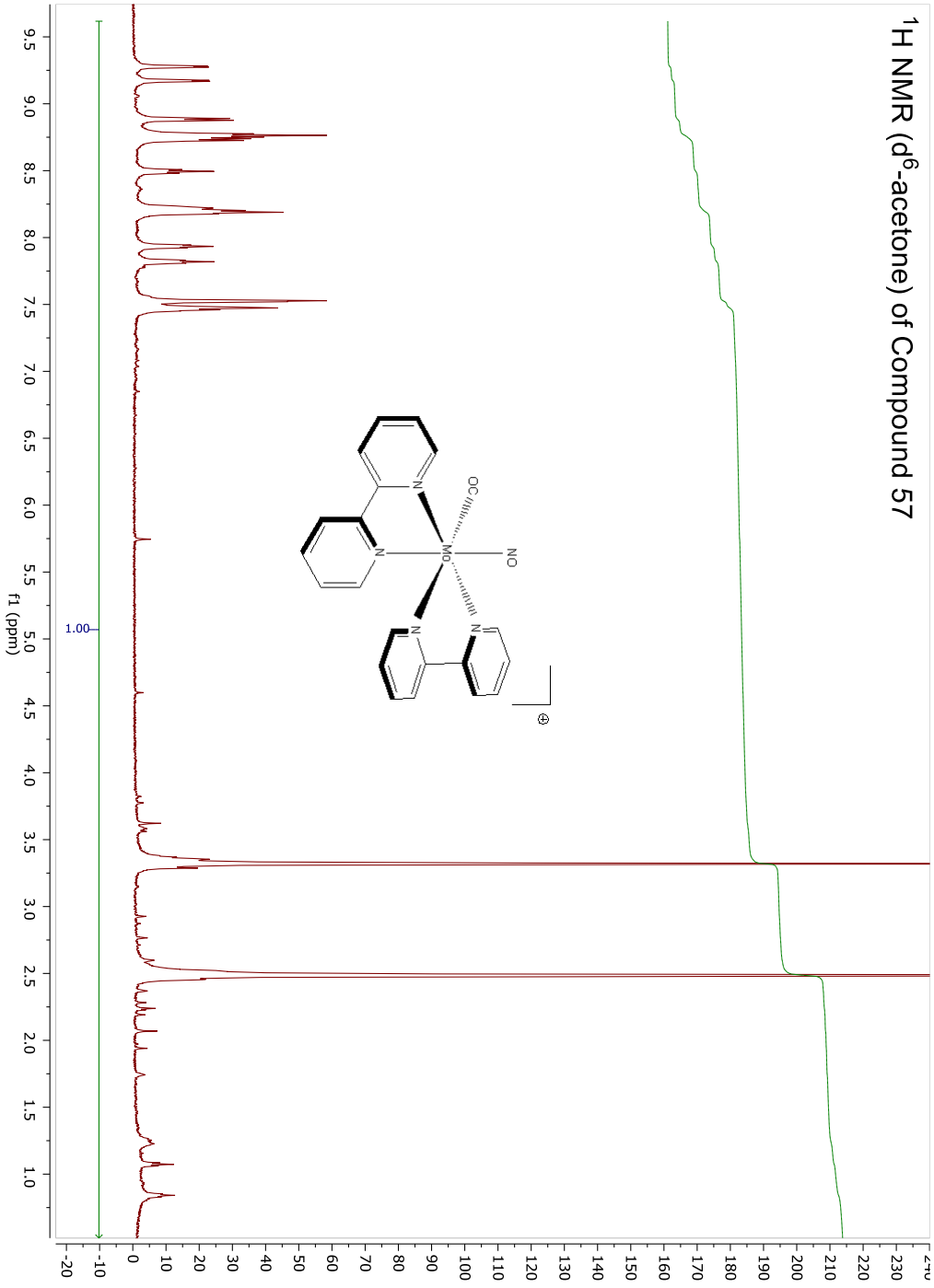
^{1}H NMR (d^6-acetone) of Compound 57
f1 (ppm)
1.00
OC
NO
Mo
N
⊕

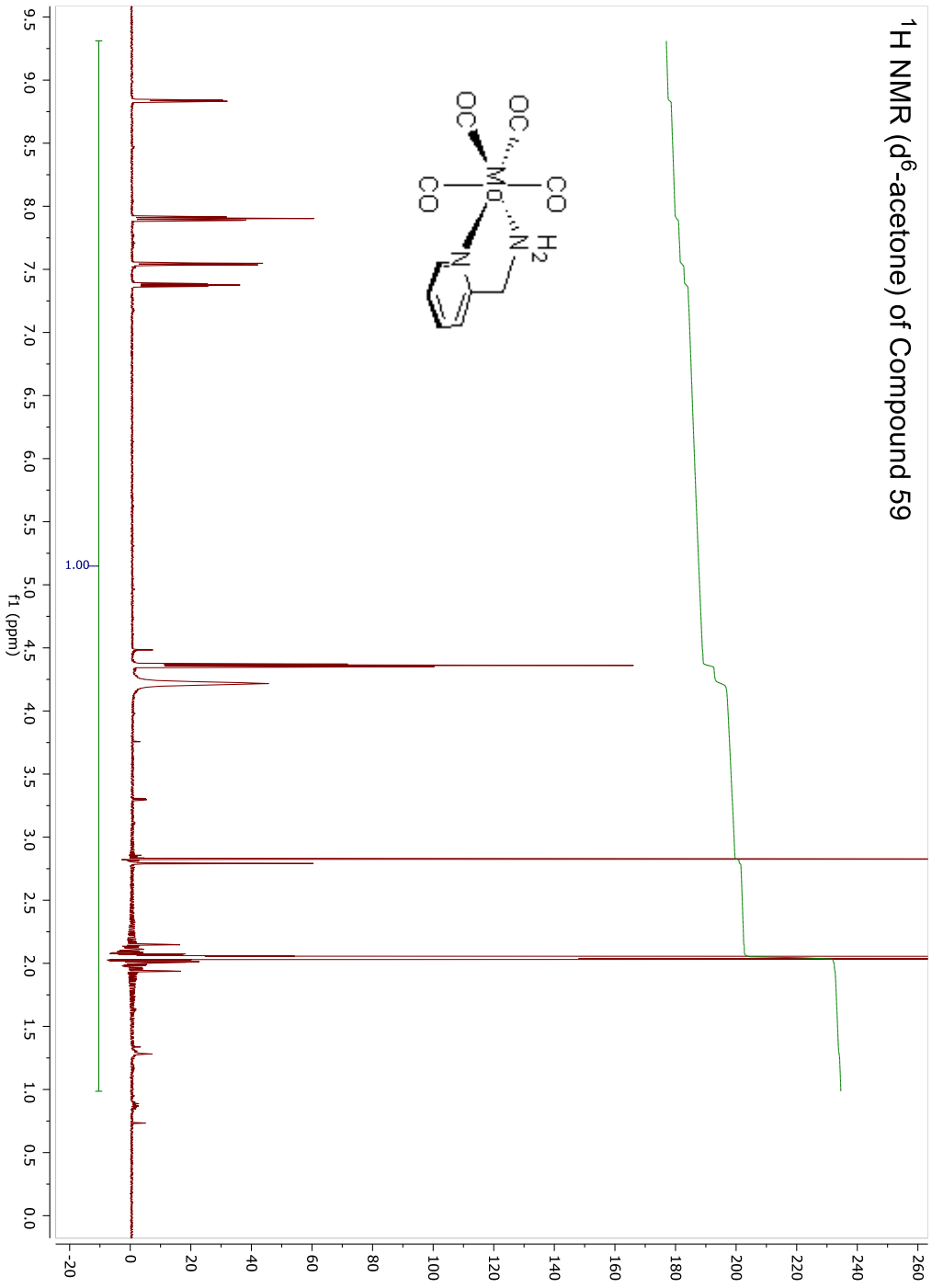
^{1}H NMR (d^6-acetone) of Compound 59
OC
OC
CO
CO
Mo
N
N
H$_2$
1.00
f1 (ppm)

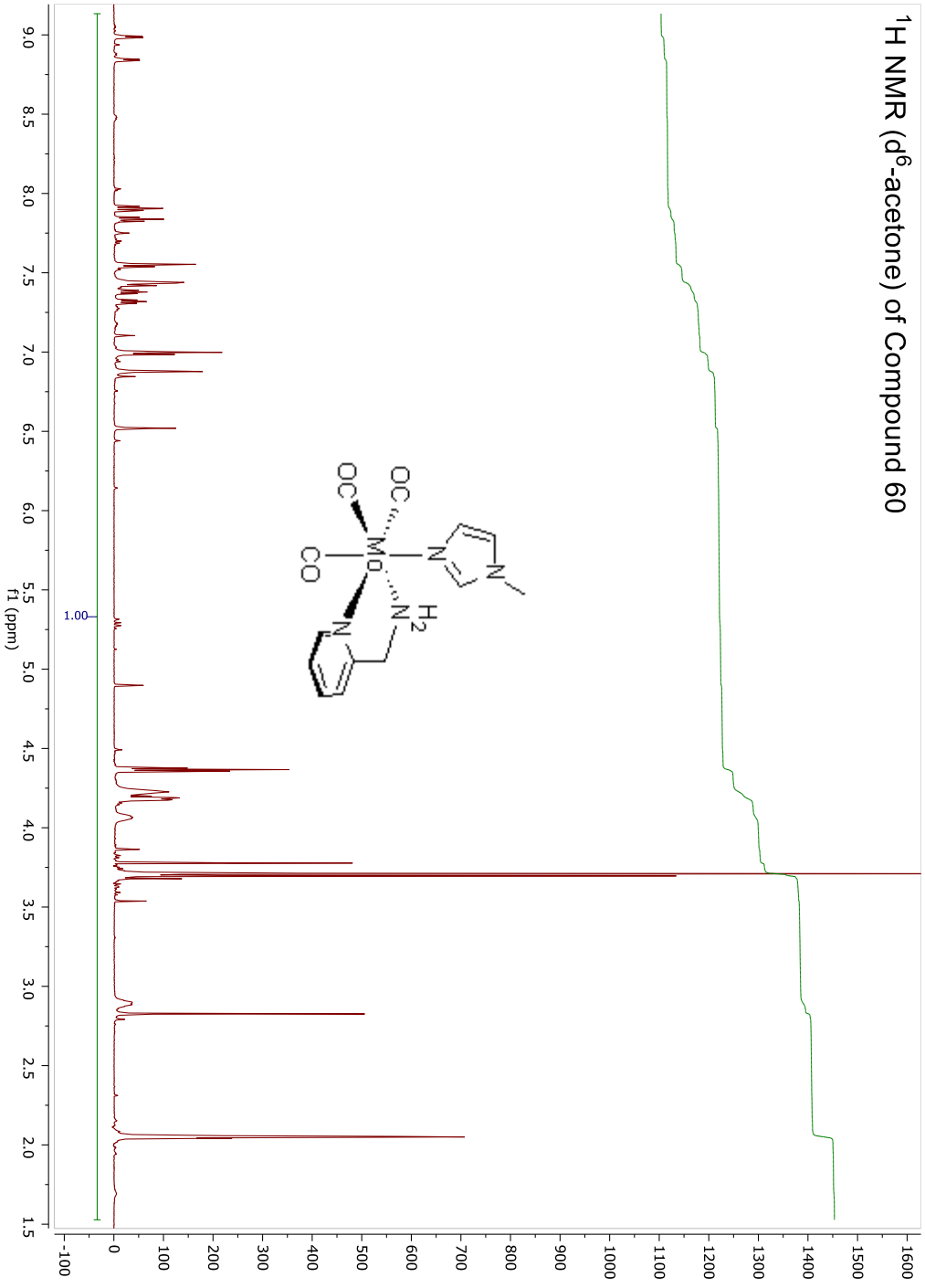
^{1}H NMR (d^6-acetone) of Compound 60
OC
OC
CO
Mo
N
N
N
H$_2$
1.00
f1 (ppm)

^{1}H NMR (d^6-acetone) of Compound 61

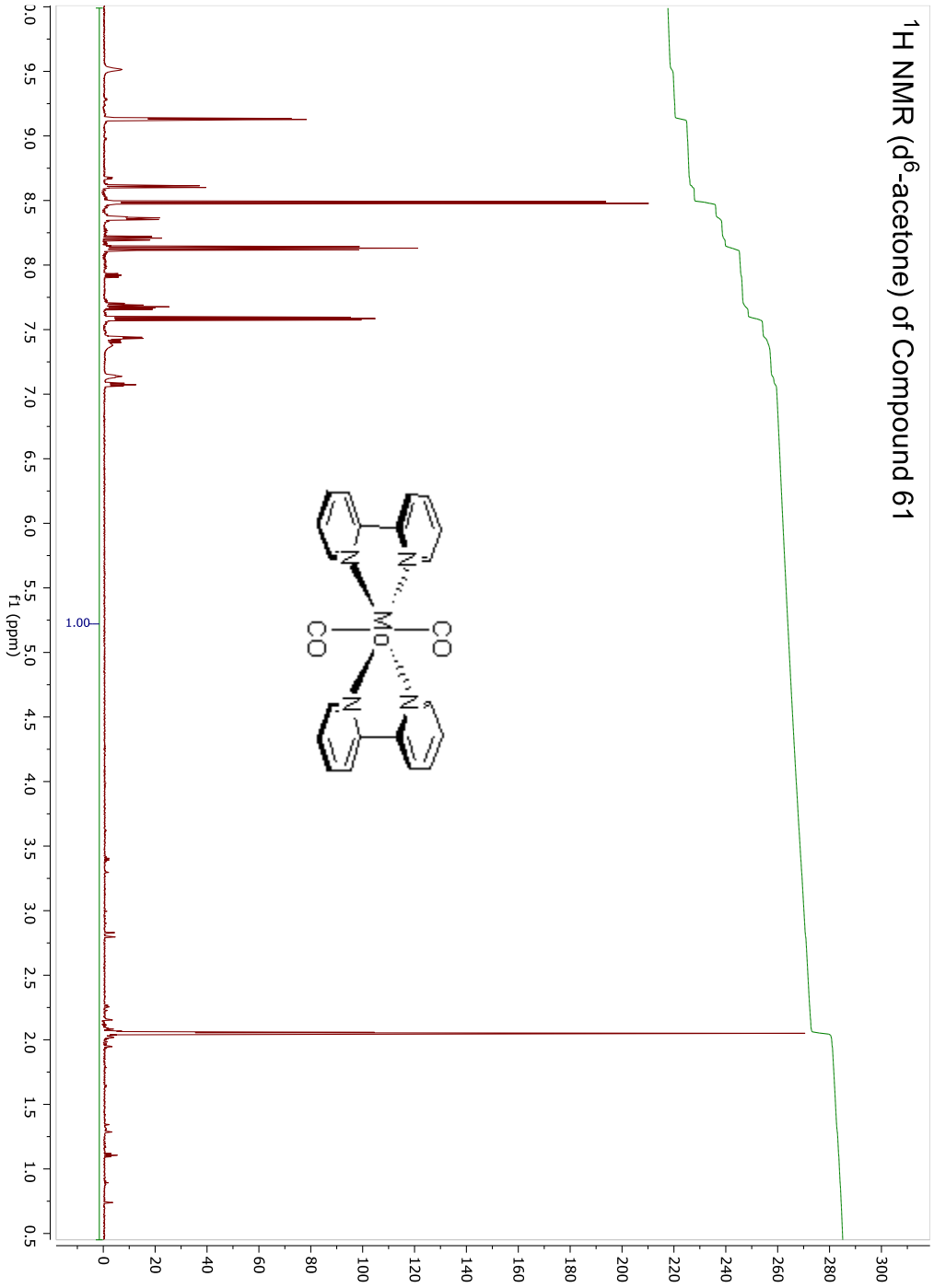

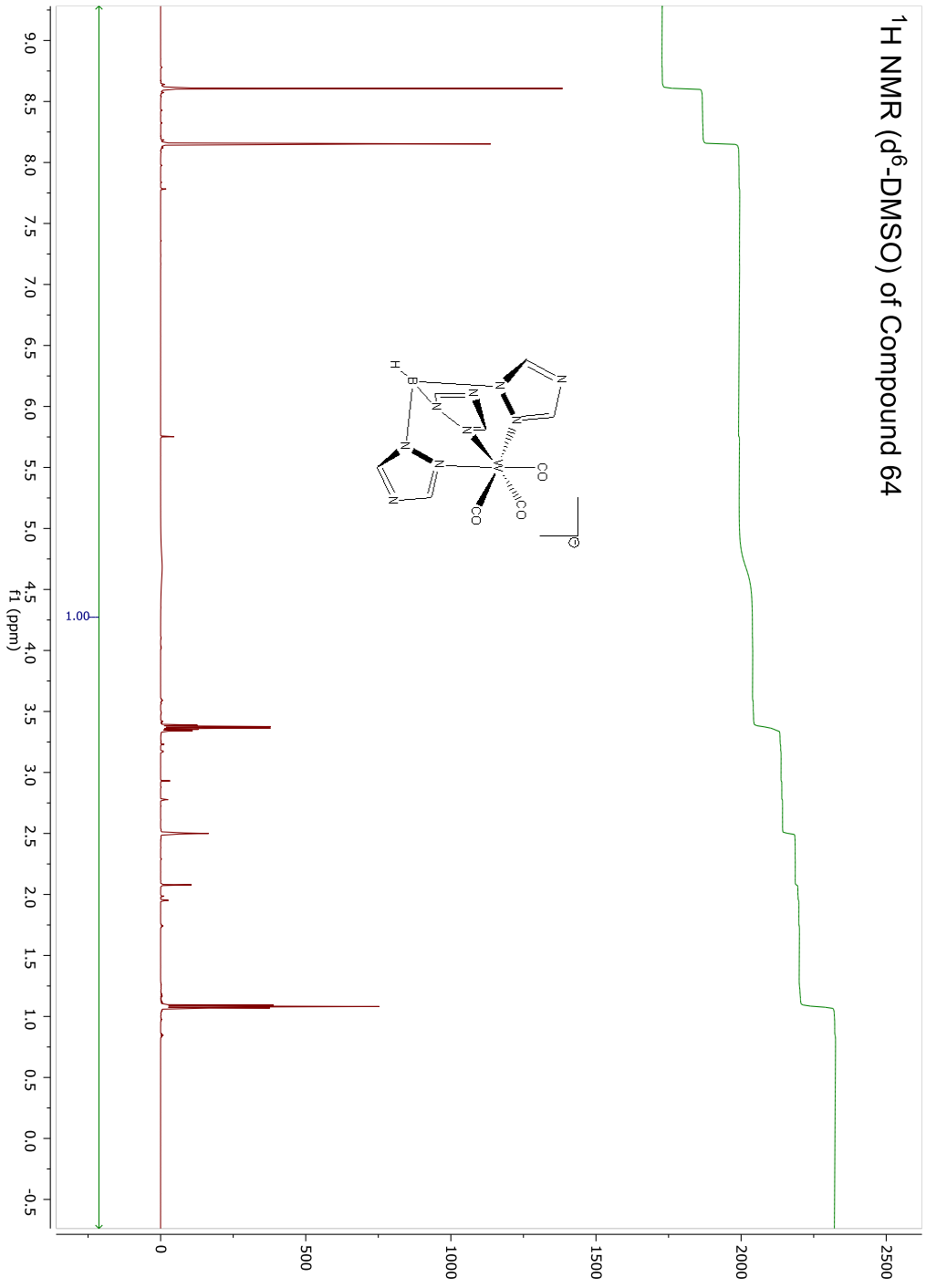
^{1}H NMR (d^6-DMSO) of Compound 64
f1 (ppm)
1.00
CO
CO
CO

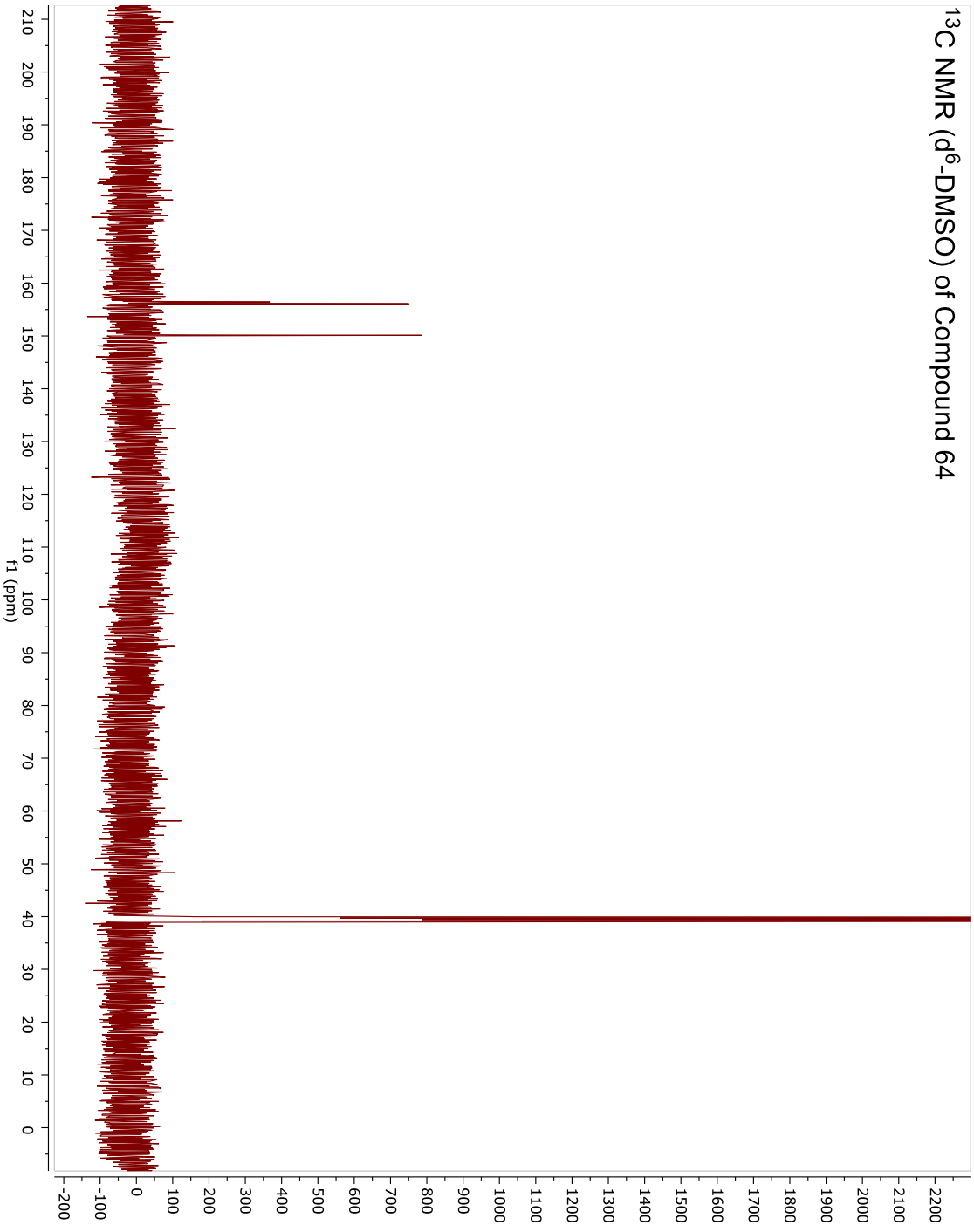
^{13}C NMR (d^6-DMSO) of Compound 64
f1 (ppm)

^{1}H NMR (d^{6}-DMSO) of Compound 65

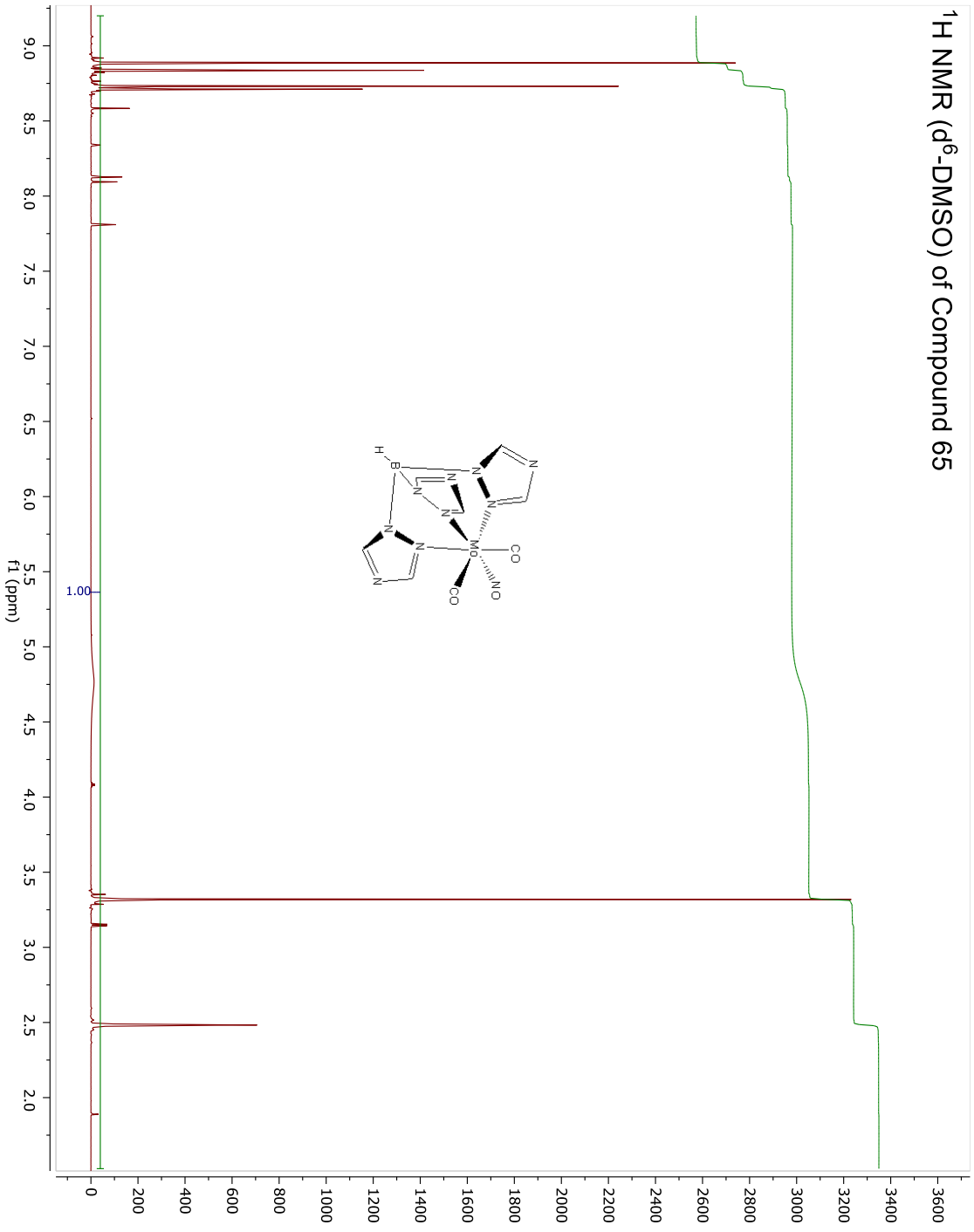

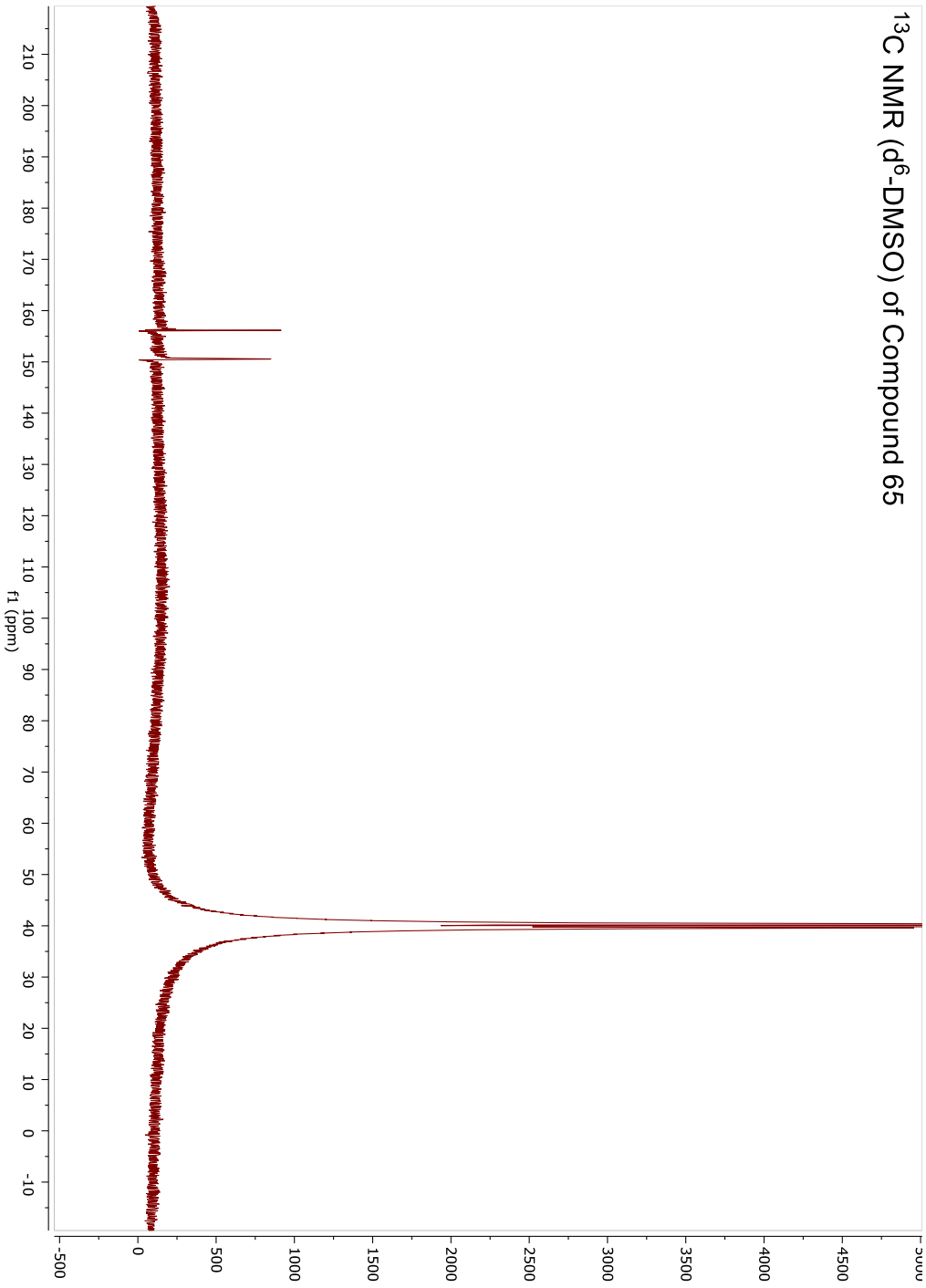
^{13}C NMR (d^6-DMSO) of Compound 65
f1 (ppm)

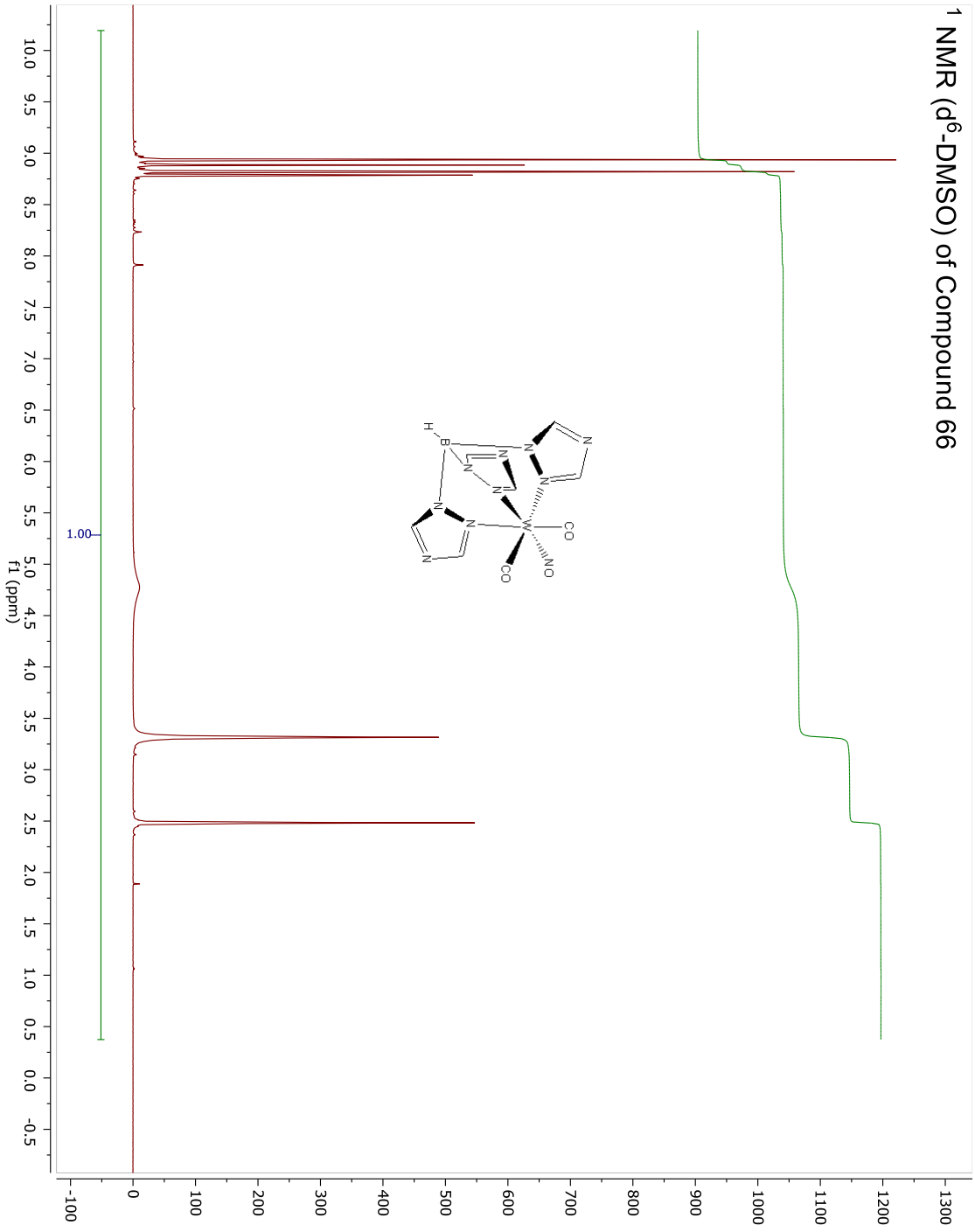
^{1} NMR (d^6-DMSO) of Compound 66
1.00
f1 (ppm)
10.0 9.5 9.0 8.5 8.0 7.5 7.0 6.5 6.0 5.5 5.0 4.5 4.0 3.5 3.0 2.5 2.0 1.5 1.0 0.5 0.0 -0.5
-100 0 100 200 300 400 500 600 700 800 900 1000 1100 1200 1300
H
B
N
CO
NO

^{13}C NMR (d^{6}-DMSO) of Compound 66